

---

# Proceedings of the 14th International Students Conference “Modern Analytical Chemistry”

Prague, 20—21 September 2018

Edited by Karel Nesměrák



FACULTY OF SCIENCE  
Charles University

Prague 2018

*Proceedings of the  
14th International Students Conference  
“Modern Analytical Chemistry”*



---

**Proceedings of the  
14th International Students Conference  
“Modern Analytical Chemistry”**

Prague, 20—21 September 2018

**Edited by Karel Nesměrák**



**FACULTY OF SCIENCE**  
Charles University

Prague 2018

CATALOGUING-IN-PUBLICATION – NATIONAL LIBRARY OF THE CZECH REPUBLIC  
KATALOGIZACE V KNIZE – NÁRODNÍ KNIHOVNA ČR

Modern Analytical Chemistry (konference) (14. : 2018 : Praha, Česko)  
Proceedings of the 14th International Students Conference “Modern Analytical Chemistry” : Prague, 20-21 September 2018 / edited by Karel Nesměrák. -- 1st edition. -- Prague : Faculty of Science, Charles University, 2018. -- x, 298 stran  
ISBN 978-80-7444-059-5 (brožováno)

543 \* (062.534)

- analytická chemie
- sborníky konferencí
- analytical chemistry
- proceedings of conferences

543 – Analytická chemie [10]

543 – Analytical chemistry [10]

The electronic version of the Proceedings is available at the conference webpage:  
<http://www.natur.cuni.cz/isc-mac/>

© Charles University, Faculty of Science, 2018.

**ISBN 978-80-7444-059-5**

## Preface

For the fourteenth time we welcome the participants of the international student conference “Modern Analytical Chemistry” in Prague at – as it can be already called – the traditional meeting of Ph.D. students of analytical chemistry. Participants from six countries (Belarus, Czech Republic, Germany, Poland, Russia, and Slovakia) are coming to present the results of their research, to master their presentation and language skills and to enjoy international community of analytical chemists. We believe that, like all previous ones, this year will be an interesting, beneficial and enjoyable encounter.

Forty eight contributions are presented in this volume of the conference proceedings, assorted by the sequence of their delivery, accompanied with the indexes at the end of the proceedings enabling easy navigation through its pages. Let’s express our hopes that all contributions will be found interesting and will prove that analytical chemistry is trendy, multifaceted, steadily developing science with new, unsuspected ways of its innovation and application. And this is what makes the organization of this meeting very fulfilling and satisfactory.

We are very grateful to the Division of Analytical Chemistry of EuCheMS for its long-lasting auspices of our conference. Also, we are thankful to our sponsors, not only for their kind financial sponsorship making the conference possible, but also for all their support and cooperation in many of our other activities.

**EuCheMS**   
European Chemical Sciences  
Division of Analytical Chemistry

prof. RNDr. Věra Pacáková, CSc.

doc. RNDr. Karel Nesměrák, Ph.D.

## Sponsors

The organizers of 14th International Students Conference “Modern Analytical Chemistry” gratefully acknowledge the generous sponsorship of following companies:



[www.ecomsro.com](http://www.ecomsro.com)



[www.thermofisher.cz](http://www.thermofisher.cz)

lach:ner

[www.lach-ner.com](http://www.lach-ner.com)

**Waters**  
THE SCIENCE OF  
WHAT'S POSSIBLE.®

[www.waters.com](http://www.waters.com)



[www.watrex.com](http://www.watrex.com)

# Contents

Milanowski M., Rudnicka J., Ligor T., Buszewski B.: <i>Determination of volatile organic compounds in headspace above saliva specimens using SPME-GC/MS technique</i> .....	1
Durner B., Ehmann T., Matysik F.N.: <i>Separation of linear and cyclic poly(dimethylsiloxanes) with interactive chromatography</i> .....	7
Dębosz M., Wieczorek M., Kościelniak P.: <i>Simple calibration approach to elimination of the additive interference effect</i> .....	14
Nguyen-Marcinczyk C.T., Karasinski J., Wojciechowski M., Krata A.A., Halicz L., Bulska E.: <i>Separation of chromium(III) and chromium(VI) by reversed-phase ion-pairing chromatography</i> .....	19
Gawor A., Konopka A., Torres Elguera J.C., Ruszczynska A., Czauderna M., Bulska E.: <i>Label-free proteomic approach to identification and quantification of proteins in animal tissue samples</i> .....	25
Granica M.: <i>Distance-based measurements using microfluidic paper-based analytical devices modified with Prussian Blue</i> .....	31
Madej M., Kochana J., Baś B.: <i>Cyclic voltammetry and staircase voltammetry in citalopram determination</i> .....	37
Jagielska A., Wagner B., Ruszczyńska A., Gawor A., Bulska E., Ziemińska E., Toczyłowska B., Jakuczun W., Szostek M.: <i>Elemental analysis of atherosclerotic plaque by ICP-MS and LA-ICP-MS</i> .....	44
Gajdár J., Barek J., Fischer J.: <i>Determination of difenzoquat at a mercury meniscus modified silver solid amalgam electrode by differential pulse voltammetry</i> .....	51
Braun P., Rabl H.P., Matysik F.M.: <i>Investigations on the electrochemically induced decomposition of AdBlue-urea</i> .....	55
Nikolaeva A.A., Bulycheva E.V., Korotkova E.I., Linert W.: <i>Simultaneous determination of synthetic dyes Ponceau 4R (E124) and Sunset Yellow (E110) by fluorimetry in soft drinks</i> .....	61
Król A., Pomastowski P., Railean-Plugaru V., Buszewski B.: <i>Analysis of Lactococcus lactis modified with zinc ions by capillary electrophoresis</i> .....	68
Festinger N., Morawska K., Smarzewska S., Ciesielski W.: <i>Voltammetric studies of acetaminophen</i> .....	77
Makrlíková A., Dejmková H., Navrátil T., Barek J., Vyskočil V.: <i>HPLC-ED/UV for determination of vanillylmandelic acid in human urine after solid phase extraction</i> .....	82
Patočka J., Krejčová A., Klausová K.: <i>ICP-MS analysis as a tool for monitoring of the efficiency of the sorption based removal of iodinated contrast agents</i> .....	87
Rogowska A., Pomastowski P., Złoch M., Railean-Plugaru V., Król A., Rafińska K., Szultka-Młyńska M., Buszewski B.: <i>The influence of pH on the electrophoretic behaviour of yeast modified by calcium ions</i> .....	93
Šoukal J., Musil S.: <i>Optimization of photochemical vapor generation of molybdenum as a sample introduction for ICP-MS</i> .....	100
Malečková M., Vrzal T., Olšovská J.: <i>Development of miniaturized extraction method used for GC-NCD screening of non-volatile nitroso compounds in malt</i> .....	105
Platonov I.A., Kolesnichenko I.N., Karapetian D.D., Igitkhanian A.E.: <i>Chromato-desorption method for producing gas mixtures of volatile organic compounds</i> .....	114
Galbavá P., Szabóová Ž., Gabrišová L., Macho O., Kubinec R., Blaško J., Mikulec J.: <i>MS/MS analysis of fatty acid methyl esters in diesel</i> .....	120
Starzec K., Kochana J.: <i>New biosensor matrices based on carbon nanomaterials for tyrosinase immobilization</i> .....	126

Gusar A., Gashevskya A., Dorozhko E., Derina K.: <i>Carbon containing electrodes modified with the iodate salts of aryl diazonium for electroanalysis</i> .....	134
Baluchová S., Taylor A., Mortet V., Schwarzová-Pecková K.: <i>Boron-doped diamond electrode fabricated by microwave plasma enhanced chemical vapour deposition process with linear antenna delivery for neurotransmitters sensing</i> .....	140
Lewińska I., Michalec M., Tymecki Ł.: <i>Fluorometric method of creatinine determination employing 3,5-dinitrobenzoic acid</i> .....	145
Zušťáková V., Dušek M., Olšovská J.: <i>Screening of pesticide in apple ciders by liquid chromatography-high resolution mass spectrometry</i> .....	152
Platonov I.A., Kolesnichenko I.N., Igitkhanian A.E., Karapetian D.D.: <i>Chromato-desorption microsystems for determination of biomarkers in the exhaled breath</i> .....	158
Korban A.: <i>A novel way of establishing the quantitative composition of gravimetrically prepared standard solutions of volatile compounds in water-ethanol matrix</i> .....	162
Shikun M., Vrublevskaya O.: <i>Method of cyclic voltammograms in the determination of Sn(II) in strongly acid electrolytes for tin electrodeposition</i> .....	169
Pegier M., Pyrzynska K., Kilian K.: <i>Adsorption of Sc(III) on oxidized carbon nanotubes for separation and preconcentration from aqueous solutions – study of mechanism</i> .....	175
Jandovská V., Dušek M.: <i>Behavior and fate of pesticides during beer brewing</i> .....	181
Bakhytkyzy I., Hewelt-Belka W., Kot-Wasik A.: <i>Design of Experiment approach for lipid extraction optimisation in lipidomics</i> .....	188
Borowska M., Kot-Wasik A., Kucińska-Lipka J.: <i>Release of active substances from polymeric coatings in medical applications</i> .....	194
Bystrzanowska M., Tobiszewski M.: <i>Multi-criteria decision analysis for selection of the best procedure for PAHs determination in smoked food</i> .....	200
Fabjanowicz M., Płotka-Wasyłka J.: <i>Metal content in wines of Polish origin</i> .....	205
Garwolińska D., Hewelt-Belka W., Namieśnik J., Kot-Wasik A.: <i>New sample preparation strategies for comprehensive lipidomics of human breast milk</i> .....	211
Glinka M., Kucińska-Lipka J., Wasik A.: <i>Determination of amikacin and ciprofloxacin by liquid chromatography with pre-column derivatization to evaluate sustained delivery of antibiotics from Drug-Eluting Biopsy Needle</i> .....	218
Kalinowska K., Wojnowski W., Płotka-Wasyłka J., Namieśnik J.: <i>Poultry meat freshness assessment based on the biogenic amines index</i> .....	224
Kempińska D., Kot-Wasik A.: <i>High resolution liquid chromatography and time of flight mass spectrometry in perfume analysis</i> .....	230
Lubinska-Szczygeł M., Różańska A., Dymerski T., Namieśnik J.: <i>Study of the effect of the hybridisation process on the content of terpenes in oroblanco fruit (Citrus paradisi × Citrus grandis)</i> .....	236
Pawlak F., Jankowska K., Polkowska Ż.: <i>Correlation between chemical composition and the presence of selected groups of bacteria in freshwater samples collected from Isfjorden and Billefjorde</i> .....	240
Pytel K., Marcinkowska R., Zabiegała B.: <i>Influence of terpenes on indoor air quality</i> .....	246
Różańska A., Lubinska-Szczygeł M., Dymerski T., Namieśnik J.: <i>Classification of adulterated raspberry juice using ultra-fast gas chromatography</i> .....	253
Świerczek L., Cieślik B., Konieczka P.: <i>The potential of raw sewage sludge in construction industry</i> .....	258
Szulczyński B., Rybarczyk P., Gębicki J.: <i>Estimation of the odour intensity of air samples undergoing biofiltration process using electronic nose and artificial neural network</i> .....	263
Wrona O., Rafińska K., Możeński C., Buszewski B.: <i>Supercritical carbon dioxide extraction as a crucial step in the enriching sample in desired group of bioactive compounds</i> .....	269

Popova V, Krivosheina A., Korotkova E.: <i>Development of a voltammetric method for detection of ethyl nitrite</i> .....	276
Khristunova Y., Berek J., Kratochvíl B., Vyskočil V., Korotkova E., Dorozhko E.: <i>Control of electrochemical signal from silver nanoparticles at different modification steps for electrochemical immunosensor development</i> .....	280
Smolejová J., Douša M.: <i>Effect of chaotropic salts addition into mobile phases on separation of model analytes on polar stationary phases in hydrophilic interaction chromatography</i> .....	285
<i>Author index</i> .....	293
<i>Keyword index</i> .....	295



## Contributions



# Determination of volatile organic compounds in headspace above saliva specimens using SPME-GC/MS technique

MACIEJ MILANOWSKI\*, JOANNA RUDNICKA, TOMASZ LIGOR, BOGUSŁAW BUSZEWSKI

*Nicolaus Copernicus University in Toruń, Faculty of Chemistry, Department of Environmental Chemistry and Bioanalytics, Gagarina 7, 87-100 Toruń, Poland ✉ bbusz@chem.uni.torun.pl*

## Keywords

HS-SPME-GC/MS  
preconcentration  
saliva  
volatile organic  
compounds

## Abstract

The aim of this study was to apply headspace-solid phase microextraction-gas chromatography/mass spectrometry (HS-SPME-GC/MS) to evaluate profiles of volatile organic compounds from saliva of nonsmokers and smokers. Also different types of SPME fibres were used and influence of such factors as sample volume, incubation, and adsorption time were evaluated. We found that 75 µm Carboxen/PDMS fibre gave the highest abundances and the greatest number of extracted volatile organic compounds from saliva. Volume of 2 mL and incubation time 20 min were chosen as the best parameters of conducted experiments. In the typical profile of salivary headspace we found at least ten compounds such as: acetaldehyde, propanal, 2,3-butanedione, ethyl ether, dimethyl sulphide, and pyrolyse. Daily variations of salivary constituents were investigated. The great diversity of compounds were observed in the afternoon. Comparison of smokers and nonsmokers revealed the presence of pyridine in salivary samples of persons smoking cigarettes.

---

## 1. Introduction

Volatile organic compounds can emanate from many different biological specimens including blood, urine, feces, saliva and skin secretions. They contain volatile organic compounds of various functional groups such as aldehydes, alcohols, alkanes, esters, fatty acids, and ketones [1]. Analyses of volatile profiles and subsequent comparison of normal and pathological states may provide important information as to the etiology, pathogenesis or diagnosis of certain diseases. Saliva can be collected noninvasively by individuals with modest training, and it offers a cost-effective approach for screening of large populations [1, 2]. Saliva provides a large number of volatile biomarkers such as volatile sulphur compounds responsible for halitosis [3], nonanal for celiac disease [4] and benzophenone for lung cancer [5]. The typical method for enrichment of volatile organic compounds

in salivary headspace are solvent extraction, stir-bar extraction and solid phase microextraction (SPME) [1]. The purpose of our study was to apply SPME-GC/MS technique to evaluate volatile profiles in the headspace above saliva. We have tested different types of polymers for SPME preconcentration. Influence of storage conditions, sample volume, incubation and adsorption time was evaluated. Volatile organic compounds were extracted using 75  $\mu\text{m}$  Carboxen/PDMS fibre and analysed by GC/MS. Daily variation of salivary profiles and comparison of smokers and nonsmokers were also investigated.

## 2. Experimental

### 2.1 Reagents and chemicals

The 15 mL sterile polypropylene tubes (ISOLAB, Wertheim, Germany) were used for collection of saliva specimens. 22 mL headspace crimp top vials and PTFE/butyl septa for HS-SPME-GC/MS experiments were purchased from PerkinElmer (Waltham, MA, USA). SPME fibres: 75  $\mu\text{m}$  Carboxen/PDMS, 100  $\mu\text{m}$  PDMS and 65  $\mu\text{m}$  PDMS/DVB were from Supelco, Bellefonte, PA, USA.

### 2.2 Instrumentation

Gas chromatograph 7890 A (Agilent) coupled with a spectrometer TruTOF (Leco). Column CP-Porabond-Q (Varian) 25 m  $\times$  0.25 m  $\times$  3  $\mu\text{m}$ . The oven temperature programme: the initial 40  $^{\circ}\text{C}$  were kept for 2 min, and ramped at 10  $^{\circ}\text{C}/\text{min}$  to 140  $^{\circ}\text{C}$  and then again ramped at 5  $^{\circ}\text{C}/\text{min}$  to 270  $^{\circ}\text{C}$  and kept for 5 min. The temperature of the split-splitless injector was 235  $^{\circ}\text{C}$ . The acquisition was performed at the mass range 30–350  $m/z$ , the acquisition rate was 50 spectra/sec. The ion source and line transfer temperatures were set at 250  $^{\circ}\text{C}$ . The collection of chromatographic data was performed by means of ChromaTOF software (Leco). Compounds were identified by comparing their mass spectra with those contained in spectral library; each peak was searched manually (including baseline subtraction and averaging over a peak). Forward and reverse match quality of at least 800/1000 was used as the lower match threshold, otherwise a compound was labelled unknown.

### 2.3 Selection of SPME fibre

Three SPME fibres: 75  $\mu\text{m}$  Carboxen/PDMS, 100  $\mu\text{m}$  PDMS and 65  $\mu\text{m}$  PDMS/DVB were tested to maximize the peaks responses. Selection was carried out with fixed extraction and adsorption conditions for all three fibres. A fibre providing the highest abundances and the greatest number of extracted volatile organic compounds was chosen.

## 2.4 Collection of saliva

Saliva samples were collected in a non-stimulated fashion from eleven healthy volunteers (8 males, 3 females), including two active smokers. They were asked to refrain from eating and drinking at least 1 h before collection of saliva samples. Participants were instructed to rinse their mouths with tap water prior to sampling, without brushing their teeth or using any mouthwashes. After 10 min, saliva samples were taken in glass vial by spitting.

## 2.5 Incubation and extraction conditions

Saliva samples were incubated finally for 20 min at 40 °C, extracted for 20 min at 40 °C with preconditioned 75 µm Carboxen/PDMS fibre and analysed with GC/MS system.

## 3. Results and discussion

### 3.1 Choosing of SPME fibre

Among three tested SPME fibres we chose 75 µm Carboxen/PDMS fibre as a device used for conducted experiments. This fibre was characterized by the highest abundances and the greatest number of extracted volatiles from saliva samples.

### 3.2 Influence of sample volume and incubation time

Influence of sample volume is demonstrated in Fig. 1(A). The results for 2 mL of saliva shows the highest abundances and comparable number of extracted

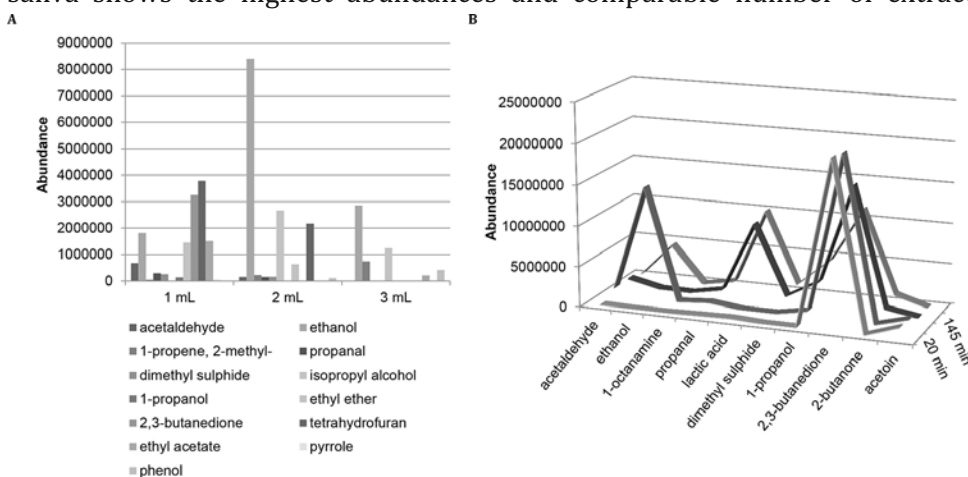


**Fig. 1** Influence of two factors affecting volatile organic compounds analysis: (A) effect of sample volume on the number volatile organic compounds released from 1 mL, 2 mL, and 3 mL of saliva samples. (B) influence of incubation time and the following extractions on the level of volatile organic compounds from single saliva sample.

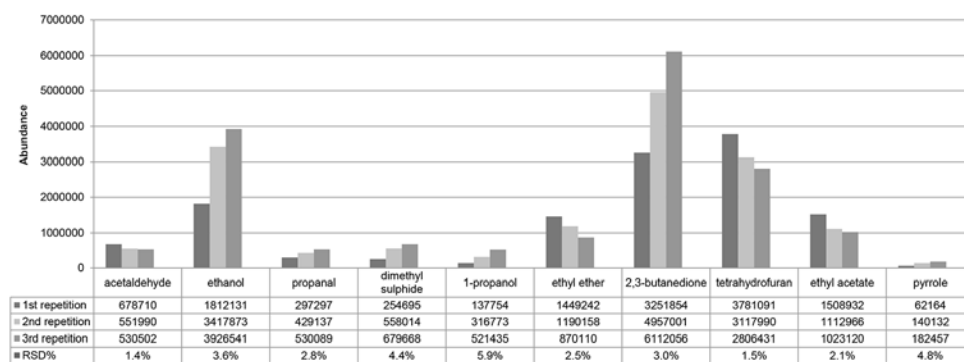


Fig. 2 The reproducibility of SPME-GC/MS method for 1 mL of saliva sample.

compounds. An effect of subsequent volatile organic compounds adsorptions from one sample with increasing incubation time from 20 min to 195 min is presented in Fig. 1 (B). It can be found that after 195 min of incubation the most noticeable observation is a decrease of 2,3-butadiene and significant raise of lactic acid level after 145 min of incubation. For further experiments we used 20 min of incubation because excessive extension of maintaining time led to appearance of compounds from bacterial metabolism in obtained salivary profiles, like ethanol. Our goal was to analyse profiles from “fresh” saliva, hence both incubation and adsorption steps were carried out at 40 °C for 20 min both. We tried to reduce the contribution of volatile organic compounds from putrefactive activity of microorganisms in mouth by shortening the time of preconcentration, but leaving sufficient time to differentiate the distinct volatile organic compound profiles of individual subjects.

### 3.3 Reproducibility of method and characteristic of typical profile

The reproducibility of the method for triplicate samples of 1 mL is shown in Fig. 2. Usage of SPME provided satisfactory level of reproducibility. Typical chromatogram of volatile organic compounds obtained from single female subject is presented in Fig. 3. We were able to detect ten volatile organic compounds in obtained profile. They were: acetaldehyde, ethanol, propanal, dimethyl sulphide, 1-propanol, ethyl ether, 2,3-butanedione, 1-propen-2-ol, acetate, ethyl acetate and pyrrole.

### 3.4 Daily variations of salivary constituents and comparison of smokers and nonsmokers

Fluctuations in daily salivary composition is demonstrated in Fig. 4 (A). Samples from single man were taken three times per day, e.g., in the morning, afternoon and evening. Subject did not have any dietary restrictions that day and was

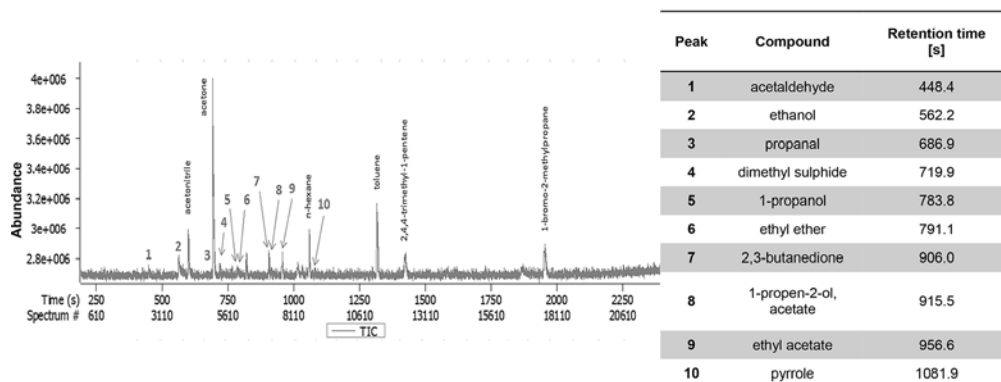


Fig. 3 SPME-GC/MS chromatogram of saliva sample from single female subject.

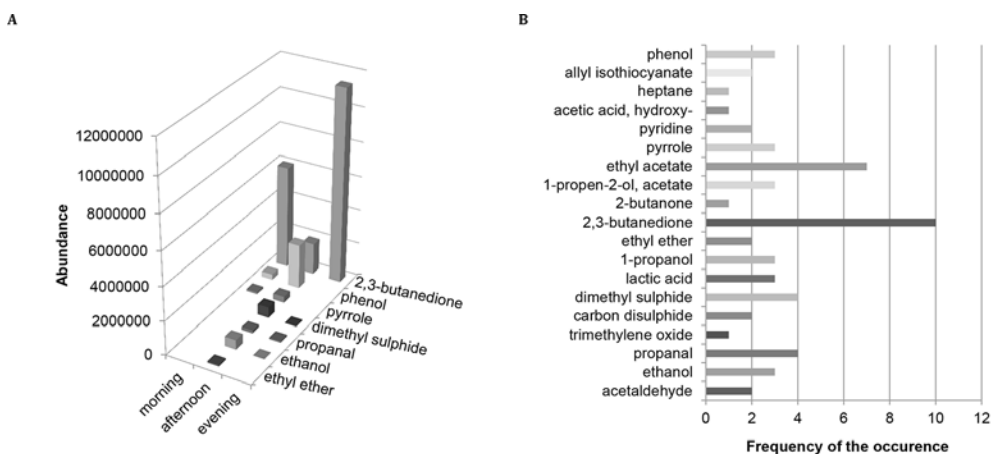
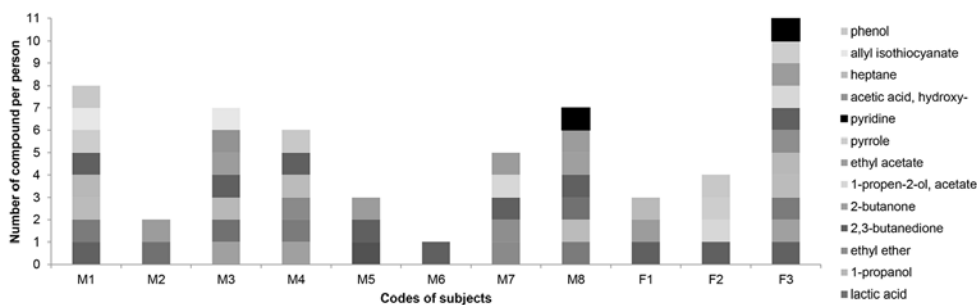


Fig. 4 (A) daily variations of volatile organic compounds from single subject. (B) frequency of occurrence of volatile organic compounds calculated for eleven healthy subjects.

allowed to perform ordinary daily routine. The great diversity of compounds were observed in the afternoon. However, the peaks of 2,3-butadienone were higher in the morning and evening. Possible origin of these fluctuations may be meals and interferences of environment.

Nineteen volatile organic compounds were identified in altogether samples from healthy non-smoking subjects. The classes of volatile organic compounds were: three alcohols and phenols, three volatile sulphur compounds, two aldehydes, two ketones, two esters, two acids, two volatile nitrogen compounds, one hydrocarbon, one ether, and an oxide (Fig. 4 (B)). 2,3-butadienone was the most frequently observed substance found in the samples. Ethyl acetate was detected in seven samples. Propanal and dimethyl sulphide were the third most seen compounds in volatile organic compound profiles. Fig. 5 demonstrates that in chromatograms obtained from active smokers (M8 and F3), one volatile from cigarette smoke was detected and it was pyridine.



**Fig. 5** Distribution of volatile organic compounds across the salivary profiles from eleven individuals, including two smokers (M8 and F3).

#### 4. Conclusions

Application of 75  $\mu\text{m}$  Carboxen/PDMS fibre allowed the extraction of the greatest number of compounds with the highest abundances, in contrast to the results from 100  $\mu\text{m}$  PDMS and 65  $\mu\text{m}$  PDMS/DVB fibres. Moreover, the proposed SPME-GC/MS method allows to obtain reproducible salivary volatile organic compound profiles that can be used for differentiation of individuals. Prolongation of time of incubation can influence the composition of salivary headspace by increasing of abundances of volatiles. Comparison of volatile organic compound profiles from eleven healthy subjects revealed significant differences in their salivary compositions as well as the diversity of distribution of certain volatiles. Pyridine was found in chromatograms of two participants in this study that were active smokers. The possible origin of this compound is tobacco smoke. Daily variations in salivary profiles were observed. The number of compounds and their different abundances can be associated with meals eaten before the collection of saliva.

#### References

- [1] de Lacy Costello B., Amann A., Al-Kateb H., Flynn C., Filipiak W., Khalid T., Osborne D, Ratcliffe N. M.: A review of the volatiles from the healthy human body. *J. Breath Res.* **8** (2014), 014001.
- [2] Pfaffe T., Cooper-White J., Beyerlein P., Kostner K., Punyadeera C.: Diagnostic potential of saliva: Current state and future applications. *Clin. Chem.* **57** (2011), 675–687.
- [3] del N. Sánchez M., García E. H., Pavón J. L., Cordero B. M.: Fast analytical methodology based on mass spectrometry for the determination of volatile biomarkers in saliva. *Anal. Chem.* **84** (2012), 379–385.
- [4] Francavilla R., Ercolini D., Piccolo M., Vannini L., Siragusa S., De Filippis F., De Pasquale I., Di Cagno R., Di Toma M., Gozzi G., Serrazanetti D. I., De Angelis M., Gobbetti M.: Salivary microbiota and metabolome associated with celiac disease. *Appl. Environ. Microbiol.* **80** (2014), 3416–3425.
- [5] Soini H. A., Klouckova I., Wiesler D., Oberzaucher E., Grammer K., Dixon S. J., Xu Y., Brereton R. G., Penn D. J., Novotny M. V.: Analysis of volatile organic compounds in human saliva by a static sorptive extraction method and gas chromatography-mass spectrometry. *J. Chem. Ecol.* **36** (2010), 1035–1042.

# Separation of linear and cyclic poly(dimethylsiloxanes) with interactive chromatography

BERNHARD DURNER<sup>a, b, \*</sup>, THOMAS EHMANN<sup>a</sup>, FRANK-MICHAEL MATYSIK<sup>b</sup>

<sup>a</sup> Wacker Chemie AG,

Johannes-Hess-Straße 24, 84489, Burghausen, Germany ✉ [bernhard.durner@wacker.com](mailto:bernhard.durner@wacker.com)

<sup>b</sup> Department of Chemistry and Pharmacy, University of Regensburg,

Universitätsstraße 31, 93040, Regensburg, Germany

## Keywords

interactive chromatography  
linear and cyclic poly(dimethylsiloxane)  
precipitation-re-dissolution mechanism  
polymer HPLC

## Abstract

Due to their attractive properties, siloxanes have found many applications in various industrial areas, e.g. cosmetics, health care or construction industries in recent years. Therefore, a method for separation of linear and cyclic poly(dimethylsiloxane), applying liquid chromatographic techniques was developed and optimized. By interactive chromatography, oligomer resolution and separation of linear from cyclic poly(dimethylsiloxane) could be achieved for poly(dimethylsiloxane) with up to 30 monomeric units. Results of investigations of the underlying separation mechanism pointed out that a combination of fractionated-re-dissolution and adsorption effects primarily depending on the adequate choice of the eluent system was essential.

## 1. Introduction

Siloxanes are used in a broad variety for different application areas. In general, siloxanes consist of alternating silicone-oxygen bonds in the backbone and different types of functional groups. An important class of siloxanes is poly(dimethylsiloxane) containing only methyl and methylene groups bounded to the polymer backbone. The basic notation of poly(dimethylsiloxane) depends on the nominal number of oxygen bonded to silicon: the basic building blocks M, D, T and Q present one, two, three or four oxygen(s) bonded to silicone, respectively. Therefore, the molecular architecture is clearly defined by the nomenclature, e.g. D4 stands for the cyclic tetramer [1–4].

The unique characteristics of siloxanes, like high flexibility in their backbone, low intermolecular forces between methyl groups or low surface energies make applications in cosmetics, medicine as well as in construction industries very attractive. Especially in case of poly(dimethylsiloxane), the usage in release agents, antifoams, heat transfer liquids or coatings demonstrate the importance of

this type of polymer [5, 6]. Concerning applications in pharmaceuticals or medical care products, comprehensive analytical methods are necessary. Therefore, investigations of low molecular weight oligomer, linear and cyclic poly(dimethylsiloxane) are mainly done with gas chromatography [7, 8]. Moreover, linear and cyclic poly(dimethylsiloxane) can also be separated with liquid chromatography at critical conditions, where the separation only depends on chemical functionalities [9]. A major drawback of liquid chromatography at critical conditions is the high susceptibility to small changes in analytical conditions, e.g. mobile phase composition, temperature changes or small variations of the investigated polymer sample [10]. Apart from liquid chromatography at critical conditions, interactive chromatography, focusing on differences in the chemical structure of macromolecules, is an appropriate alternative. Compared to conventional HPLC, peculiarities like small diffusion coefficients in solution, reduced solubility or a more complex retention mechanism on the stationary phase, occur. Thus, polymer elution is controlled by different types of interactions of various separation mechanisms, caused by adsorption, partition or solubility effects. Consequently, optimizing various parameters in method development, e.g. choice of mobile and stationary phase, LC flow rate, temperature, are necessary for explaining the main separation mechanism [11–13]. The present contribution is concerned with corresponding method developments.

## 2. Experimental

### 2.1 Reagents and chemicals

All solvents used were HPLC grade. Acetonitrile, acetone, methanol, ethanol, isopropanol, and non-stabilized tetrahydrofuran were purchased from Merck (Darmstadt, Germany) and used without further purification. Water of a Milli-Q-Advantage A10 water system (Merck Millipore) was used. All used analytical stationary phases applied in this study are summarized in Table 1. For fraction collection of single linear and cyclic oligomers a Thermo-Fisher (Waltham, USA) Accucore C30 (150×4.6 mm, 2.6 μm) was used. The used linear and cyclic poly(dimethylsiloxane) samples were obtained from Wacker Chemie AG (Burghausen, Germany). As reference material for linear poly(dimethylsiloxane) a silicone oil with a viscosity of 10 mPa s and for cyclic poly(dimethylsiloxane) a mixture of D8–D17 was used.

### 2.2 Instrumentation

The investigations were performed on a 1100 series LC system of Agilent (Waldbronn, Germany) with a tetrahydrofuran-resistant 3215α degasser from ERC (Riemerling, Germany) and a 385 ELSD of Agilent equipped with an enhanced parallel-path MiraMist® poly(tetrafluoroethylene) nebulizer from Burgener

**Table 1**

Overview of investigated stationary phases for the separation of poly(dimethylsiloxane); columns were purchased by Agilent (Waldbronn, Germany), Macherey-Nagel (Düren, Germany), MicroSolv Technology Corporation (Leland, USA), Thermo-Fisher (Waltham, USA), Phenomenex (Aschaffenburg, Germany), and YMC (Dinslaken, Germany).

Number	Manufacturer	Name	Particle type	Dimensions / mm
1	Thermo-Fisher	Accucore C18	2.6 $\mu\text{m}$ , 80 $\text{\AA}$	100×4.6
2	Thermo-Fisher	Accucore C8	2.6 $\mu\text{m}$ , 80 $\text{\AA}$	100×4.6
3	Thermo-Fisher	Accucore C30	2.6 $\mu\text{m}$ , 150 $\text{\AA}$	50×4.6
4	Phenomenex	Kinetex PFP	2.6 $\mu\text{m}$ , 100 $\text{\AA}$	100×4.6
5	YMC	Carotenoid C30	3 $\mu\text{m}$ , 80 $\text{\AA}$	100×4.6
6	Thermo-Fisher	Accucore C18 aQ	2.6 $\mu\text{m}$	100×4.6
7	Agilent	Eclipse C18	5 $\mu\text{m}$ , 80 $\text{\AA}$	150×4.6
8	Phenomenex	EVO C18	2.6 $\mu\text{m}$ , 100 $\text{\AA}$	100×4.6
9	MicroSolv Technology	Cogent Bidentate C18	4.2 $\mu\text{m}$ , 100 $\text{\AA}$	150×4.6
10	Macherey-Nagel	Nucleosil 100 C18	5 $\mu\text{m}$ , 100 $\text{\AA}$	125×4
11	Macherey-Nagel	Nucleodur Pyramid C18	5 $\mu\text{m}$ , 110 $\text{\AA}$	150×4.6
12	Thermo-Fisher	Hypersil BDS C18	2.4 $\mu\text{m}$ , 120 $\text{\AA}$	100×4.6
13	Phenomenex	HyperClone BDS C18	5 $\mu\text{m}$ , 130 $\text{\AA}$	150×4.6
14	Thermo-Fisher	HyPurity C18	5 $\mu\text{m}$ , 190 $\text{\AA}$	150×4.6
15	Macherey-Nagel	Nucleosil C18 EC	5 $\mu\text{m}$ , 50 $\text{\AA}$	100×4.6
16	Macherey-Nagel	Nucleosil C18 EC	5 $\mu\text{m}$ , 100 $\text{\AA}$	100×4.6
17	Macherey-Nagel	Nucleosil C18 EC	5 $\mu\text{m}$ , 300 $\text{\AA}$	150×4.6
18	Macherey-Nagel	Nucleosil C18 EC	7 $\mu\text{m}$ , 1000 $\text{\AA}$	150×4.6
19	Self-prepared	Silica beads	75 $\mu\text{m}$	50×7.0

Research (Mississauga, Ontario, Canada) at 40 °C evaporator temperature, 90 °C nebulizer temperature and 1.2 SLM (standard liter per minute) gas flow. All test measurements were done with a linear gradient from 100% A to 100% B in 40 min, unless otherwise stated. Changing column dimensions, the gradient parameters were adapted to obtain the same effective linear gradient. The final method development was done on an Accucore C30 (50×4.6 mm, 2.6  $\mu\text{m}$ ) at a LC flow rate of 2 mL·min<sup>-1</sup> starting at (methanol:water (75:25, v/v)): acetone 50:50 and ending at 100% acetone in 160 min. Applying silica beads the stepwise gradient was performed with 5% step height, 5 min step length with water and acetone as eluent system.

### 3. Results and discussion

#### 3.1 Optimization of stationary phase

According to common literature for poly(dimethylsiloxane) separation [9] with RP-Polymer-HPLC, acetonitrile as adsorption promoting solvent and tetrahydrofuran as desorption promoting solvent were chosen in preliminary experiments. Thus, a C8 stationary phase was selected separating linear and cyclic poly(dimethylsiloxane), Fig. 1. The separation performance of this system is limited by repea-

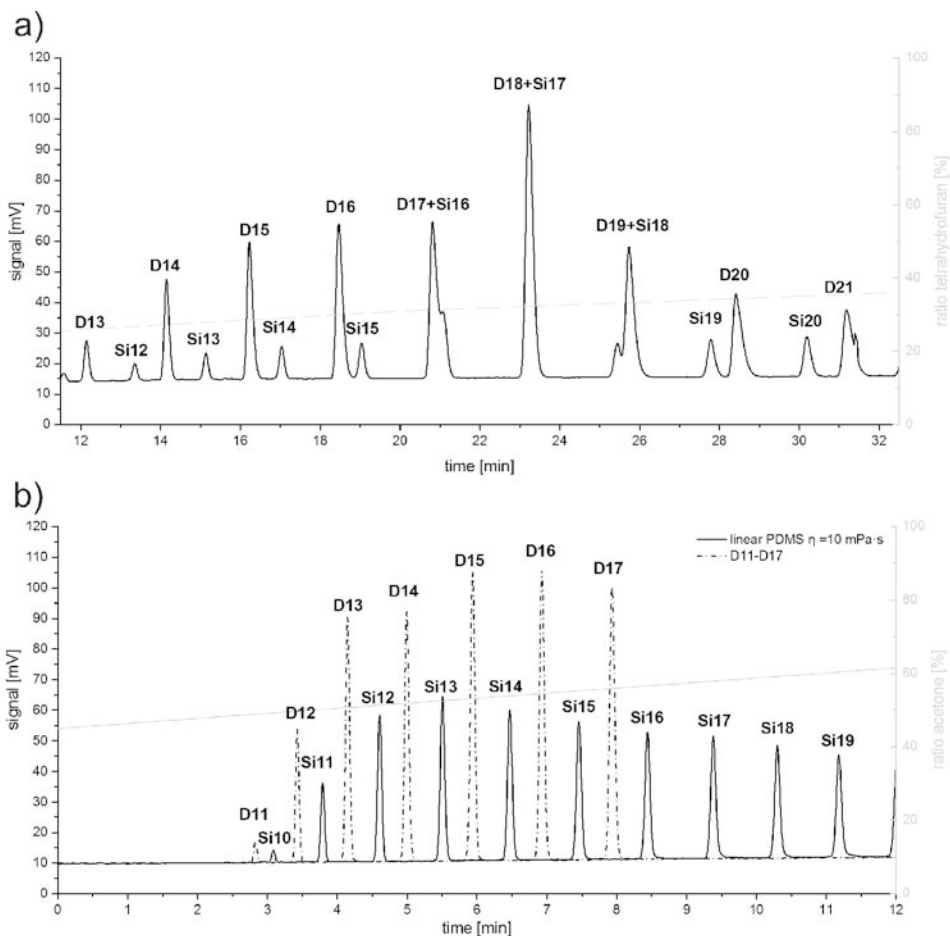


**Fig. 1** Separation of linear and cyclic poly(dimethylsiloxane) with (a) acetonitrile/tetrahydrofuran on an Accucore C8 column (100×4.6 mm, 2.6 μm) and with (b) methanol:water (75:25)/acetone on a Kinetex pentafluorophenyl column (100×4.6 mm, 2.6 μm); cyclic poly(dimethylsiloxane) is annotated as D plus monomeric number, and linear poly(dimethylsiloxane) is annotated as Si plus monomeric number.

ted peak overlap of linear and cyclic siloxanes. Following a classical HPLC approach, different stationary phases (Table 1) were tested for improving the separation performance. With a pentafluorophenyl (PFP) column an improvement of the separation could be achieved by replacing the adsorption promoting solvent from acetonitrile to an adequate mixture of methanol:water (75:25) – the triple bond of acetonitrile prevents the interaction of analyte and stationary phase. Finally, the determination could considerably be improved when using an Accucore C30 stationary phase in combination with the eluent system methanol: water/ acetone (Fig. 2).

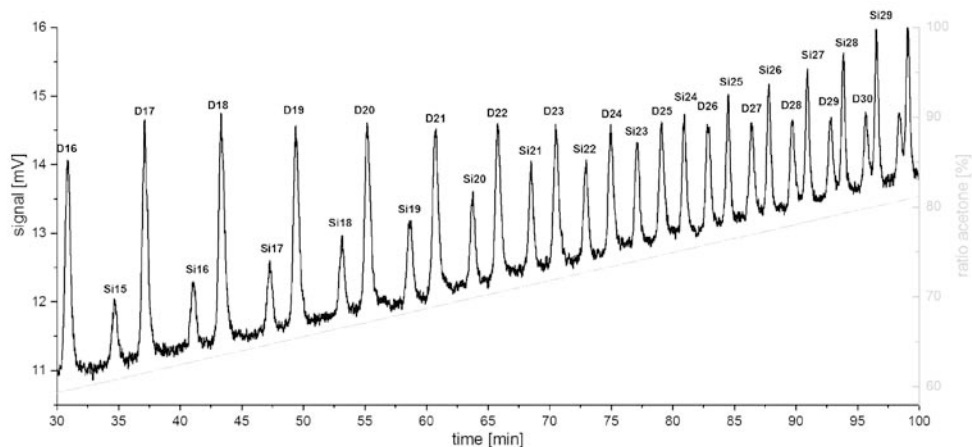


**Fig. 2** Optimized separation of poly(dimethylsiloxane) applying an Accucore C30 (50×4.6 mm, 2.6  $\mu\text{m}$ ) a LC flow rate of 2.0  $\text{mL min}^{-1}$ , methanol:water (75:25) as adsorption promoting solvent and acetone as desorption promoting solvent, the chromatogram in detail highlights the oligomeric separation of linear and cyclic oligomers up to 30 repetition units.

### 3.2 Optimization of mobile phase composition

Using acetonitrile, methanol or water as adsorption promoting solvent and acetone, ethanol, isopropanol or tetrahydrofuran as desorption promoting solvent and mixtures thereof, allowed the investigation of various solvent combinations while optimizing the stationary phase for separating poly(dimethylsiloxane). The choice of an appropriate mobile phase composition interfered with separation improvement in terms of polymer solubility in stationary and mobile phase. Consequently, the originally used eluent system for the pentafluorophenyl column considerably improved the analysis method on other more robust stationary phases, too, e.g. Accucore C30 (Fig. 2). This particular combination of stationary and mobile phases enabled an extended separation range, mainly caused by precipitation-re-dissolution and adsorption of the polymer at the column.

### 3.3 Explanation of separation mechanism

According to the aforementioned findings, a more detailed description of the predominant separation mechanism was possible. Particularly, when investigating low molecular weight poly(dimethylsiloxane) (up to 3000  $\text{g mol}^{-1}$ ) liquid adsorption chromatography is the prominent separation mode because separation efficiency was highly depending on the applied stationary phase. Apart from this, the significance of well-defined mobile phase composition suggested that an adsorption mechanism is superimposed by a mechanism of precipitation

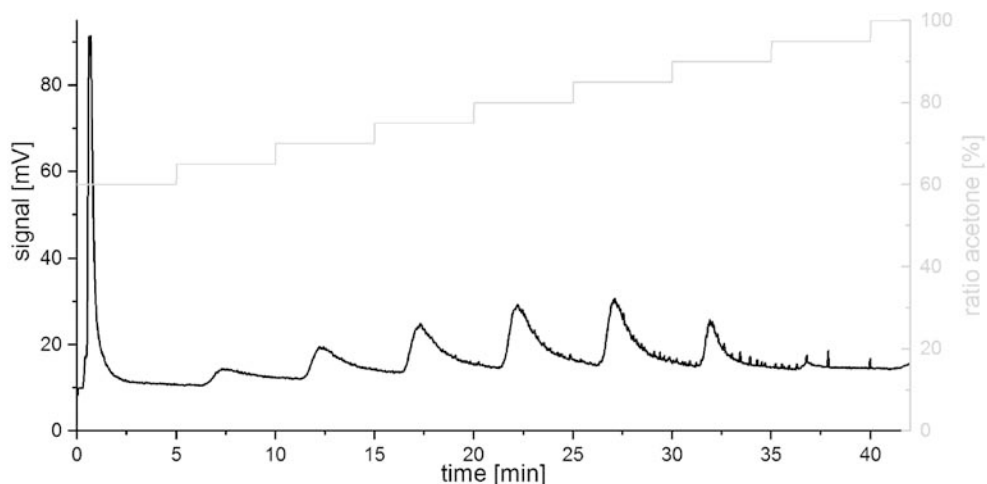


**Fig. 3** Separation of a silicone oil with a viscosity of 10 mPa s, containing only linear poly(dimethylsiloxane) oligomers, when applying a stepwise gradient (step length 5 min and step height 5%) using water and acetone as mobile phase on a silica beads (75  $\mu\text{m}$ ) column excluding HPLC adsorption effects of the stationary phase.

and re-dissolving. Further measurements were performed with a silica beads column (Fig. 3), which showed no useful HPLC separation due to absence of stationary phase modifications. Applying a stepwise gradient, the poly(dimethylsiloxane) (viscosity of 10 mPa s) polymeric distribution was measured primarily to fraction re-dissolution mechanism. Fractionated re-dissolving elution overlaying HPLC adsorption effects indicated the significance of mobile phase composition. With ideal settings, resolving various molecular weight oligomers become possible.

#### 4. Conclusion

An interactive chromatography method was developed for separating linear and cyclic poly(dimethylsiloxane) up to 30 repetition units (D30). Therefore, the mobile phase composition and selection of stationary phases were optimized. Applying preparative HPLC, pure single oligomeric standards of linear and cyclic poly(dimethylsiloxane) can be obtained for improving quantitative analyses in interactive chromatography as well as in gas chromatography. Based on the combination of precipitation-re-dissolution and adsorption mechanisms various other types of polymers might be analyzed with interactive chromatography.

#### Acknowledgments

The authors thank the group of Process Chemistry Polymer and Fluids of the Business Unit Basics and Intermediates at Wacker Chemie AG Burghausen for support with silicone oils.

## References

- [1] Fendinger N.J., Lehmann R.G.: Polydimethylsiloxanes. In: *Organosilicon Materials*. G. Chandra (ed.). Berlin, Springer 1997.
- [2] Liu, Y.: Silicone dispersions. In: *Surfactant Science Series*, Vol. 159. London, CRC Press 2017.
- [3] Noll W.: *Chemie und Technologie der Silicone*. 2nd ed. Weinheim, Chemie 1968.
- [4] Koerner G., Schulze, M., Weis J.: *Silicone. Chemie und Technologie. Symposium am 28. April 1989*. Essen, Vulkan-Verlag 1989.
- [5] Lambrecht J., Brünnig M.: Advantages of silicones and future challenges in the world of T&D. In: *Silicone Elastomers*. Berlin, Smithers Rapra Technology 2012.
- [6] *Silicone Elastomers* Shawbury, Smithers Rapra Technology 2013.
- [7] Bletsou A.A., Asimakopoulos A.G., Stasinakis A.S., Thomaidis N.S., Kannan K.: Mass loading and fate of linear and cyclic siloxanes in a wastewater treatment plant in Greece. *Environ. Sci. Technol.* **47** (2013), 1824–1832.
- [8] Brothers H.M., Boehmer T., Campbell R.A., Dorn S., Kerbleski J.J., Lewis S., Mund C., Pero D., Saito K., Wieser M., Zoller W.: Determination of cyclic volatile methylsiloxanes in personal care products by gas chromatography. *Int. J. Cosmetic Sci.* **39** (2017), 580–588.
- [9] Macko T., Hunkeler D.: Liquid chromatography under critical and limiting conditions: A survey of experimental systems for synthetic polymers. In: *Liquid Chromatography / FTIR Microspectroscopy / Microwave Assisted Synthesis*. A. Abe, A.C. Albertsson (eds.). Berlin, Springer 2003.
- [10] Berek D.: Critical assessment of “critical” liquid chromatography of block copolymers. *J. Sep. Sci.* **39** (2016), 93–101.
- [11] Glöckner G.: *Gradient HPLC of Copolymers and Chromatographic Cross-Fractionation*. Berlin, Springer 1991.
- [12] Pasch H., Trathnigg B.: *HPLC of Polymers. Springer Laboratory*. Berlin, Springer 1998.
- [13] Berek D.: Polymer HPLC. In: *Handbook of HPLC*. D. Corradini (edit.), 2nd ed., Boca Raton, Taylor & Francis 2010, p. 447–504.

# Simple Calibration Approach to Elimination of the Additive Interference Effect

MAREK DĘBOSZ\*, MARCIN WIECZOREK, PAWEŁ KOŚCIELNIAK

*Department of Analytical Chemistry, Faculty of Chemistry, Jagiellonian University in Krakow, Gronostajowa 2, 30-387, Krakow, Poland ✉ [marek.debosz@doctoral.uj.edu.pl](mailto:marek.debosz@doctoral.uj.edu.pl)*

## Keywords

analytical calibration  
flow analysis  
iron  
interference effects  
spectrophotometry

## Abstract

The determination of analytes usually requires the calibration procedure to be carried out. To do this the calibration curve method is commonly met in laboratory practice. However, its use is faced with serious problems. For instance, the final result might be affected by serious systematic error in the case when the interference effects are present. In this work it is shown how the calibration curve method can be modified in order to eliminate the additive interference effect. The concept is based on the measurements of both the standard solutions and the samples at two various wavelengths selected so to keep the signals measured for an interferent constant. As the result, the analyte in a sample is determined with the use of two calibration curves more accurately than in the conventional way. In contrast to the alternative H-point standard addition method the proposed approach allows the calibration curves to be used for analysis of a series of samples. The method was verified on the example of the spectrophotometric determination of Fe(II) in the presence of Fe(III) as the interferent.

---

## 1. Introduction

Over the last few decades various calibration methods were proposed with the aim of obtaining the result that is accurate, meaning that it reflects the true amount of the analyte in the sample. Unfortunately, most of those methods is not used in laboratory practice and the calibration curve method is still the most popular one. However, when this method is employed, the final result is affected by a serious systematic error since the composition of the sample's matrix is not taken into considerations. Moreover the interference effects might cause the calibration relationship to be changed. The standard addition method is also well-known calibration approach and might be used for elimination of the interference effect when the change of the analytical signal is proportional to the analyte concentration (it is caused because all calibration solutions contain the analyte in the environment of all sample components). The standard addition method, however, doesn't allow elimination of the additive interference effect, which cause a constant change of a measured signal regardless of the analyte concentration. The other drawback is that the calibration curve has to be constructed for each

analysed sample separately making the calibration procedure laborious and time-consuming [1–2].

The one of the calibration method which is not popular in laboratory practice, but compensates both the multiplicative and additive interference effect is H-point standard addition method [3]. This approach is based on the analytical measurements carried out according to the standard addition method at two different wavelengths. The conditions has to be selected to measure the analytical signal with different sensitivities but to keep the signals produced by the interferents constant. Under such conditions calibration graphs are crossed at the H-point indicating both the additive effect and the analyte concentration. However, as for the case of the standard addition method, the requirement of preparing several working solutions for each sample needs to be met.

To overcome this issue a new approach is presented in this work. Namely, it is proposed to prepare two calibration curves according to the calibration curve method at two wavelengths (selected as above) and to measure the signals for the sample in the same conditions separately from the standard solutions. When both calibration graphs are linear ( $R_i = A_i + B_i c_x$ ,  $i = 1, 2$ ) and the additive effect is constant at both wavelengths ( $A_1 = A_2 = A$ ), the concentration  $c_x$  of an analyte in a sample and the value  $A$  of the additive interference effect are calculated from the equations:

$$c_x = (R_1 - R_2)/(B_1 - B_2) \quad (1)$$

$$A = (R_2 B_1 - R_1 B_2)/(B_1 - B_2) \quad (2)$$

where  $R_i$  and  $B_i$  ( $i = 1, 2$ ) are the signals for the sample and the slopes of the calibration graphs, respectively.

The suitability of this approach was verified on the example of the spectrophotometric determination of Fe(II) in the presence of Fe(III), which played the role of the interferent (as in [4]).

## 2. Experimental

### 2.1 Reagents and samples

The reagents, all of which were analytical grade chemicals, were used to prepare the appropriate solutions: phenantroline monohydrate (Lachner, Czech Republic), salicylic acid (Fabryka Odczynników Chemicznych, Gliwice, Poland), iron (III) nitrate nonahydrate (Sigma Aldrich, Germany), ammonium iron(II) sulphate hexahydrate (Chempur, Poland), 37% fuming hydrochloric acid (Merck, Germany) and potassium hydrogen phthalate (Fabryka Odczynników Chemicznych, Gliwice, Poland).

Stock iron solutions containing  $1000 \text{ mg L}^{-1}$  Fe(II) and Fe(III) were prepared by water dissolving of an adequate amount of  $\text{Fe}(\text{NH}_4)_2(\text{SO}_4)_2 \cdot 6\text{H}_2\text{O}$  and  $\text{Fe}(\text{NO}_3)_3 \cdot 9\text{H}_2\text{O}$ , respectively. Stock solution of mixture of 1,10-phenantroline

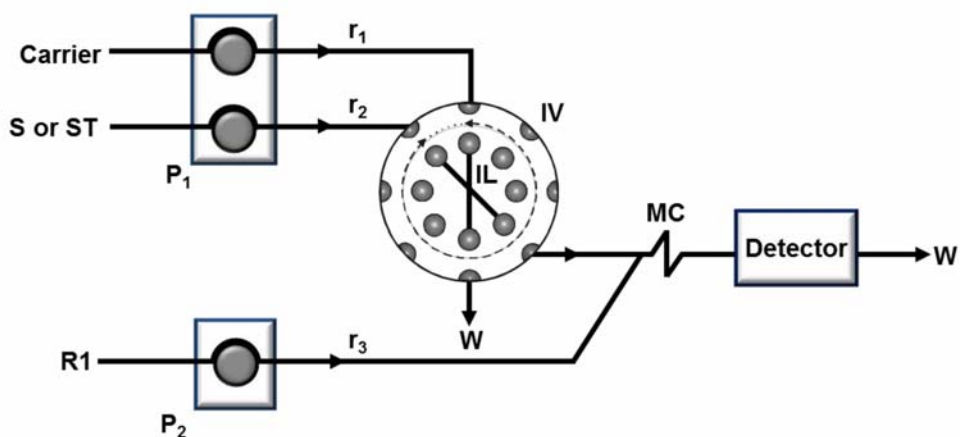


**Fig. 1** Scheme of the constructed flow-injection manifold: (S) sample, (ST) standard solution, (P1) and (P2) peristaltic pumps, (IV) injection valve (MC) mixing coil, (W) waste, ( $r_1$ ,  $r_2$ ,  $r_3$ ) flow rates.

monohydrate and salicylic acid was prepared by dissolving 0.843 g and 0.575 g of these reagents, respectively, in 10,0 mL of ethanol and adjusting the volume to 100 mL with distilled water. The use of ethanol was utilized to increase the solubility of salicylic acid. Buffer solution (pH = 3.0) was prepared by mixing appropriate volume of 0.2 mol dm<sup>-3</sup> solutions of potassium hydrogen phthalate and hydrochloric acid [5]. All stock solutions were prepared fresh daily. The solutions were prepared in distilled water. The distilled water from an HLP 5 system (Hydrolab, Poland) was used throughout the work.

## 2.2 Instrumentation

The instrumental flow-injection manifold dedicated to the proposed calibration method is presented in Fig. 1. It consisted of an eight-port injection valve equipped with a homemade, electric switching system, two peristaltic pumps (Minipuls 3, Gilson, France) and 16-channel controller UVCTR-16 (KSP Electronics Laboratory, Poland). Lambda 25 spectrometer (Perkin Elmer, USA) equipped with a glass flow cell with path length equal 10 mm, was utilized as the detector. The work of pumps and injection valve was controlled by Valve and Pump Controller Software (KSP Electronics Laboratory, Poland).

## 2.3. Procedure

Samples or standard solutions were prepared by adding 1 mL of buffer solution and 7 mL of samples or appropriate volume of stock solutions of Fe(II) and Fe(III) to 10 mL volumetric flask and made up to mark with deionized water. The concentration of Fe(II) in the calibration solutions was in the range of 0–5 mg L<sup>-1</sup> (with 1 mg L<sup>-1</sup> step). The sample or standard solution was injected into a stream of water,

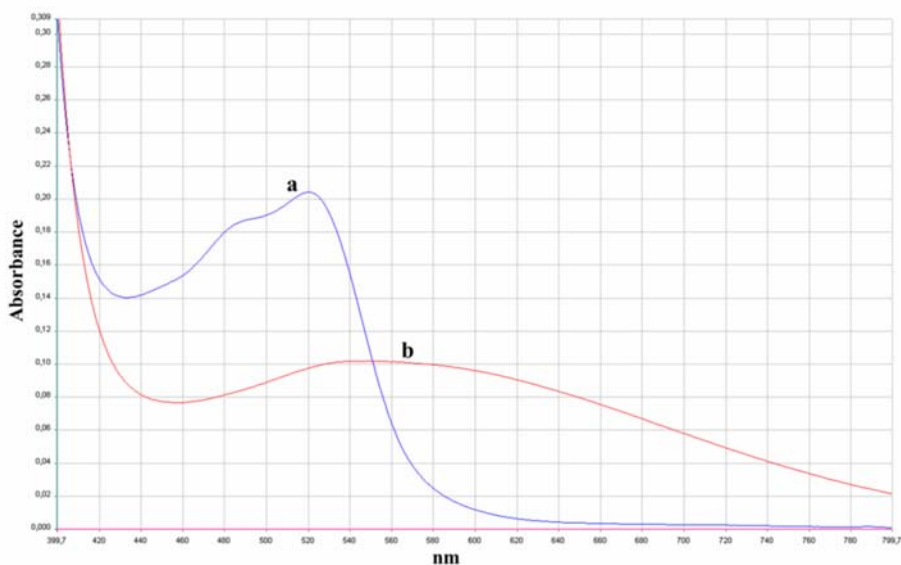


**Fig. 2** Absorption spectra of (a)  $5 \text{ mg L}^{-1}$  Fe(II), and (b)  $10 \text{ mg L}^{-1}$  Fe(III) with the mixed reagents at pH = 3.

which was connected with a stream of mixture of phenantroline and salicylic acid, resulting in formation of an orange or purple derivative complex of Fe(II) and Fe(III), respectively. The formed product was directed towards the detector where absorbance was recorded at two selected set wavelengths. Height of recorded characteristic peaks was treated as an analytical signal. Each determination was repeated three times in the same instrumental conditions.

### 3. Results and discussion

Working parameters of the flow-injection manifold, such as: flow rate, reaction loop length and the volume of injected sample, were optimized. The following parameters were chosen: flow rates  $2.0 \text{ mL min}^{-1}$ , the length of the reaction coil 100 cm and the volume of injected sample  $200 \mu\text{L}$ . The linearity range of the proposed method is  $0\text{--}25 \text{ mg L}^{-1}$  for both analytes.

Based on the spectra of 1,10-phenantroline and salicylic acid complexes with Fe(II) and Fe(III) (Fig. 2) three pairs of wavelength were chosen in accordance with principle of the method: 530 and 573 nm, 542 and 549 nm, 542 and 551 nm.

Table 1 presents the results of analysis of several synthetic samples with different concentrations of Fe(II) (analyte) and Fe(III) (interferent). The results obtained by the proposed method are compared with these obtained conventionally, i.e. using the calibration curve method. The results obtained with the calibration curve method in terms of the relative error are unacceptable. This is due to the presence of Fe(III) that acts as an interferent. The calibration curve method evidently cannot deal with the interference effect. However, the use of the

**Table 1**

Results obtained by the calibration curve method (CCM) and the proposed method (PM) in three synthetic samples (*A* is additive effect in absorbance).

Sample	$\lambda$ / nm	Concentration / mg L <sup>-1</sup>			Relative error / %		<i>A</i>
		Expected	CCM		CCM	PM	
			Fe(II) / Fe(III)	Fe(II)			
I	530/573	1.00 / 5.00	6.20	1.10	520.0	10.0	0.0498
	542/549		3.19	1.13	219.0	13.0	0.0498
	542/551		3.62	1.01	262.0	1.0	0.0529
II	530/573	5.00 / 10.00	13.92	4.88	178.4	-2.4	0.0935
	542/549		8.79	4.89	75.8	-2.2	0.0947
	542/551		9.02	4.86	80.4	-2.6	0.0953
III	530/573	5.00 / 20.00	22.36	4.58	347.2	-8.4	0.1861
	542/549		12.30	4.66	146.0	-6.8	0.1910
	542/551		12.71	4.71	154.2	-5.8	0.1895

proposed method is able to take into account such effect and, as it can be seen in Table 1, the results are quite satisfactory. The exception are the results obtained for Fe(II) in sample I at two pairs of wavelengths. It can be caused by the fact that selected concentration of Fe(II) is nearby the limit of detection and the influence of interferent is especially strong in this case. In addition, the values of the additive effect caused by Fe(III) were calculated. The validity of these parameters is evident when compared with the increasing value of interferent's concentration – the higher the concentration the higher the additive effect.

#### 4. Conclusions

The presented study shows that the presented calibration method is an effective and helpful analytical tool. It offers determination of an analyte with improved accuracy due to elimination of the additive interference effect. Furthermore, it allows the value of this effect to be estimated. As the method is faster and simpler in comparison with H-point standard addition method, it can be recommended to be used in routine analytical practice.

#### References

- [1] Kościelniak P., Wieczorek M., Kozak J.: Calibration problems in trace analysis. In: *Handbook of Trace Analysis. Fundamentals and Applications*. I. Baranowska (Ed.). Springer 2016.
- [2] Kościelniak P., Wieczorek M.: Univariate analytical calibration methods and procedures: A review. *Analytica Chimica Acta* **944** (2016), 14–28.
- [3] Bosch R.F., Campins F.P.: H-point standard addition method: Part 1 fundamentals and application to analytical spectroscopy. *Analyst* **113** (1988), 1011–1016.
- [4] Safavi A., Abdollahi H.: Application of the H-point standard addition method to the speciation of the Fe(II) and Fe(III) with chromogenic mixed reagents. *Talanta* **54** (2001), 727–734.
- [5] [http://www.ochemonline.com/Buffer\\_solutions](http://www.ochemonline.com/Buffer_solutions) (accessed 5th May 2018)

# Separation of chromium(III) and chromium(VI) by reversed-phase ion-pairing chromatography

CUC THI NGUYEN-MARCINCYK<sup>a,\*</sup>, JAKUB KARASINSKI<sup>a</sup>, MARCIN WOJCIECHOWSKI<sup>a</sup>,  
AGNIESZKA ANNA KRATA<sup>a</sup>, LUDWIK HALICZ<sup>b</sup>, EWA BULSKA<sup>a</sup>

<sup>a</sup> *Biological and Chemical Research Center, Faculty of Chemistry, University of Warsaw, Żwirki I Wigury 101, 02-089, Warsaw, Poland* ✉ [cuc.marcinczyk@chem.uw.edu.pl](mailto:cuc.marcinczyk@chem.uw.edu.pl)

<sup>b</sup> *Geological Survey of Israel, 30 Malkhei Israel Street, Jerusalem 95501, Israel*

## Keywords

chelation  
chromium  
RPIP HPLC  
reduction

## Abstract

The separation of Cr(III) and Cr(VI) by reversed-phase ion pairing liquid chromatography for a specific purpose has been investigated. Chromium(III) was chelated with EDTA at pH = 6.0 prior to analysis. The mobile phase (pH = 6.0) consisted of a 0.32 mmol L<sup>-1</sup> EDTA and 0.83 mmol L<sup>-1</sup> tetrabutylammonium hydroxide. The method showed that Cr(III) and Cr(VI) were effectively separated at low mobile phase flow rate which is suitable for a future experiment design of isotopic ratio measurements. The most difficult task was not only to ensure the effective separation but also to avoid any possible inter-conversion between two chromium forms. For a better detection of chromium species, the chromatographic system was coupled with a typical quadrupole inductively coupled plasma mass spectrometry.

## 1. Introduction

Chromium with different oxidation states exhibits widely different behaviours in terms of potential toxic effects on environmental and biological system. Chromium(VI) is toxic and known as carcinogenic while Cr(III) is a trace essential element for the proper functioning of living organism [1, 2]. Because chromium is used widely in industrial activities such as electrical plating, Cr(VI) is easily released into the environment, especially in surface water and groundwater and could pose a health risk. Therefore, extraction and chemical treatment of contaminated groundwater in order to remove Cr(VI) become an important issue. Chromium (VI) can be reduced into immobile Cr(III) form which is much less toxic. It was reported that Cr(VI) reduction is often associated an isotopic fractionation and is the dominant process causing the change of <sup>53</sup>Cr/<sup>52</sup>Cr ratio [3, 4]. As a result of which, Cr stable isotopic ratios can be served as indicators to quantify the extent of Cr(VI) reduction in environmental remediation efforts.

According to our best knowledge, there has not been any published article yet which studies the isotopic ratio of each chromium form Cr(III) and Cr(VI) existing simultaneously in an analytical sample. Therefore, the aim of this work is to develop a method to separate two forms of chromium: Cr(III) and Cr(VI) by using reversed-phase ion pairing liquid chromatography. The separation method should be capable for coupling with a multicollector inductively coupled plasma mass spectrometry (MC ICP-MS) in a future experiment design which allows chromium isotopic ratio measurement.

## 2. Experimental

### 2.1 Reagents and chemicals

Reagents were analytical grade chemicals and were used without any further purification. Standards and other solutions including a mobile phase were prepared with deionized water (18,2 M $\Omega$  cm) obtained by Milli-Q System (Merck Millipore, Germany). Standard solutions of 10 mg L<sup>-1</sup> Cr(III) and Cr(VI) were prepared by diluting the standard stock solution of Cr(NO<sub>3</sub>)<sub>3</sub> and K<sub>2</sub>CrO<sub>4</sub> at 1000 mg L<sup>-1</sup> (Merk, Germany). The mobile phase was obtained by dissolution of an appropriate amount of ethylenediaminetetraacetic acid disodium dehydrate (EDTA, EDM Millipore, Germany) in deionized water and by an addition of tetrabutylammonium hydroxide (40% in water, Sigma-Aldrich, USA). For adjusting pH sodium hydroxide (NaOH 50%, Fisher Scientific, USA) and acid nitric (HNO<sub>3</sub> 65% Suprapur<sup>®</sup>, Merck, Germany) were used.

### 2.2 Instrumentation

An Agilent 1200 Infinity series high-performance liquid chromatography (Agilent Technologies, USA) equipped with a peltier-cooled autosampler tray, quaternary pump, a peltier-heated column oven, and an UV/ VIS detector with variable wavelength was used. A reversed-phase Agilent Zorbax C8 (2.1×150 mm, 1.8  $\mu$ m) was utilized as the separation column, its temperature was set at 35 °C. Mobile phase in isocratic mode consisted of 0.32 mmol L<sup>-1</sup> EDTA and 0.83 mmol L<sup>-1</sup> tetrabutylammonium hydroxide; its pH was maintained to 6.0. The separation was carried out within total analysis time of 16 min with the flow rate of mobile phase 0.25 ml min<sup>-1</sup> and sample injection volume 20  $\mu$ L. The ICP-MS detector was a model of Elan 6100 DRC (Perkin-ElmerSCIEX, Canada). The operational conditions for ICP-MS were: RF power 1200 W, nebulizer gas (argon) flow 0.92 L min<sup>-1</sup>, lens voltage 15 V. Monitored ion was <sup>52</sup>Cr<sup>+</sup>.

### 2.3 Procedure

Working standards with different concentrations containing Cr(III) and/or Cr(VI) were prepared by mixing an appropriate volume of standards solutions of Cr(III)

and Cr(VI) with EDTA 0.05 or 0.1 mol L<sup>-1</sup> at pH = 6.0 (adjusted by NaOH) in glass vials (volume ratio of 1/1). The obtained volume then was brought up to 500 μL by adding the mobile phase. The solutions were kept at an ambient temperature for 1 hour prior to analysis or were incubated at 40 °C/60 °C in a water bath for 15–60 minutes to allow formation of Cr(III)-EDTA.

For the optimization of chromatographic conditions, several factors which affect the separation such as the concentration of EDTA and tetrabutylammonium hydroxide in the mobile phase as well as the pH (adjusted by HNO<sub>3</sub>) were investigated to get the best separation.

### 3. Results and discussion

In this work, reversed-phase ion-pairing chromatography was used for the separation of Cr(III) and CrO<sub>4</sub><sup>2-</sup>. Firstly, EDTA was used to chelate and stabilize Cr(III) in the form of [Cr-EDTA]<sup>-</sup>, which is also an anionic ion as CrO<sub>4</sub><sup>2-</sup>. These anionic ions interacted with tetrabutylammonium as the cation ion-pairing reagent, which in turn interacted with reversed phase C8 column.

It was reported that the inter-conversion between chromium species occurs at acidic pH, and Cr(VI) is much more stable in neutral and basic pH [5]. The Cr(III)-EDTA chelation is pH dependent. A high pH favours the complexation, however, Cr(III) can be precipitated in a form of chromium hydroxide [6]. Therefore in this work, the chelation of Cr(III) with EDTA prior to analysis was carried out at pH=6.0 which allows to keep Cr(VI) stable and avoid Cr(III) precipitation. To examine the effect of temperature on the chelation efficiency, the complexation was performed at ambient room temperature and at 60 °C. The results showed that, after several hours Cr(III)-EDTA was not formed at room temperature while an intensive violet colour was obtained when the solution was heated at 60 °C for 30 min, which indicated the formation of Cr(III)-EDTA. Therefore, unlike other works [7, 8] heating was required because of Cr(III)-EDTA complexation reaction kinetic.

The mobile phase flow rate of 0.25 ml min<sup>-1</sup> was used due to the planning utilization of a desolvating nebulizer system designed for the MC ICP-MS. This value is almost maximum for the sample flow rate at which the nebulizer can still operate. The future experiment design for isotopic ratio measurements by coupling HPLC with MC ICP-MS will not be discussed in this work. However, to be capable for being coupled with MS ICP-MS, the separation by using reversed-phase ion pairing liquid chromatography should fulfil some criteria such as: good resolution and acceptable long retention times. The best separation was obtained with mobile phase (pH = 6.0) containing 0.32 mmol L<sup>-1</sup> EDTA and 0.83 mmol L<sup>-1</sup> tetrabutylammonium hydroxide. A typical obtained chromatogram is shown in Fig. 1.

The most difficult task in this work was to avoid inter-conversion between two chromium forms during the experiment. As aforementioned the Cr(VI) reduction

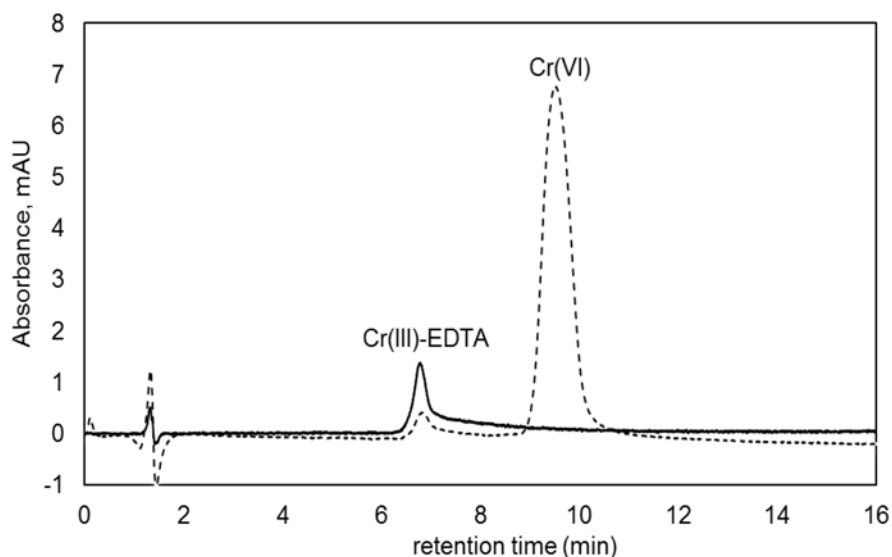


**Fig. 1** Typical chromatogram obtained for the separation of Cr(III)-EDTA and Cr(VI). Concentration of chromium was  $500 \mu\text{g L}^{-1}$ . Mobile phase (pH = 6.0) contained  $0.32 \text{ mmol L}^{-1}$  EDTA and  $0.83 \text{ mmol L}^{-1}$  tetrabutylammonium hydroxide. Detector UV/VIS, detection wavelength 540 nm (continuous line) and 370 nm (dotted line).

is often associated with an isotopic fractionation, hence the inter-conversion between two forms is not beneficial for the further isotopic ratio analysis. The oxidation of Cr(III) to Cr(VI) did not occur at the optimal chromatographic conditions. Unfortunately, Cr(III)-EDTA peak was observed in the chromatogram of the Cr(VI) standard solutions. This could be caused by the reduction of Cr(VI). Other investigations were carried out in order to confirm whether the reduction of Cr(VI) to Cr(III) occurred before or during the experiments. The effect of EDTA concentration, temperature and time in the chelation step was examined (see procedure). It was observed that after heating the Cr(VI) working standard solutions containing equal chromium concentrations with EDTA  $0.05 \text{ mol L}^{-1}$  or  $0.1 \text{ mol L}^{-1}$  at  $40 \text{ }^\circ\text{C}$  or  $60 \text{ }^\circ\text{C}$  for 15–60 min, in all cases the same peak areas for Cr(VI) were obtained. Interestingly, Cr(III)-EDTA peak was also observed when experiment was performed without any pre-treatment (Fig. 2), and the same peak area was also obtained for Cr(VI). These results implied that the EDTA concentration, temperature and time were not the reasons for the observation of Cr(III) in Cr(VI) standard solutions. The effect of the pH of mobile phase was also tested. The results showed that the more acidic the mobile phase was, the bigger Cr(III)-EDTA peak area was obtained. However, for pH bigger than 5.5 (6.0, 6.5 and 7.0) Cr(III)-EDTA peak areas were the same. Calibration curves (Fig. 3) show a very good regression coefficient ( $R^2 > 0.99$ ) for both Cr(VI) and Cr(III). One possibility explaining this phenomena could be that Cr(III) already exists in the

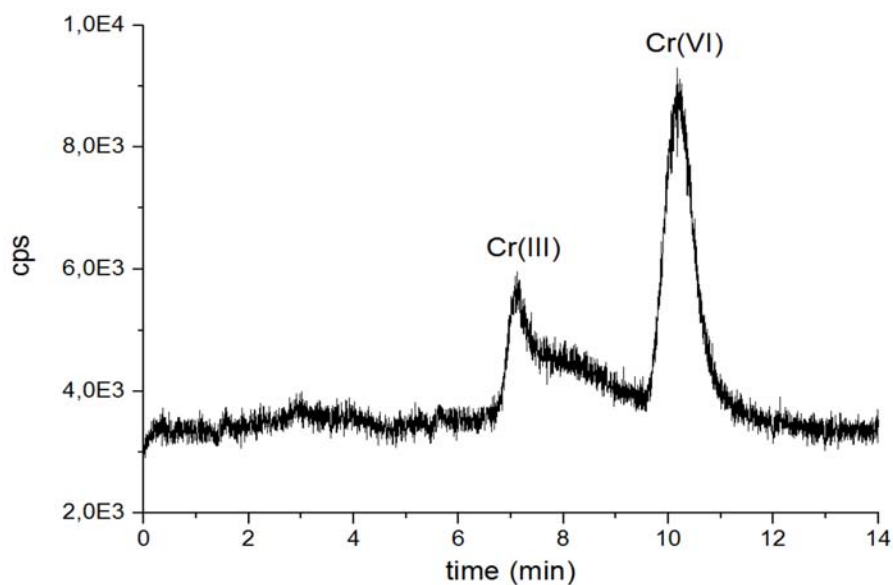


**Fig. 2** Chromatogram of  $^{52}\text{Cr(VI)}$  standard solution obtained when no sample pre-treatment was carried out. Concentration of Cr(VI) was  $100\ \mu\text{g L}^{-1}$ . Mobile phase (pH = 6.0) contained  $0.32\ \text{mmol L}^{-1}$  EDTA and  $0.83\ \text{mmol L}^{-1}$  tetrabutylammonium hydroxide. Detector ICP-MS.

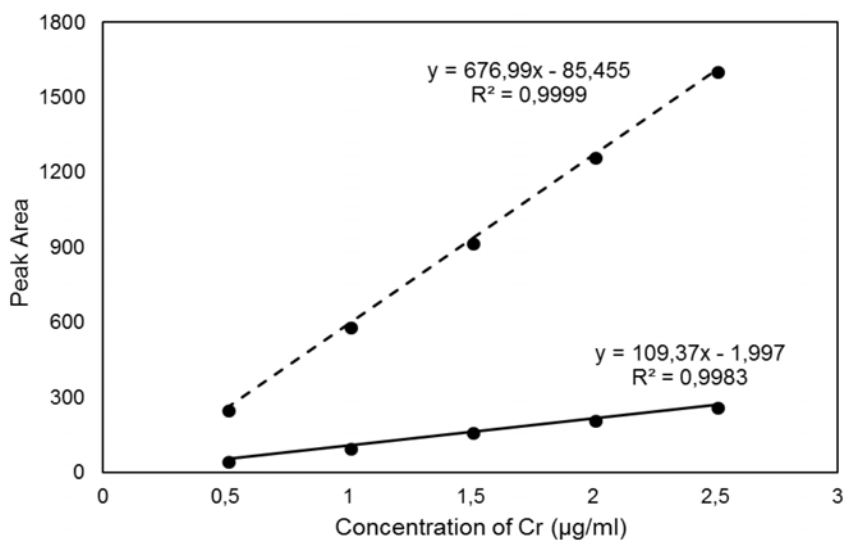


**Fig. 3** Calibration curves of chromium standard solutions obtained by using the optimized HPLC procedure: Cr(VI) = dotted line, Cr(III)-EDTA = continuous line.

initial standard stock solution of chromate ( $1000 \text{ mg L}^{-1}$ ) due to the reduction (about 25%). The reduction might occur during transportation and/or storage.

#### 4. Conclusions

In this work, reversed-phase ion pairing liquid chromatography was shown to be a good technique with easy sample preparation for effective separation of two different chromium forms Cr(III) and Cr(VI). The mobile phase ( $\text{pH} = 6.0$ ) containing  $0.32 \text{ mmol L}^{-1}$  EDTA and  $0.83 \text{ mmol L}^{-1}$  tetrabutylammonium hydroxide and the used low flow rate  $0.25 \text{ ml min}^{-1}$  ensured the good separation resolution and acceptable long retention times, which are required for the future experiment design of isotopic ratio measurements. However, 25% of Cr(VI) was found to be reduced into Cr(III) even when there was no pre-treatment prior to analysis carried out. The experiments showed that the reduction of Cr(VI) might occur in the initial standard stock solution due to an inappropriate transportation or storage. However, further work needs to be done in order to find the exact problem causing this transformation.

#### Acknowledgments

This research is financial supported by the Nation Center of Science (NCN, Poland), project 501-D312-66-0004878. A special thank to Julio Torres for your technical support.

#### References

- [1] Gomez V., Callao MP.: Chromium determination and speciation since 2000. *Trends Anal. Chem.* **25** (2006), 1006–1015.
- [2] Kotaś J., Stasicka Z.: Chromium occurrence in the environment and methods of its speciation. *Environ. Pollut.* **107** (2000), 263–283.
- [3] Ellis Andre S., Johnson Thomas M., Bullen Thomas D.: Using chromium stable isotope ratios to quantify Cr (VI) reduction: lack of sorption effects. *Environ. Sci. Technol.* **38** (2004), 3604–3607.
- [4] Cole D.B., Wang X., Qin L., Planavsky N.J., Reinhard C.T.: Chromium isotopes. In: *Encyclopedia of Geochemistry*. Springer 2018.
- [5] Sun J., Ma L., Yang Z., Wang L.: Optimization of species stability and interconversion during the complexing reaction for chromium speciation by high-performance liquid chromatography with inductively coupled plasma mass spectrometry. *J. Sep. Sci.* **37** (2014), 1944–1950.
- [6] Jen J.F., Ou-Yang G.L., Chen C.S., Yang S.M.: Simultaneous determination of chromium(III) and chromium(VI) with reversed-phase ion-pair high-performance liquid chromatography. *Analyst* **118** (1993), 1281–1284.
- [7] Barańkiewicz D., Pikoś B., Belter M., Marcinkowska M.: Speciation analysis of chromium in drinking water samples by ion-pair reversed-phase HPLC–ICP–MS: validation of the analytical method and evaluation of the uncertainty budget. *Accredit. Qual. Assur.* **18** (2013), 391–401.
- [8] Wolf R.E., Morrison J.M., Goldhaber M.B.: Simultaneous determination of Cr(III) and Cr(VI) using reversed-phased ion-pairing liquid chromatography with dynamic reaction cell inductively coupled plasma mass spectrometry. *J. Anal. At. Spectrom.* **22** (2007), 1051–1060.

# Label-free proteomic approach to identification and quantification of proteins in animal tissue samples

ANDRZEJ GAWOR<sup>a,\*</sup>, ANNA KONOPKA<sup>a</sup>, JULIO CESAR TORRES ELGUERA<sup>a</sup>,  
ANNA RUSZCZYNSKA<sup>a</sup>, MARIAN CZAUDERNA<sup>b</sup>, EWA BULSKA<sup>a</sup>

<sup>a</sup> *Biological and Chemical Research Centre, Faculty of Chemistry, University of Warsaw, Zwirki i Wigury 101, 02-093 Warsaw, Poland ✉ agawor@chem.uw.edu.pl*

<sup>b</sup> *The Kielanowski Institute of Animal Physiology and Nutrition, Polish Academy of Sciences, Instytucka 3, 05-110 Jabłonna, Poland*

## Keywords

label-free proteomics  
mass spectrometry  
selenoproteins

## Abstract

Mass spectrometry-based proteomics is recognised as a useful procedure for large-scale identification and quantification of proteins in natural samples. Here, we present the label-free proteomic approach for liver tissue samples obtained from lambs fed with the diet enriched with inorganic compounds of Se(VI) and organic selenium compounds (selenomethionine in selenium yeast). The study aimed to examine how the presence of inorganic and organic forms of selenium in the lambs' forage affects the expression of the proteins, in particular, those containing selenium. In the course of the study, protein tissue homogenates were in-solution digested by trypsin. Peptide analysis was performed using high-resolution electrospray mass spectrometer equipped with Orbitrap mass analyser coupled to ultra-high performance liquid chromatography (nano-UHPLC-ESI-(ORBITRAP)-MS/MS). Based on registered data, using the appropriate proteomic software (Mascot, MaxQuant) with access to the SwissProt protein database, qualitative and quantitative analysis of proteins was achieved.

---

## 1. Introduction

Selenium is an essential element for the proper function of human and animal organisms. Selenium is a component of many proteins, thus contributing to biochemical processes. For many years, research has continued on the role of selenium in both physiological and pathological processes of living organisms [1, 2]. It is suggested that the beneficial effects of selenium on living organisms is mainly caused by the activity of a low molecular compound Se-methyl-Selenocysteine and selenoproteins (containing selenium in the form of selenocysteine), enzymes that protect the body from oxidative stress by reducing free radicals [3]. Dietary supplementation with selenium compounds may lead to an increase in the

concentration of these enzymes and affects the expression of the proteins. Identifying a specific protein in tissues, then comparing its concentrations between physiological and pathological states of tissues can support the detection of those associated with the specific disease and contribute to the development of new drugs and therapies.

The study aimed to examine how the presence of inorganic and organic forms of selenium in the lambs' forage affects the expression of the proteins, in particular, those containing selenium. Here, we present the complete label-free proteomics methodology for identification and quantification of the proteins using nano-UHPLC-ESI-(ORBITRAP)-MS/MS and the appropriate proteomic software (Mascot, MaxQuant) with access to the SwissProt protein database [4].

## 2. Experimental

### 2.1 Examined objects

The subject of the study was lamb liver from animals on an experimental diet supplemented with selenium. Breeding of animals and tissue collection was carried out by the Regulation of the Council of the European Union (EC) No. 130 1099/2009 of 24 September 2009 on the protection of animals at the time of their killing [5]. Thirty Corriedale male lambs of similar age after a 3-week standard diet were divided into control and two diet groups enriched in selenium compounds (0.35 mg of Se(VI)/1 kg standard diet and 0.35 mg of selenomethionine/1 kg standard diet). After 35 days of experimental dietary enrichment and decapitation of animals, the liver tissue were collected. The samples of tissues were freeze-dried (below  $-40\text{ }^{\circ}\text{C}$ ) and stored at  $4\text{ }^{\circ}\text{C}$  before conducting proper sample preparation.

### 2.2 Reagents and chemicals

Analytical reagent grade chemicals were purchased from Sigma Aldrich (Germany), Baker (USA), Promega (USA) and Bio-Rad (USA). Solutions including a mobile phase for UHPLC-ESI-MS/MS were prepared with LC MS grade water (Baker, USA).

### 2.2 Instrumentation

The separation of supernatants from liver tissue residue was achieved using the centrifuge 5804/5804R (Eppendorf, USA). The vacuum centrifuge (Eppendorf, USA) was used for concentration of the extracts solution. The measurements were carried out using the nano-UHPLC system equipped with Accucore<sup>®</sup> column ( $75\text{ }\mu\text{m} \times 500\text{ mm}$ ; C-18;  $2.6\text{ }\mu\text{m}$ ) purchased from Thermo Scientific coupled to the ESI-MS/MS mass spectrometer (Orbitrap Fusion Tribrid<sup>™</sup> Mass Spectrometer, Dionex Ultimate Series UHPLC, Thermo Scientific, USA).

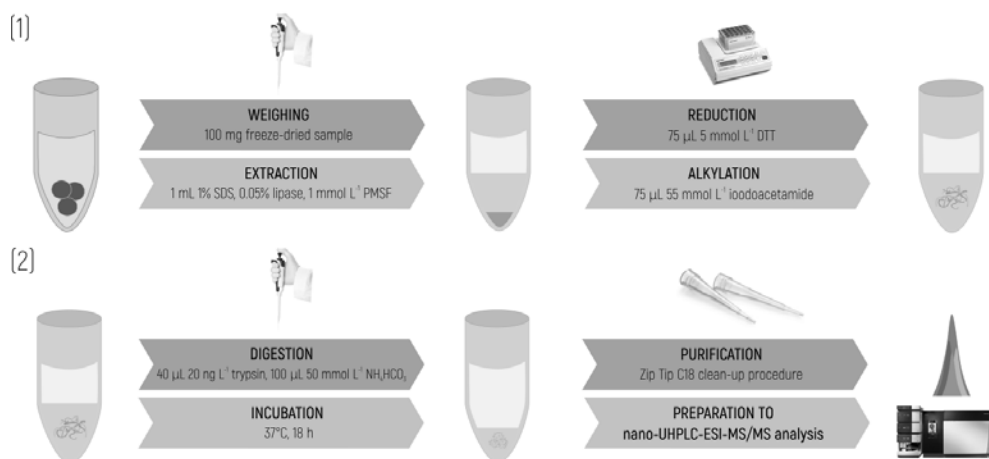


**Fig. 1** Scheme of the analytical procedure.

### 2.3 Procedure

Around 100 mg of tissues were extracted with 1 mL of lysis buffer (1% SDS, 0.05% lipase, 1 mmol L<sup>-1</sup> phenylmethylsulfonyl) in room temperature over 6 hours supported by mixing and ultrasonic baths. The supernatant was separated from the residue by centrifugation for 30 min at 20 000× g. Total protein concentration was determined using the Bradford method [6]. All extracts were kept at -80 °C before the proteins digestion. The 5 μL of protein extracts were reduced with 75 μL of 5 mmol L<sup>-1</sup> 1,4-dithiothreitol for 45 min at 56 °C, then alkylated with 75 μL of 55 mmol L<sup>-1</sup> iodoacetamide for 30 min in the dark. The samples were subjected to enzymatic digestion for 18 hours at 37 °C with 75 μL of 20 ng L<sup>-1</sup> trypsin and 100 μL of 50 mmol L<sup>-1</sup> ammonium bicarbonate. The reaction was quenched with the addition of 150 μL 5% formic acid. The solutions containing the eluted peptides were purified by the Zip Tip C18 clean-up procedure (EMD Millipore, Germany) and concentrated in a vacuum centrifuge at 20 °C and resuspended in 0.1% formic acid. The samples were injected (1 μL) into UHPLC system in a reverse phase at a flow rate of 300 nL min<sup>-1</sup> using gradient elution consisted of 0.1% formic acid in water (solvent A) and 0.1% formic acid in acetonitrile (solvent B) for 360 min. Scheme of the procedure is presented in Fig. 1.

## 3. Results and discussion

Figure 2A shows an example of Total Ion Current (TIC) chromatogram from the group supplemented in selenium organic compounds. Registered MS/MS spectra of peptides were analysed to identify selenium-containing proteins using Mascot software (Matrix Science, USA). Mascot is a powerful search engine which uses mass spectrometry data to identify proteins from primary sequence databases. The program searches all possible peptides from the theoretical digestion of

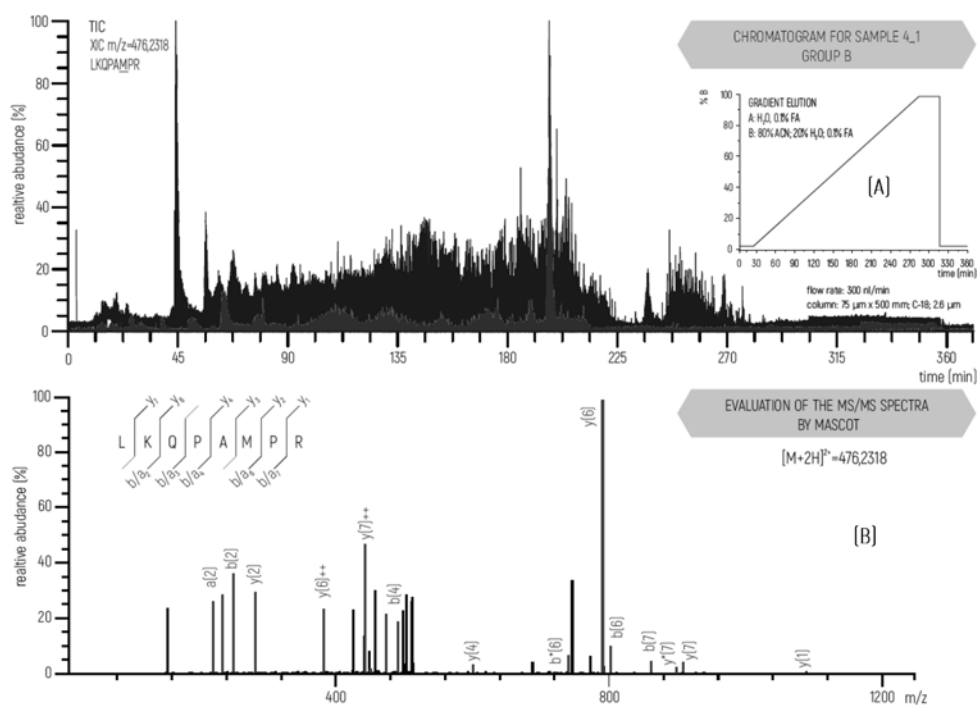


**Fig. 2** (A) TIC chromatogram for peptide extracts from lambs supplemented in organic form of selenium. (B) Evaluation of MS/MS spectra by Mascot for peptide LKQPAMPR.

available protein sequences in the database and then, indicates those, which mass and fragmentation spectra correspond to the result of experimental MS analysis. Search parameters used during research were followed: SwissProt database, mammalian taxonomy, fixed modification: cysteine carbamidomethylation, variable modifications: Se-cysteine, Se-methionine and oxidation of Se-cysteine, Se-methionine and carbamidomethylation of Se-cysteine. About 30 proteins containing selenium in the form of selenomethionine or selenocysteine with various modifications were found in the studied liver lambs' samples (score parameter above 23). In order to confirm the protein identification proposed by the Mascot, the registered isotopic pattern for the identified selenium-containing peptide was compared manually to the theoretical one. Manual verification of experimental isotopic pattern allowed the confirmation of the presence of selenium in only one of them: dipeptidyl peptidase. Figure 2B shows the evaluation of the MS/MS spectrum for the peptide LKQPAMPR with Se-methionine modification from dipeptidyl peptidase protein. The differences in experimental and theoretical isotopic patterns observed for others may be related to a very low concentration of those selenium-containing proteins in the examined liver samples, which have been already reported by others [7, 8].

Quantitative analysis was performed manually by comparing the intensities of a given unique peptide, which correlates with a given protein, on the TIC

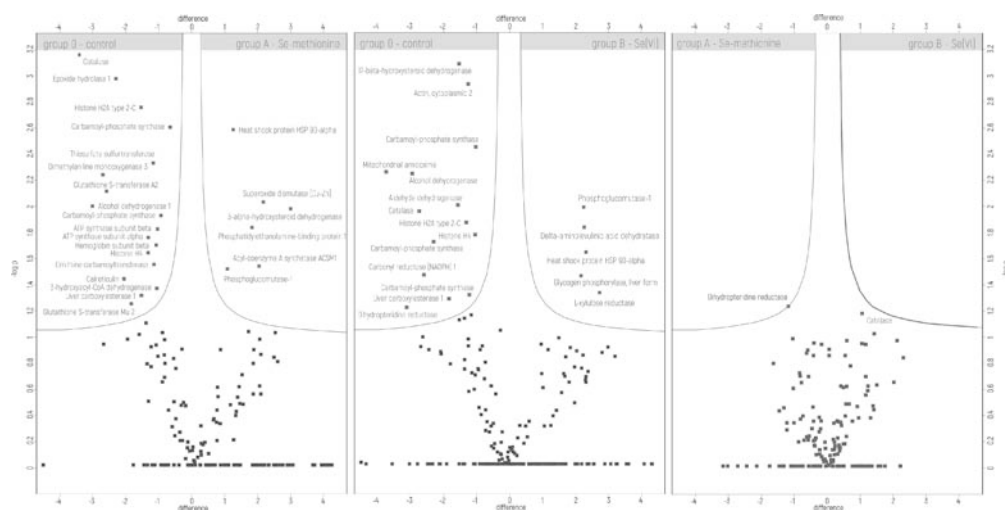


**Fig. 3** Volcano plot chart showing differing in the proteins expression between the control group and groups with selenium supplementation.

chromatograms using MaxQuant. For determining the variations between the proteome expressed in various conditions, it is necessary not only to identify the proteins present but also to perform statistical tests to determine if the observed expression changes are statistically significant (Principle Component Analysis, PCA). Perseus was used for statistical analysis and visualisation of the received data. Fig. 3 shows the quantitative analysis revealed that the selenium supplementation of lambs' diet, both in organic and inorganic forms, changes the expression of some proteins (comparisons of groups A and B vs group 0). In contrast, no expression change was observed when two groups with selenium supplementation were compared to each other (comparison of group A vs group B). It can be concluded that whereas selenium presence itself in the diet has some influence on the protein expression in the liver cells of lambs, the selenium form (organic or inorganic) is not so crucial.

#### 4. Conclusions

The applied analytical procedure allows automatic identification of thousands of proteins. Nearly 30 proteins containing selenium in the form of selenomethionine or selenocysteine with various modifications were found in the studied liver lambs' samples (score parameter above 23). Manual verification of experimental isotopic pattern allowed the confirmation of the presence of selenium in only one of them. Quantitative analysis revealed that the selenium supplementation of lambs' diet, both in organic and inorganic forms, changes the expression of some proteins, but no expression change was observed when two groups with selenium supplementation were compared to each other. Further studies of protein expression in other tissues of lambs (muscles, brain, serum, etc.) are in progress.

## Acknowledgments

The study was carried out at the Biological and Chemical Research Centre, University of Warsaw established within the project co-financed by European Union from the European Regional Development Fund under the Operational Programme Innovative Economy 2007–2013.

## References

- [1] Navarro A., López-Martinez M.C.: Essentiality of selenium in the human body: relationship with different diseases. *Sci. Total Environ.* **249** (2000), 347–371.
- [2] Wierzbicka A., Bulska E., Pyrżyńska K., Wysocka I., Zachara B.A.: *Selen. Pierwiastek ważny dla zdrowia, fascynujący dla badacza*. Warszawa, Wydawnictwo Malamut 2007. (In Polish.)
- [3] Rusczyńska A., Konopka A., Kurek E., Torres Elguera J C., Bulska E.: Investigation of biotransformation of selenium in plants using spectrometric methods. *Spectrochim. Acta B* **130** (2017), 7–16.
- [4] Cox J., Mann M.: MaxQuant enables high peptide identification rates, individualized p.p.b.-range mass accuracies and proteome-wide protein quantification. *Nat. Biotechnol.* **26** (2008), 1367–1372.
- [5] Rusczyńska A., Bulska E., Czauderna M., Krajewska-Bienias L.: Dietary selenium, carnolic acid and fish oil affect the concentrations of selected elements, fatty acids, tocopherols, cholesterol and oxidative stress in the liver and selected muscles of lambs. *Ital. J. Anim. Sci.* **21** (2017), 285–301.
- [6] Bradford M.: Rapid and sensitive method for the quantitation of microgram quantities of protein utilizing the principle of protein-dye binding. *Anal. Biochem.* **72** (1976), 248–254.
- [7] Guillaume B., Lisa E., Eric L., Clay W.: Detection and characterization of selenoproteins by tandem mass spectrometry assisted by laser ablation inductively coupled plasma mass spectrometry: application to human plasma selenoproteins. *J. Anal. At. Spectrom.* **26** (2011), 383–394.
- [8] Gammelgaard B.: Complementary use of molecular and element-specific mass spectrometry for identification of selenium compounds related to human selenium metabolism. *Anal. Bioanal. Chem.* **390** (2008), 1691–1706.

# Distance-based measurements using microfluidic paper-based analytical devices modified with Prussian blue

MATEUSZ GRANICA\*

*Faculty of Chemistry, University of Warsaw,  
Pasteur 1 St., 02-093, Warsaw, Poland* ✉ [mgranica@chem.uw.edu.pl](mailto:mgranica@chem.uw.edu.pl)

## Keywords

distance-based detection  
microfluidic paper  
analytical devices  
Prussian blue

## Abstract

In the course of this research the distance-based microfluidic paper analytical devices ( $\mu$ PADs) were investigated. Prussian blue was used as a sensing substrate, deposited in the working zone of the system. As a result of the capillary action, the sample introduced on the dry paper surface was transported along the channel, and the analyte was reacting with Prussian blue. As effect the discolorization of the sensing zone, proportional to the analyte concentration was observed. using created  $\mu$ PADs the calibration curves for ascorbic acid was recorded within the experiment and optimization of the dye deposition was provided.

---

## 1. Introduction

Modern analytic trends are focused on the miniaturization, cost-effectiveness, and portability of the created systems or methodologies [1]. The ability to perform qualitative and quantitative analysis in source limited conditions or in the field is one of the significant factors that caused the growth of the idea of quick paper-made tests. Microfluidic paper-based analytical devices ( $\mu$ PADs), were introduced as fully utilize platforms capable of performing complete analytical procedures, providing results comparable to these one obtained using standard laboratory equipment. Minimal, user-friendly operation and versatility stay in excellent agreement to the challenges they forced, and for this reason, paper based-system are intensively investigated.

With years, simple tests evolve to more complicated planar or even three-dimensional systems, where sample could proceed with many individual operations providing the opportunity for simultaneous testing or analyte multistep derivatization within one  $\mu$ PAD [2]. Development of this devices was connected with the possibility to cover the paper matrix with hydrophobic substances. The paper patterning allows for remote sample splitting or mixing within one microfluidic system without user intervention. Wax-printing technique is one of the

most used for  $\mu$ PAD preparation [3] due to computer designing, simple preparation with solid ink printers and good reproducibility.

The most problematic in a matter of  $\mu$ PAD usefulness is the signal detection step. Colorimetric schemes show the greatest popularity because of the fast signal readout and a plurality of available colorimetric procedures dedicated to the determination of common analytes. However, the biggest concern is still focused on color intensity evaluation because this kind of measurements requires reliable photosensitive devices. The unaided eye color intensity detection, which is the unquestionably most convenient to perform in the source-limited localization is disrupted with user individual attributes and impressions [4] and is not recommended in quantitative analysis. To solve this problem the different idea for colorimetric signal quantification with the naked eye was proposed by Zuk et al. [5]. This idea applied in flow paper-based system utilize the effect of the analyte consumption during sample flow through the system. When the flow channel is covered with the reagent in advance, the analyte from the sample is reacting with the reagent in the restricted zone. If the reaction product is colored, a color band proportional to the analyte concentration present in the sample is generated. The quantification of the signal is accomplished by simply measuring the length/size of the colored zone. Extremely facile readout of the signal with the absence of the electronic equipment is described with proper reproducibility and accuracy [6]. This kind of detection has been already used in the aspect of environmental pollution analysis [7] and point of care testing [8] where its application potential in real scenarios was confirmed.

## 2. Experimental

### 2.1 Reagents and chemicals

All used solutions were prepared using deionized water (Mili-Q Purification System) and analytical grade reagents. The Prussian blue deposition was carried from the 1-M hydrochloric acid solutions of the iron(III) chloride and potassium hexacyanoferrate(III) (Sigma-Aldrich). The concentrations of the applied solutions were experimentally adjusted. The stock  $0.1 \text{ mol dm}^{-3}$  standard of ascorbic acid was prepared daily from the pure reagents of the Ascorbic Acid (PoCH, Poland) to limit the storage time and avoid breakdown of the analyte. Working standards of the ascorbic acid in  $2\text{--}10 \text{ mmol dm}^{-3}$  was prepared with an appropriate dilution of the stock standard with water.

### 2.2 Instrumentation and research methodology

Paper-based systems were prepared using Whatman Qualitative paper Grade No. 1 as a support. Using solid ink printer (Xerox 8580DN) the patterns, which design is presented on the Fig. 1, were printed and then heated in standard

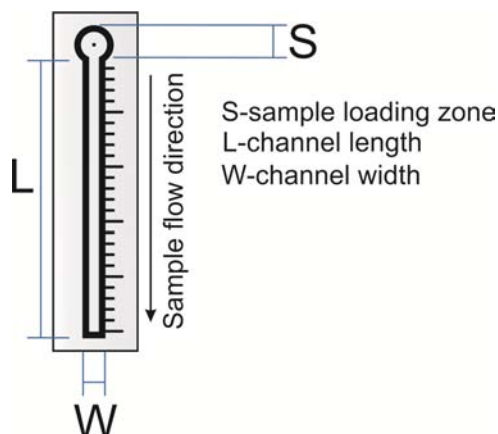


**Fig. 1** The system design used during the experiments. The Prussian blue was deposited along the channel described with  $S = 5$  mm diameter,  $W = 3$  mm, and  $L = 50$  mm.

laboratory drier for 2 min in 120 °C. The heat treatment ensure the paper penetration with wax, causing that obtained barriers were fully impermeable for aqueous solutions. In the next step, patterns were covered with Prussian blue. The solutions used for Prussian blue deposition were mixed together equally just before the introduction into the paper surface. The 25  $\mu$ L of the mixture was spread along the channel using the pipette, and soaked systems were left for the deposition for 24 h. After that time, systems were washed with deionized water and dried in the open air. The sample was placed in the  $S$  part of the system using the pipette. For signal readout, the colored band length was measured using conventional ruler.

### 3. Results and discussion

The first part of the work was devoted to examining the influence of the Prussian blue amount deposited on the sensitivity and resolution of the created systems. Because the distance-based detection uses the analyte consumption effect, as a primary reason why the signals for different standard concentration are observed, the amount of the dye deposited in the channel has significant importance. The decolorization occurs only in the zone where the sensing dye was able to react with the reductant (in this contribution as a model reductant an ascorbic acid was chosen). The amount of the Prussian blue deposited into the paper can be easily controlled by the concentration of the iron(III) chloride and potassium hexacyanoferrate(III) solutions used for its fabrication. Higher concentrations provide enhanced Prussian blue deposition, what is manifested with lower sensitivity but the wider linearity of the calibration curves, as presented in Fig. 2.

As can be noticed from the Fig. 2, when the channel is modified with a high amount of Prussian blue, the signals (measured distance) obtained for low concentrations of analyte are low, due to the high rate of the ascorbic acid oxidation at the beginning of the channel. For diluted standards, a small amount (a mixture of the 10 mM standards) of the dye is preferable, because it provides high sensitivity

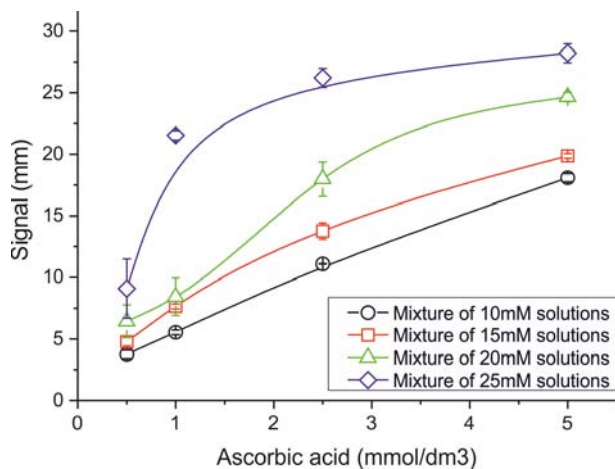


**Fig. 2** The different sensitivity of the systems obtained using different concentrations of  $\text{FeCl}_3$  and  $\text{K}_3[\text{Fe}(\text{CN})_6]$  applied for Prussian Blue deposition.

and high measurement resolution. From the other hand, for highly concentrated samples, a significant amount of the dye (a mixture of 25 mM solutions) deposited on the systems provide constant decolorization during the sample flow, thus expanded calibration curves linearity can be observed, but also lower sensitivity is noticeable. Based on the results the mixture of the  $2.5 \times 10^{-4} \text{ mol dm}^{-3}$  of  $\text{Fe}^{3+}$  and  $[\text{Fe}(\text{CN})_6]^{3-}$  solutions was chosen as optimal for distance-based paper analytical systems preparation. All further investigations will be conducted with the Prussian blue deposited in this description.

The systems prepared using optimized conditions were used to record calibration curve for ascorbic acid. The obtained calibration curve is presented in Fig. 3. The calibration shows good linearity in all respected range of ascorbic acid applied. The system also is characterized by high reproducibility and facile signal readout. The error bars represent the standard deviation for three-time repeated measurements for the same standard solution.

#### 4. Conclusions

In the course of these preliminary investigations, the fully working distance-based microfluidic sensoric system was developed. The system allows ascorbic acid determination in the millimolar range of concentrations with good reproducibility and accuracy. Moreover, due to its chemical properties, Prussian blue can be used as hydrogen peroxide sensor. After the reduction into Prussian white form it is sensitive to any oxidizing agent present in the sample. Using this property, presented platform will be in the future reduced with ascorbic acid and then modified with enzymes to provide high-selectively devices dedicated to the specified analyte recognition. The oxidases generate the hydrogen peroxide

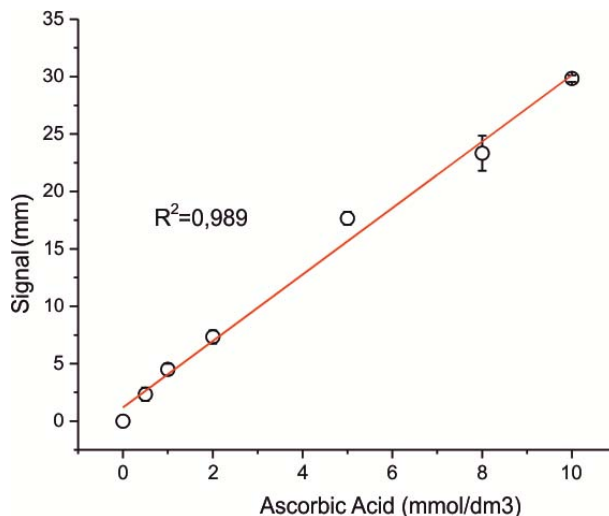


**Fig. 3** Calibration graph for ascorbic acid obtained under optimized conditions.

during its catalytic activity and show great potential to be involved in distance-based sensors development.

Distance-based detection shows excellent application possibility in the aspect of the paper-based microfluidic systems due to its simplicity and device-free readout. However, this kind of detection still requires an evaluation of the factors influencing the signal generation, e.g., the geometry and deposited reagent concentration.

### Acknowledgments

Helpful comments to this paper from Dr Łukasz Tymecki (University of Warsaw) are kindly acknowledged. The author thanks the support from the University of Warsaw (DSM 501-D112-86-DSM-115 100 project). These investigations were supported by the Polish National Science Centre (project OPUS NCN no. 2014/13/B/ST4/04528).

### References

- [1] Akyazi T., Basabe-Desmouts L., Benito-Lopez F.: *Review on microfluidic paper-based analytical devices towards commercialisation*. *Anal. Chim. Acta* **1001** (2017), 1–17.
- [2] Yetisen A.K., Akram M.S., Lowe C.R.: Paper-based microfluidic point-of-care diagnostic devices. *Lab. Chip.* **13** (2013), 2210–2251.
- [3] Carrilho E., Martinez A.W., Whitesides G.M.: Wax printing – a simple micropatterning process for paper-based microfluidics. *Anal. Chem.* **81** (2009), 1–5.
- [4] Morbioli G.G., Mazzu-Nascimento T., Stockton A.M., Carrilho E.: Technical aspects and challenges of colorimetric detection with microfluidic paper-based analytical devices ( $\mu$ PADs): A review. *Anal. Chim. Acta* **970** (2017), 1–22.
- [5] Zuk R.F., Ginsberg V.K., Houts T., Rabbie J., Merrick H., Ullman E.F., Fischer M.M., Sizto C.C., Stiso S.N., Litman D.J.: Enzyme immunochromatography: A quantitative immunoassay requiring no instrumentation. *Clin. Chem.* **31** (1985), 1144–1150.
- [6] Cate D.M., Dungchai W., Cunningham J.C., Volckens J., Henry C.S.: Simple, distance-based measurement for paper analytical devices. *Lab. Chip.* **13** (2013), 2397–2404.

- [7] Quinn C.W., Cate D.M., Miller-Lionberg D.D., Reilly T., Volckens J., Henry C.S.: Solid-phase extraction coupled to a paper-based technique for trace copper detection in drinking water. *Environ. Sci. Technol.* **52** (2018), 3567–3573.
- [8] Wei X., Tian Tian T., Jia S., Zhu Z., Ma Y., Sun J., Lin Z., Yang C.J.: Microfluidic distance readout sweet hydrogel integrated paper-based analytical device ( $\mu$ DiSH-PAD) for visual quantitative point-of-care testing. *Anal. Chem.* **88** (2016), 2345–2352.

# Cyclic voltammetry and staircase voltammetry in citalopram determination

MARIA MADEJ<sup>a,\*</sup>, JOLANTA KOCHANA<sup>a</sup>, BOGUSŁAW BAŚ<sup>b</sup>

<sup>a</sup> Department of Analytical Chemistry, Faculty of Chemistry, Jagiellonian University in Kraków, Gronostajowa 2, 30-387, Kraków, Poland ✉ [marysia.madej@doctoral.uj.edu.pl](mailto:marysia.madej@doctoral.uj.edu.pl)

<sup>b</sup> Department of Analytical Chemistry, Faculty of Materials and Ceramics, AGH University of Science and Technology Adama Mickiewicza 30, 30-059, Kraków, Poland

## Keywords

citalopram  
cyclic voltammetry  
electrochemistry  
staircase voltammetry

## Abstract

This work deals with electrochemical detection of citalopram, commonly used antidepressant. The comparison of two electrochemical techniques: cyclic voltammetry (CV) and staircase voltammetry (SCV) are presented. The measurement parameters, influencing peak currents recorded using both studied techniques, i.e. scan rate for CV, and potential step and step time for SCV were verified and examined. The research has shown that employing SCV technique allowed to obtain larger calibration slope in comparison to CV, and consequently better sensitivity of the analytical method. Employing SCV instead of standard CV seems to provide better opportunities for more sensitive electrochemical detection of organic compounds.

## 1. Introduction

Citalopram (Fig. 1) is known chemically as (±)-1-(3-dimethylaminopropyl)-1-(4-fluorophenyl)-1,3-dihydroisobenzofuran-5-carbonitrile. It is a selective serotonin-reuptake inhibitor and exhibits broad spectrum of therapeutic activity against depressive disorders [1]. Citalopram is one of the most commonly used antidepressants, hence there is a great need to develop fast and reliable methods for its determination in tablets, biological fluids or even in the environment. The application of voltammetric techniques for this purpose could be very promising due to the low cost of the apparatus, the simplicity, rapidity and high sensitivity of voltammetric measurements [2].

Cyclic voltammetry (CV) is one of the most commonly used voltammetric technique for analytical and mechanism of electrochemical reactions studies of organic and inorganic compounds. Its effectiveness is limited by the charging

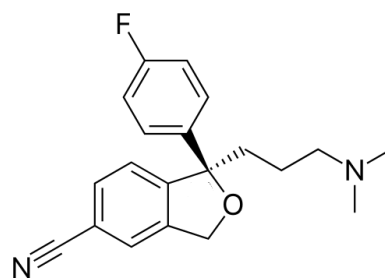


Fig. 1 Chemical structure of citalopram.

current, always occurring due to the continuously changing potential. Staircase voltammetry (SCV), the equivalent technique in the pulse version, allows to separate the Faradaic current from the non-Faradaic and thus to eliminate the charging current [3].

According to Randles-Sevcik equation (1) peak current depends only on one measuring parameter: the speed of changing potential applied to the working electrode, commonly known as a scan rate

$$I_p = kz^{3/2}AD^{1/2}v^{1/2}c \quad (1)$$

where:  $I_p$  is peak current,  $k$  constant value,  $z$  number of electrons involved in the redox process,  $A$  electrode surface,  $D$  diffusion coefficient,  $v$  scan rate, and  $c$  is concentration of electroactive compound.

In cyclic voltammetry, potential is changed linearly, therefore scan rate does not depend on any other parameters. During staircase voltammetric measurements, potential of working electrode is changed in the form of intervals, so-called stairs, with a certain potential value (step potential) and the specified duration (step time). Therefore, the scan rate in SCV technique is determined by these two parameters [4].

The aim of this work was to compare two electrochemical technics: SCV and CV in citalopram determination. For this purpose, the CV and SCV measurements at different experimental conditions were carried out. The influence of experimental parameters on recorded signals was compared, particularly in terms of analytical method sensitivity.

## 2. Experimental

### 2.1 Reagents and chemicals

The following reagents were used: MicroPolish Alumina suspension with grain size 0.5  $\mu\text{m}$  (Buechler, USA); potassium chloride 99.5% (Poch, Poland); sodium nitrate 99.5% (Merck, Germany); nitric acid 65% (Merck, Germany); disodium hydrogen phosphate 99% (Poch, Poland); sodium dihydrogen phosphate 99.5% (Chempur, Poland); citalopram hydrobromide (LGC Standards, Canada); distilled water derived from a HLP 5 system (Hydrolab, Poland).

### 2.2 Instrumentation

The voltammetric measurements were conducted with the M161 electrochemical analyzer (Mtm-Anko, Poland). The EALab 2.1 software was used for data acquisition. The measurements were carried in three-electrode system in quartz vessel of 5mL volume covered with a plastic cover with four holes that matched the size of each electrode and an additional hole for adding standard solution. The role of

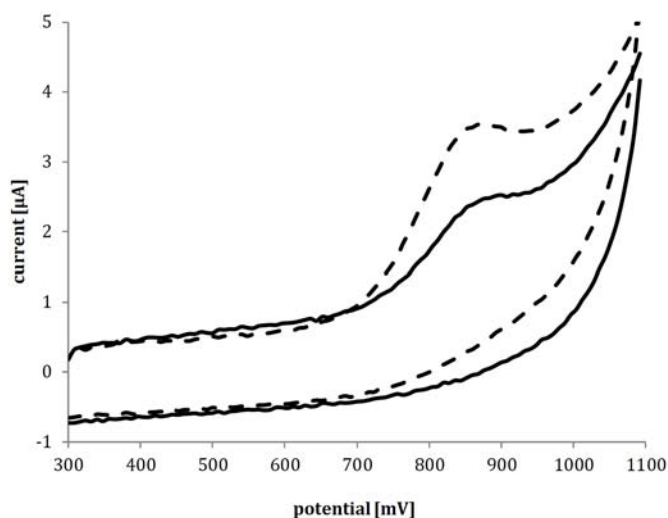


**Fig. 2** Voltammograms recorded for  $10 \mu\text{mol L}^{-1}$  citalopram in phosphate buffer solution ( $\text{pH} = 8.00$ ;  $100 \text{ mmol L}^{-1}$ ) using cyclic (solid line) and staircase voltammetry (dotted line) techniques.

working electrode played glassy carbon electrode consisting of 3 mm silver wire covered by glassy carbon layer placed in teflon holder (MTM Anko M10X1). Silver chloride electrode with double coat ( $\text{Ag}/\text{AgCl}$ , saturated  $\text{KCl}/2 \text{ mol L}^{-1} \text{ NaNO}_3$ ; MTM Anko M6) was used as a reference electrode and platinum plate placed in teflon holder was used as an auxiliary electrode. Also ultrasonic bath Sonic-3 (Polsonic, Poland) and magnetic stirrer MS 11 (Wigo, Poland) were used.

### 3. Results and discussion

According to Randles-Sevcik equation peak current recorded in cyclic voltammetric measurements depends on square root of scan rate. To confirm this relationship cyclic voltammograms were registered using different scan rates: 12.5, 25, 50, 100, 200, 250 and  $500 \text{ mV s}^{-1}$ . The measurements were conducted in phosphate buffer solution ( $\text{pH} = 8.00$ ;  $100 \text{ mmol L}^{-1}$ ) containing citalopram at concentration of  $10 \mu\text{mol L}^{-1}$  in potential range from 300 to 1100 mV. The example of recorded CV voltammogram is presented in Fig. 2. As can be seen, citalopram undergoes an irreversible oxidation process, therefore oxidation peak current was taken as analytical signal in further stages of research. The obtained dependence of peak current in function of scan rate is presented in Fig. 3. As shown in this chart, the correlation of peak current and square root of the scan rate assumed the linear function, which is consistent with the Randles-Sevcik equation and proves that the citalopram oxidation is a process controlled by diffusion [5].

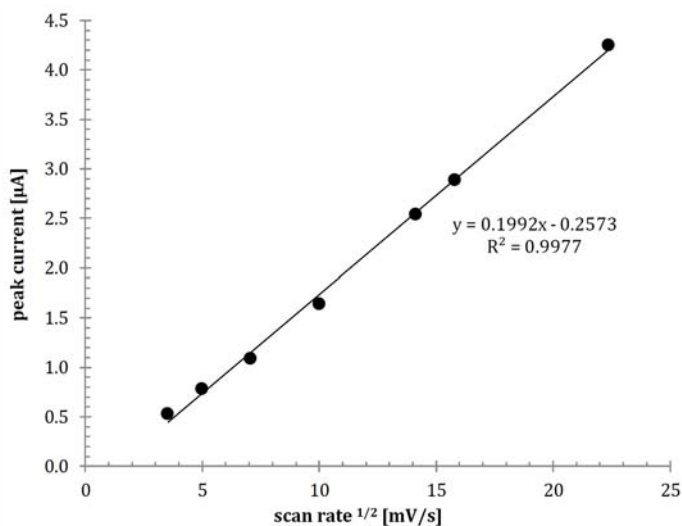


**Fig. 3** Dependence of peak current in a function of square root of the scan rate obtained in cyclic voltammetry measurements.

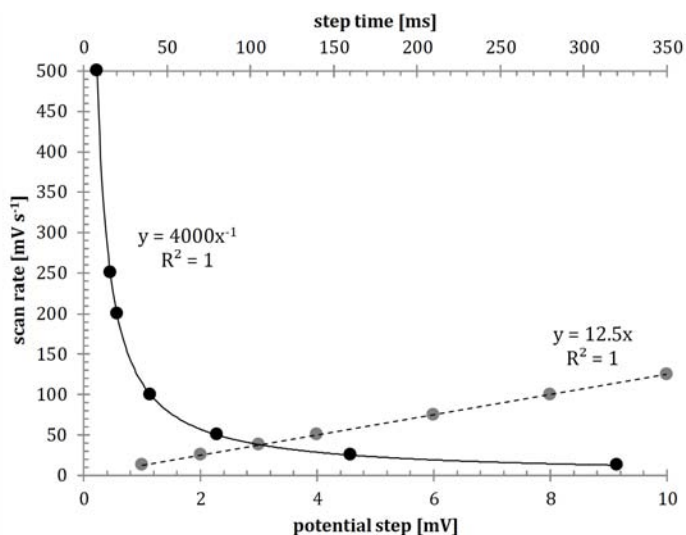


**Fig. 4** Dependence of scan rate from step time (black points with solid line) or potential step (grey points with dotted line) achieved in staircase voltammetric measurements.

To study the impact of the change in the potential step and step time on recorded signal SCV voltammograms were registered using various values of the potential step (1, 2, 3, 4, 6, 8, and 10 mV) and constant value of step time (40 ms). Subsequently, one value of the potential step (8 mV) was selected and voltammograms using different values of step time (8, 16, 20, 40, 80, 160 and 320 ms) were recorded (Fig. 4). The measurements were conducted in the same

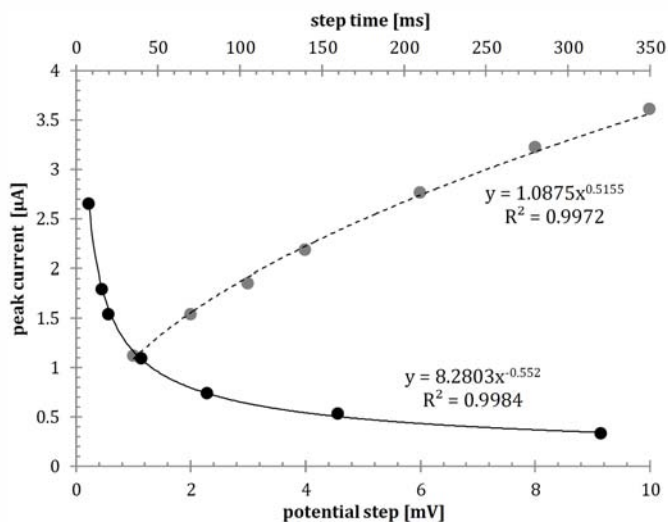


**Fig. 5** Influence of potential step (grey points with dotted line) and step time (black points with solid line) on registered peak current in staircase voltammetric measurements.

electrolyte solution as CV measurements were carried out with the corresponding potential range and citalopram hydrobromide concentration. The graph presented in Fig. 4 proves the growing linear relationship between the potential step and scan rate. With the increase of the potential step, the number of registered points decreased, thus the scan rate grew up. Therefore, due to decreasing measurement resolution, it is recommended to apply potential step not higher than 10 mV. If the step potential is not higher than 8 mV, the SCV measurements correspond to the CV technique [4]. For step time the reverse relationship was observed: the scan rate decreased with the growth of the each step duration, which can be described as inversely proportional relationship. Registered values of peak current for different potential steps and step times are shown in Fig. 5. It can be seen that peak current increased with the growth of potential step and decreased with growing of step time. According to obtained correlations between scan rate and step parameters it was observed that dependences of peak current on potential step and step time were consistent with the Randles-Sevcik equation (1).

In order to verify the influence of applied voltammetric technique on citalopram calibration graphs measurements were performed using both CV and SCV methods. For this purpose, the appropriate volumes of  $1.0 \text{ mmol L}^{-1}$  citalopram solution were gradually added to the measuring vessel filled with 5 mL of phosphate buffer solution ( $\text{pH}=8.00$ ;  $100 \text{ mmol L}^{-1}$ ), obtaining citalopram concentrations of 0, 10, 20, 30, 40 and  $50 \text{ }\mu\text{mol L}^{-1}$ . For both techniques, measurements were conducted in potential range from 300 to 1100 mV and scan rate equal  $100 \text{ mV s}^{-1}$ . For SCV, potential step equal 8mV and step time 40 ms, was applied, which correspond to mentioned scan rate value. For each analyte concentration voltammograms were registered three times and peak current

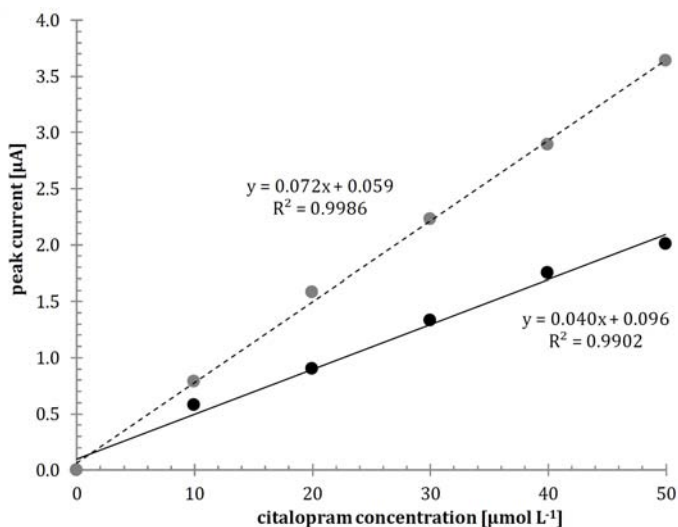


**Fig. 6** Calibration graphs obtained from cyclic voltammetric (black points with solid line) and staircase voltammetric (grey points with dotted line) measurements conducted in phosphate buffer solution (pH = 8.00; 100 mmol L<sup>-1</sup>) containing citalopram with potential range 300–1100 mV and scan rate equal 100 mV s<sup>-1</sup>.

value was calculated as the average of performed repetitions. The peak current was read from the maximum of the oxidation peak and then the value from base voltammogram (registered for buffer solution) was subtracted. The results of this experiment are presented in the Fig. 6. Both calibration graphs exhibit good linearity, however estimated linear function achieved for SCV measurements is characterized by a greater slope value than calibration graph obtained by CV technique. The phenomenon may be related to the fact that SCV method eliminates the charging current which is responsible for the high background in CV method, especially disturbing at high potential values: the citalopram oxidation peak is recorded near to 900 mV, were noticeable increasing of background current in CV measurements was observed (Fig. 2).

#### 4. Conclusions

The conducted preliminary studies proved that staircase voltammetry can be applied for electrochemical determination of citalopram instead of cyclic voltammetry. In SCV measurements scan rate, so also peak current, depends on potential step value and step duration. Appropriate selection of these parameters allows for the modification of the measurement resolution: higher potential step value decreases number of recorded points and the resolution is descending. Thus, the values of the step potential greater than 10 mV are not recommended in the quantitative analysis. It was observed that SCV technique allowed to obtain

calibration graph with a larger slope than using CV and so improved sensitivity of determination. According to literature, also the point in the step duration, when the current starts to be measured, seems to have significant impact on registered value of peak current [3]. The investigation of this parameter's impact on the peak current would be an important part of further research.

### Acknowledgments

This research has been partly supported by the EU Project POWR.03.02.00-00-I004/16.

### References

- [1] Atmaca M., Kuloglu M., Tezcan E., Semercioz A.: The efficacy of citalopram in the treatment of premature ejaculation: a placebo-controlled study. *Int. J. Impot. Res.* **14** (2002), 502–505.
- [2] Keypour H., Saremi S.G., Veisi H., Noroozi M.: Electrochemical determination of citalopram on new Schiff base functionalized magnetic Fe<sub>3</sub>O<sub>4</sub>nanoparticle/MWCNTs modified glassy carbon electrode. *J. Electroanal. Chem.* **780** (2016), 160–168.
- [3] Seralathan M., Osteryoung R., Osteryoung J.: General equivalence of linear scan and staircase voltammetry. *J. Electroanal. Chem.* **222** (1987), 69–100.
- [4] Cygański A.: *Podstawy metod elektroanalitycznych*. 3rd ed. Warszawa, WNT 1999.
- [5] Gosser D.K.: *Cyclic Voltammetry: Simulation and Analysis of Reaction Mechanisms*. 2nd ed. New York, VCH 1993.

# Elemental analysis of atherosclerotic plaque by ICP-MS and LA-ICP-MS

AGATA JAGIELSKA<sup>a,\*</sup>, BARBARA WAGNER<sup>a</sup>, ANNA RUSZCZYŃSKA<sup>a</sup>, ANDRZEJ GAWOR<sup>a</sup>,  
EWA BULSKA<sup>a</sup>, ELŻBIETA ZIEMIŃSKA<sup>b</sup>, BEATA TOCZYŁOWSKA<sup>c</sup>, WAWRZYNIEC JAKUCZUN<sup>d</sup>,  
MAŁGORZATA SZOSTEK<sup>d</sup>

<sup>a</sup> *Biological and Chemical Research Centre, Faculty of Chemistry, University of Warsaw,  
ul. Żwirki i Wigury 101, 02-093 Warsaw, Poland ✉ ajagielska@chem.uw.edu.pl*

<sup>b</sup> *Mossakowski Medical Research Centre, Polish Academy of Sciences,  
ul. Pawińskiego 5, 02-106 Warsaw, Poland*

<sup>c</sup> *Nałęcz Institute of Biocybernetics and Biomedical Engineering, Polish Academy of Sciences,  
ul. ks. Trojdena 4, 02-109 Warsaw, Poland*

<sup>d</sup> *Department of General and Endocrine Surgery, Medical University of Warsaw,  
ul. Banacha 1a, 02-097 Warsaw, Poland*

## Keywords

atherosclerosis  
laser ablation  
mass spectrometry

## Abstract

Atherosclerosis can be described as narrowing the lumen of an artery due to the build-up of plaque. Chemical composition of an atherosclerotic plaque strongly depends on its clinically important stability. The aim of a study was elemental analysis of atherosclerotic plaque by using inductively coupled plasma mass spectrometry (ICP-MS) and creating the elemental distribution maps by using laser ablation inductively coupled plasma mass spectrometry (LA-ICP-MS). Elements such as Li, Mg, Ca, V, Mn, Fe, Co, Cu, As, Se, Rb, Sr, Ag, Cd, Pb were successfully quantified, with the greatest content of typical calcification components: Ca and Mg. LA-ICP-MS analysis was performed with no need of sample mineralization. Inhomogeneous distribution of several elements was observed, again mainly in case of calcification (Ca, Mg, Sr, P). Moreover, the influence of sample preparation was stated. Lyophilisation enhanced analytes concentration, but also caused the loss of several elements, such as Pb or S.

---

## 1. Introduction

According to statistical reports vascular diseases remain the first cause of death in Poland, responsible for nearly 46% of deceases in 2013 [1]. That kind of decease is usually associated with atherosclerosis, defined as narrowing the lumen of an artery due to the build-up of plaque [2]. Atherosclerotic plaque is composed of glycolipoprotein part and inorganic part, mainly calcium compounds [3]. The most clinically important differentiation of atherosclerotic plaque distinguishes two types: stable and unstable plaque [4]. Stable plaque has small lipid pool and thick fibrous cap. It can grow in many years without any symptoms. In turn, bigger

lipid pool and thinner fibrous cap in unstable plaque make it much more vulnerable and easier to rupture. Chemical composition of a plaque can vary depending on its stable or unstable character. Currently, there are no drugs available to stabilize unstable atherosclerotic plaque [5]. However, it is important to quickly diagnose the stability or instability of the plaque in order to decide about surgery and to plan further treatment.

## 2. Experimental

### 2.1 Reagents and chemicals

Stock solutions were prepared by diluting ICP multi-element standard Merck VI (Merck, Germany). Certified Reference Materials (CRM) were used: MODAS-4, cormorant tissue (MODAS, Poland), MODAS-3, herring tissue (MODAS, Poland), NIST 1577c, bovine liver tissue (NIST, USA). For sample mineralization 65% nitric acid, analytical grade, was used (Merck, Germany). Samples and standards were diluted with deionized water obtained by Milli-Q System (Merck, Millipore, Germany).

### 2.2 Instrumentation

The measurement were carried out using inductively coupled plasma mass spectrometer NexION 300D (Perkin Elmer, USA). Laser ablation was performed with LSX-213 (Cetac Technologies, USA). Instruments conditions are presented in Table 1. Sample lyophilisation was executed with Liofilizator Alpha model 1-2 LDplus (Donserv, Germany).

**Table 1**

Laser ablation inductively coupled plasma mass spectrometry and inductively coupled plasma mass spectrometry instrumentation conditions.

	LA-ICP-MS	ICP-MS
Sample introduction system	LSX-213 (CETAC)	Meinhard nebulizer
Number of ablation lines	5	–
Laser energy / mJ	2.5	–
Laser shot frequency / Hz	20	–
Spot size / $\mu\text{m}$	100	–
Scan rate / $\mu\text{m s}^{-1}$	50	–
Plasma power / W	1400	1350
Carrying gas (Ar) flow / $\text{dm}^3\text{min}^{-1}$	0.9	0.8
Dwell time / ms	5	50
Shutter delay / s	30	–

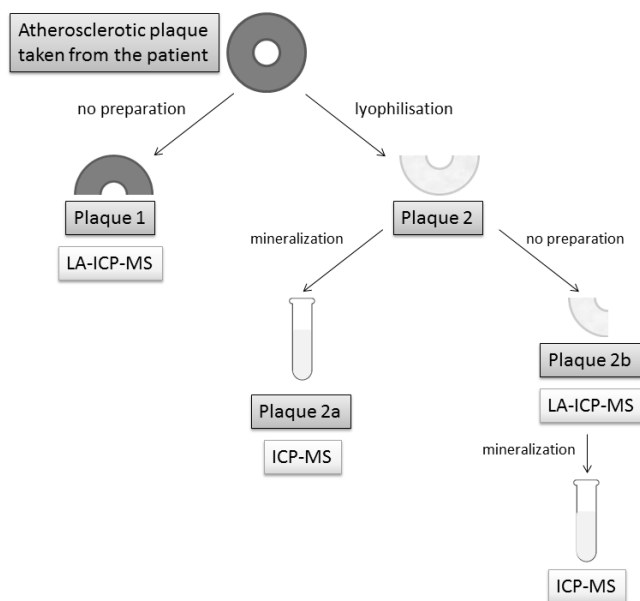


Fig. 1 Scheme of used analytical procedure.

### 2.3 Analytical procedure

Scheme of the analytical procedure is presented in Fig. 1. Atherosclerotic plaque taken intraoperatively from the patient's femoral artery was divided into two pieces (Plaque 1 and Plaque 2). The first piece remained unchanged (Plaque 1) and the second (Plaque 2) was lyophilized (temperature:  $-15\text{ }^{\circ}\text{C}$ , pressure: 1 mbar, time: 6 h). A half of lyophilized material (Plaque 2a) was treated with microwave-assisted mineralization in the closed system ( $65\% \text{HNO}_3$ ,  $220\text{ }^{\circ}\text{C}$ ) and analysed by using inductively coupled plasma mass spectrometry (ICP-MS). The unchanged piece (Plaque 1) and the second half of lyophilized sample (Plaque 2b) were analysed by using laser ablation inductively coupled plasma mass spectrometry (LA-ICP-MS). After laser ablation it is still possible to mineralise the sample and that is why Plaque 2b could be transferred to the solution and also analysed by ICP-MS.

## 3. Results and discussion

In order to estimate total elemental content in atherosclerotic plaque, the screening ICP-MS method was used. Preliminary screening analysis relies on mass spectrum registration in a wide range mass to charge ratio. Then, the results are interpreted by using mathematical algorithm with automatic correction for typical isobaric and multielemental interferences. Registered signal intensities

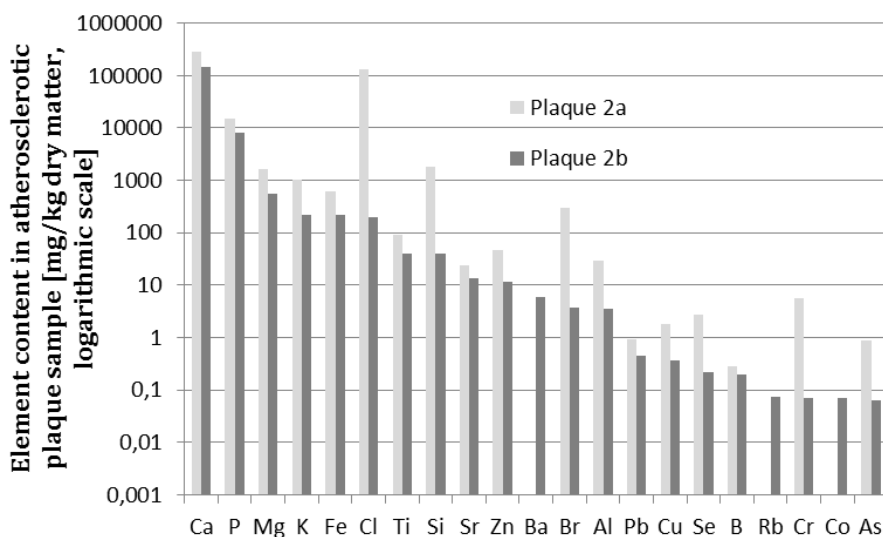


**Fig. 2** Laser ablation inductively coupled plasma mass spectrometry screening method results for two samples of atherosclerotic plaque.

are compared with available table of results for each element and presented as approximate concentrations.

Results obtained by using ICP-MS screening method are presented in Fig. 2. Preliminary testing allowed to narrow down the list of elements designed for further quantitative analysis by external standard calibration. The results were referred to CRM in order to prove the reliability of the method. Chosen elemental content in atherosclerotic plaque is presented in Table 2 (*next page*). Elements such as calcium (above 10% of plaque dry matter) or magnesium (above 0.1%) can be considered as typical components of calcified plaque areas. Significant iron content (above 0.01%) comes probably from the rest of morphotic component of the blood. Apart from these elements, quantitative results for cobalt, copper, lead and cadmium were achieved that may be a starting point for investigation about metal accumulation in atherosclerotic plaque.

Direct analysis of elemental distribution in atherosclerotic plaque was performed using LA-ICP-MS. Linear laser ablation was chosen in order to obtain the information of elemental content on sample surface. Signals reconstruction allowed visualising elemental distribution in chosen area ( $1.35 \text{ mm}^2$ ) of a plaque (Fig. 3, *page 49*). For each element, signal intensities were normalised and presented as percent of maximum signal intensity. Most of the elements are inhomogeneously distributed, particularly characteristic components of calcification (Ca, Mg, Sr, P). A correlation between high content of these elements can be observed in the maps. It is worth mentioning that phosphorus not only is the component of calcified parts, but also it occurs in phospholipids. Additionally, phosphates may be not the only anions in calcification.

**Table 2**  
Chosen elemental content in atherosclerotic plaque quantified by using external standard method (*CV* – coefficient of variation, *LOD* – limit of detection, *LOQ* – limit of quantitation).

Sample	Quantification / mg kg <sup>-1</sup> dry matter														
	Li	Mg	Ca	V	Mn	Fe	Co	Cu	As	Se	Rb	Sr	Ag	Cd	Pb
Plaque 2a	<LOD	3454	230361	4.86	1.39	1179	0.206	5.65	1.01	0.986	0.668	53.5	0.097	0.397	2.088
<i>CV</i> / %	644	0.6	3.8	5.2	2.0	2.0	4.8	4.3	6.4	14.5	18.2	1.5	112.6	3.6	1.8
Plaque 2b	0.024	1819	126672	<LOD	<LOD	485.3	0.287	<LOQ	<LOD	0.251	0.206	39.8	<LOD	0.059	0.928
<i>CV</i> / %	3.1	0.8	0.9	2.6	0.7	0.7	1.4	1.1	1.0	5.0	1.2	1.5	4.8	0.5	0.9
<i>LOD</i>	0.012	15	46	0.02	0.09	4.7	0.003	1.07	0.21	0.018	0.196	0.2	0.024	0.003	0.062
<i>LOQ</i>	0.016	15	55	0.02	0.13	7.6	0.005	1.76	0.25	0.029	0.210	0.2	0.037	0.004	0.079

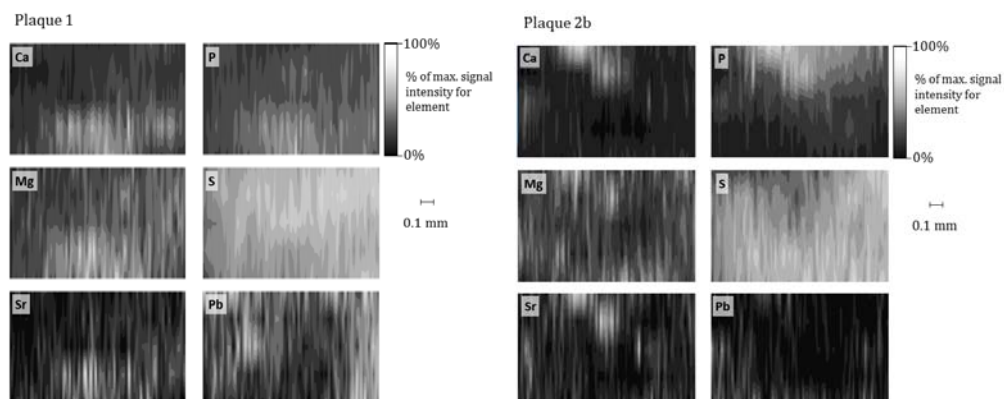


**Fig. 3** Elemental distribution maps of chosen elements in atherosclerotic plaque with no preparation (Plaque 1) and in lyophilized sample (Plaque 2b) performed by using laser ablation inductively coupled plasma mass spectrometry

Multielemental composition of an atherosclerotic plaque from heart vessels was performed for the first time by Zhuravskaya et al. in 2016 [6]. Authors used synchrotron radiation-induced X-ray fluorescence (SRXRF) method and also stated the correlation between calcium and strontium distribution, as in presented research. Moreover, in the cited study [6], the association between calcium, zinc and iron was observed.

Sample preparation was considered as an important factor influencing LA-ICP-MS measurements. Lyophilisation has many advantages, such as increasing stability and inhibition of metabolic processes [7]. There are reports that lyophilisation preserves tissue cellular structure [8, 9]. Concentration of the analytes increases after removing water that make it possible to determine trace contents. However, there are also some limitations of the process, among others being a consequence of sample specificity. Atherosclerotic plaque is composed of cellular rests rich in water, but it contains also lipid pools and calcification with much lower water contribution. For such inhomogeneous samples, results calculated as percent of dry matter may not be the best way of measurement data presentation. The second considerable drawback of lyophilisation observed during the preliminary research was losing the information about several elements (mainly sulphur and lead). Average signal for these elements was much lower for lyophilized sample in comparison with unprepared samples that is in opposition to normally observed effect of increasing content after removing water.

## 4. Conclusions

Atherosclerotic plaque analysis by using mass spectrometry techniques is complementary in relation to histological examination that provides only the information about cellular composition of the sample. ICP-MS method gives a possibility to analyse elemental content and its combination with laser ablation allows visualizing superficial distribution of many elements. Inhomogeneous distribution of several elements was observed mainly in case of calcification (Ca, Mg, Sr, P) that can become an important tool in atherosclerotic plaque differentiation. The influence of sample preparation was stated, seeing that lyophilisation enhances analytes concentration, but also causes the loss of several elements, such as Pb or S. Presented study can be a good starting point for further research leading to chemical differentiation of atherosclerotic plaque in clinical practice.

## Acknowledgments

The study was carried out at the Biological and Chemical Research Centre, University of Warsaw established within the project co-financed by European Union from the European Regional Development Fund under the Operational Programme Innovative Economy 2007–2013.

## References

- [1] Strzelecki Z., Szymborski J.: *Zachorowalność i umieralność na choroby układu krążenia a sytuacja demograficzna Polski*. Rządowa Rada Ludnościowa 2015.
- [2] Herrington W., Lacey B., Sherliker P., Armitage J., Lewington S.: Epidemiology of atherosclerosis and the potential to reduce the global burden of atherothrombotic disease. *Circ. Res.* **118** (2016), 535–546.
- [3] Lara M.J., Ros E., Sierra M., Dorronsoro C., Aguilar J.: Composition and genesis of calcium deposits in atheroma plaques. *Ultrastruct. Pathol.* **38** (2014), 167–177.
- [4] Liu J., Wang Z., Wang W.M., Li Q., Ma Y.L., Liu C.F., Lu M.Y., Zhao H.: Feasibility of diagnosing unstable plaque in patients with acute coronary syndrome using iMap-IVUS. *J. Zhejiang. Univ. Sci. B* **16** (2015), 924–930.
- [5] Thompson P.L., Nidorf S.M., Eikelboom J.: Targeting the unstable plaque in acute coronary syndromes. *Clin. Ther.* **35** (2013), 1099–1107.
- [6] Zhuravskaya E.Y., Savchenkob T.I., Chankinab O.V., Polonskayaa Y.V., Chernyavskii A.M., Ragino Y.I., Shcherbakova L.V.: SRXRF study of chemical elements content in the atherosclerotic plaque of heart vessels. *Phys. Procedia* **84** (2016), 270–274.
- [7] Shukla S.: Freeze drying process: a review. *Int. J. Pharm. Sci. Res.* **2** (2011), 3061–3068.
- [8] Tang M., Wolkers W.F., Crowe J.H., Tablin F.: Freeze-dried rehydrated human blood platelets regulate intracellular pH. *Transfusion* **46** (2006), 1029–1037.
- [9] Wolkers W.F., Walker N.J., Tablin F., Crowe J.H.: Human platelets loaded with trehalose survive freeze-drying. *Cryobiology* **42** (2001), 79–87.

# Determination of difenzoquat at a mercury meniscus modified silver solid amalgam electrode by differential pulse voltammetry

JÚLIUS GAJDÁR\*, JIŘÍ BAREK, JAN FISCHER

*UNESCO Laboratory of Environmental Electrochemistry, Department of Analytical Chemistry, Faculty of Science, Charles University, Hlavova 8, 128 43 Prague 2, Czech Republic*  
✉ *julius.gajdar@natur.cuni.cz*

## Keywords

difenzoquat  
herbicide  
mercury meniscus  
modified silver solid  
amalgam electrode  
voltammetry

## Abstract

In this study herbicide difenzoquat is determined by differential pulse voltammetry at a mercury meniscus modified silver solid amalgam electrode. The optimal medium for the determination is Britton-Robinson buffer pH = 11.0. At this pH difenzoquat gives one cathodic signal at  $-1.33$  V (vs. Ag|AgCl|3M KCl reference electrode). An addition of a few drops of gelatin as a surface-active compound greatly improves repeatability of determination of difenzoquat and removes sharp maxima in voltammograms. Under these conditions it is possible to achieve limits of quantitation in submicromolar range.

## 1. Introduction

Recently, there has been a decrease in the use of mercury electrodes caused by the fear of its toxicity that prompted research of novel electrode materials with similar properties. Mercury electrodes are generally considered as the best for studies of reducible substances. Non-toxic amalgam electrodes proved to be a worthy replacement of mercury electrodes with similarly wide potential window, comparable sensitivity and they also offer advantage of better mechanical stability [1]. They were introduced by Novotny and Yosypchuk [2] and since then they have been widely used for voltammetric determination of various organic compounds, environmental pollutants and pesticides [3–7]. A mercury meniscus modified silver solid amalgam electrode (m-AgSAE) is considered to be the most similar to a mercury electrode with its wide potential window and high sensitivity [8].

The analyte in this study is a herbicide difenzoquat (Fig. 1), a quaternary ammonium salt, usually distributed as 1,2-dimethyl-3,5-diphenyl-pyrazolium methyl sulfate. This

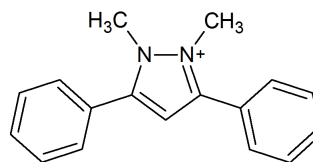


Fig. 1 Structural formula of difenzoquat

herbicide is used for wild oat (*Avena fatua*) control in barley and wheat. It bears almost no acute or chronic threat to avian, water or mammalian species [9]. This compound was studied by electrochemical methods at mercury electrodes with either pure organic or mixed solvents and the determination was unsuccessful in aqueous media [10, 11]. In this work, a studied herbicide difenzoquat has been determined by differential pulse voltammetry at m-AgSAE in aqueous medium.

## 2. Experimental

### 2.1 Reagents and chemicals

A stock solution of difenzoquat ( $1 \text{ mmol L}^{-1}$ , 1,2-dimethyl-3,5-diphenylpyrazolium methyl sulfate, CAS number: 43222-48-6, 99.9% from Sigma Aldrich) was prepared in deionized water. Britton-Robinson buffers were prepared by mixing  $0.04 \text{ mol L}^{-1}$  phosphoric, acetic, and boric acid with  $0.02 \text{ mol L}^{-1}$  sodium hydroxide (all p.a., Lach-Ner).

### 2.2 Instrumentation

All voltammetric measurements were carried out on Eco-Tribo Polarograph controlled by Polar Pro 5.1 software (both Polaro-Sensors, Czech Republic). Voltammetric measurements were carried out in a three-electrode system with working m-AgSAE (0.5 mm diameter, Eco-Trend Plus, Czech Republic), Ag|AgCl| $3 \text{ mol L}^{-1}$  KCl reference electrode (Elektrochemické detektory, Turnov, Czech Republic) and a platinum wire auxiliary electrode (Eco-Trend Plus, Czech Republic). Samples for voltammetric measurements were prepared by measuring an appropriate amount of the stock solution of difenzoquat into a 10.0 mL volumetric flask, two drops of 0.5% gelatin solution were then added and the volumetric flask was filled with Britton-Robinson buffer pH = 11.0 to the mark. The solution was purged with nitrogen for 5 min and corresponding voltammogram was recorded. The purging was repeated for 30 s before every single measurement. Working m-AgSAE was pre-treated as described in [12]. The m-AgSAE was activated before every series of measurements by applying potential  $-2.2 \text{ V}$  for 300 s in  $0.2 \text{ mol L}^{-1}$  KCl. differential pulse voltammetry parameters were: scan rate  $20 \text{ mV s}^{-1}$ , pulse width of 100 ms, pulse amplitude  $-50 \text{ mV}$ , and sampling time 20 ms.

## 3. Results and discussion

Voltammetric response of difenzoquat was investigated in the Britton-Robinson buffer. Reduction at m-AgSAE was observed only at pH = 8.0 and more alkaline buffer solutions; in neutral and acidic pH the reduction response coincided with the hydrogen evolution. The potential of reduction was constant at  $-1.33 \text{ V}$  in the

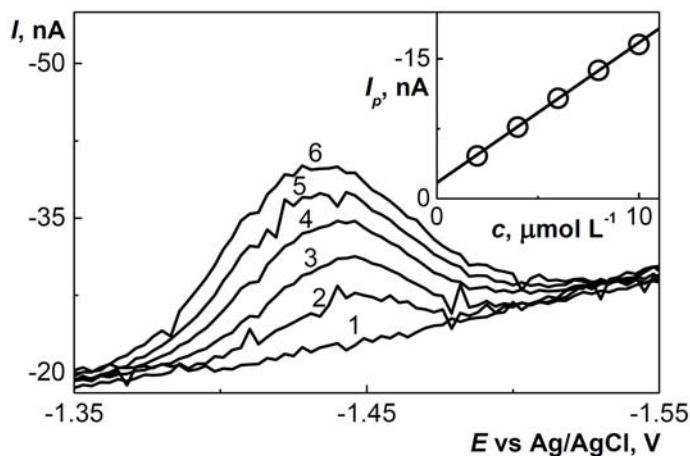


**Fig. 2** Differential pulse voltammograms of difenzoquat (0 (1); 2 (2); 4 (3); 6 (4); 8 (5); and 10 (6)  $\mu\text{mol L}^{-1}$ ) at m-AgSAE in Britton-Robinson buffer pH = 11.0 medium in the presence of gelatin ( $25 \mu\text{g mL}^{-1}$ ). The calibration curve is shown in the inset.

pH range 8.0–12.0. The peak current response did not significantly change in the pH range 10.0–12.0 and the value in the middle of this range pH = 11.0 was chosen as optimal for the voltammetric determination of the compound. A few drops of gelatin were added to the measured solution because it eliminated some sharp maxima that were observed in voltammograms at more negative potentials than the reduction peak. Under these conditions it was possible to measure 20 curves with good reproducibility after the activation of m-AgSAE without any regenerating step in-between measurements.

Difenzoquat was at first successfully determined in the Britton-Robinson buffer with the addition of two drops of 0.5% gelatin solution. Voltammetric curves and a calibration dependency for the concentration range 2–10  $\mu\text{mol L}^{-1}$  are shown in Fig. 2. Difenzoquat was also determined in real matrices (drinking and river water) spiked with concentrated difenzoquat solution and in the presence of 10% Britton-Robinson buffer of pH = 11.0 and the surface-active compound gelatin. Parameters of calibration curves for the linear dynamic range of the method are summarized in Table 1. At higher concentrations of the

**Table 1**

Calibration straight line parameters for differential pulse voltammetry determination of difenzoquat in linear dynamic range of 0.2–10  $\mu\text{mol L}^{-1}$  at m-AgSAE in various matrices using Britton-Robinson buffer pH = 11.0 as a supporting electrolyte and after the addition of gelatin ( $25 \mu\text{g mL}^{-1}$ ) to suppress observed maxima.

Matrix	Slope / $\text{mA L mol}^{-1}$	Intercept / nA	R	LOQ / $\mu\text{mol L}^{-1}$
Deionized water	$-1.78 \pm 0.05$	$+0.13 \pm 0.15$	-0.9978	0.46
Drinking water	$-2.14 \pm 0.04$	$-0.36 \pm 0.14$	-0.9983	0.34
River water	$-1.59 \pm 0.06$	$-0.55 \pm 0.09$	-0.9946	0.47

herbicide (more than  $10 \mu\text{mol L}^{-1}$ ) slopes of the concentration dependencies were significantly different (lower) in case of all matrices.

#### 4. Conclusions

The herbicide difenzoquat was successfully determined by differential pulse voltammetry at the m-AgSAE in the Britton-Robinson buffer buffer solution (pH = 11.0) and in real matrices of drinking and river water with limits of quantitation in submicromolar range. An addition of gelatin eliminated some sharp maxima that were present in aqueous medium.

#### Acknowledgments

Financial support of the Czech Science Foundation (project 17-03868S) is gratefully acknowledged.

#### References

- [1] Gajdar J., Horakova E., Barek J., Fischer J., Vyskocil V.: Recent applications of mercury electrodes for monitoring of pesticides: A critical review. *Electroanalysis* **28** (2016), 2659–2671.
- [2] Novotný L., Yosypchuk B.: Pevné stříbrné amalgamové elektrody. *Chem. Listy* **94** (2000), 1118–1120.
- [3] Danhel A., Barek J.: Amalgam electrodes in organic electrochemistry. *Curr. Org. Chem.* **15** (2011), 2957–2969.
- [4] Chorti P., Fischer J., Vyskocil V., Economou A., Barek J.: Voltammetric determination of insecticide thiamethoxam on silver solid amalgam Electrode. *Electrochim. Acta* **140** (2014), 5–10.
- [5] Hajkova A., Vyskocil V., Josypcuk B., Barek J.: A miniaturized electrode system for voltammetric determination of electrochemically reducible environmental pollutants. *Sens. Actuators B* **227** (2016), 263–270.
- [6] Janikova-Bandzuchova L., Selesovska R., Chylkova J., Nesnidalova V.: Voltammetric analysis of herbicide picloram on the silver solid amalgam electrode. *Anal. Lett.* **49** (2016), 19–36.
- [7] Novakova K., Hrdlicka V., Navratil T., Harvila M., Zima J., Barek J.: Application of silver solid amalgam electrode for determination of formamidine amitraz. *Monatsh. Chem.* **147** (2016), 181–189.
- [8] Danhel A., Josypcuk B., Barek J., Fojta M.: Možnosti a perspektivy stříbrného amalgámu v elektroanalytické chemii. *Chem. Listy* **110** (2016), 215–221.
- [9] Donald W.W.: Difenzoquat. In: *Systems of Weed Control in Wheat in North America*. Donald W.W. (edit.). Champaign, Weed Science Society of America 1990, p. 298–320.
- [10] Pospíšil L., Colombini M.P., Fuoco R., Strelets V.V.: Electrochemical properties of difenzoquat herbicide (1,2-dimethyl-3,5-diphenyl-pyrazolium). *J. Electroanal. Chem. Interfacial Electrochem.* **310** (1991), 169–178.
- [11] Rühling I., Schäfer H., Ternes W.: HPLC online reductive scanning voltammetric detection of diquat, paraquat and difenzoquat with mercury electrodes. *Fresenius J. Anal. Chem.* **364** (1999), 565–569.
- [12] Yosypchuk B., Barek J.: Analytical applications of solid and paste amalgam electrodes. *Crit. Rev. Anal. Chem.* **39** (2009), 189–203.

# Investigations on the electrochemically induced decomposition of AdBlue-urea

PETER BRAUN<sup>a, b, \*</sup>, HANS-PETER RABL<sup>b</sup>, FRANK-MICHAEL MATYSIK<sup>a</sup>

<sup>a</sup> *Institute of Analytical Chemistry, Chemo- and Biosensors, Faculty of Chemistry and Pharmacy, University of Regensburg, Universitätsstraße 31, 93053, Regensburg, Germany*

✉ [peter.braun@ur.de](mailto:peter.braun@ur.de)

<sup>b</sup> *Laboratory Combustion Engines and Emission Control, Faculty of Mechanical Engineering, Ostbayerische Technische Hochschule, Galgenbergstraße 30, 93053, Regensburg, Germany*

## Keywords

DeNO<sub>x</sub> systems  
diesel engine  
NiOOH  
selective catalytic  
reduction  
urea decomposition

## Abstract

Ammonia based selective catalytic reduction systems are the most widely used technology for reduction of nitrogen oxide emissions from lean-burn engines such as diesel engines. However, at low exhaust temperatures the selective catalytic reduction process is limited by difficulties in decomposition of the ammonia precursor urea, which is carried on-board using an aqueous solution "AdBlue". In previous work the nickel species NiOOH was shown to be catalytically active in decomposing urea at low temperatures, for the case of highly concentrated potassium hydroxide in AdBlue. Since this approach is difficult to apply in practice, in the present study the electrochemical behaviour of a nickel surface in ammonium carbonate was compared to that in sodium hydroxide using cyclic voltammetry. It was found that the electrochemical behaviour changes significantly when changing the electrolyte.

---

## 1. Introduction

In order to counteract environmental air pollution, legislation worldwide increasingly limits the permitted amounts of exhaust gases from internal combustion engines. Nitrogen oxides (NO<sub>x</sub>), meaning the sum of nitrogen monoxide NO and nitrogen dioxide NO<sub>2</sub> have attracted attention in recent years in connection with the discussions about the diesel-engine's NO<sub>x</sub> emissions. In contrast to gasoline engines, diesel engines are in general operated with a lean combustion mixture, meaning that a stoichiometric excess of oxygen compared to the amount of fuel is present inside the combustion chamber [1]. For this case, the on-board chemical reduction of NO<sub>x</sub> is a complex process due to undesired reactions of exhaust's potential reducing agents (unburned hydrocarbons, carbon monoxide) with the oxygen present in the lean exhaust gas. Therefore, vehicles operated by diesel engines require an additional technology for reduction of NO<sub>x</sub> emissions since the

introduction of the EURO VI standard. Besides the lean  $\text{NO}_x$ -trap catalyst, which is mainly used for light duty applications, the selective catalytic reduction process is the most commonly used technology for elimination of  $\text{NO}_x$  emissions from lean exhaust gas [2]. The selective catalytic reduction process requires ammonia as external reducing agent and must be carried on-board as additional operating material. However, as ammonia is a toxic gas at ambient conditions, the reducing agent is carried on-board in form of the precursor urea. Therefore, urea as 32.5% by mass solution in water (“AdBlue” or “DEF”) is used as external reducing agent. The process of  $\text{NO}_x$  reduction is thus preceded by the process of urea decomposition to ammonia. While modern SCR catalytic coatings reach 90%  $\text{NO}_x$  reduction at exhaust temperatures of 165 °C [2], for the case of available ammonia, the decomposition of urea to ammonia requires temperatures of at least 180–190 °C even when applying a hydrolysis catalyst (e.g.,  $\text{TiO}_2$ ) [3]. Since modern diesel engines have become more and more efficient over the last years, a decline of exhaust temperature could be observed concurrently [4]. Hence, in case of low-load driving like in city traffic, the decomposition process of urea to ammonia limits the applicability of the overall selective catalytic reduction system. Consequently, methods enabling preparation of ammonia at lower temperatures would reduce  $\text{NO}_x$  emissions of diesel vehicles at low exhaust temperatures [5].

One electrochemical approach for decomposing urea in the liquid phase at low temperatures was presented by Lu et al. [6]. In their study they showed that a nickel-based electrode was able to increase the rate of ammonia generation by a factor of ~28 in comparison to the thermal hydrolysis of urea at a temperature as low as 70 °C. The investigations were carried out in AdBlue containing 7 M KOH. In a further publication the same authors presented mechanistic studies on this electrochemically induced conversion of urea to ammonia [7]. They concluded that nickel oxyhydroxide,  $\text{NiOOH}$  is the species catalytically active in the decomposition of urea on the nickel surface [8]. However, since all these studies were carried out in urea solutions containing potassium hydroxide at relatively high concentrations, the experiments represent an approach which is difficult to implement in practice. The most desirable approach in terms of practicability would be to use AdBlue without any additives or in general without changing its composition. Along with the decomposition of urea in aqueous solution, the evolution of carbon dioxide takes place in addition to the formation of ammonia. If the reaction is carried out in aqueous solution, an ammonium carbonate solution is formed by dissolution.

Because of that, in this study the electrochemical behaviour of a nickel electrode in ammonium carbonate solutions was investigated by cyclic voltammetry studies and compared to the behaviour of the nickel electrode in sodium hydroxide solution.

## 2. Experimental

### 2.1 Reagents and chemicals

Sodium hydroxide, purity "p.a." was purchased from Merck. Ammonium carbonate, purity "pure food grade" was purchased from AppliChem. Millipore water was used throughout the experiments.

### 2.2 Instrumentation

A laboratory-made nickel-disc electrode was used in the experiments. A nickel wire (diameter 0.5 mm) was embedded into the tip of a glass pipette, using epoxy resin. For the cyclic voltammetry studies a three electrode configuration was applied consisting of the working electrode (nickel disc) which was polished before each experiment, the auxiliary electrode (platinum wire) and the reference electrode (Ag/AgCl/3 M KCl). The schematic setup is shown in Fig. 1.

A 797 VA Computrace of Metrohm was used as potentiostat. To enable cyclic voltammetry experiments at elevated temperatures, a reaction vessel with a thermostat jacket and a Haake D8 thermostat were used. To keep the reference electrode at a constant temperature and thereby enable comparability of the potentials in the different experiments, the reference electrode was placed in an external compartment, connected to the reaction vessel via a salt bridge filled with 3 M KCl. The experiments were performed with the following voltammetric parameters: sweep rate:  $50 \text{ mV s}^{-1}$ , voltage step: 0.001 V, number of sweeps: 30.

## 3. Results and discussion

Since signals in the cyclic voltammograms of ammonium carbonate were growing during the experiments, cyclic voltammograms in both electrolytes were repeated 30 times and the 30th sweep of each experiment is shown in Figs. 2 and 3. First, the behaviour of the nickel electrode in sodium hydroxide solutions of different concentrations (0.1 M, 0.5 M, 1.0 M, 2.0 M and 4.0 M) was investigated at 25 °C and 40 °C. The results of each cyclic voltammetry experiment are shown in Fig. 2.

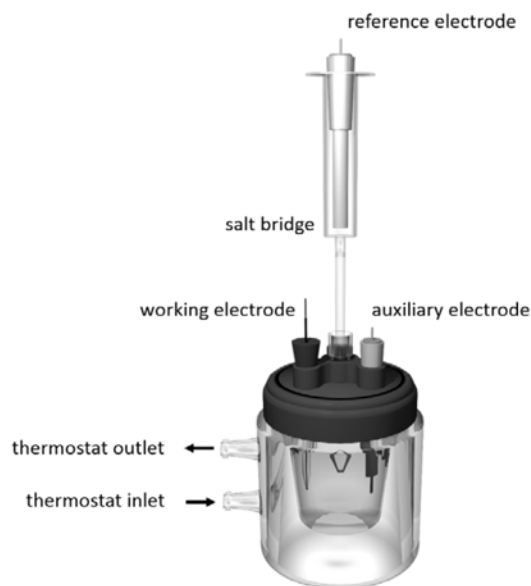


**Fig. 1** Schematic setup of the electrochemical cell configuration.

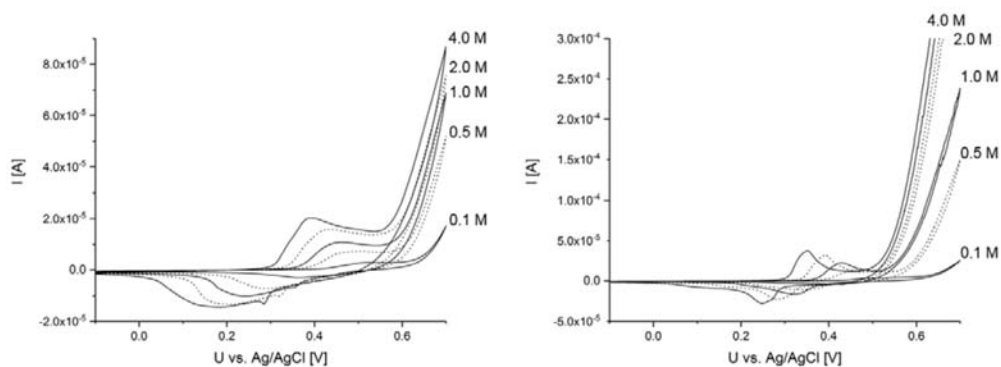


**Fig. 2** Cyclic voltammograms of a nickel-disc electrode ( $d = 0.5$  mm) in sodium hydroxide solutions of various concentrations, left: at 25 °C, right: at 40 °C.

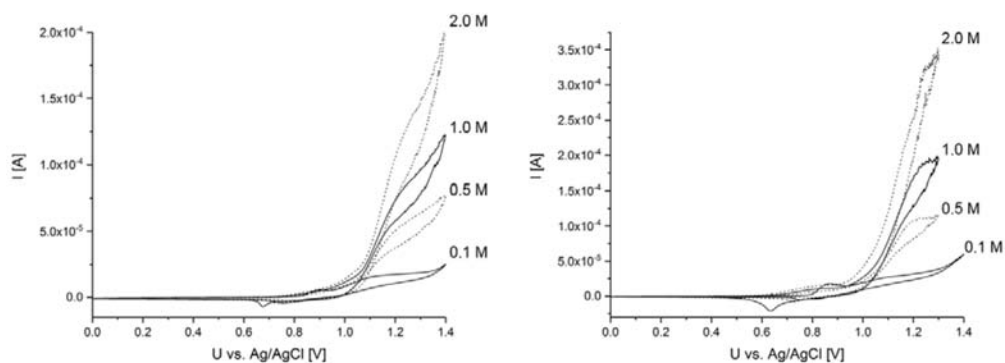


**Fig. 3** Cyclic voltammograms of a nickel-disc electrode ( $d = 0.5$  mm) in ammonium carbonate solutions of various concentrations, left: at 25 °C, right: at 40 °C.

As can be seen for all investigated concentrations, at 25 °C and 40 °C there is a signal of oxidation and reduction for the nickel surface. According to literature the process can be attributed to the oxidation of  $\text{Ni}^{2+}$  to  $\text{Ni}^{3+}$  [9] by



thereby forming NiOOH which was shown to be catalytically active concerning the decomposition of urea [7].

In the next step the cyclic voltammetry experiments were carried out in ammonium carbonate solutions of different concentrations (0.1 M, 0.5 M, 1.0 M, and 2.0 M). The experiments were again carried out at 25 °C and 40 °C. The results of these experiments are shown in Fig. 3.

Regarding the 0.1 M ammonium carbonate solution, two oxidation signals at potentials of about 0.9 V and 1.1 V and one reduction signal at about 0.65 V were

found in the cyclic voltammetry experiments for both temperatures. The reduction signal was of similar size as the oxidation peak at 0.9 V. The oxidation, as well as the reduction, signals were growing with the number of sweeps during the experiment, meaning the signals did not reach a steady state even after the recording of 30 cyclic voltammograms. As can be seen, the intensity of the signals at 0.65 V and 0.9 V was most pronounced in the experiments with low ammonium carbonate concentrations. In the experiments with 0.5 M, 1.0 M and 2.0 M ammonium carbonate at 25 °C and 40 °C, these signals were much weaker. This finding was additionally confirmed by an experiment with a 0.05 M ammonium carbonate solution. Literature indicates that these signals could be related to the transition  $\text{Ni}^{2+}/\text{Ni}^{3+}$  [10]. However, as visible in Fig. 3 the intensity of the second oxidation peak increased by increasing the ammonium carbonate concentration, which can be an indication that the oxidation peak at about 1.1 V is due to the oxidation of ammonia on the nickel surface [10]. Besides the experiments shown in Fig. 3, the cyclic voltammetry experiment with 0.1 M ammonium carbonate was also carried out with the upper vertex potential being 1.0 V instead of 1.4 V. In this case the signals at 0.65 V and 0.9 V could not be detected. This observation shows that this process cannot proceed independently of processes occurring at potentials >1.0 V. One possible explanation might be a local acidic pH shift at the nickel electrode, which is associated with the formation of oxygen at high potentials with progressing experiment.

#### 4. Conclusions

The presented results show that the behaviour of the nickel electrode studied by cyclic voltammetry experiments changes significantly by changing the electrolyte from sodium hydroxide to ammonium carbonate. Oxidation of the nickel surface might also occur in the ammonium carbonate solutions. However, further detailed studies are necessary. Experiments with urea dissolved in sodium hydroxide as well as ammonium carbonate solutions are planned in order to evaluate possible interactions between the species formed on the nickel surface and urea.

#### References

- [1] Tschöke H., Mollenhauer K., Maier R.: *Handbuch Dieselmotoren*, 4th ed. Wiesbaden, Springer 2018.
- [2] Braun P., Gebhard J., Matysik F.M., Rabl H.P.: Potential technical approaches for improving low-temperature  $\text{NO}_x$  conversion of exhaust aftertreatment systems. *Chem. Ing. Tech.* **90** (2018), 762–773.
- [3] Bernhard A.M., Peitz D., Elsener M., Schildhauer T, Kröcher O.: Catalytic urea hydrolysis in the selective catalytic reduction of  $\text{NO}_x$ : catalyst screening and kinetics on anatase  $\text{TiO}_2$  and  $\text{ZrO}_2$ . *Catal. Sci. Technol.* **3** (2013), 942–951.
- [4] Braun P., Gebhard J., Rabl H.P.: Low temperature De $\text{NO}_x$ . *Final Report FVV project 1155*, 2017.
- [5] Roppertz A., Föger S., Kureti S.: Investigation of urea-SCR at low temperatures. *Top. Catal.* **60** (2017), 199–203.

- [6] Lu F, Botte G.G.: Electrochemically induced conversion of urea to ammonia. *ECS Electrochem. Lett.* **4** (2015), E5–E7.
- [7] Lu F, Botte G.G.: Understanding the electrochemically induced conversion of urea to ammonia using nickel based catalysts. *Electrochim. Acta* **246** (2017), 564–571.
- [8] Daramola D.A., Singh D., Botte G.G.: Dissociation rates of urea in the presence of NiOOH catalyst: A DFT analysis. *J. Phys Chem. A* **114** (2010), 11513–11521.
- [9] Hahn F, Floner D., Beden B., Lamy C.: In situ investigation of the behaviour of a nickel electrode in alkaline solution by UV-Vis and IR reflectance spectroscopies. *Electrochim. Acta* **32** (1987), 1631–1636.
- [10] Zheng G., Cao H., Zheng L.: Influence of ammonia concentration on anodic deposition of nickel oxide. *J. Appl. Electrochem.* **37** (2007), 799–803.

# Simultaneous determination of synthetic dyes Ponceau 4R (E124) and Sunset Yellow (E110) by fluorimetry in soft drinks

ALENA A. NIKOLAEVA<sup>a,\*</sup>, ELIZABETH V. BULYCHEVA<sup>a</sup>, ELENA I. KOROTKOVA<sup>a</sup>,  
WOLFGANG LINERT<sup>b</sup>

<sup>a</sup> Department of Chemical Engineering, Engineering School of Natural Resources, National Research Tomsk Polytechnic University, Lenin avenue 30, 634050, Tomsk, Russia

✉ [ivanovaaa@tpu.ru](mailto:ivanovaaa@tpu.ru)

<sup>b</sup> Institute of Applied Chemistry, Technical University of Vienna, Getreidemarkt 9, 1060, Vienna, Austria

## Keywords

fluorimetry  
simultaneous  
determination  
synthetic dyes

## Abstract

A fluorimetric method for simultaneous determination and quantification for of the synthetic food azo dyes Sunset Yellow (E110) and Ponceau 4R (E124) in soft drinks is proposed, which is characterized by high sensitivity and selectivity. These dyes are widely used in soft drinks, as they have a bright and attractive orange color. For determination of the dyes in beverages the working conditions for the analysis were selected: excitation wavelength is 330 nm, logging interval is from 350 to 500 nm for Ponceau 4R; the excitation wavelength is 250 nm, logging interval is from 280 to 450 nm for Sunset Yellow. The possibility of simultaneous determination of two dyes of a red shade in a mixture is proved, as well as the repeatability of measurements of food azo dyes determination in non-alcoholic beverages by fluorimetric and spectrophotometric methods of analysis.

---

## 1. Introduction

The most frequently used of synthetic food colours is the group of azo dyes [1], which is characterized by the presence of one or more azo groups  $-N=N-$  in the molecule. Unfortunately, azo dyes are often potential carcinogens [2].

“Ponceau”, identical to “Crimson” (food additive E124) is a dye of synthetic origin, which exhibiting a red colour [3]. Sunset Yellow (food additive E110) is used to coloration of many products in orange colours [4]. A mixture of synthetic dyes E110 and E124 is often used to produce caramel shades in the production of fruit fillings “Rowan with cognac” and soft drinks “pear”.

Feketea et al. [5] commissioned by the Food Standards Agency of the United Kingdom (FSA) conducted studies that showed that the use of products containing azo dyes leads to increased hyperactivity and reduced attention concentration in children.

This encouraged us to develop rapid, inexpensive and accurate methods to determination of dyes in food as an urgent task for solving problems of quality control and food safety. To date, many analytical methods are used to analyze the synthetic dyes [6]: chromatographic, spectrophotometric, electrochemical and capillary electrophoresis. But among the listed methods of determination of several dyes in a mixture is possible only with the help of expensive and time consuming chromatographic methods.

In the literature, there are also references concerning the application of the fluorimetric method for the determination of dyes [7, 8]. However, despite a number of merits of fluorimetric analysis, such as high sensitivity, a wide range of detectable concentrations, simplicity of instrumentation, the application of this method to dye studies has not been paid enough attention.

The aim of this research was to develop a fluorimetric technique for the simultaneous determination of synthetic food dyes Ponceau 4R (E124) and Sunset Yellow (E110) in a mixture in model solutions and non-alcoholic beverages. As a comparison method, a spectrophotometric analysis method was used.

## 2. Experimental

### 2.1 Reagents and chemicals

Work solutions of the dyes Ponceau 4R and Sunset Yellow ( $c = 10.00 \text{ mg dm}^{-3}$ ) were prepared using a reference substance of dye with 95% purity. Soft drinks were chosen as the main target of the research for the determination of synthetic food colors of Ponceau 4R (E124) and Sunset Yellow (E110): “Japanese pear”, manufacturer of TM Irbis, Russia, Novokuznetsk; “Mirinda”, manufacturer of PepsiCo, Spain; “Irn-Bru” (Iron brew), manufacturer of A.G. Barr p.l.c., Scotland.

### 2.2 Instrumentation

The investigations were carried out on a Fluorat-02-Panorama Fluid Analyzer. The principle of the analyzer is based on measuring the intensities of the light fluxes from the object under investigation, which arise under the action of exciting optical radiation of the selected spectral range and recorded by the optical receivers of the device.

Spectrophotometric determination of Ponceau 4R and Sunset Yellow in beverages was carried out using the Agilent Technology Cary 60 UV-Vis spectrophotometer. The quantitative concentration of E124 and E110 dyes in the beverages studied was determined using a calibration curve of the dependence of the optical density of beverage solutions on the concentration of standard dye solutions. Sample preparation of the beverages for spectrophotometric determination was carried out in accordance with GOST P 52470-2005 “Food products. Methods for identification and determination of the mass concentration of

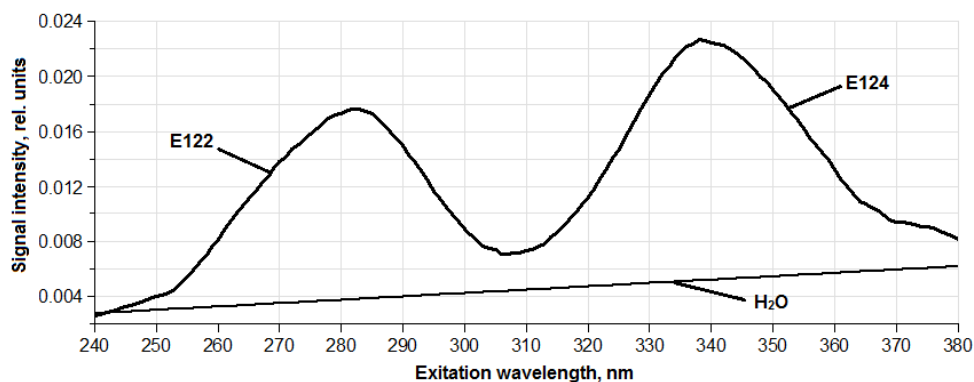


**Fig. 1** Synchronous scanning of a mixture of azo dyes ( $c = 10 \text{ mg dm}^{-3}$ ,  $V = 3 \text{ ml}$ ) with a monochromator displacing 60 nm: E110 – Sunset Yellow, E124 – Ponceau 4R, and water.

synthetic dyes in alcohol products” and GOST P 52671-2006 “Food products. Methods for identification and determination of the mass concentration of synthetic dyes in caramel”.

### 2.3 Sample preparation

The sample preparation of the beverages studied consisted of diluting the initial sample 1:100 with distilled water, which made it possible to get rid of the harmful influence of other components in the beverages. The quantitative concentration of the test dyes in the samples of soft drinks was determined using a calibration curve of the dependence of fluorescence signal intensity on the concentration of the dye, which was constructed using standard solutions.

## 3. Results and discussion

At the first stage of the work, the dyes Sunset Yellow (E110) and Ponceau 4R (E124) were synchronously scanned in order to search for all potential excitation wavelengths at which the dye luminescence process is possible [9]. The investigation showed that the highest signal intensity is observed at an excitation wavelength of 330 nm for Ponceau 4R and 250 nm for the Sunset Yellow. In this regard, the synchronous scanning mode was subsequently used as the major mode for simultaneous identification of two dyes E110 and E124 in the mixture (Fig. 1).

With the benefit of the addition option of fluoride-02-Panorama is “Analysis of a multicomponent mixture”, mixtures of two dyes Ponceau 4R and a Sunset Yellow in different splits were investigated (Table 1). As the Table 1 shows, using fluorimetric analysis, it is possible to quantitatively determine synthetic food dyes in a mixture without constructing a calibration curve with a single standard solution of each dye in the mixture.

**Table 1**

Fluorimetric analysis of the simultaneous determination of dyes E110 – Sunset Yellow and E124 – Ponceau 4R ( $c_{\text{total}} = 10 \text{ mg dm}^{-3}$ ).

Dyes ratio (E110:E124)	$c_{\text{added}} / \text{mg dm}^{-3}$	$c_{\text{assay}} / \text{mg dm}^{-3}$
3:1	7.50:2.50	8.00:2.20
1:3	2.50:7.50	3.58:7.22
3:3	5.00:5.00	5.45:4.43

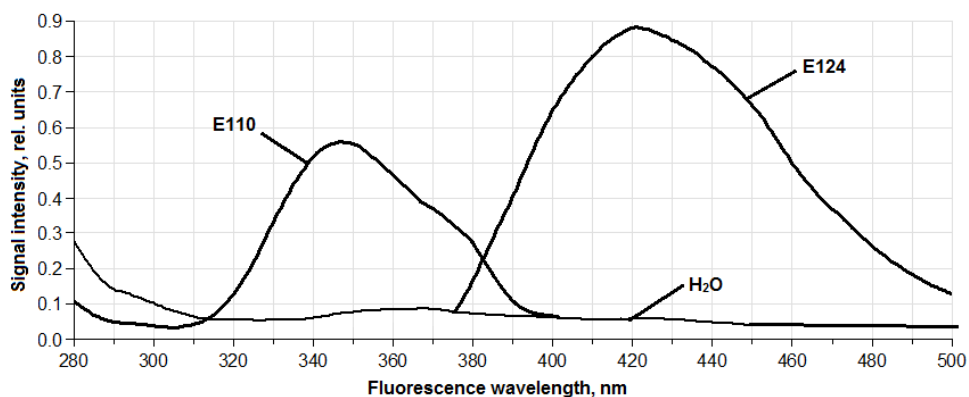


**Fig. 2** Luminescent spectrums of aqueous solutions of dye standards ( $c = 10 \text{ mg dm}^{-3}$ ): E110 – Sunset Yellow, E124 – Ponceau 4R, and water.

It can be seen from Fig. 2 that a maximum of fluorescence is observed at a detection wavelength of 420 nm for Ponceau 4R and 347 nm for a Sunset Yellow. The obtained wavelengths are used as operating fluorescence wavelengths to determine the dyes in the test beverages.

To determine the dyes to be studied in beverage samples, a series of standard dye solutions of various concentrations were prepared using a calibration plot and the fluorescence intensity of dyes under the same conditions was measured. According to the calibration graph in the concentration range from 0.10 to 1.00  $\text{mg dm}^{-3}$  with regression equation for Sunset Yellow (E110)

$$I = 0.0442x + 0.1478 \quad (1)$$

$$R^2 = 0.9919$$

and for Ponceau 4R (E124)

$$I = 0.0355x + 0.0081 \quad (2)$$

$$R^2 = 0.9922$$

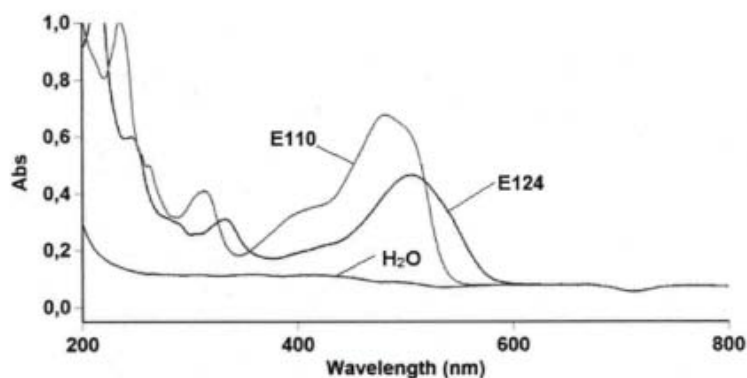


**Fig. 3** Absorbance spectrums of aqueous solutions of dye standards ( $c = 10 \text{ mg dm}^{-3}$ ): E110 – Sunset yellow, E124 – Ponceau 4R, and water.

a quantitative determination of the dyes in non-alcoholic beverages has been carried out. As a comparison method, a spectrophotometric method for the analysis of synthetic food dyes was used.

To determine the wavelength corresponding to the maximum of absorptivity, the spectrums of standard solutions of the Sunset Yellow and Ponceau 4R and the research beverages were recorded in the wavelength range 400–650 nm (Fig. 3). From the figure becomes obvious that the absorption maximum, both for the standard solution and for the test beverage, corresponds to the Sunset Yellow is 482 nm, and for the Ponceau 4R is 505 nm, which corresponds to GOST R and literature [10].

For the quantitative determination of food dyes in the research samples of beverages, the calibration curve for the dependence of the optical density of the solution on the concentration of standard solutions E110 and E124 at a wavelength of 482 nm and 505 nm, respectively, was constructed. The calibration graph is linear in the concentration range  $1.00\text{--}10.00 \text{ mg dm}^{-3}$  with the regression equation for Sunset Yellow (E110)

$$\begin{aligned} A &= 0.0579x + 0.0923 \\ R^2 &= 0.9972 \end{aligned} \quad (3)$$

and for Ponceau 4R

$$\begin{aligned} A &= 0.0391x + 0.0827 \\ R^2 &= 0.9995 \end{aligned} \quad (4)$$

The results of the determination of the synthetic food dyes of the Sunset Yellow and Ponceau 4R in soft drinks by two methods of analysis are presented in Table 2.

**Table 2**

Results of the determination of the E110 –Sunset Yellow and E124 –Ponceau 4R in soft drinks by fluorimetric and spectrophotometric methods of analysis ( $n = 3, p = 0.95, t_{\text{table}} = 4.3$ ).

Soft drink	Dye	Fluorimetric method		Spectrophotometric method		$t_{\text{calc}}$
		$c_{\text{dye}}/\text{mg dm}^{-3}$	$s_r$	$c_{\text{dye}}/\text{mg dm}^{-3}$	$s_r$	
“Mirinda”	E110	45.29±1.42	0.02	44.78±1.86	0.03	1.37
“Japanese pear”	E124	30.05±0.09	0.01	30.03±0.03	0.02	1.41
“Irn-Bru”	E110	21.18±0.07	0.03	–	–	–
	E124	17.08±1.06	0.02	–	–	–

From the table it is seen that the repeatability measurements of fluorimetric and spectrophotometric analysis is appeared. Besides, it was found that the concentration of dyes in all samples of beverages studied does not exceed the permissible norm of  $50 \text{ mg dm}^{-3}$ .

#### 4. Conclusions

The investigations carried out show the possibility and usefulness of fluorimetric method for the simultaneous analysis of qualitative and quantitative determination of synthetic food dyes Sunset Yellow (E110) and Ponceau 4R (E124) in a mixture in soft drinks without using complex and prolonged sample preparation. Compared to the spectrophotometric analysis for the determination of dyes in food products, the fluorimetric analysis are characterized by higher sensitivity, selectivity and simple sample preparation, and also allows the simultaneous detection of two dyes of red shades in the mixture.

#### Acknowledgments

The work is supported by grant of Ministry of Education and Science of Russian Federation for program “Science”.

#### References

- [1] Dotto G.L., Vieira M.L.G., V. M. Esquerdo M.V., Pinto L.A.A.: Equilibrium and thermodynamics of azo dyes biosorption onto *Spirulina platensis*. *Braz. J. Chem. Eng.* 30 (2013), 13–21.
- [2] Abe F.R., Mendonça J.N., Moraes L.A., Oliveira G.A., Gravato C., Soares A.M., Oliveira D.P.: Toxicological and behavioral responses as a tool to assess the effects of natural and synthetic dyes on zebrafish early life. *J. Chemosphere* 178 (2017), 282–290.
- [3] Bevzuik K., Chebotarev A., Snigur D., Bazel Y., Fizer M., Sidey V.: Spectrophotometric and theoretical studies of the protonation of Allura Red AC and Ponceau 4R. *J. Mol. Struct.* 1144 (2017), 216–224.
- [4] Hamza M.S., Al-Sibaai A.A., Bashammakh A.S., Al-Saidi H.M. A new method for analysis of sunset yellow in food samples based on cloud point extraction prior to spectrophotometric determination. *J. Ind. Eng. Chem.* 19 (2013), 529–535.
- [5] Feketea G., Tsadouri S.: Common food colorants and allergic reactions in children: Myth or reality? *J. Food Chem.* 230 (2017), 578–588.

- [6] Yamjala K., Nainar M.S., Ramiseti N.R.: Methods for the analysis of azo dyes employed in food industry. *J. Food Chem.* **192** (2016), 813–824.
- [7] Kashi A., Waxman S.M., Komaiko J.S., Draganski A., Corradini M.G., Ludescher R.D.: Potential use of food synthetic colors as intrinsic luminescent probes of the physical state of foods. *J. Chem. Sens. Inf. Food: Measum. Anal.* **1191** (2015), 253–267.
- [8] Zhang J., Na L., Jiang Y., Han D., Lou D., Jin L.: A fluorescence-quenching method for quantitative analysis of Ponceau 4R in beverage. *J. Food Chem.* **221** (2017), 803–808.
- [9] Samari F., Yousefinejad S.: Quantitative structural modeling on the wavelength interval in synchronous fluorescence spectroscopy. *J. Mol. Struct.* **1148** (2017), 101–110.
- [10] Benvindi A., Abbasi S., Gharaghani S., Dehghan M.D., Masoum S.: Spectrophotometric determination of synthetic colorants using PSO-GA-ANN. *J. Food Chem.* **220** (2017), 377–384.

# Analysis of *Lactococcus lactis* modified with zinc ions by capillary electrophoresis

ANNA KRÓL<sup>a, b, \*</sup>, PAWEŁ POMASTOWSKI<sup>b</sup>, VIORICA RAILEAN-PLUGARU<sup>a, b</sup>,  
BOGUSŁAW BUSZEWSKI<sup>a, b</sup>

<sup>a</sup> Department of Environmental Chemistry and Bioanalytics, Faculty of Chemistry, Nicolaus Copernicus University, Gagarina Street 7, 87-100 Toruń, Poland ✉ annkrol18@gmail.com

<sup>b</sup> Interdisciplinary Centre for Modern Technologies, Nicolaus Copernicus University, Toruń, Poland

## Keywords

bacterial aggregation  
capillary electrophoresis  
*Lactococcus lactis*  
zinc ions

## Abstract

Adhesion to the capillary surface and uncontrolled aggregation of bacterial cells is a significant drawback of capillary electrophoresis. In our study, the influence of the *Lactococcus lactis* surface modification by zinc ions at different concentration was determined. Results of the study indicated that using a  $Zn^{2+}$  caused the uncontrolled aggregation of bacterial cells and new peaks of microbial agglomerates were observed in the electropherogram. Capillary electrophoresis was performed in an isotachopheretic mode using Tris + boric acid + hydrochloric acid (inlet) and Tris + boric acid (outlet) buffers at pH = 7.3 and 8.0, respectively. In addition, data from fluorescence microscopy pointed out if capillary electrophoresis does not cause the death of microbial cells but only their damage. Therefore, CE may be a potential method for evaluating the aggregation activity of different types of metal ions against microbial cells.

---

## 1. Introduction

Nowadays, the use of capillary electrophoresis (CE) for the analysis, identification, and characterization of different types of microorganisms has received much attention. This technique has been found to provide many advantages such as high separation efficiency, short analysis time or the possibility of direct analysis of biological samples [1, 2]. There is a few examples of the CE use for the determination of bacterial pathogens [3], yeast cells [4] or various types of viruses [5]. Unfortunately, this analytical method has limitations such as uncontrolled aggregation of bacterial cells and their adhesion to the capillary surface [6]. Microorganisms are often consider as a biocolloids, mainly due to the complex structure of their cell wall, and the understanding of the electrophoretic process is more complicated for such a particles. The cell wall composition is characteristic for various types of bacterial species, they have different content of proteins, phospholipids, polysaccharides or another organic components [7]. All compounds present in the bacterial cell wall structure strongly affects the surface

charge of microorganisms. It can be explained by the presence of many functional groups undergoing the protonation process. Therefore, it is important to develop a method allowing to eliminate the aggregation and adhesion problem. Some research groups have proposed the addition of poly(ethylene oxide) to the buffer solution [8, 9] which functioned as a focussing agent. Another approach is capillary surface modification by the chemicals such as divinylbenzene or trimethylchlorosilane acrylamide [10, 11]. Recently, the new approach was suggested; it is based on the modification of the bacterial surface by specific divalent metal ions such as, e.g. calcium [12]. Application of this method may result in the controlled aggregation of microorganisms cells. Although several surface modifications by calcium ions have been evaluated for the separation of microorganisms [12], there is a lack of papers described bacteria surface modification via another types of divalent metal ions, e.g. zinc ions. Therefore, understanding the influence of different ions on microorganisms surfaces and their potential use for further modifications, is pivotal for analytical chemistry. Such a problem led our research group to the main task of the conducted experiment. The main aim of this study was to investigate the electrophoretic behavior of lactic acid strain of Gram(+) *Lactococcus lactis* during CE analysis and to examine the influence of  $Zn^{2+}$  ions at different concentration on the bacterial cells aggregation. Additionally, the viability of *Lactococcus lactis* before and after CE analysis by using fluorescence microscopy was performed.

## 2. Experimental

### 2.1. Sample preparation for CE analysis

The required number of cells in 1 mL of the suspension was achieved by the serial dilution. The bacterial pellet were then suspended in the solution of zinc nitrate at 1, 3 or 10 mM concentration and incubated for 1 hour at the room temperature. After the incubation, the suspension was centrifuged (20 °C, 9000 rpm, 15 min) and the obtained precipitate was washed twice with distilled water and transferred to the outlet TB buffer (Tris and boric acid; pH = 8.0). As a control, unmodified *Lactococcus lactis* cells were used.

### 2.2 Capillary electrophoresis analysis

Capillary electrophoresis analysis were performed using PA 800 plus (Beckman Coulter system, Brea, USA) equipped with a DAD with the use of fused silica capillary (i.d. = 75  $\mu$ m;  $L_{tot}$  = 33.5 cm;  $L_{eff}$  = 25 cm; Composite Metal Services, Shipley, UK). The bacterial samples were injected into the capillary with a pressure mode (10 psi, 8 s) and the analysis were performed at a constant voltage (20 kV) and the temperature at 23°C. As the inlet buffer, TBH (Tris, boric acid and hydrochloric acid; pH = 7.3) were choose. The samples were detected at  $\lambda$  = 214 nm.

### 2.3. Fluorescence microscopy analysis

Determination of *Lactococcus lactis* cells viability after the CE analysis was performed by using fluorescence microscopy approach according to the [13]. During the CE analysis, fractions of bacterial cells not and modified with zinc ions were collected. Obtained bacterial samples were then stained using acridine orange (0.12 µg/mL) and ethidium bromide (0.4 µg/mL) and analyzed using a Zeiss Axiocom D1 (Germany) fluorescence microscope with the set of filters (43 He and 38). Recorded images were analyzed with Axio Vision 4.8. software.

### 3. Results and discussion

In this study, Gram(+) *Lactococcus lactis* modified with the different concentration of zinc ions (1, 3, and 10 mM) were examined in an applied voltage of 20 kV. Bacterial strain without any surface modification was tested as a control sample (Fig. 1A). The electromigration time of the probiotic strain modified by the zinc nitrate solution at concentration of 1, 3 and 10 mM was 2.026 ( $RSD = 0.784\%$ ), 2.064 ( $RSD = 1.287\%$ ) and 2.083 ( $RSD = 0.512\%$ ) min respectively. Application of electrophoretic buffers with different ionic strength (TB and TBH) allowed focusing the zone of control sample at the electromigration time of 1.670 min ( $RSD = 1.794\%$ ). It is in a good correlation with the results obtained by Pomastowski et al. [14], who have observed the peak of *Lactococcus lactis* ATCC 11454 at migration time of about 2 minutes. All electrophoretic analysis were reproducible because of the migration times low standard deviation values (Table 1). Moreover, the value of *Lactococcus lactis* electrophoretic mobility non- and modified with zinc ions, were decreasing with the increasing CE duration time (Table 1). Outcomes of our study show that after the *Lactococcus lactis* surface modification by  $Zn^{2+}$  ions, the formation of bacterial aggregates with different size and surface charge occurred; it was observed by an increasing number of signals in the electropherograms (Fig. 1B, C and D). The number of bacterial agglomerates rises with an increasing concentration of modifier. In the case of 1 and 3mM modification, the number of CE zones occurred at 18, whereas using of 10mM zinc nitrate resulted in the observation of 23 signals. The observed differences in the intensity, number and time of some signals, can be a consequence of the various sorption and interaction of zinc at different concentration level with bacterial proteins. Król et al. [15] have observed that addition of 3mM zinc nitrate to the probiotic strain (*Lactobacillus paracasei* LB3) have resulted in the intracellular formation of zinc oxide nanocomposites which could also form aggregates and be observed as a multiplied signals on the CE electropherogram. According to their data from FT-IR analysis, the main groups involved in the ZnO biosynthesis were carboxyl and amid groups derived from bacterial proteins. It is strongly related with results obtained in our study.

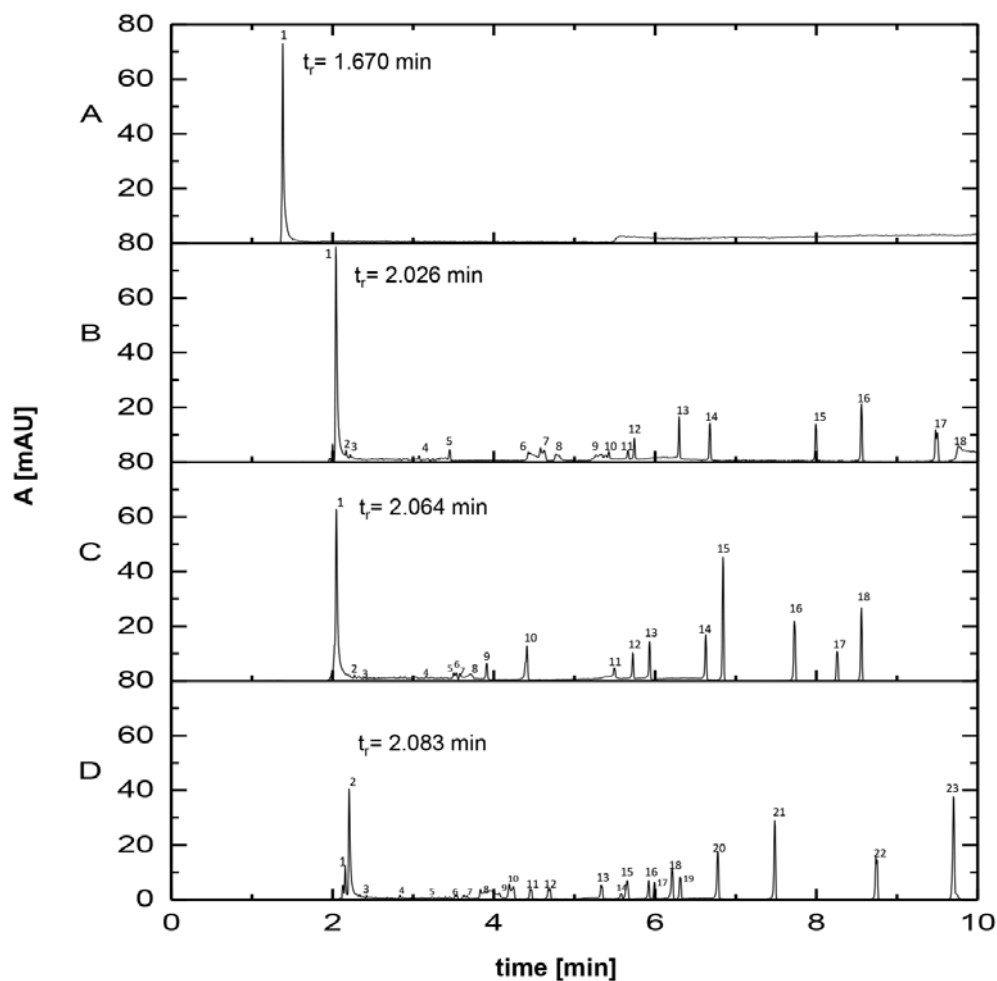
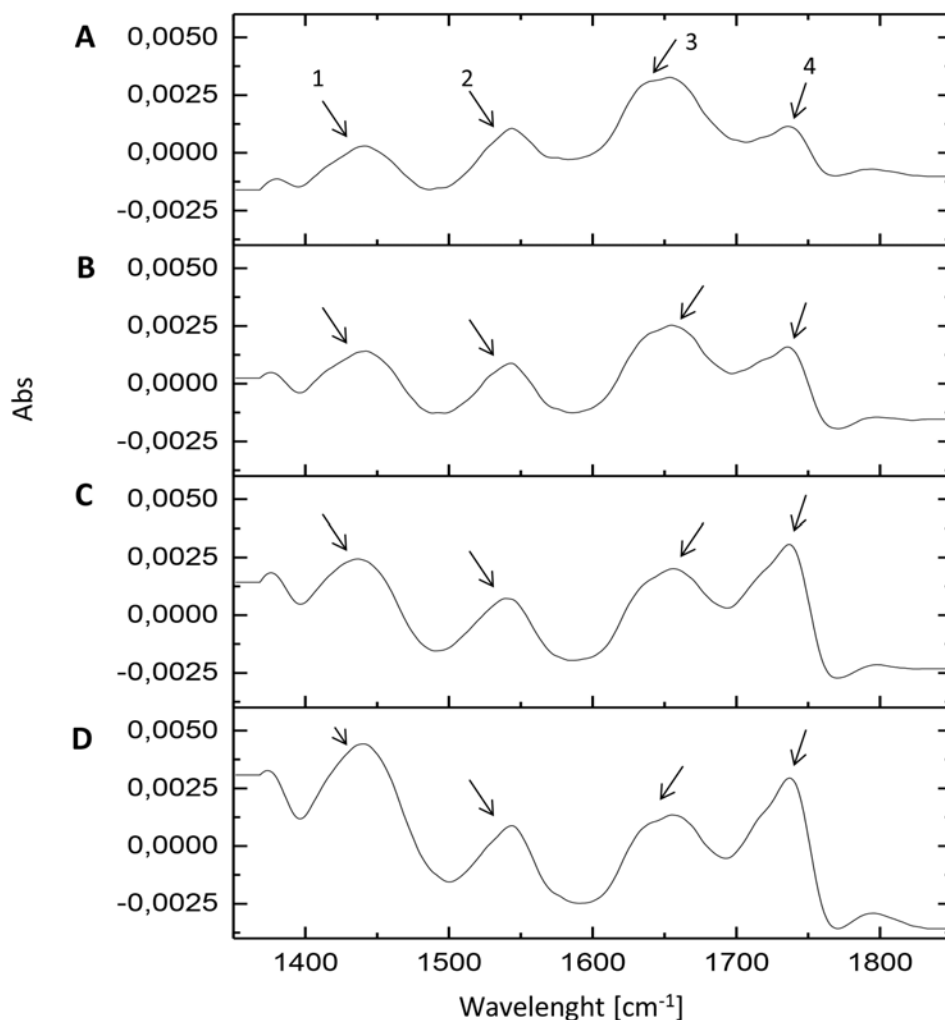


**Fig. 1** Electropherogram of (A) non-modified *Lactococcus lactis*, and modified *Lactococcus lactis* by (B) 1 mM, (C) 3mM, and (D) 10 mM of  $Zn(NO_3)_2$ . Conditions: inlet buffer: TBH (pH = 7.3), outlet buffer: TB (pH = 8.0), suspensive buffer: TB (pH = 8.0);  $I = 100 \mu A$ ,  $U = 20$  kV,  $t = 23$  °C,  $\lambda = 214$  nm,  $L = 33.5$  cm,  $L_{eff} = 25$  cm,  $\varphi = 100 \mu m$ , injection: 10 psi,  $t = 8$  s.

**Table 1**  
Migration times and electrophoretic mobility of *Lactococcus lactis* modified with different concentration of zinc ions.

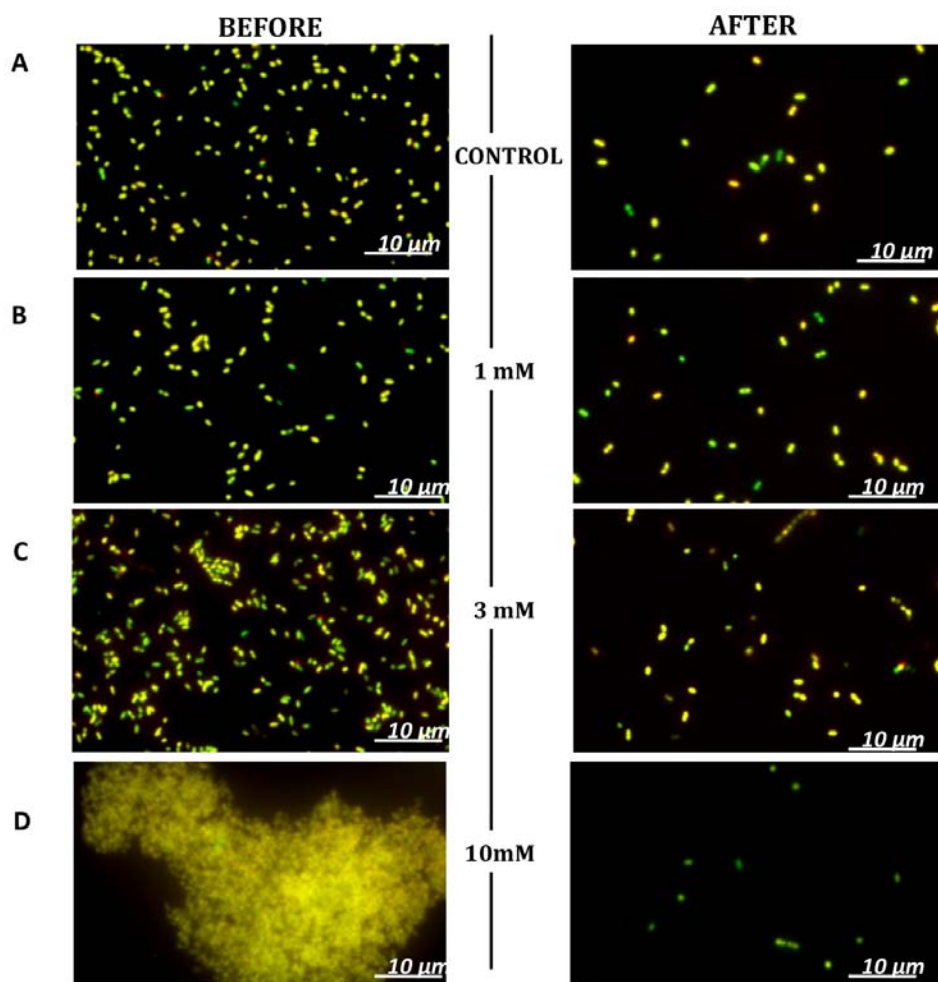
1mM Zn <sup>2+</sup>			3mM Zn <sup>2+</sup>			10mM Zn <sup>2+</sup>		
t / min	μ / cm <sup>2</sup> V <sup>-1</sup> s <sup>-1</sup>	RSD / %	t / min	μ / cm <sup>2</sup> V <sup>-1</sup> s <sup>-1</sup>	RSD / %	t / min	μ / cm <sup>2</sup> V <sup>-1</sup> s <sup>-1</sup>	RSD / %
2.026	2.07×10 <sup>-2</sup>	0.784	2.064	2.03×10 <sup>-2</sup>	1.287	2.083	2.01×10 <sup>-2</sup>	0.512
2.173	1.93×10 <sup>-2</sup>	0.981	2.241	1.87×10 <sup>-2</sup>	1.427	2.143	1.95×10 <sup>-2</sup>	0.498
2.230	1.88×10 <sup>-2</sup>	0.713	2.372	1.77×10 <sup>-2</sup>	1.490	2.407	1.74×10 <sup>-2</sup>	0.443
3.093	1.35×10 <sup>-2</sup>	1.397	3.024	1.38×10 <sup>-2</sup>	0.705	2.896	1.45×10 <sup>-2</sup>	1.473
3.427	1.22×10 <sup>-2</sup>	0.802	3.182	1.32×10 <sup>-2</sup>	0.670	3.306	1.27×10 <sup>-2</sup>	0.164
4.464	9.38×10 <sup>-3</sup>	0.899	3.455	1.21×10 <sup>-2</sup>	2.063	3.430	1.22×10 <sup>-2</sup>	0.927
4.598	9.11×10 <sup>-3</sup>	1.494	3.539	1.18×10 <sup>-2</sup>	1.664	3.642	1.15×10 <sup>-2</sup>	0.246
4.631	9.04×10 <sup>-3</sup>	1.494	3.656	1.15×10 <sup>-2</sup>	1.744	3.920	1.07×10 <sup>-2</sup>	0.272
5.309	7.89×10 <sup>-3</sup>	0.878	3.908	1.07×10 <sup>-2</sup>	0.412	4.062	1.03×10 <sup>-2</sup>	1.008
5.410	7.74×10 <sup>-3</sup>	0.197	4.451	9.41×10 <sup>-3</sup>	1.315	4.198	9.98×10 <sup>-3</sup>	1.519
5.580	7.51×10 <sup>-3</sup>	2.005	5.546	7.55×10 <sup>-3</sup>	1.554	4.496	9.32×10 <sup>-3</sup>	0.828
5.862	7.15×10 <sup>-3</sup>	2.725	5.685	7.37×10 <sup>-3</sup>	0.842	4.725	8.86×10 <sup>-3</sup>	0.451
6.299	6.65×10 <sup>-3</sup>	0.169	5.859	7.15×10 <sup>-3</sup>	1.342	5.166	8.11×10 <sup>-3</sup>	0.883
6.773	6.18×10 <sup>-3</sup>	1.886	6.524	6.42×10 <sup>-3</sup>	2.135	5.542	7.56×10 <sup>-3</sup>	1.056
8.082	5.18×10 <sup>-3</sup>	1.430	6.788	6.17×10 <sup>-3</sup>	1.245	5.704	7.34×10 <sup>-3</sup>	0.935
8.591	4.87×10 <sup>-3</sup>	0.557	7.812	5.36×10 <sup>-3</sup>	1.499	5.945	7.04×10 <sup>-3</sup>	0.717
9.400	4.46×10 <sup>-3</sup>	1.359	8.188	5.11×10 <sup>-3</sup>	1.430	6.059	6.91×10 <sup>-3</sup>	1.252
9.712	4.31×10 <sup>-3</sup>	0.930	8.635	4.85×10 <sup>-3</sup>	1.286	6.212	6.74×10 <sup>-3</sup>	0.087
						6.310	6.64×10 <sup>-3</sup>	0.252
						6.709	6.24×10 <sup>-3</sup>	1.508
						7.560	5.54×10 <sup>-3</sup>	1.195
						8.752	4.78×10 <sup>-3</sup>	0.113
						9.639	4.34×10 <sup>-3</sup>	1.019

Fig. 2 shows the FT-IR spectra of *Lactococcus lactis* unmodified and modified by Zn<sup>2+</sup> ions. It indicated that the main groups involved in the bacterial cells aggregation process are deprotonated carboxyl groups (spectral bands at 1530–1560 cm<sup>-1</sup>) which can derive from both amino-acids of bacterial proteins and peptidoglycan of their cell wall [16]. The spectra band at 1610–1670 cm<sup>-1</sup> corresponds with amide groups of bacterial proteins. Another characteristic band appears at 1440 cm<sup>-1</sup> may derives from the stretching vibration of C–N and N–H bond from surface microbial proteins. Furthermore, as a result of the modification, the increase of the signal at 1720 cm<sup>-1</sup> intensity can be observed. It is related with the stretching vibration of carbonyl groups (C=O). Additionally, it can



**Fig. 2** FT-IR spectra for (A) non-modified *Lactococcus lactis*, and modified *Lactococcus lactis* by (B) 1 mM, (C) 3mM, and (D) 10 mM of  $Zn(NO_3)_2$ . Spectral bands: (1)  $1420-1480\text{ cm}^{-1}$ , (2)  $1530-1560\text{ cm}^{-1}$ , (3)  $1610-1670\text{ cm}^{-1}$ , and (4)  $1710-1740\text{ cm}^{-1}$ .

be observed that the most significant changes occur in the spectrum of the *Lactococcus lactis* modified by 10 mM zinc nitrate. Among the common use of capillary electrophoresis in the identification of pathogens, yeast cells and various types of viruses [3–5], a CE approach has also been applied for the direct detect of the cell viability determination. Szumski et al. [17] have performed the assessment of the viability of *Staphylococcus aureus* and *Escherichia coli* cells during capillary electrophoretic process. They have tested two different applied voltage (20 kV and 30 kV) and collected bacterial zones after CE were cultivated on the Broth Agar. In comparison to the control sample (without electric treatment),



**Fig. 3** Fluorescent microscopy analysis after the capillary electrophoresis (A) *Lactococcus lactis* non-modified, and *Lactococcus lactis* modified by (B) 1 mM, (C) 3mM, and (D) 10 mM of  $Zn(NO_3)_2$ .

only 3.4% and 0.7% of the *Escherichia coli* cells survived the applied voltage treatment of 20 kV and 30 kV, respectively. *Staphylococcus aureus* strains were found to be more resistant to the electric field, results of the experiment have shown that about 35% and 20% *Staphylococcus aureus* cells survived voltage of 20 kV and 30 kV, respectively. Szumski et al. [17] have emphasized such a significant differences is related to the different cell wall composition of treated strains. The bigger peptidoglycan layer of Gram(+) (*Staphylococcus aureus*) cell wall make them more tough and resistant to capillary electrophoresis conditions. It is in a good correlation with data received in our study. In the fluorescence microscopy assay the amount of total cells before CE were compared to the control after the CE analysis (Fig. 3). The results of the fluorescent microscopy analysis indicated that

capillary electrophoresis do not cause the death of microbial cells but only their damage. It can be explained by the fact that *Lactococcus lactis* is the Gram(+) strain with the thick peptidoglycan layer in its bacterial cell wall. Application of the fluorescence microscopy confirmed also that the modification of the bacterial cell surface with 1, 3 and 10 mM zinc ions causes their uncontrolled aggregation (Fig. 3B, C and D). The results obtained during the experiment also indicate that zinc ions with the highest concentration (10 mM) caused the greatest aggregation of the *Lactococcus lactis*.

#### 4. Conclusions

In this work, CE was used to evaluate the effect of zinc ions at different concentration level (1, 3 and 10 mM) on the *Lactococcus lactis* cells aggregation. This study confirms the occurrence the formation of bacterial cells agglomerates under the specific surface modification. According to the FT-IR data, the main groups involved in those process are carboxyl and amid groups which may derive from surface bacterial proteins. The results of the fluorescence microscopy showed that *Lactococcus lactis* cells stay alive after surface modification and during capillary electrophoresis. In comparison with previous papers focussed on the microbial surface modification by calcium ions, it can be concluded that  $Zn^{2+}$  is not sufficient for the *Lactococcus lactis* controlled clumping in CE approach. However, the described work shed new light on several important issues, including an interpretation of probiotic bacteria aggregation process and understanding the influence of zinc ions on microorganisms surfaces and their potential use for further modifications, which seems to be crucial for separation science field.

#### Acknowledgments

This work was supported by the Opus 11 No. 2016/21/B/ST4/02130 (2017–2020) from the National Science Centre, Poland.

#### References

- [1] Klodzinska E., Kupczyk W., Jackowski M., Buszewski B.: Capillary electrophoresis in the diagnosis of surgical site infections. *Electrophoresis* **34** (2013), 3206–3213.
- [2] Desai M.J., Armstrong D.W.: Separation, identification, and characterization of microorganisms by capillary electrophoresis. *Microbiol Mol Biol Rev.* **67** (2003), 38–51.
- [3] Horka M., Tesarova M., Karasek P., Ruzicka F., Hola V., Sittova M., Roth M.: Determination of methicillin-resistant and methicillin-susceptible *Staphylococcus aureus* bacteria in blood by capillary zone electrophoresis. *Anal. Chim. Acta.* **868** (2015), 67–72.
- [4] Shen Y., Berger S.J., Smith R.D.: Capillary isoelectric focusing of yeast cells. *Anal. Chem.* **72** (2000), 4603–4607.
- [5] Okun V.M., Moser R., Blaas D., Kenndler E.: Complexes between monoclonal antibodies and receptor fragments with a common cold virus: determination of stoichiometry by capillary electrophoresis. *Anal. Chem.* **73** (2001), 3900–3906.
- [6] Dziubakiewicz E., Buszewski B.: Capillary electrophoresis of microbial aggregates. *Electrophoresis* **35** (2014), 1160–1164.

- [7] Salton M.R.J.: Studies of the bacterial cell wall: IV. The composition of the cell walls of some gram-positive and gram-negative bacteria. *Biochim. Biophys. Acta* **10** (1953), 512–523.
- [8] Schneiderheinze J.M., Armstrong D.W., Schulte G., Westenberg D.J.: High efficiency separation of microbial aggregates using capillary electrophoresis. *FEMS Microbiol. Lett.* **189** (2000) 39–44.
- [9] Klodzińska E., Dahm H., Rozycki H., Szeliga J., Jackowski M., Buszewski B.: Rapid identification of *Escherichia coli* and *Helicobacter pylori* in biological samples by capillary zone electrophoresis. *J. Sep. Sci.* **29** (2006), 1180–1187.
- [10] Buszewski B., Szumski M., Kłodzińska E., Dahm H.: Separation of bacteria by capillary electrophoresis. *J. Sep. Sci.* **26** (2003), 1045–1049.
- [11] Buszewski B., Kłodzińska E.: Determination of pathogenic bacteria by CZE with surface-modified capillaries. *Electrophoresis* **29** (2008), 4177–4184.
- [12] Rogowska A., Pomastowski P., Złoch M., Railean-Plugaru V., Król A., Rafińska K., Szultka-Młyńska M., Buszewski B.: The influence of different pH on the electrophoretic behaviour of *Saccharomyces cerevisiae* modified by calcium ions. *Sci. Rep.* **8** (2018), DOI: 10.1038/s41598-018-25024-4.
- [13] Railean-Plugaru V., Pomastowski P., Rafińska K., Wypij M., Kupczyk W., Dahm H., Buszewski B.: Antimicrobial properties of biosynthesized silver nanoparticles studied by flow cytometry and related techniques. *Electrophoresis* **37** (2016), 752–761.
- [14] Pomastowski P., Szultka-Młyńska M., Kupczyk W., Jackowski M., Buszewski B.: Evaluation of intact cell Matrix-Assisted Laser Desorption/Ionization Time-of-Flight Mass Spectrometry for Capillary Electrophoresis detection of controlled bacterial clumping. *J. Anal. Bioanal. Tech.* **S13** (2015), 008. DOI: 10.4172/2155-9872.S13-008.
- [15] Król A., Railean-Plugaru V., Pomastowski P., Złoch M., Buszewski B.: Mechanism study of intracellular zinc oxide nanocomposites formation. *Colloids Surf. A* **553** (2018), 349–358.
- [16] Naumann D., Keller S., Helm D., Schultz C., Schrader B.: FT-IR spectroscopy and FT-Raman spectroscopy are powerful analytical tools for the non-invasive characterization of intact microbial cells. *J. Mol. Struct.* **347** (1995), 399–405.
- [17] Szumski M., Kłodzińska E., Dziubakiewicz E., Hryniewicz K., Buszewski B.: Effect of applied voltage on viability of bacteria during separation under electrophoretic conditions. *J. Liq. Chromatogr. Relat. Technol.* **34** (2011), 2689–2698.

# Voltammetric studies of acemetacin

NATALIA FESTINGER\*, KAMILA MORAWSKA, SYLWIA SMARZEWSKA, WITOLD CIESIELSKI

*Department of Inorganic and Analytical Chemistry, Faculty of Chemistry, University of Lodz,  
12 Tamka Street, 91-403, Lodz, Poland ✉ natalia.festinger@chemia.uni.lodz.pl*

## Keywords

acemetacin  
carbon paste electrode  
determination  
voltammetry

## Abstract

A voltammetric method for the sensitive determination of acemetacin using carbon paste electrode is proposed. Under the optimum conditions, the calibration curve was linear in the concentration range from  $3.0 \times 10^{-8}$  to  $1.0 \times 10^{-6}$  mol L<sup>-1</sup>. The limit of detection and limit of quantification were calculated and were equal to  $6.45 \times 10^{-9}$  mol L<sup>-1</sup> and  $2.15 \times 10^{-8}$  mol L<sup>-1</sup>, respectively. The developed method was successfully applied for the determination of acemetacin in the pharmaceutical formulations.

---

## 1. Introduction

Since the date of their invention in 1958, carbon paste electrodes underwent a very impressive development, pursuing the progress in electrochemistry, electroanalysis, and instrumental analysis as such. This year, 60 years have passed since the design of the carbon paste electrodes by R. N. Adams [1]. Over the past six decades, carbon paste – a mixture of graphite powder and a binder (pasting liquid), has become one of the most popular electrode materials used for the preparation of various electrodes and sensors [2]. Graphite is commonly used in the electrochemical studies due to its low background current and wide potential window. Moreover, the graphite paste electrodes have high sensitivity and low cost which makes them more and more popular [3, 4]. Carbon paste electrodes are used as working electrodes in voltammetry for the determination of electrochemical active compounds, such as pharmaceuticals [5] or pesticides [6]. Typical properties of the respective carbon paste mixture depends on the type and quality of used graphite, as well as its amount in the mixture. The paraffin oils are the most popular binding agents used for preparation of carbon paste mixtures [2].

Acemetacin, the glycolic acid ester of indometacin, is non-steroidal anti-inflammatory drug, which is commonly used in rheumatoid arthritis treatment. Acemetacin may inhibit prostaglandin synthesis and produce anti-inflammatory, analgesic, and antipyretic effects [7]. The drug is practically insoluble in water.

In this paper, the voltammetric method of acemetacin determination in pharmaceuticals was developed.

## 2. Experimental

### 2.1 Reagents and chemicals

All chemicals were provided from commercial sources. These materials were used without further purification. The standard solutions of acetaminophen were made daily by appropriate dilution of the stock solution ( $c = 1.0 \times 10^{-3} \text{ mol L}^{-1}$ ), which was made by dissolving appropriate amount of the compound in acetone. The 0.04M Britton–Robinson buffer was used in experiments as the supporting electrolyte. The pharmaceutical formulation (Rantudil Retard, 90 mg) was obtained from local pharmacy store and used as received. The content of six capsules was mixed with proper amount of acetone and then diluted to receive appropriate acetaminophen concentration.

### 2.2 Instrumentation

Electrochemical experiments were conducted using Multi Autolab potentiostat/galvanostat with Nova 1.10 software and electrode stand M164 type (mtm-anko) with three-electrode system consisting of carbon paste electrode as a working electrode, Ag/AgCl ( $3 \text{ mol L}^{-1} \text{ KCl}$ ) as a reference electrode and Pt wire as an auxiliary electrode. The carbon paste electrode was made by placing the paste (300  $\mu\text{L}$  of paraffin oil and 1.0 g of graphite) in a piston-driven carbon paste electrode holder with inner diameter 6 mm. Before each set of measurements, the surface of electrode was refreshed by polishing on wet filter paper. All measurements were carried out at room temperature.

## 3. Results and discussion

The Britton-Robinson buffer in wide pH range (1.5–9.0) was tested as supporting electrolyte for acetaminophen determination. The highest signals of acetaminophen were recorded in Britton-Robinson buffer pH = 2.1 (Fig. 1), therefore Britton-Robinson buffer pH = 2.1 was selected for further studies as supporting electrolyte. Next, parameters of square wave voltammetry were chosen (Table 1) according to acetaminophen signals' shape and height.

Using the optimized parameters of square wave voltammetry technique, the calibration curve of acetaminophen determination was found in the range from 0.03 to  $1.0 \mu\text{mol L}^{-1}$  (Fig. 2). The limit of determination (*LOD*) and limit of quantification (*LOQ*) for acetaminophen were calculated from the calibration curve using the following equations:

$$LOD = 3 SD/b \quad (1)$$

$$LOQ = 10 SD/b \quad (2)$$

where *SD* is standard deviation and *b* is a slope of the linear calibration curve.

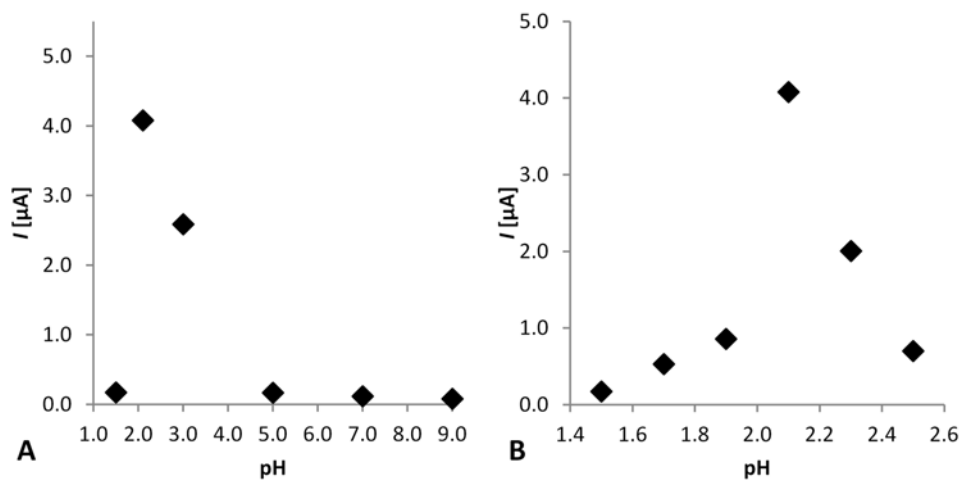


**Fig. 1** Relationship between the acemetacin peak current and the pH of Britton-Robinson buffers in (A) pH range 1.5–9.0, and (B) pH range 1.5–2.5.

**Table 1**

Optimum parameters of square wave voltammetry technique for acemetacin determination

Parameter	Examined range	Optimal value
Step potential / mV	1–15	7
Amplitude / mV	10–100	20
Frequency / Hz	2–100	20

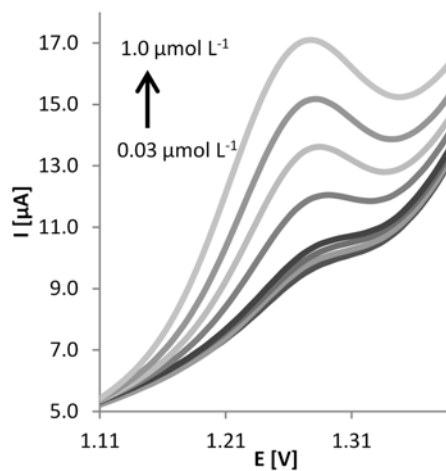


**Fig. 2** Square wave voltammograms for acemetacin calibration curve. Acemetacin concentrations: 0.03, 0.05, 0.07, 0.10, 0.30, 0.50, 0.70, and 1.00 μmol L<sup>-1</sup>. Voltammograms recorded in Britton-Robinson buffer pH = 2.1.

**Table 2**

Regression data of the calibration curve for the determination of acetaminophen in Britton-Robinson buffer pH = 2.1.

Parameter	Value
Linear range / mol L <sup>-1</sup>	3.0×10 <sup>-8</sup> –1.0×10 <sup>-6</sup>
Linear regression equation	$I [A] = 5.66 c [\text{mol L}^{-1}] + 3.55 \times 10^{-7}$
<i>R</i> <sup>2</sup>	0.9993
<i>LOD</i> / mol L <sup>-1</sup>	6.45×10 <sup>-9</sup>
<i>LOQ</i> / mol L <sup>-1</sup>	2.15×10 <sup>-8</sup>

Limit of determination and limit of quantification were equal to 6.45 and 21.5 nmol L<sup>-1</sup>, respectively (Table 2). To check the correctness of the developed method, the accuracy and precision of square wave voltammetry were calculated for increasing concentrations of acetaminophen in the linear range. The CV was equal in the range of 4.5–9.0%. From the obtained results, it can be concluded that the proposed method provides good sensitivity and repeatability for the acetaminophen determination.

Because the acetaminophen is frequently used as anti-inflammatory drug in rheumatoid arthritis, its determination in real samples is very important. The determination of acetaminophen in pharmaceutical formulations was conducted using triple standard addition method under the optimum conditions of experiment. For analysed pharmaceutical formulation with declared amount of 90.00 mg of acetaminophen, the found amount was 90.09 mg of acetaminophen; the recovery was 100.11% and CV 1.70%. Developed method gave satisfying results of recovery. It was observed that pharmaceutical formulation matrix do not produce additional signals and do not interfere in acetaminophen determination.

#### 4. Conclusions

An innovative, simple and low-cost method for the acetaminophen determination was developed. The calibration curve was obtained for acetaminophen concentration in range 0.03 to 1.0 μmol L<sup>-1</sup>. The carbon paste electrode was applied for acetaminophen determination in real samples with good recovery (100.1% for Rantudil Retard). To our knowledge, this is the first study to demonstrate the possibility of electrochemical determination of acetaminophen based on oxidation process.

#### Acknowledgments

This work was supported by the University of Lodz, Poland under Grant for young investigators B1711100001602.02.

## References

- [1] Adams R.N.: Carbon paste electrodes. *Anal. Chem.* **30** (1958), 1576–1576.
- [2] Švancara I., Vytřas K., Kalcher K., Walcarius A., Wang J.: Carbon paste electrodes in facts, numbers, and notes: a review on the occasion of the 50-years jubilee of carbon paste in electrochemistry and electroanalysis. *Electroanalysis* **21** (2009), 7–28.
- [3] Švancara I., Walcarius A., Kalcher K., Vytřas K.: Carbon paste electrodes in the new millennium. *Cent. Eur. J. Chem.* **7** (2009), 598–656.
- [4] AlAqad K.M., Suleiman R., Al-Hamouz O.C., Saleh T.A.: Novel graphene modified carbon-paste electrode for promazine detection by square wave voltammetry. *J. Mol. Liq.* **252** (2018), 75–82.
- [5] Smarzewska, S., Pokora, J., Leniart, A., Festinger, N., Ciesielski, W.: Carbon paste electrodes modified with graphene oxides – comparative electrochemical studies of thioguanine. *Electroanalysis* **28** (2016), 1562–1569.
- [6] Papp I., Švancara I., Guzsvány V., Vytřas K., Gaál F.: Voltammetric determination of imidacloprid insecticide in selected samples using a carbon paste electrode. *Microchim. Acta* **166** (2009), 169–175.
- [7] hehata T.M., Abdallah M.H., Ibrahim M.M.: Proniosomal oral tablets for controlled delivery and enhanced pharmacokinetic properties of acemetacin. *AAPS PharmSciTech* **16** (2015), 375–383.

# HPLC-ED/UV for determination of vanillylmandelic acid in human urine after solid phase extraction

ANNA MAKRLÍKOVÁ<sup>a, b, \*</sup>, HANA DEJMKOVÁ<sup>a</sup>, TOMÁŠ NAVRÁTIL<sup>b</sup>, JIŘÍ BAREK<sup>a</sup>,  
VLASTIMIL VYSKOČIL<sup>a</sup>

<sup>a</sup> UNESCO Laboratory of Environmental Electrochemistry, Department of Analytical Chemistry, Faculty of Science, Charles University, Hlavova 2030/8, 128 43 Prague 2, Czech Republic

✉ [anna.makrlikova@natur.cuni.cz](mailto:anna.makrlikova@natur.cuni.cz)

<sup>b</sup> J. Heyrovský Institute of Physical Chemistry of the AS CR, v.v.i., Dolejškova 3, 182 23 Prague 8, Czech Republic

## Keywords

HPLC  
solid phase extraction  
tumor biomarker  
vanillylmandelic acid

## Abstract

HPLC with electrochemical and spectrophotometric detection (ED/-UV) after solid phase extraction (SPE) was used for determination of vanillylmandelic acid in human urine. HPLC-ED was performed at a glassy carbon electrode in a “wall-jet” arrangement in acetate-phosphate buffer at pH = 2.5 and gradient elution (increasing content of acetonitrile from 5 to 25% in 10 minutes) was used. Optimized parameters were following: flow rate of mobile phase 1 mL min<sup>-1</sup>, detection potential +1.1 V, detection wavelength 279 nm, injected volume 20 μL. Dependence of the peak current on the analyte concentration was linear in the concentration range from 10 to 150 μmol L<sup>-1</sup>, with obtained limits of detection 2.6 μmol L<sup>-1</sup> (calculated from peak height) and 1.9 μmol L<sup>-1</sup> (calculated from peak area) for HPLC-ED, and 11.0 μmol L<sup>-1</sup> (calculated from peak height) and 9.8 μmol L<sup>-1</sup> (calculated from peak area) for HPLC-UV.

---

## 1. Introduction

Vanillylmandelic acid (DL-4-hydroxy-3-methoxybenzeneacetic acid) is found in urine with other catecholamine metabolites (homovanillic acid, metanephrine, and normetanephrine). Normal concentrations of vanillylmandelic acid in urine described in the bibliography are from 11.6 to 28.7 μmol L<sup>-1</sup> [1]. Increased urinary vanillylmandelic acid level is found in patients with tumors, pheochromocytoma and neuroblastoma [2]. The most common methods for determination of vanillylmandelic acid are HPLC and ELISA (enzyme-linked immunosorbent assay) [3]. Due to hydroxyl group on aromatic system, vanillylmandelic acid is electrochemically oxidizable and thus suitable for electroanalytical determination.

In this work, determination of vanillylmandelic acid in human urine using HPLC with electrochemical and spectrophotometric detection (ED/UV) with solid phase extraction (SPE) will be presented. The aim of this study was to determine vanillylmandelic acid in human urine without difficult sample pre-treatment. Solid phase extraction was used for filtration of samples to protect the HPLC column from clogging.

## 2. Experimental

### 2.1 Reagents and chemicals

For testing experiments, the stock solution ( $1000 \mu\text{mol L}^{-1}$ ) of vanillylmandelic acid was prepared by dissolving 4.95 mg of the pure substance in 25 mL of deionized water and then diluted to  $100 \mu\text{mol L}^{-1}$  solution containing 25% of acetonitrile. To obtain high recovery during the SPE procedure, 10% acetic acid was added to each sample of urine. Acetate-phosphate buffer ( $0.05 \text{ mol L}^{-1}$  in phosphoric acid and  $0.05 \text{ mol L}^{-1}$  in acetic acid with the appropriate amount of  $0.2 \text{ mol L}^{-1}$  sodium hydroxide solution) at pH = 2.5 was used as a mobile phase.

### 2.2 Instrumentation

HPLC-ED measurements were performed in a “wall-jet” arrangement with a glassy carbon working electrode (3 mm, Metrohm, Switzerland), a reference argentochloride electrode ( $3 \text{ mol L}^{-1}$  KCl, Monokrystal, Czech Republic), and a platinum counter electrode (Monokrystal, Czech Republic). Apparatus for HPLC-ED/UV consists of high pressure pump Beta 10 (Ecom, Czech Republic), injection valve with a 20  $\mu\text{L}$  loop (Ecom, Czech Republic), degasser DG 4014 (Ecom, Czech Republic), UV/VIS detector Sapphire 800 (Ecom, Czech Republic), and amperometric detector ADLC 2 (Laboratorní přístroje, Czech Republic) connected in series. A Kromasil Eternity-5-PhenylHexyl  $4.6 \times 150 \text{ mm}$  (AkzoNobel, Netherlands) HPLC column was used for separations. Apart from vanillylmandelic acid, other tumor biomarkers (5-hydroxyindole-3-acetic acid and homovanillic acid) were added into human urine for separation and detection. For simultaneous separation, a gradient elution program was used, linearly increasing the content of acetonitrile in the mobile phase from 5 to 25% in 10 minutes. Optimum conditions for obtaining best results were as follows: flow rate of mobile phase was  $1 \text{ mL min}^{-1}$ , detection potential for ED was set up to +1.1 V, and for UV detection, wavelength 279 nm was used.

Sample pre-treatment included only SPE as a filtration technique with commercially available SPE columns (LiChrolut EN 200 mg 3 mL standard PP-tubes, Merck Millipore, Germany), where methanol was used as a SPE eluent.

Software Clarity 2.3 (DataApex, Czech Republic) was used for recording HPLC chromatograms, Microsoft Office Excel 2010 (Microsoft, USA) and OriginPro 8.0

(Origin Lab, USA) were used for calculating calibration curve parameters and graphic expressions of results. The limit of detection (*LOD*) was calculated according equation

$$LOD = 3s/a \quad (1)$$

where *s* is the standard deviation of three repetitive measurements of the lowest measurable concentration and *a* is the slope of the calibration curve [4].

### 3. Results and discussion

Firstly, pilot experiments with buffer (composition of the used buffer was adopted from paper [5]) were done. Mobile phase was a mixture of acetate-phosphate buffer at pH=2.5 and acetonitrile, where the content of acetonitrile linearly increased from 5 to 25% in 10 minutes. Calibration dependences for biomarkers in buffer were linear in the whole tested concentration range (0.5 to 10  $\mu\text{mol L}^{-1}$ ). Relative standard deviations for 10 measurements (concentration of vanillyl-mandelic acid was 100  $\mu\text{mol L}^{-1}$ ) were not higher than 16% for HPLC-ED and not higher than 3.5% for HPLC-UV.

Next step of this research was to develop the optimum SPE procedure. Methanol provided better extraction recovery (almost 100%) in comparison with acetonitrile. The SPE column was used only for filtration to avoid destruction of the HPLC column. Activation of the SPE column and elution were performed with 5 mL of methanol, and also injection of samples (20  $\mu\text{L}$ ) was performed from 5 mL of each sample.

Last part of this research was devoted to application of this method for determination of vanillylmandelic acid in human urine. Fig. 1 shows HPLC-ED recordings of urine and urine with addition of 1 mL of the stock solution of vanillylmandelic acid, 5-hydroxyindole-3-acetic acid, and homovanillic acid (each of 1000  $\mu\text{mol L}^{-1}$ ) into a 7 mL urine sample. Fig. 2 then depicts HPLC-UV recordings of the same analysis as in Fig. 1. There were no problems with interferences in HPLC-ED; found native concentrations ( $\sim 13 \mu\text{mol L}^{-1}$ ) in urine fully correspond with published concentrations (from 11.6 to 28.7  $\mu\text{mol L}^{-1}$ ) [1]. On the other hand, there were some interferences observed in HPLC-UV, and found native concentrations are thus not corresponding with the published values. For the determination of the concentration of the analyte, the standard addition method was used. Dependences were linear in the tested concentration range from 10 to 150  $\mu\text{mol L}^{-1}$ ; obtained *LODs* were 2.6  $\mu\text{mol L}^{-1}$  (calculated from peak height) and 1.9  $\mu\text{mol L}^{-1}$  (calculated from peak area) for HPLC-ED, and 11.0  $\mu\text{mol L}^{-1}$  (calculated from peak height) and 9.8  $\mu\text{mol L}^{-1}$  (calculated from peak area) for HPLC-UV.

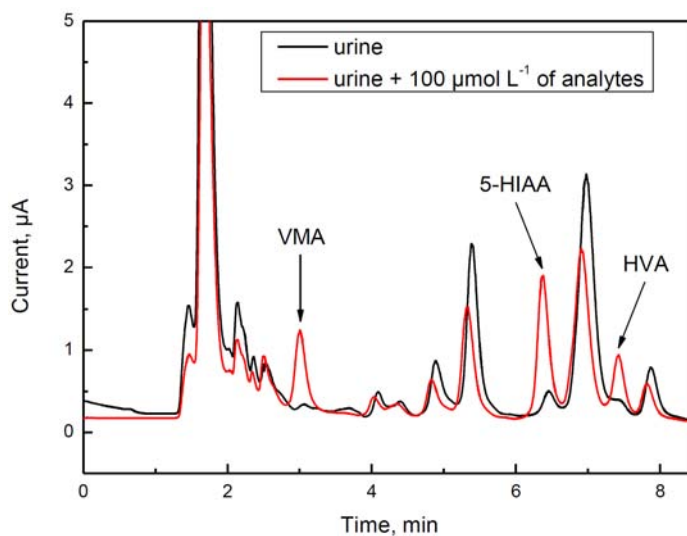


**Fig. 1** HPLC-ED recordings of urine and urine with addition of vanillylmandelic acid (VMA), 5-hydroxyindole-3-acetic acid (5-HIAA), and homovanillic acid (HVA), each  $100 \mu\text{mol L}^{-1}$ . Glassy carbon electrode, acetate-phosphate buffer at  $\text{pH} = 2.5$ , gradient elution (increasing content of acetonitrile from 5 to 25% in 10 minutes), flow rate of mobile phase  $1 \text{ mL min}^{-1}$ , detection potential  $+1.1 \text{ V}$ , injected volume  $20 \mu\text{L}$ .

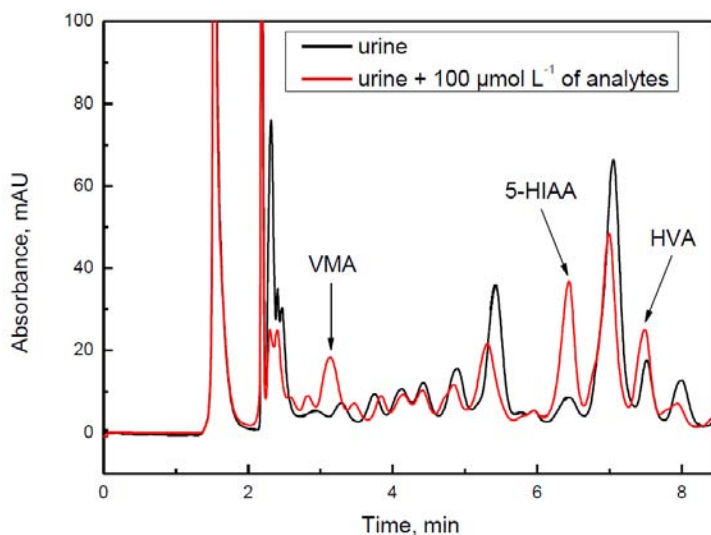


**Fig. 2** HPLC-UV recordings of urine and urine with addition of vanillylmandelic acid (VMA), 5-hydroxyindole-3-acetic acid (5-HIAA), and homovanillic acid (HVA), each  $100 \mu\text{mol L}^{-1}$ . Acetate-phosphate buffer at  $\text{pH} = 2.5$ , gradient elution (increasing content of acetonitrile from 5 to 25% in 10 minutes), flow rate of mobile phase  $1 \text{ mL min}^{-1}$ , detection wavelength  $279 \text{ nm}$ , injected volume  $20 \mu\text{L}$ .

## 4. Conclusions

HPLC-ED/UV after SPE was successfully used for determination of vanillylmandelic acid in human urine. Solid phase extraction procedure replaced filtration of samples of human urine to avoid problems with clogging an HPLC column; any other sample pre-treatment was not used. Presented method could be used for screening of human urine, especially of infants, because HPLC-ED is very sensitive method and allows simultaneous determination of all three tumor biomarkers, vanillylmandelic acid, 5-hydroxyindole-3-acetic acid, and homovanillic acid.

## Acknowledgments

This research was carried out within the framework of the Specific University Research (SVV260440). A.M. thanks the Grant Agency of the Charles University (Project GAUK734216) for the financial support. J.B. and T.N. thank the Grant Agency of the Czech Republic (project 17-03868S).

## References

- [1] García A., Heinänen M., Jimenéz L. M., Barbas C.: Direct measurement of homovanillic, vanillylmandelic and 5-hydroxyindoleacetic acids in urine by capillary electrophoresis. *J. Chromatogr. A* **871** (2000), 341–350.
- [2] Magera M. J., Thompson A. L., Matern D., Rinaldo P.: Liquid chromatography-tandem mass spectrometry method for the determination of vanillylmandelic acid in urine. *Clin. Chem.* **49** (2003), 825–826.
- [3] Shirao M. K., Suzuki S., Kobayashi J., Nakazawa H., Mochizuki E.: Analysis of creatinine, vanilmandelic acid, homovanillic acid and uric acid in urine by micellar electrokinetic chromatography. *J. Chromatogr. B* **693** (1997), 463–467.
- [4] Inczédy J., Lengyel T., Ure A. M.: *Compendium of Analytical Nomenclature: Definitive Rules 1997*. 3rd Ed. Blackwell Science, Malden 1998, p. 106–127.
- [5] Dejmková H., Adamková H., Barek J., Zima J.: Voltammetric and amperometric determination of selected catecholamine metabolites using glassy carbon paste electrode. *Monatsh. Chem.* **148** (2017), 511–515.

# ICP-MS analysis as a tool for monitoring of the efficiency of the sorption based removal of iodinated contrast agents

JAN PATOČKA\*, ANNA KREJČOVÁ, KATEŘINA KLAUSOVÁ

*Department of Environmental and Chemical Engineering, University of Pardubice, Studentská 95, 532 10 Pardubice, Czech Republic ✉ jan.patocka@student.upce.cz*

## Keywords

ICP-MS  
iodinated contrast agents  
iodine  
sorption

## Abstract

The inductively coupled plasma mass spectrometry (ICP-MS) method for the iodine determination was developed. The instrumental limit of detection ( $3\sigma$ ) for  $^{127}\text{I}$  was  $0.28\text{ ng l}^{-1}$ , recoveries 100–118%, repeatabilities 1.23–4.99 %. Iodine in the certified reference material NCS ZC81002b (human hair, the certified value  $0.96\pm 0.2\text{ }\mu\text{g kg}^{-1}$ ) was found  $1.15\pm 0.07\text{ }\mu\text{g kg}^{-1}$ . The method was used for the evaluation of the sorption based removal of iodinated contrast agents from water and artificial urine using activated carbon, humic acids and dry biomass of green algae *Chlorella kessleri*. The tested iodinated contrast agents were Iomeron and Xenetix. Potassium iodide was used to evaluate the sorption of inorganic iodine in order to assess fully the applicability of proposed approaches in real hospital wastewaters containing iodine in various forms.

## 1. Introduction

The presence and ecotoxicological effects of medicinal products in the water environment are one of current problems in environmental chemistry. More than eighty pharmaceutically active substances, including iodine X-ray contrast agents, were found up to the level of  $\mu\text{g L}^{-1}$  in sewage, surface, and ground water. Their increased abundance in the water environment is connected to the improvement of health care over the past fifty years. From tens up to hundreds grams of iodinated contrast agents are required for one diagnostic test. Then iodinated contrast agents are eliminated from human body in the urine in non-metabolized form, which is not completely removed in water treatment plants and leads to the enhanced adsorbable organic halides formation [1].

Analytical techniques suitable for the determination of single iodinated contrast agents are, e.g., high performance liquid chromatography or capillary electrophoresis with suitable detection as UV-Vis, photometric and mass spectrometry. Liquid chromatography connected to mass spectrometry using electro-

spray ionization, in the comparison with the others, allows performing not only quantification but also identification of iodinated contrast agents in unknown samples [2–4]. Total iodine can be determined using spectral techniques such as inductively coupled plasma optical emission spectrometry and inductively coupled plasma mass spectrometry (ICP-MS) [5].

In case of our laboratory research experiments, iodinated contrast agents can be monitored as iodine.

## 2. Experimental

### 2.1 Reagents and chemicals

The deionized water purified using the system Milli-Q (Merck, Germany) was used in this work. All reagents were of analytical-reagent grade. Nitric acid 65% (v/v), analytical grade (LachNer, Czech Republic) was distilled in sub-boiling distillation equipment (BSB 939 IR, Berghof, Germany). For stabilization of iodine solutions, 25% tetramethylammonium hydroxide (analytical grade, Sigma-Aldrich, Germany) was used.

The stock artificial urine was prepared according to Dawson [6]: 3.9 g  $\text{NH}_4\text{H}_2\text{PO}_4$ , 5.08 g NaCl, 2.86 g KCl, 0.312 g  $\text{CaCO}_3$ , 0.418 g  $\text{MgCl}_2 \cdot 6\text{H}_2\text{O}$ , 18.1 g of urea, 8.7 mL 35% HCl, and 0.67 mL 96%  $\text{H}_2\text{SO}_4$  to the final volume of 100 mL (all analytical grade from Lach-Ner, Czech Republic). For next experiments, the stock artificial urine was ten times diluted.

The iodine calibration standard solutions of concentrations 0.1, 0.5, 1.0, 5.0, and 10.0  $\mu\text{g L}^{-1}$  were prepared from potassium iodide (analytical grade, Lach-Ner, Czech Republic) in 1% tetramethylammonium hydroxide. However, tetramethylammonium hydroxide was used only at the method developing and validating stage. For the iodine determination in samples from sorption experiments, tetramethylammonium hydroxide was not used and calibration standards were prepared fresh right before analysis.

The single element standard solution of tellurium  $1.000 \pm 0.002 \text{ g L}^{-1}$  (SCP Science, Canada) was used for the internal standard preparation.

The certified reference material NCS ZC81002b (human hair, China) with the certified value of iodine  $0.96 \pm 0.2 \mu\text{g kg}^{-1}$  was used for the method validation.

The evaluated sorbents were activated carbon Hydrarffin CC 8X30 (Donau-chem, Czech Republic), the *Chlorella kessleri* algae biomass (Institute of Botany of the Czech Academy of Sciences, Czech Republic) and humic acids (sodium humate, Humatex, Czech Republic).

### 2.2 Sample preparation

The tested iodinated contrast agents (structures in Fig. 1; [7, 8]) were Iomeron containing jomeprol ( $400 \text{ g L}^{-1}$  of iodine, Bracco Imaging Deutschland, Germany) and Xenetix containing jobitridol ( $350 \text{ g L}^{-1}$  of iodine, Guerbert, France).

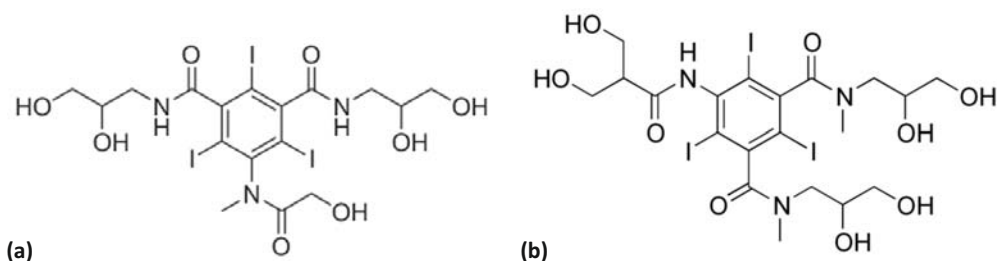


**Fig. 1** Chemical structures of (a) Iomeprol, and (b) Iobitridol.

Samples of liquid phase from sorption experiments were taken after the centrifugation (5 minutes) and subsequently 1000fold diluted for analysis.

The original iodinated contrast agents were mineralized using the microwave oven: 1 mL of 1000fold diluted sample in 6 mL of 65% HNO<sub>3</sub>, (i) 160 °C at 50 bars, (ii) 200 °C at 75 bars, (iii) 50 °C at 75 bars, filled up to 100 mL and subsequently 1000fold diluted for analysis.

About 0.3 g of the CRM NCS ZC81002b was mineralized under the same conditions as were the iodinated contrast agents, filled up to 25 mL and diluted to get the theoretical iodine concentration 4 μg L<sup>-1</sup> for Iomeron and 3.5 μg L<sup>-1</sup> for Xenetix.

Wastewaters obtained from the Pardubice Hospital were stabilized in 1% tetramethylammonium hydroxide and then: (i) filtrated and hundred times diluted, (ii) filtrated and five hundred times diluted for a series of spiked samples with potassium iodide (1, 2 and 4 μg L<sup>-1</sup>) for standard addition approach, and (iii) digested (1 ml of raw wastewater, the same conditions as for the iodinated contrast agents, filled up to 50 mL, four times diluted).

### 2.3 Instrumentation

The inductively coupled plasma orthogonal acceleration time-of-flight mass spectrometer (oaTOF-ICP-MS) Optimass 9500 (GBC Scientific Equipment, Australia) equipped with the concentric nebuliser MicroMist (0.4 mL min<sup>-1</sup>) and a 70 mL thermostatted (10 °C) cyclonic spray chamber (both Glass expansion, Australia) was used for the determination of iodine.

The microwave system Speedwave Xpert (Berghoff, Germany) was used for mineralization of samples.

The sorption experiments were realized using the laboratory shaker Heidolph Vibramax 100 (Heidolph Instruments GmbH & CO. KG, Germany) and the Eppendorf Centrifuge 5804 R (Eppendorf AG, Germany).

### 3. Results and discussion

#### 3.1 The ICP-MS method validation

Iodine was measured on the isotope  $^{127}\text{I}$ . Based on the literature [9],  $^{125}\text{Te}$  was added as an internal standard ( $10\ \mu\text{g L}^{-1}$ ) in calibration standards and mineralized samples of certified reference material NCS ZC81002b.

The reliability of the ICP-MS method was proven by recoveries and repeatabilities obtained from the repetitive analysis of iodine standard solutions, which were 101–112% and 1.08–4.91% when using the internal standard  $^{125}\text{Te}$  and 100–118% and 1.23–4.99% without the internal standard.

The determined iodine concentration in certified reference material NCS ZC81002b was  $1.15 \pm 0.07\ \text{mg kg}^{-1}$  ( $n = 4$ ) complied with the certified value  $0.96 \pm 0.2\ \text{mg kg}^{-1}$ .

The limits of detection calculated as the concentration related to three times the standard deviation of the integrated peak area measured near the monitored ion peak for the standard solution containing  $0.1\ \mu\text{g L}^{-1}$  of I in three replicates were  $0.28\ \text{ng L}^{-1}$  (instrumental) and  $0.28\ \mu\text{g L}^{-1}$  (procedural for sorption experiments).

#### 3.2 The analysis of iodinated contrast agents

The diluted or mineralized iodinated contrast agents were analysed in order to assess the ICP-MS method applicability for the monitoring of sorption experiments. Tetramethylammonium hydroxide was not used for the stabilization of these samples because they are considered to be very stable.

The iodine concentration for Iomeron was  $371 \pm 18.2\ \text{g L}^{-1}$  (diluted) and  $385 \pm 44.7\ \text{g L}^{-1}$  (digested) and for Xenetix  $287 \pm 12.9\ \text{g L}^{-1}$  (diluted) and  $294 \pm 39.1\ \text{g L}^{-1}$  (digested). The lower recoveries were probably caused by the sample matrix in case of only diluted iodinated contrast agents and by analyte losses during digestion in case of digested samples. Possible systematic errors in sorption experiments were overcome by relating of actual to origin concentration. For the sorption monitoring, the samples were only diluted and no tetramethylammonium hydroxide or technetium was added.

#### 3.3 Sorption experiments

The sorption experiments were realized using activated carbon, biomass of algae *Chlorella kessleri* and humic acids as sorbents for iodinated contrast agents Iomeron and Xenetix and potassium iodide removal from water and the artificial urine. The sorption experiments were performed in 15 mL centrifuge tubes with 0.1; 0.2; 0.5; 1.0 g of sorbents and tested substances with iodine concentration  $20\ \text{mg L}^{-1}$  for Iomeron and potassium iodide and  $17.5\ \text{mg L}^{-1}$  for Xenetix. The testing tubes were placed on laboratory shaker for 2 hours. Then, samples of liquid phase were taken for iodine analysis.

**Table 1**

The percentage efficiency of iodinated contrast agents removal from chosen media using evaluated sorbents ( $m_s$  – mass of used sorbent).

$m_s$ /g	Removal efficiency / %					
	Water			Artificial urine		
	Activated carbon	Biomass of <i>Chlorella kessleri</i>	Humic acid	Activated carbon	Biomass of <i>Chlorella kessleri</i>	Humic acid
<i>Iomeron</i>						
0.1	88	5	7	69	6	4
0.2	98	16	3	73	– <sup>a</sup>	– <sup>a</sup>
0.5	99	10	8	89	– <sup>a</sup>	1
1.0	98	11	11	89	– <sup>a</sup>	9
<i>Xenetix</i>						
0.1	62	2	– <sup>a</sup>	– <sup>a</sup>	– <sup>a</sup>	– <sup>a</sup>
0.2	95	– <sup>a</sup>	2	– <sup>a</sup>	– <sup>a</sup>	– <sup>a</sup>
0.5	96	4	2	– <sup>a</sup>	– <sup>a</sup>	– <sup>a</sup>
1.0	97	– <sup>a</sup>	– <sup>a</sup>	– <sup>a</sup>	– <sup>a</sup>	– <sup>a</sup>
<i>Potassium iodide</i>						
0.1	46	– <sup>a</sup>	– <sup>a</sup>	67	– <sup>a</sup>	– <sup>a</sup>
0.2	31	– <sup>a</sup>	1	79	– <sup>a</sup>	– <sup>a</sup>
0.5	75	1	– <sup>a</sup>	89	– <sup>a</sup>	– <sup>a</sup>
1.0	90	– <sup>a</sup>	– <sup>a</sup>	89	– <sup>a</sup>	– <sup>a</sup>

<sup>a</sup> Impossible to evaluate; no sorption has occurred.

The sorption experiments were carried out for every combination of tested iodinated contrast agents with sorbents used in water and artificial urine. The results are presented in Table 1. For the experiments showing very low iodine removal efficiency, the iodine removal percentage could not have been calculated because the determined iodine concentration at the end of the experiment was slightly higher than the starting one. This situation may have occurred from several reasons and their combinations: (i) memory effects for iodine at sub  $\mu\text{g L}^{-1}$  levels were noticed during ICP-MS measurements, (ii) severe iodine memory effects occurred during sample preparation and manipulation, which was diminished but not completely avoided using disposable laboratory equipment, and (iii) the absence of internal standardization, which may have led to the short time nebulizing efficiency changes and the instrument signal instability.

### 3.4 Analysis of real hospital wastewater

The iodine concentrations in the real hospital wastewater were: (i)  $0.85 \pm 0.02 \text{ mg L}^{-1}$  for filtered and diluted, (ii)  $1.07 \pm 0.04 \text{ mg L}^{-1}$  for filtered, diluted and quantified using the standard addition approach, and (iii)  $0.71 \pm 0.03 \text{ mg L}^{-1}$  for mineralized samples. The obtained results support the

idea of analyte losses during microwave digestion and mild matrix interference when external calibration standards used for quantification.

#### 4. Conclusions

The developed ICP-MS method provided sufficient sensitivity ( $LOD_{\text{procedure}} = 0.28 \mu\text{g L}^{-1}$ ) for iodine monitoring in the sorption experiments and real samples of hospital wastewater. The results revealed that the best of sorbents used was activated carbon with the removal efficiencies 99, 97, and 90% for Iomeron, Xenetix and potassium iodide in water and 89% for both Iomeron and potassium iodide in the artificial urine. The *Chlorella kessleri* algae biomass and humic acids revealed significantly lower removal efficiencies: 11, 2, and 1% for Iomeron, Xenetix and potassium iodide in water and 9% for Iomeron in the artificial urine when the difference between these two sorbents was insignificant. Activated carbon seems to be a suitable sorbent for the removal of iodine in both organic and inorganic forms even in the presence of complex matrix.

#### Acknowledgments

Authors acknowledge the support from the University of Pardubice, Faculty of Chemical Technology projects SG FCHT 05/17 and SG FCHT 05/18.

#### References

- [1] Steger-Hartmann R, Lange R, Schweinfurth H.: Environmental risk assessment for the widely used iodinated X-ray contrast agent iopromide (Ultravist). *Ecotoxicol. Environ. Saf.* **42** (1999), 274–281.
- [2] Arbughi T, Bertani F, Celeste R, Grotti A, Tirone P.: High-performance liquid chromatographic determination of the X-ray imaging contrast agent, iofratol, in plasma and urine. *J. Chromatogr. B* **701** (1997), 103–103.
- [3] Van Houcke S.K., Seaux L., Cavalier E., Speeckaert M.M., Dumoulin E., Lecocq E., Delanghe J.R.: Determination of iohexol and iothalamate in serum and urine by capillary electrophoresis. *Electrophoresis* **37** (2016), 2363–2367.
- [4] Hirsch R., Ternes T.A., Lindart A., Haberer K., Wilken R.D.: A sensitive method for the determination of iodine containing diagnostic agents in aqueous matrices using LC-electrospray-tandem-MS detection. *Fresenius J. Anal. Chem.* **366** (2000), 835–841.
- [5] Oliveira A.A., Trevizan L.C., Nobrega J.A.: Iodine determination by inductively coupled plasma spectrometry. *Appl Spectrosc Rev.* **45** (2010), 447–473.
- [6] Dawson J.B., Ellis D.J., Newton-John H.: Direct estimation of copper in serum and urine by atomic absorption spectroscopy. *Clin Chim Acta.* **21** (1968), 33–42.
- [7] Whitehouse G.H.: Foreword. *Eur. J. Radiol.* **18** (1994), vii.
- [8] Conti M., Motta R., Puggioli C., Brambilla P.: Surface-activated chemical ionization-electrospray ionization mass spectrometry combined with two-dimensional serial chromatography is a powerful tool for drug stability studies. *Rapid. Commun. Mass. Spectrom.* **27** (2013), 1231–1236.
- [9] Jerše A., Jaćimović R., Maršić N.K., Germ M., Šircelj H., Stibilj V.: Determination of iodine in plants by ICP-MS after alkaline microwave extraction. *Microchem. J.* **137** (2018), 355–362.

# The influence of pH on the electrophoretic behaviour of yeast modified by calcium ions

AGNIESZKA ROGOWSKA<sup>a, b</sup>, PAWEŁ POMASTOWSKI<sup>a</sup>, MICHAŁ ZŁOCH<sup>b</sup>,  
VIORICA RAILEAN-PLUGARU<sup>a, b</sup>, ANNA KRÓL<sup>a, b</sup>, KATARZYNA RAFIŃSKA<sup>a, b</sup>,  
MAŁGORZATA SZULTKA-MŁYŃSKA<sup>b</sup>, BOGUSŁAW BUSZEWSKI<sup>a, b, \*</sup>

<sup>a</sup> Centre for Modern Interdisciplinary Technologies, Nicolaus Copernicus University,  
Wileńska 4, 87-100 Torun, Poland

<sup>b</sup> Department of Environmental Chemistry and Bioanalytics, Faculty of Chemistry, Nicolaus  
Copernicus University, Gagarina 7, 87-100 Torun, Poland ✉ [bbusz@chem.uni.torun.pl](mailto:bbusz@chem.uni.torun.pl)

## Keywords

capillary zone  
electrophoresis  
cells clumping  
MALDI-TOF MS  
yeast

## Abstract

The influence of a different pH on *Saccharomyces cerevisiae* yeast cells modified with calcium ions was investigated by the capillary zone electrophoresis. The obtained results indicate that the modification of surface functional groups by calcium ions significantly affected the efficiency of electrophoretic mobility. Moreover, the microscopic and spectrometric analysis shows that the pH value of the calcium ions solution has a significant effect on the intensity yeast cells clumping. However, these changes did not affect on the accuracy of *S. cerevisiae* identification by MALDI equipment with BioTyper platform. These results form the analytical solution for coupling of electrophoresis and MALDI-TOF MS technique.

---

## 1. Introduction

Capillary zone electrophoresis (CZE) is a well known and widely used technique enabling the separation, and identification of microorganisms [1]. Despite such widespread use of CZE, this technique is in the process of evolution and requires the development of new methods for sample preparation. In recent years a lot of interest has been focused on the possibility of applying this technique to electroanalysis to provide the identification of wild stains of microorganisms in diagnostics laboratory. However, the electrophoretic analysis of such complicated systems as microorganisms can cause many difficulties associated with uncontrolled cell aggregation and adhesion to the inner surface of the capillary. The new approach to eliminate this problem involves changes of functional groups on the microbial surface by divalent metal ions resulting in controlled cells clumping [2].

*Saccharomyces cerevisiae* can be called a model organism because they are small with a short generation time and can be easily cultured [3]. The yeasts cell wall structure is composed of polysaccharides and proteins [4]. Such a construction of the yeast cell wall results in there being many functional groups on its

surface such as phosphate, carboxyl and amino groups. Under appropriate conditions of pH, these groups are deprotonated, which allows their interaction with positive charged metal ions results in cells flocculation [5]. Many metal ions such as  $Mg^{2+}$  or  $Zn^{2+}$  have been described as yeast cell aggregation inducers. However, calcium ions are known as the most effective in flocculation promotion [6].

The aim of this study was to investigate the impact of the cells surface modification by calcium ions on its clumping and on the effectiveness of the electrophoretic mobility. The novel approach of the microbial sample preparation for the CZE analysis may constitute a significant contribution to the future use of this technique in diagnostics laboratory. Moreover, the spectrometric analysis of yeast modified by calcium ions may be a foundation for the coupling of capillary electrophoresis and MALDI-TOF MS analysis to eliminate the preconcentration problem of microbiological samples.

## 2. Experimental

All solvents and materials were purchased from Sigma Aldrich (Poznan, Poland). Ultra-pure water was purified using the Milli-Q RG system (Bedford, USA).

In order to preparation of yeast cells modified by calcium ions at different pH *S. cerevisiae* samples were suspended in 5 mM  $Ca(NO_3)_2$  adjusted to the desired pH by the addition of  $Ca(OH)_2$ . After 60 minutes of incubation, the suspension was centrifuged. The resulting precipitate was washed twice with water to remove unbound calcium ions.

In order to performed microscopic analysis, sample of modified yeast was dropped on the watch glass and observed using stereoscopic fluorescent microscope with Cell software (Olympus, SZX16, Shinjuku, Tokyo, Japan).

For the spectrometric analysis the sample of modified and non-modified yeast was analyzed according to the previously described methodology [7].

To performed capillary zone electrophoresis analysis modified and non-modified *S. cerevisiae* cells were transferred to the outlet TB buffer of pH = 7.98 (4.5 mM tris(hydroxymethyl)aminomethane, 50 mM boric acid) as the inlet buffer was used TBH of pH = 7.31 (4.5 mM tris(hydroxymethyl)aminomethane, 50 mM boric acid, 3.31 mM hydrochloric acid). Directly before the CZE analysis the obtained yeast sample was sonificated. The CZE analysis was performed using PA 800 plus (Beckman Coutner system, USA) equipped with a DAD detector with the use of fused silica capillaries ( $id = 75 \mu m$ ;  $L_{tot} = 33.5 cm$ ;  $L_{eff} = 25 cm$ ; Composite Metal Services, UK).

## 3. Results and discussion

To determine the effect of the surface modification of *S. cerevisiae* on the electrophoretic mobility, the electrophoretic analysis was conducted. Fig. 1 shows

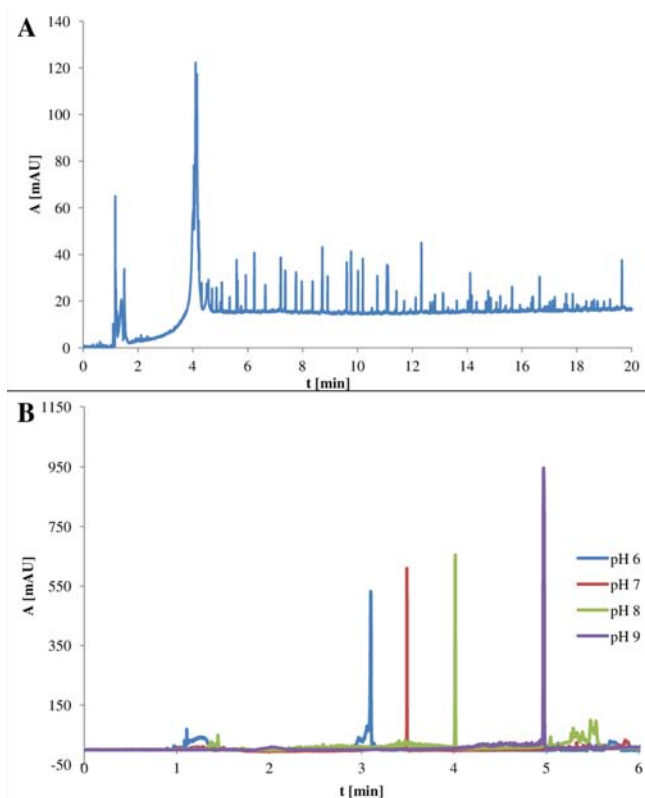


**Fig. 1** Electropherogram of (A) non-modified *Saccharomyces cerevisiae*, and (B) and modified *Saccharomyces cerevisiae* by  $\text{Ca}(\text{NO}_3)_2$  at pH = 6.0, 7.0, 8.0 and 9.0.

the electropherograms of the yeast unmodified and modified by calcium ions at different pH conditions. The electromigration time of the yeast modified by the calcium solution of pH = 6.0, 8.0 and 9.0 was 3.099, 4.013 and 4.099 min, respectively. The results indicate that the surface modification of (bio)colloid has a significant impact on its electrophoretic mobility. This phenomenon was also observed by Pomastowski et al. [7] in the case of bacteria. Moreover, after the modification, the sharpening of the peaks and improvement of the shape of the base line on the electropherogram as well as the reduction in the number of aggregates and the improvement of the reproducibility can be observed. Another interesting observation is the effect of pH on modified (bio)colloid behavior during the electrophoretic analysis. With the increase in the pH of medium in which sorption was conducted, the increase in the electromigration time of modified yeast cells and as a decrease in the electrophoretic mobility. The highest reproducibility ( $RSD < 5\%$ ) of the electrophoretic analysis was obtained for *S. cerevisiae* which was modified at pH=9.0. This phenomenon is probably connected with the total deprotonation of surface functional groups.

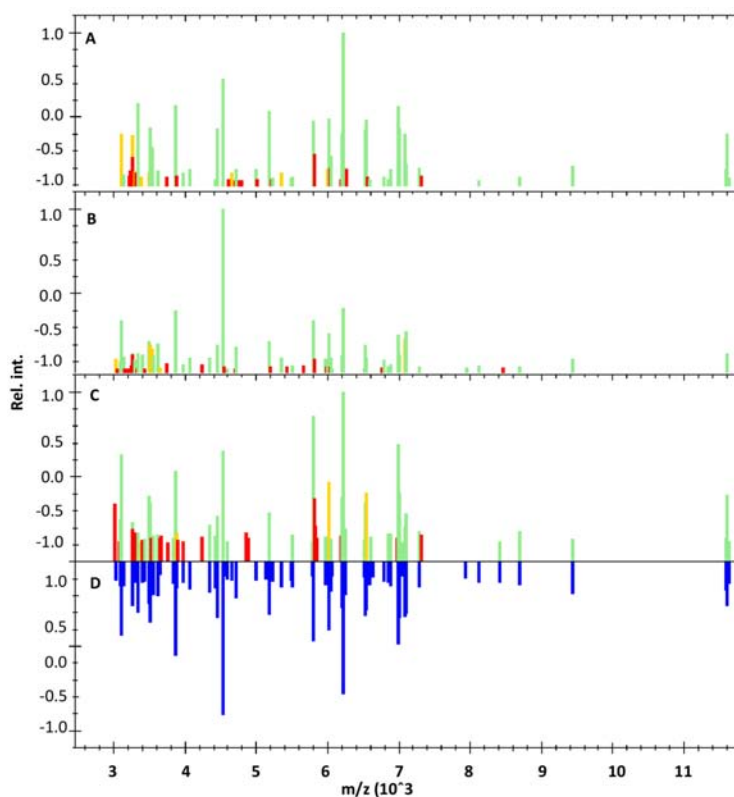


**Fig. 2** MALDI-TOF MS spectra of *Saccharomyces cerevisiae* suspended in  $\text{Ca}(\text{NO}_3)_2$  solution at (A) pH = 6.0, (B) pH = 8.0, (C) pH = 9.0, and (D) native *S. cerevisiae*.

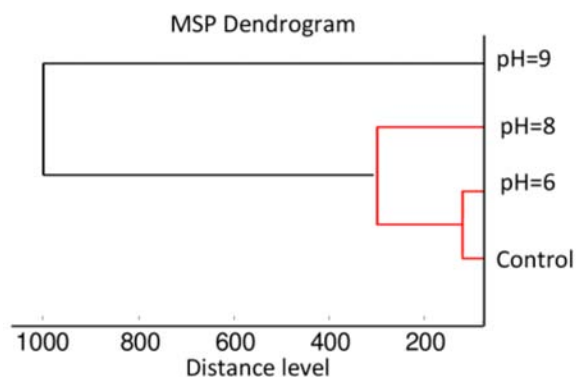


**Fig. 3** MSP dendrogram for MALDI-TOF MS spectra of *Saccharomyces cerevisiae* modified with  $\text{Ca}(\text{NO}_3)_2$  solution at pH = 6.0, 8.0, 9.0 and native *S. cerevisiae*.

In order to highlight the changes on molecular profile of (bio)colloids under different pH conditions, the influence the electrophoretic properties, microscopic and spectrometric studies of modified yeasts were performed. On the MALDI spectra (Fig. 2) for calcium-modified yeast, can be observed many significant changes in comparison to spectra of native cells. However, cluster analysis of MSP

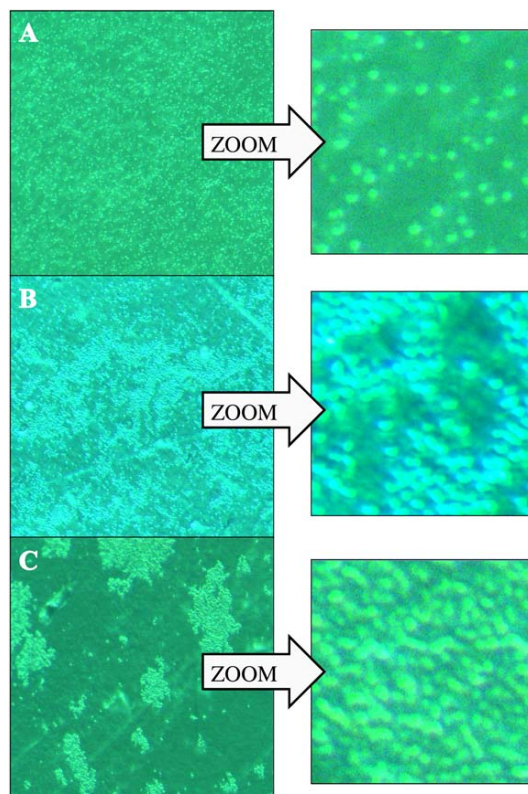


**Fig. 4** Microscopic images of *Saccharomyces cerevisiae* suspended in 5 mM  $\text{Ca}(\text{NO}_3)_2$  solution at (A) pH = 6.0, (B) pH = 8.0, and (C) pH = 9.0.

(Main Spectrum Profile) spectra (Fig. 3) of control and yeasts incubated in calcium solution at pH = 6.0, 8.0 and 9.0 show that the greatest change in molecular profiles, as compared to the control sample, was observed for the yeast incubated in calcium solution at pH = 9.0. The changes were observed at molecular level of ribosomal, cytosol and membrane proteins. It is known that presence of the  $\text{Ca}^{2+}$  in the culture medium may strongly influence the expression of proteins in *S. cerevisiae* cells, mainly ribosomal or ribosome-associated proteins as well as proteins related to the cell wall. High concentrations of  $\text{Ca}^{2+}$  leads to overexpression of cell wall integrity regulators as a response to the osmotic and ionic changes that occur in the media [8] which can explain the observations in this work changes of protein profiles during MALDI TOF/MS analysis.

The microscopic observation shows that the highest aggregation of the yeast cells was achieved for the system, where solution at pH = 9.0 was used. In the case of the calcium solution at pH = 6.0, cluster formation wasn't observed (Fig. 4). Moreover, microscopic results prove that the yeast surface changes with a calcium ion affect the aggregates formation. A similar phenomenon was observed by Dziubakiewicz et al. for the bacterial cells [2]. As a result of the bacteria surface

charge modification by calcium ions, the cells created a compact aggregates, whereby, fewer high-intensity signals on the electropherograms were observed. They attributed this score to the bridging effect of calcium ions between bacterial cells. According to the well-known theory of dicationic bridges, carboxyl and amine surface groups are involved in the formation of aggregates. Partially deprotonated carboxyl groups and protonated amino groups are not able to form bridges between (bio)colloids. After yeast centrifugation from calcium salt solution and suspended in TB buffer, probably borate ions associate and/or complex adsorbed calcium ions. The created ions of TB buffer respectively associate components of the microorganisms surface. In turn, yeast suspended in a calcium solution at pH = 8.0 form aggregates with part-compact structure (Fig. 4).

#### 4. Conclusion

Capillary zone electrophoresis allows for the determination of a variety of biological systems. However, the complexity of the microorganism surface morphology forced us to carry out a series of research on the physicochemical properties in order to interpret the phenomena occurring at the interface of (bio)colloids. The microscopic and spectrometric studies performed for non-modified and modified *S. cerevisiae* have shown that under specified conditions the tested system tends to aggregate. This phenomenon explains the stability of (bio)colloid subjected to the biosorption process in electrophoretic separation conditions. In addition, it was observed that along with the increasing pH of modifier the weight and surface of particles of colloidal system increases, which results in the reduction of the (bio)colloid electrophoretic mobility. Obtained results indicate that the proposed new sample preparation approach of wild microorganisms strains may be a foundation for the application of capillary electrophoresis in diagnostics laboratory in the future. Moreover, the results show that the different pH and modification of the cells by  $\text{Ca}^{2+}$  influence the molecular profiles of yeast cells but do not affect the identification quality by the MALDI-TOF MS equipment with the BioTyper database. Such results may provide a basis enabling for coupling of capillary electrophoresis and the MALDI-TOF MS analysis.

#### Acknowledgments

This study was financially supported by Opus 11 No. 2016/21/B/ST4/02130 (2017–2020) from the National Science Centre, Poland.

#### References

- [1] Buszewski B., Kłodzińska E.: Rapid microbiological diagnostics in medicine using electro-migration techniques. *Trends Anal. Chem.* **78** (2016), 95–108.
- [2] Dziubakiewicz E., Buszewski B.: Capillary electrophoresis of microbial aggregates. *Electrophoresis* **35** (2014), 1160–1164.
- [3] Blackwell M.: The Fungi: 1, 2, 3 ... 5.1 million species? *Am. J. Bot.* **98** (2011), 426–438.

- [4] Somerville C., Bauer S., Brininstool G., Facette M., Hamann T., Milne J., Osborne E., Paredez A., Persson S., Raab T., Vorwerk S., Youngs H.: Toward a systems approach to understanding plant cell walls. *Science* **306** (2004), 2206-2211.
- [5] Mill P.J.: The nature of the interactions between flocculent cells in the flocculation of *Saccharomyces cerevisiae*. *J. Gen. Microbiol.* **35** (1964), 61–68.
- [6] Miki B.L.A., Poon N.H., James A.P., Seligy V.L.: Possible mechanism for flocculation interactions governed by gene FLO1 in *Saccharomyces cerevisiae*. *J. Bacteriol.* **150** (1982), 878–889.
- [7] Pomastowski P., Szultka-Młyńska M., Kupczyk W., Jackowski M., Buszewski B.: Evaluation of intact cell Matrix-Assisted Laser Desorption/Ionization Time-of-Flight Mass Spectrometry for capillary Electrophoresis detection of controlled bacterial clumping. *J. Anal. Bioanal. Tech.* S13 (2015), 008.
- [8] Haramati O., Brodov A., Yelin I., Atir-Lande A., Samra N., Arava Y.: Identification and characterization of roles for Puf1 and Puf2 proteins in the yeast response to high calcium. *Sci. Rep.* **7** (2017) 3037.

# Optimization of photochemical vapor generation of molybdenum as a sample introduction for ICP-MS

JAKUB ŠOUKAL<sup>a, b, \*</sup>, STANISLAV MUSIL<sup>a</sup>

<sup>a</sup> Department of Trace Element Analysis, Institute of Analytical Chemistry of the Czech Academy of Sciences, Veveří 97, 602 00 Brno, Czech Republic

<sup>b</sup> Department of Analytical Chemistry, Faculty of Science, Charles University, Hlavova 8, 128 43 Prague, Czech Republic ✉ soukalkuba@gmail.com

## Keywords

ICP-MS  
molybdenum  
photochemical vapor  
generation  
UV

## Abstract

This article deals with optimization of conditions of photochemical vapor generation of molybdenum. The volatile species of molybdenum were generated in the flow arrangement, when sample was injected to a stream of a reaction medium. Efficient generation was accomplished using a 19W high-efficiency flow-through photoreactor using formic acid as the reaction medium. The generated volatile product (most probably molybdenum hexacarbonyl) was introduced to an inductively coupled plasma mass spectrometer for sensitive detection. Irradiation time, formic acid concentration and effect of additives were carefully studied with the aim to reach the highest generation efficiency. Interferences from inorganic anions ( $\text{NO}_3^-$ ,  $\text{Cl}^-$ ,  $\text{SO}_4^{2-}$ ,  $\text{NO}_2^-$ , and  $\text{ClO}_4^-$ ) were also in detail investigated. The limit of detection achieved at optimal conditions was  $1.2 \text{ pg mL}^{-1}$ .

---

## 1. Introduction

Photochemical vapor generation is an expanding and promising sample introduction technique for analytical atomic spectrometry. In photochemical vapor generation, an analyte is converted to the volatile species through the action of UV-radiation. The presence of a photochemical agent in the liquid phase is required (e.g., formic acid). The photochemical generator usually consists of a source of UV-radiation, most often a mercury UV tube lamp (emitting mainly at 254 nm), and a reaction coil that is tightly wrapped around and where the sample is converted to the volatile species. The material of the reaction coil must be made of a material transparent for UV (quartz or teflon). The advanced photoreactors (high-efficiency flow-through photoreactors) utilize a modified mercury UV lamp where the sample is irradiated in the inner channel (quartz tube) that passes through the discharge of the UV lamp. Since UV light has to transmit only a quartz wall of the inner channel, these photoreactors were shown to irradiate the sample

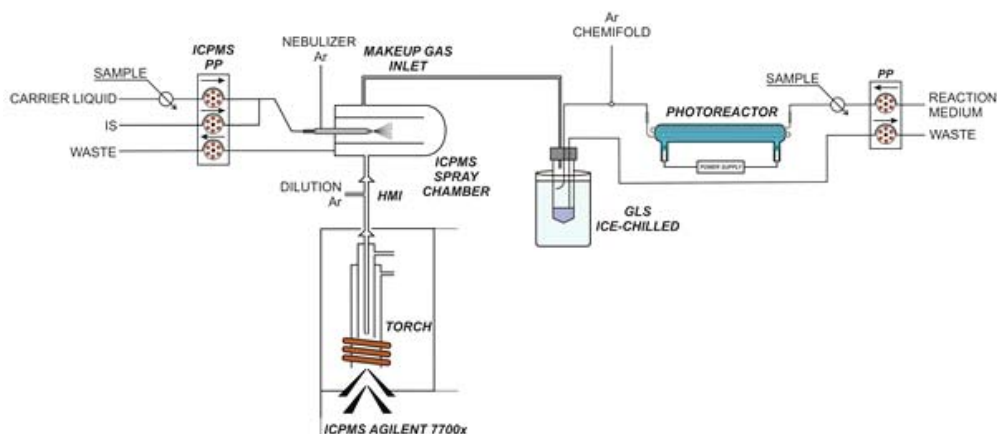


**Fig. 1** Schematic diagram of the flow injection-photochemical vapor generation system hyphenated to ICP-MS for vapor introduction of volatile molybdenum species

with photochemical agent more efficiently. Photochemical vapor generation is applicable not only to mercury and hydride forming elements (Se, As, Sb, Te, Pb, Bi) but also nonmetals (I, Br, Cl, S) and some transition metals (Ni, Fe, Co, Cu, Cd, Os) [1–4]. In this work, we present the photochemical vapor generation of molybdenum, which has never been earlier reported.

## 2. Experimental

A schematic diagram of the UV-photochemical vapor generation system in a flow-injection mode hyphenated to ICP-MS is depicted in Fig. 1. Photochemical vapor generation was accomplished using a 19W high-efficiency flow-through photo-reactor (Beijing Titan Instruments, China). The generated volatile product was directed by an argon carrier gas to a plastic gas-liquid separator (50 mL) and introduced into a spray chamber of an Agilent 7700x inductively coupled plasma mass spectrometer (ICP-MS). A solution of 1% nitric acid mixed with a solution of rhodium internal standard was nebulized into the spray chamber creating robust wet plasma conditions. The typical conditions of ICP-MS used for detection are: RF power 1600 W, nebulizer Ar  $1.02 \text{ L min}^{-1}$ , dilution Ar (via HMI)  $0 \text{ L min}^{-1}$ , Ar chemifold for photochemical vapor generation  $100 \text{ mL min}^{-1}$ , ICP-MS pump  $0.35 \text{ mL min}^{-1}$  carrier liquid and  $0.06 \text{ mL min}^{-1}$  internal standard, spray chamber temperature  $2 \text{ }^\circ\text{C}$ , He collision cell gas  $4.1 \text{ mL min}^{-1}$ , measurement mode: time resolved analysis, measured isotopes (dwell time):  $^{95}\text{Mo}$  (0.1 s),  $^{98}\text{Mo}$  (0.1 s),  $^{103}\text{Rh}$  (internal standard, 0.05 s).

### 3. Results and discussion

Firstly, a flow rate of Ar (chemifold) for photochemical vapor generation was optimized but it had no significant influence on sensitivity in the range between 100 and 500 mL min<sup>-1</sup>. The important aspect for photochemical vapor generation is an irradiation time. The influence of irradiation time of analyte was investigated by changing the flow rate of the reaction medium (30% formic acid). The highest sensitivity was found at 1.25 ml min<sup>-1</sup>. This flow rate of the reaction medium is equal to irradiation time of 39 s in the photoreactor. The flow rate 1.25 ml min<sup>-1</sup> of the reaction medium is reflected in a total time of the measurement of 350 s per one sample injection. Afterward, a concentration of formic acid as the reaction medium was optimized. The works published on photochemical vapor generation of Ni so far suggest that the higher generating efficiency is achieved by using formic acid as a reaction medium for photochemical vapor generation [5–6]. In this work, the maximum sensitivity at 50% formic acid was found for molybdenum. However, this concentration was not used further due to an inevitable dilution of sample, instability of the signal baseline, increase in signal baseline level due to contamination and formic acid vapors load into plasma. Hence, 30% formic acid was chosen as a compromise for further experiments. An influence of various additives (transition metals Fe<sup>3+</sup>, Ni<sup>2+</sup>, Cu<sup>2+</sup> ions or acetic acid, etc.) as well as adjustment in pH of the reaction medium with respect to potential enhancement in generation efficiency was also investigated. Only Fe<sup>3+</sup> ions increased significantly generation efficiency by a factor of around 1.4. A part of the research was targeted on interference from common inorganic acids and their salts (Fig. 2). Especially nitric acid and nitrates were found serious interferences during photochemical vapor generation of molybdenum.

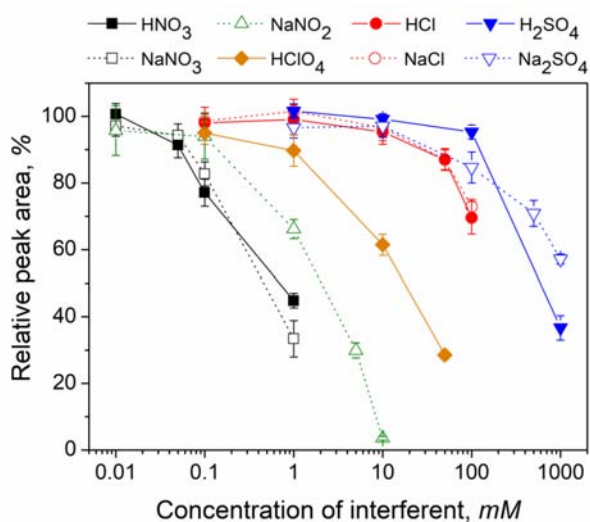


**Fig. 2** Relative effects of added inorganic acids and salts on photochemical vapor generation of 1 ng mL<sup>-1</sup> molybdenum in 30% formic acid.

**Table 1**

Concentrations of molybdenum in water certified reference materials determined by flow injection photochemical vapor generation ICP-MS using standard addition technique.

Certified reference material	Concentration of molybdenum / ng mL <sup>-1</sup>	
	Certified	Found
SRM 1643e (Fresh water)	121.4±1.3	127.7±18.9
NASS-7 (Seawater)	9.29±0.4	9.51±0.37
CASS-6 (Nearshore seawater)	9.15±0.52	8.98±0.07

**Table 2**

Concentrations of molybdenum in dietary supplement samples (µg per 1 tablet) determined by flow injection photochemical vapor generation ICP-MS (FI-PVG-ICP-MS) using standard addition technique and by nebulization-ICP-MS using external calibration.

Dietary supplement		Concentration of molybdenum / µg per tablet		
		declared	FI-PVG-ICP-MS	nebulization-ICP-MS
Centrum AZ	50		56.8±5.1	56.7±1.9
Supradyn CoQ10 energy	50		45.7±2.9	46.8±1.6

The achieved limit of detection at chosen optimal conditions was 1.2 pg mL<sup>-1</sup>. Repeatability of the measurement at 1 ng mL<sup>-1</sup> of molybdenum was better than 3%. The accuracy and feasibility of this sensitive methodology was successfully verified by analysis of certified reference materials: one fresh water (SRM 1643e) and two seawater materials (NASS-7 and CASS-6). Due to nitric acid presence used for stabilization of the certified reference materials, the materials had to be diluted and measured using standard addition technique (Table 1). The flow injection photochemical vapor generation ICP-MS was also successfully applied on two samples of dietary supplements. The tablets purchased at a local pharmacy were dissolved in 30% formic acid, sonicated at 50 °C and further diluted with 30% formic acid (for photochemical vapor generation ICP-MS) or with 1% nitric acid (nebulization-ICP-MS). All the results are compared in Table 2.

#### 4. Conclusion

Photochemical vapor generation of molybdenum has been thoroughly investigated using ICP-MS as a detector. The method is extremely sensitive with a very good repeatability. Molybdenum hexacarbonyl is supposed to be the generated volatile product. Very high efficiency of photochemical vapor generation has been reached using 30% formic acid. Further enhancement can be achieved with addition of Fe<sup>3+</sup> ions. Accuracy of the developed method has been verified on water certified reference materials and on two samples of dietary supplements. Photochemical vapor generation is prone to serious interferences from nitrates

but also chlorides which have to be taken into account with respect to real sample preparation.

### Acknowledgments

The support of the Grant Agency of the Czech Republic (P206/17-04329S), Czech Academy of Sciences (Institutional support RVO: 68081715) and Charles University (project SVV260440) is gratefully acknowledged.

### References

- [1] Rybínová M., Červený V., Hraníček J., Rychlovský P.: UV-fotochemické generování těkavých sloučenin pro potřeby atomových spektrometrických metod. *Chem. Listy* **109** (2015), 930–937.
- [2] Yin Y.G., Liu J.F., Jiang G.B.: Photo-induced chemical-vapor generation for sample introduction in atomic spectrometry. *TrAC Trends Anal. Chem.* **30** (2011), 1672–1684.
- [3] He Y.H., Hou X.D., Zheng R.E., Sturgeon R.E.: Critical evaluation of the application of photochemical vapor generation in analytical atomic spectrometry. *Anal. Bioanal. Chem.* **30** (2007), 769–774.
- [4] Sturgeon R.E.: Photochemical vapor generation: a radical approach to analyte introduction for atomic spectrometry. *J. Anal. Atom. Spectrom.* **32** (2017), 2319–2340.
- [5] Guo X., Sturgeon R.E., Mester Z., Gardner G.: UV photosynthesis of nickel carbonyl. *Appl. Organometal. Chem.* **18** (2004), 205–211.
- [6] Liu L., Deng H., Wu L., Zheng C., Hou X.: UV-induced carbonyl generation with formic acid for sensitive determination of nickel by atomic fluorescence spectrometry. *Talanta* **80** (2010), 1239–1244.

# Development of miniaturized extraction method used for GC-NCD screening of non-volatile nitroso compounds in malt

MICHAELA MALEČKOVÁ<sup>a, b, \*</sup>, TOMÁŠ VRZAL<sup>a, b</sup>, JANA OLŠOVSKÁ<sup>a</sup>

<sup>a</sup> *Research Institute of Brewing and Malting, Inc., Lípová 15, 120 44 Prague 2, Czech Republic*

<sup>b</sup> *Department of Analytical Chemistry, Faculty of Science, Charles University, Hlavova 8, 128 43 Prague 2, Czech Republic* ✉ [maleckm@natur.cuni.cz](mailto:maleckm@natur.cuni.cz)

## Keywords

chemiluminescence  
detector  
derivatization  
extraction  
gas chromatography  
nitroso compounds

## Abstract

The aim of this study was to develop a miniaturized extraction method for a fast screening of non-volatile nitroso compounds using gas chromatography with a nitroso specific chemiluminescence detection. According to a final methodology, the samples were prepared by extraction of grinded malt using a mixture of pyridine and acetonitrile in ratio 60:40 (v/v). To enhance volatility of the determined analytes, the two-step derivatization using hexamethyldisalazane and *N,O*-bis(trimethylsilyl)trifluoroacetamide was used. The total volume of the sample was 200 µl and the preparation time after optimization was 80 min. The extraction method was connected to a classification method, which can divide chromatographic peaks into the groups of *N*-nitroso and *C*-nitroso compounds, and interfering substances. After application of the methods mentioned above to real malt samples, the specific chromatographic peaks of *C*-nitroso and *N*-nitroso compounds were selected.

## 1. Introduction

Volatile *N*-nitrosamines are well-known carcinogens, which were detected in food, cosmetic products, beer, and malt. The determination of volatile *N*-nitrosamines in a malt and beer are routinely measured by a gas chromatography with mass spectrometric (GC-MS) or a nitroso specific chemiluminescence detection (GC-NCD). The sum of all nitroso groups in the sample is characterized by apparent total nitroso compounds. Volatile *N*-nitrosamines forms less than 5% of apparent total nitroso compounds in malt [1]. The rest of apparent total nitroso compounds consisted of non-volatile nitroso compounds of unknown structure. Study of these compounds more deeply would reveal their health effect.

The aim of this study was to develop a miniaturized extraction method for screening of non-volatile nitroso compounds using the GC-NCD. An extraction method consists of the preparation of a malt sample, namely an extraction and

a derivatization by hexamethyldisilazane and *N,O*-bis(trimethylsilyl)trifluoroacetamide [2].

For a total GC-NCD screening of the non-volatile nitroso compounds in malt, used extraction method is coupled with a classification method [3], that can distinguish chromatographic peaks into the groups of *N*-nitroso, *C*-nitroso, *C*-nitroso/nitro compounds and interfering substances.

## 2. Experimental

### 2.1 Reagents and chemicals

Used chemicals: pyridine ( $\geq 99.8\%$ ), acetonitrile ( $\geq 99.9\%$ ), ethyl acetate ( $\geq 99.5\%$ ), *N,O*-bis(trimethylsilyl)trifluoroacetamide with trimethylchlorosilane (99:1, v/v), hexamethyldisilazane ( $\geq 99.0\%$ ), and trifluoroacetic acid ( $\geq 99.0\%$ ), all from Sigma-Aldrich, chloroform ( $\geq 99.8\%$ , Merck), diethyl ether (99.9%), acetone (99.97%), and toluene ( $\geq 99\%$ ) all from Lach-Ner.

### 2.2 Instrumentation

Extraction and derivatization steps were performed on a heating block Pierce Reacti-Therm I. The samples were analysed on the chromatograph Thermo Trace 1310, equipped with capillary column TG-200 MS (30 m, 0.25 mm ID and 0.25  $\mu\text{m}$  df, trifluoropropyl methylpolysiloxane). Sample injections of 2.0  $\mu\text{l}$  were performed at 210 °C by a split technique (1:10). A constant flow of argon, as a carrier gas, was maintained at 0.6 ml min<sup>-1</sup>. A temperature programme was chosen as follows: 50 °C (1 min); 20 °C min<sup>-1</sup>; 150 °C (5 min); 10 °C min<sup>-1</sup>; 210 °C (3 min); 10 °C min<sup>-1</sup>; 320 °C (6 min). Detection was carried out by Ellutia 820 TEA NCD at different temperatures of a pyrolytic tube (500, 650, 700, 750 and 800 °C) to obtain related pyrolytic profiles. An oxygen flow for ozone generation was 3.2 ml min<sup>-1</sup>.

### 2.3 Sample preparation

Used malts were pilsner, munich, caramel, wheat and coloured type. Barley grains were also used. Ground malt or husk or malt flour (50 mg) was extracted by 50  $\mu\text{l}$  of a mixture of pyridine: acetonitrile (60:40, v/v) for 10 min at 65 °C. Hexamethyldisilazane (100  $\mu\text{l}$ ) and trifluoroacetic acid (1  $\mu\text{l}$ ) was added, and after 30 min at 65 °C, *N,O*-bis(trimethylsilyl)trifluoroacetamide (50  $\mu\text{l}$ ) was added. Samples were established for 30 min at 65 °C and subsequently were cooled for 10 min at laboratory temperature. The extract was transferred to a new vial insert and analysed by the GC-NCD.

## 2.4 Data processing

Experimental designs were evaluated by the ANOVA with a back elimination strategy. Data were analysed by the principal component analysis (PCA), the ANOVA and hierarchical clustering with Euclidean distance and Ward method. Data were evaluated at a significance level of 0.05.

## 3. Results and discussion

### 3.1 Development of the extraction method

In primary experiment, ground malt husks were extracted by 100  $\mu$ l of solvent and derivatized by 100  $\mu$ l of *N,O*-bis(trimethylsilyl)trifluoroacetamide for 60 minutes at 65 °C. In the first three samples, the pyridine, chloroform, and *N,O*-bis(trimethylsilyl)trifluoroacetamide were used as solvents. Resulting chromatograms showed satisfying peak intensities of the extracted analytes, therefore, other aprotic solvents were tested in the next experiment. Causentively, pyridine, chloroform, acetone, acetonitrile, diethyl ether, ethyl acetate and toluene were used and tested as solvents, separately. After comparing intensities of the chromatographic peaks, the samples extracted using pyridine, acetonitrile, and ethyl acetate had the highest analytes' abundance. To find out the best mixture of these three solvents, the 3-factor mixture design was applied. The samples were prepared using 100  $\mu$ l of the mixture of the different solvents ratio and 100  $\mu$ l of the *N,O*-bis(trimethylsilyl)trifluoroacetamide and analysed by GC-NCD. Because of the difference of the chromatographic peaks' intensities, the data were divided into two blocks as follows: **Block 1** includes peaks eluting in the range of retention times 4–16 min and **Block 2** in the range of retention times 23–27 min. The sum of the chromatographic peak area of the blocks was used as a response ( $y$ ) in the mixture design experiments described by a linear mathematical model

$$y = \sum \beta_i (\pm \varepsilon_i) x_i + \sum \beta_{ij} (\pm \varepsilon_{ij}) x_i x_j \quad (1)$$

where  $\beta_i$  is the regression coefficient of the factor  $x_i$ , and  $\beta_{ij}$  is the regression coefficient of the  $ij$  interaction between the factors  $x_i$  and  $x_j$ , and  $\varepsilon_i$ ,  $\varepsilon_{ij}$  are standard errors of the regression coefficients  $\beta_i$ ,  $\beta_{ij}$ , respectively. The linear mathematical model with evaluated regression coefficients and their standard errors are described by the equation (2) for **Block 1**, and equation (3) for **Block 2**

$$y = 18.66 (\pm 5.86) x_p + 10.11 (\pm 5.86) x_a + 4.91 (\pm 5.86) x_e + 73.66 (\pm 27.00) x_p x_a + 24.19 (\pm 27.00) x_p x_e + 10.90 (\pm 27.00) x_a x_e \quad (2)$$

$$y = 321.40 (\pm 89.42) x_p + 157.00 (\pm 89.42) x_a + 223.70 (\pm 89.42) x_e + 1024.60 (\pm 412.14) x_p x_a + 184.20 (\pm 412.14) x_p x_e - 255.10 (\pm 412.14) x_a x_e \quad (3)$$

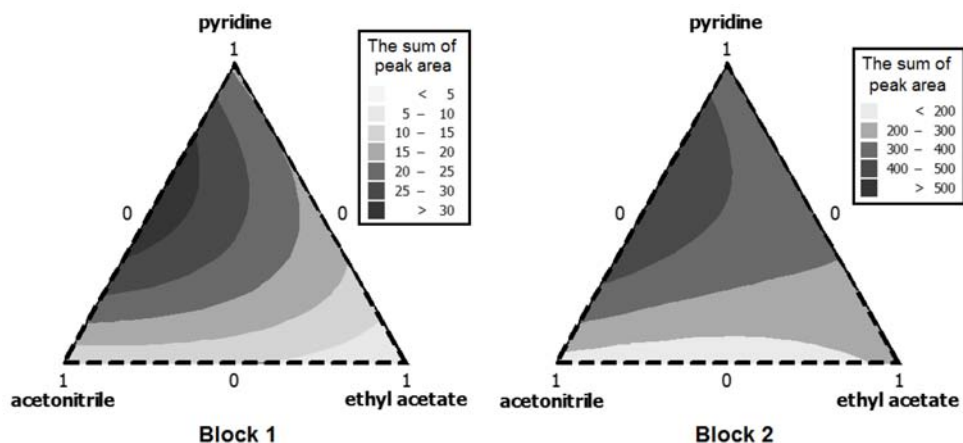


Fig. 1 The contour plot of the 3-factor mixture design.

where factors  $x_p$ ,  $x_a$  and  $x_e$  represents the volume ratio of the pyridine, acetonitrile and ethyl acetate, respectively. The coefficients of determination of these models were 81.04% and 76.20%, respectively. The models projected into the contour plots are in Fig. 1. According to both linear mathematical models, the optimum mixture of pyridine: acetonitrile: ethyl acetate is 60:40:0 (v/v/v).

In the next step of the method development, acetone and chloroform were tested, in addition to the previous solvents by a 5-factor mixture design. The sum of classified chromatographic peak area was used as a response. The linear mathematical model with the evaluated regression coefficients and their standard errors are in equation

$$y = 191.00 (\pm 51.51) x_{ac} + 283.00 (\pm 56.00) x_a + 42.00 (\pm 56.00) x_{ch} + 448.00 (\pm 56.00) x_p + 322.00 (\pm 56.00) x_e - 2690.00 (\pm 821.87) x_a x_e + 1344.00 (\pm 821.87) x_{ch} x_p \quad (4)$$

where factors  $x_{ac}$ ,  $x_a$ ,  $x_{ch}$ ,  $x_p$  and  $x_e$  represents volume ratio of the acetone, acetonitrile, chloroform, pyridine and ethyl acetate, respectively. The coefficient of determination for this model was 89.46%. The model projected into the contour plot is in Fig. 2, where factors of acetone and acetonitrile were constant. According to the linear mathematical model, the optimum mixture of acetone: acetonitrile: chloroform: pyridine: ethyl acetate is 0:0:35:65:0 (v/v/v/v/v).

Two optimum mixtures were obtained and compared in the following experiment (simultaneously tested the effect of ultrasound on the extraction). The samples were treated in the ultrasound bath for 0, 1, 5 and 15 min before the derivatization. The sum of all chromatographic peak areas was used as response values, which were evaluated by the two-way analysis of variance (ANOVA) for the six repeats. According to two-way ANOVA, the effect of ultrasound on the extraction was statistically significant ( $\alpha = 0.05$ ). The samples extracted by the

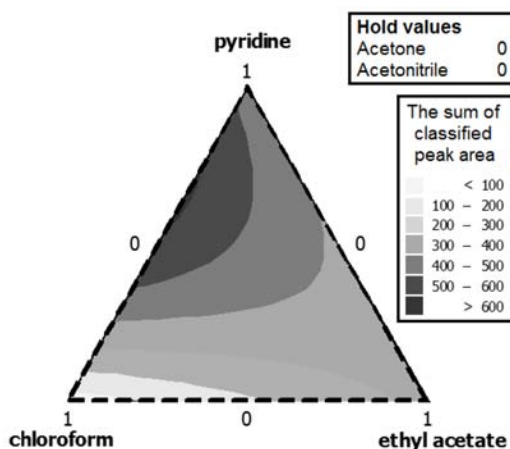


**Fig. 2** The response area plot of the 5-factor mixture design.

mixture of pyridine: acetonitrile (60:40, v/v) showed decreasing response with increasing ultrasound treatment time. Samples extracted by the mixture of pyridine: chloroform (65:35, v/v) showed constant responses in the whole time range of the ultrasound treatment. The mixture of pyridine: acetonitrile shows at least two-times higher response area than the mixture of pyridine: chloroform. This observation leads to a conclusion, that the mixture of pyridine: acetonitrile had a higher extractivity for target analytes.

According to Wainwright [4], the most abundance of nitroso compounds are located in the husk. The next experiment tested the differences among the samples prepared from the extraction of malt husk, malt flour, and malt grain. The chromatographic peak areas of selected 14 peaks eluting in all samples were used as response values and were evaluated by PCA. Fig. 3 depicts the biplot of PCA analysis, where 14 variables are represented by a vector. The samples were divided into three clusters according to a used matrix. Points of malt husk and malt

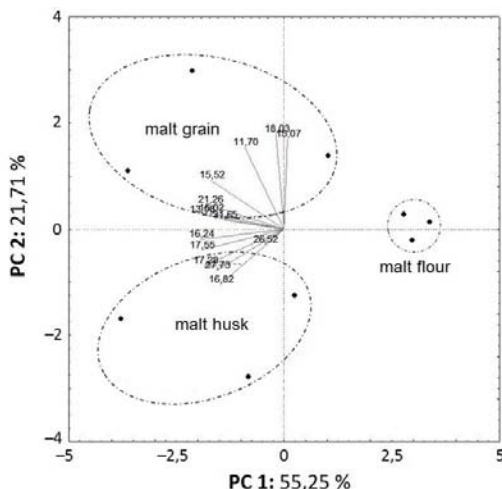


**Fig. 3** The biplot of PCA of samples prepared by extraction of malt grain, malt husk and malt flour. Vectors represent retention time of selected peaks.

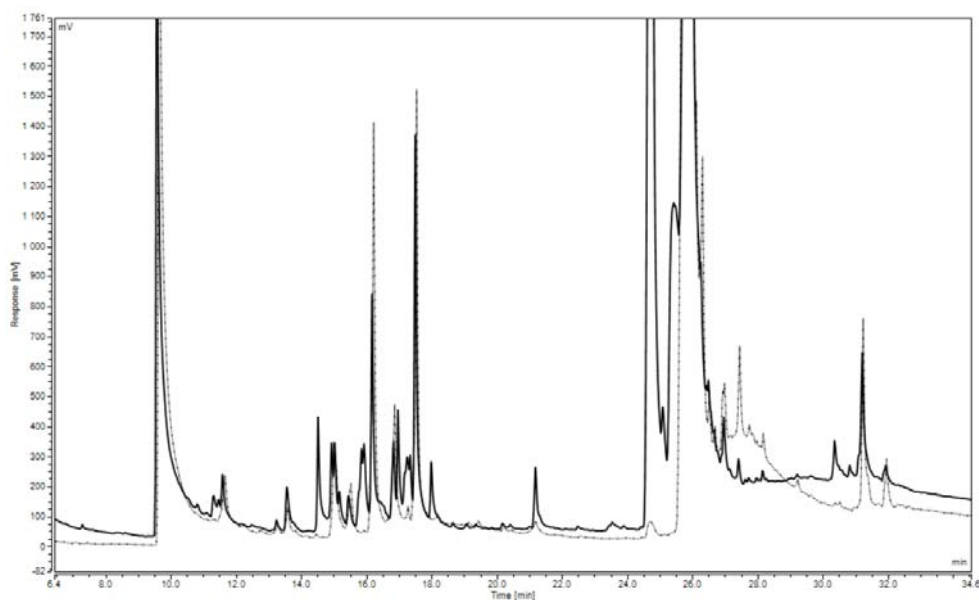


**Fig. 4** The chromatograms of the samples prepared by one-step (dashed line) and two-step derivatization (solid line).

grain matrices are in the area of higher peak areas. The samples from malt grains were chosen as the optimal matrix, due to the simpler preparation in comparison with malt husk.

So far, only *N,O*-bis(trimethylsilyl)trifluoroacetamide was used for the derivatization. A new derivatizing agent hexamethyldisilazane was added and revealed some new analytes (Fig 4). The ratio of extraction solution: hexamethyldisilazane: *N,O*-bis(trimethylsilyl)trifluoroacetamide (50:100:50, *v/v/v*) were chosen according to previously published method [2]. The whole process including the two-step derivatization was optimized using the Plackett-Burman design. The sum of standardized chromatographic peak area was used as the response ( $y$ ) in the Plackett-Burman design experiments described by a linear mathematical model

$$y = \beta_0(\pm \varepsilon_0) + \sum \beta_i(\pm \varepsilon_i) x_i \quad (5)$$

where  $\beta_0$  is an intercept, and  $\beta_i$  is a regression coefficient of the factor  $x_i$  and  $\varepsilon_i$  is standard error of the regression coefficients. Linear mathematical model, with evaluated regression coefficients and their standard errors, is described in equation

$$y = 3.67 (\pm 0.63) + 0.33 (\pm 0.63) x_{\text{ex}} - 0.67 (\pm 0.63) x_{\text{H}} + 0.83 (\pm 0.63) x_{\text{B}} + 0.00 (\pm 0.63) x_{\text{st}} \quad (6)$$

where factors  $x_{\text{ex}}$ ,  $x_{\text{H}}$ ,  $x_{\text{B}}$ , and  $x_{\text{st}}$  represent times of extraction, 1<sup>st</sup> and 2<sup>nd</sup> derivatization and time to the stabilization of the solution. This model was evaluated as very poor ( $R^2 = 0.3082$ ), therefore the decision about significance level of the factors would be inaccurate. All prior factors were maintained at 30 min (in total 120 min) and after the optimization, only factor  $x_{\text{ex}}$  and  $x_{\text{st}}$  were cut down for 10 min (in total 80 min).

### 3.2 Real sample application

The developed extraction method together with the classification method was applied to nine pilsner, three munich, three caramel, one wheat, one coloured, and two artificially nitrosated malts, and three samples of barley grains. Result classified peaks into the groups of *N*-nitroso, *C*-nitroso, *C*-nitroso/nitro compounds and interferences are depicted by a heat map in Fig. 5 (on page 112). According to the similar classification, the samples were clustered into three groups (**A**, **B**, **C**). There was observed an association between the *N*-nitrosodimethylamine concentrations in malts of particular groups and characters of clusters: the group **A** includes malts with *N*-nitrosodimethylamine concentration  $\geq 0.9$  ppb and it is characterized by a high number of detected *C*-nitroso compounds, the cluster **B** contains malts of *N*-nitrosodimethylamine concentration  $\leq 0.9$  ppb and it is characterized by the lower number of *C*-nitroso compounds but the higher number of *C*-nitroso/nitro compounds. The cluster **C** contains mostly the barley samples and the special malt, in which the concentration of *N*-nitrosodimethylamine is  $\leq 0.2$  ppb, this cluster is characteristic with no or very low number of the nitroso compounds detected.

## 4. Conclusions

Miniaturizes extraction method for the screening of the non-volatile nitroso compounds in malt samples, using the GC-NCD, was developed. For the sample preparation, the grained malt was chosen to be appropriate for the screening analysis. The method uses 50  $\mu\text{l}$  of the pyridine: acetonitrile mixture in ratio 60:40 ( $v/v$ ) and none ultrasonication treatment are required. Two-step derivatization is also suitable. The optimum ratio of extraction solution: hexamethyldisilazane: *N,O*-bis(trimethylsilyl)trifluoroacetamide is 50:100:50 ( $v/v/v$ ). The total time of sample preparation is 80 min (including 10 min of the extraction at 65 °C, two-times 30 min of the two-step derivatization at 65 °C and 10 min of stabilizing at 20 °C). The real sample application reveals the association between *N*-nitrosodimethylamine concentration and the characteristic classification of the nitroso compounds among the samples within the same clusters.

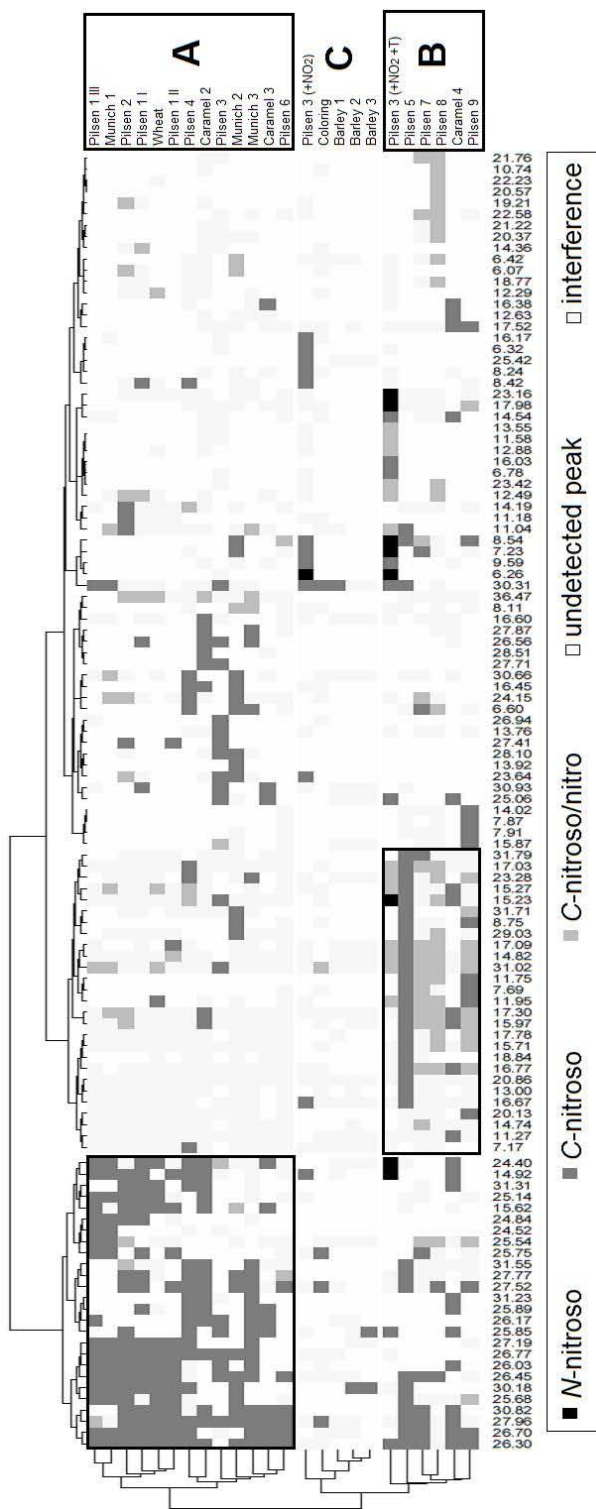


Fig. 5 The heatmap of peak classification in malt samples.

### Acknowledgments

This study was supported by the project of Ministry of Education Youth and Sports of the Czech Republic No. LO 1312.

### References

- [1] Johnson P, Pfab J., Tricker A., Key P., Massey R.: An investigation into the apparent total *N*-nitroso compounds in malts. *J. Inst. Brew.* **93** (1987), 319–321.
- [2] Gabrišová L., Kotora P, Peciar, P.: Characterization of nutritional supplement with content of vaccinium macrocarpon based on comparison of chosen flavonol glycosides by HTGC-MS. In: *Proceedings of the 13th ISC Modern Analytical Chemistry*. Prague, Faculty of Science, Chales University 2017, p. 126–130.
- [3] Vrzal T., Matoulková D., Olšovská, J.: A new method for detection and classification of non-volatile nitroso compounds in beer combining gas chromatography with chemiluminescence detection and discriminant analysis. In: *Proceedings of the 13th ISC Modern Analytical Chemistry*. Prague, Faculty of Science, Chales University 2017, p. 12–19.
- [4] Wainwright T.: Nitrosamines in malt and beer. *J. Inst. Brew.* **92** (1986), 73–80.

# Chromato-desorption method for producing gas mixtures of volatile organic compounds

IGOR ARTEMYEVITCH PLATONOV<sup>a</sup>, IRINA NIKOLAEVNA KOLESNICHENKO<sup>a</sup>,  
DIANA DAVIDOVNA KARAPETIAN<sup>b,\*</sup>, ASTKHIK EDIKOVNA IGITKHANIAN<sup>b</sup>

<sup>a</sup> *Department of Chemistry, Samara National Research University,  
Moskovskoye shosse, 443086 Samara, Russia* ✉ [pia@ssau.ru](mailto:pia@ssau.ru)

<sup>b</sup> *Institute of Space Rocket Engineering, Samara National Research University,  
Moskovskoye shosse, 443086 Samara, Russia* ✉ [dianik2@mail.ru](mailto:dianik2@mail.ru)

## Keywords

calibration mixtures  
chromato-desorption  
microsystems  
ecological control  
gas chromatography

## Abstract

A new simple chromato-desorption method for the preparation of calibration gas mixtures containing microconcentrations of volatile organic compounds is proposed. Various methods for the preparation of calibration mixtures are considered. The possibility of obtaining calibration gas mixtures in the concentration range 3–10 mg m<sup>-3</sup> ( $\delta_{\max} = 15\%$ ) is shown. A comparative evaluation of the proposed and standardized methods is carried out. It is proved that the chromatography-desorption method allows to increase the accuracy of preparation of calibration mixtures, and also to reduce the total error of the analysis by 13–15%.

---

## 1. Introduction

To date, the environmental situation in the world can be characterized by a high level of anthropogenic impact on the natural environment. In addition, recently, human habitat has dramatically changed, including in connection with pollution with mutagenic and teratogenic factors of various origins, which puts the vast majority of the population in other conditions of existence than in previous generations [1].

World over wide chemical, metallurgical, oil refining and gas processing industries are widespread, which lead to an increase in the release of industrial waste. One of the most common production-related air pollutants is acetone, whose high content in the air can cause serious harm to the human body.

Despite the fact that acetone is a natural metabolite of the human body, exceeding its permissible concentrations in the blood with prolonged external action is accompanied by a disturbance of metabolic processes, a manifestation of signs of liver dysfunction [2]. The liver is the central body of neutralization and utilization of foreign compounds of exogenous origin and further the severity of damage to its metabolic systems may depend on the subsequent toxic effects of ecotoxicants on all organs and systems of the body [3].

At present, gas analyzers and gas chromatographs are used to reliably and systematically control the level of environmentally hazardous substances in air environments [4]. At the same time, the accuracy of the measurements depends on the efficiency of calibration and calibration of gas analyzing equipment [5], which is associated with the use of liquid, gas and vapor-gas mixtures with a standardized content of volatile organic compounds.

The purpose of this work is the development of new methods and devices to improve the accuracy and adequacy of the preparation of calibration mixtures for the subsequent quantification of volatile organic compounds in air environments.

## 2. Experimental

### 2.1. Preparation of liquid and gas-vapor grading mixtures

Liquid acetone calibration mixtures in the range of measurable concentrations from 0.05 to 5.00 mg m<sup>-3</sup> were prepared by the volumetric method, by successively diluting the pure substance.

Vapor-gas calibration acetone mixtures in the range of measured concentrations from 0.0005 to 5.0000 mg m<sup>-3</sup> were obtained using static gas extraction [6].

### 2.2 Gas mixtures obtained by dynamic chromatography-desorption method

To build the calibration characteristics, also used gas mixtures of acetone, obtained by the chromato-desorption method. This method is based on the equilibrium saturation of the inert gas flow of volatile organic compounds as it passes through the chromato-desorption microsystem [7]. The system is a medical needle (length 32 mm, internal diameter 0.5 mm) filled with a sorbent with a known amount of volatile organic compounds. In this study, the following sorbents: Chromaton N-AW-DMCS/25% CaCl<sub>2</sub>, Chromaton N-AW-DMCS/25% CoCl<sub>2</sub> and Fiberglass/50% PEG.

To obtain gas mixtures of acetone by a chromatographic-desorption method, a outline was implemented, the algorithm of which is shown in Fig. 1.

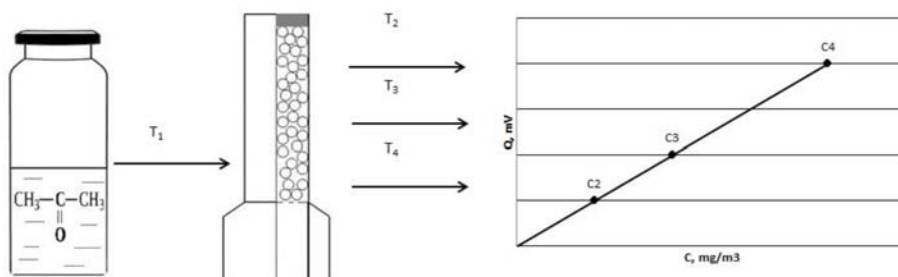


Fig. 1 Preparation of gas mixtures by a chromato-desorption method.

The process of obtaining gas mixtures was carried out in two stages [7]:

1. The chromato-sorption stage includes the preparation of a sorbent, the filling of a column, and the equilibrium saturation of the sorbent with impurities of volatile substances. In this case, there is a multiple redistribution of the analyte in the volume of the sorbent, so that an insignificant concentration gradient of the analyte can be achieved during the use of chromato-desorption micro-system. Thus, by changing the temperature, by adjusting the value of the distribution constant of substances in the system, it is possible to obtain gas flows containing micro-quantities of volatile components.
2. The chromato-desorption stage consists in the equilibrium desorption of volatile substances at temperatures equal to the sorption temperature.

### 2.3 Calibration of analytical equipment

The experiment was carried out on a gas chromatograph Crystal 5000.1 with a flame ionization detector. To separate the sample components, a quartz capillary column 50 m long, 0.32 mm inner diameter and 0.5  $\mu\text{m}$  thick non-polar stationary phase OV-351 film was used. The measurements were carried out under the conditions of programming the temperature from 600  $^{\circ}\text{C}$  (for 7 minutes) to 200  $^{\circ}\text{C}$  with a gradient of 20  $^{\circ}\text{C min}^{-1}$ , temperature of the detector 220  $^{\circ}\text{C}$ , evaporator temperature of 100  $^{\circ}\text{C}$ . As the carrier gas, nitrogen was used (osm., GOST 9093-74), consumption 20.9  $\text{cm}^3\text{min}^{-1}$ , hydrogen and air consumption 20  $\text{cm}^3\text{min}^{-1}$  and 200  $\text{cm}^3\text{min}^{-1}$ , respectively. In the case of chromato-desorption microsystem, the column temperature ranged from 50, 70 or 100  $^{\circ}\text{C}$  to provide gas mixtures with different concentrations of the target component.

## 3. Results and discussion

Estimation of convergence limit and reproducibility limit of the calibration mixtures preparation are presented in Table 1. It should be noted that the use of liquid calibration mixtures is limited by the level of purity of the solvent, which has matrix microimpurities in its composition, which makes it impossible to directly determine the analyte at the level of microconcentrations and at values close to

**Table 1**

Estimation of convergence limit ( $r$ ), reproducibility limit ( $R$ ), and correlation coefficient ( $K$ ) of the calibration mixtures preparation.

Calibration mixtures	$r / \%$	$R / \%$	$K$
Liquid	6.1	7.7	0.90
Vapor-gas	10.2	15.8	0.93
Gas, obtained by a discrete chromato-desorption system method	12.4	17.6	0.95

the threshold of the sensitivity of the detector. To reduce the measurement error, it is possible using the subtraction method of the solvent background, but even in this case it is not possible to achieve the required accuracy.

The use of chromato-desorption microsystem makes it possible to obtain calibration gas mixtures with an acetone content of 3 to 10 mg m<sup>-3</sup> when operating in the temperature range 50-100 °C.

It was experimentally established that when discrete dosing of a gas mixture containing a standardized microcumulative amount of acetone, the operating life of chromato-desorption microsystem is at least 6 cycles with a standard deviation of  $\delta = 15\%$ . At the same time, the renewable resource of the system was at least 3 cycles. Fig. 2–4 shows relation between acetone concentration and the number of consecutively obtained gas mixtures with the use of chromato-desorption microsystem filled with different type of sorbents.

An important advantage of chromato-desorption microsystem is the possibility of obtaining multi-point calibrations, without additional dilution of the flow, by varying the desorption temperature.

Comparison of data on calibrations obtained using standard methods and using chromato-desorption microsystem shows that the application of the developed systems makes it possible to improve the accuracy of the linear dependence description by reducing the total error of the analysis when using chromato-desorption microsystem by 13–15%.

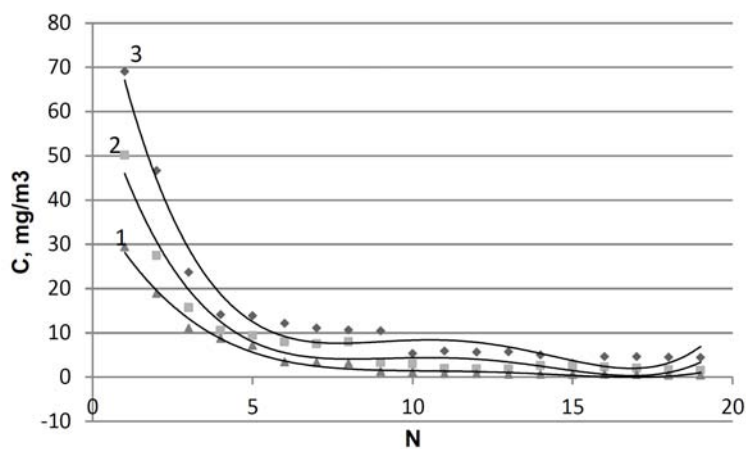


**Fig. 2** Dependence of acetone concentration on duration of use chromato-desorption microsystem (Chromaton N-AW-DMCS/25% CoCl<sub>2</sub>) at temperatures (1) 50 °C, (2) 70 °C, and (3) 100 °C.

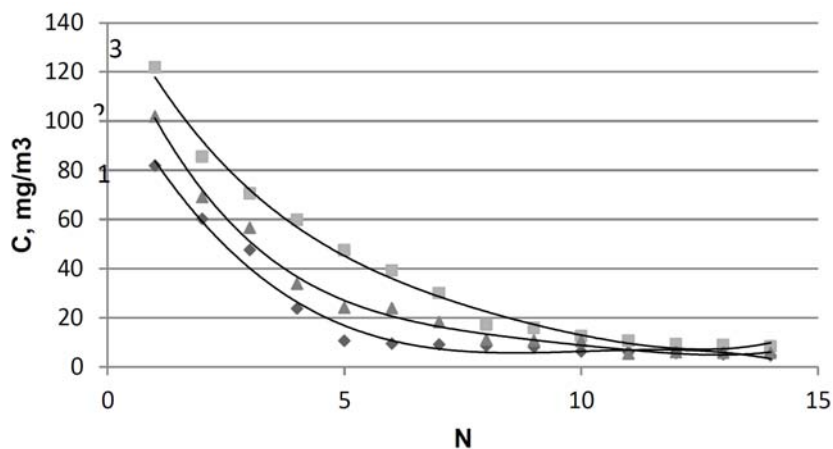


**Fig. 3** Dependence of acetone concentration on duration of use chromato-desorption microsystem (Chromaton N-AW-DMCS/25% CaCl<sub>2</sub>) at temperatures (1) 50 °C, (2) 70 °C, and (3) 100 °C.

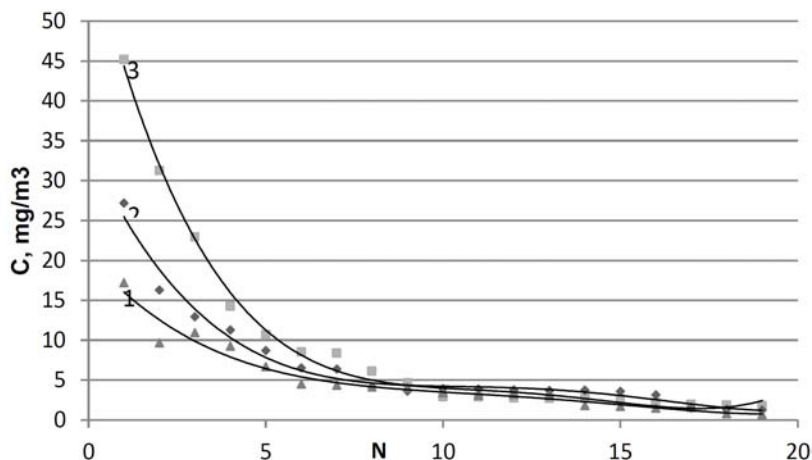


**Fig. 4** Dependence of acetone concentration on duration of use chromato-desorption microsystem (Fiberglass/50% PEG) at temperatures (1) 50 °C, (2) 70 °C, and (3) 100 °C.

#### 4. Conclusions

A new simple method for obtaining calibration gas mixtures containing known constant microconcentrations of volatile organic compounds is proposed. The experimental verification of the proposed method showed the expediency of its practical use. Gas mixtures obtained by the chromatographic-desorption method are applicable for calibration and calibration of gas analytical equipment for the quantitative analysis of organic and inorganic contaminants in ambient air, workplace air, and also for other purposes, for example, in the analysis of biomarkers in exhaled air. It should be noted that the use of developed microanalytical

systems has several advantages, the main of which are simplicity of hardware design, universality, efficiency, exponentiality and the possibility of automation of analysis.

### Acknowledgments

The reported study was funded by the Ministry of the Education and Science of the Russian Federation under project No. 4.6875.2017/8.9.

### References

- [1] Delgado-Saborit J.M., Aquilina N.J., Meddings C., Baker S., Harrison R.M.: Model development and validation of personal exposure to volatile organic compound concentrations. *Environ. Health Perspect.* **117** (2009), 1571–1579.
- [2] Фоменко С.Е., Кушнерова Н.Ф.: Экспериментальная оценка токсического влияния ацетона на метаболические реакции печени в условиях повышенной влажности воздуха. *Токсикологический вестник* **2** (2013), 9–14.
- [3] Мышкин В.А., Еникеев Д.А., Срубиллин Д.В., Гимадиева А.Р.: Экспериментальная оценка производных пиримидина на моделях токсического поражения печени: обзор. *Научное обозрение. Медицинские науки* **3** (2016), 88–98.
- [4] Bellar T, Sigsby J.E., Clemons C.A., Altshuller A.P.: Direct application of gas chromatography to atmospheric pollutants. *Anal. Chem.* **34** (1962), 763–765.
- [5] McKinley J., Majors R.E.: The preparation of calibration standards for volatile organic compounds – a question of traceability. *LC-GC Eur.* **13** (2000), 892–895.
- [6] Vitenberg, A. G., Konopelko L.A.: Gas chromatographic headspace analysis: metrological aspects. *J. Anal. Chem.* **66** (2011), 438–457.
- [7] Platonov I.A., Kolesnichenko I.N., Lange P.K.: Chromatographic-desorption method for preparing calibration gas mixtures of volatile organic compounds. *Meas. Tech.* **59** (2017), 1330–1333.

# MS/MS analysis of fatty acid methyl esters in diesel

PAULÍNA GALBAVÁ<sup>a,\*</sup>, ŽOFIA NIŽNANSKÁ<sup>a</sup>, ĽUDMILA GABRIŠOVÁ<sup>b</sup>, OLIVER MACHO<sup>b</sup>, RÓBERT KUBINEC<sup>a</sup>, JAROSLAV BLAŠKO<sup>a</sup>, JOZEF MIKULEC<sup>c</sup>

<sup>a</sup> *Institute of Chemistry, Faculty of Natural Sciences, Comenius University in Bratislava, Illkovičova 6, 842 15 Bratislava, Slovakia ✉ galbava11@uniba.sk*

<sup>b</sup> *Institute of Process Engineering, Faculty of Mechanical Engineering, Slovak University of Technology in Bratislava, Námetie slobody 17, 821 43 Bratislava, Slovakia*

<sup>c</sup> *VÚRUP, a.s., Vlčie hrdlo, 820 03 Bratislava, Slovakia*

## Keywords

biodiesel  
diesel  
GC-FID  
fatty acid methyl ester  
MS/MS  
restrictor

## Abstract

The work is focused on the development of a new method for fatty acid methyl ester analysis in diesel. The method allows rapid analysis of individual fatty acid methyl ester in diesel. The linearity of the method is in the range of 0.5% to 40% for biodiesel, providing comparable results with the GC-FID method with a 10-fold shorter analysis time. Unlike the standard method (STN EN 14078), with this new method it is possible to identify individual methyl esters in diesel and due to high selectivity, the analysis is not burdened by the interference of other components present in diesel. The content of fatty acid methyl esters in diesel obtained from the local gas station at the level 6.1% with a relative standard deviation of 3% was determined.

---

## 1. Introduction

Interest in biodiesel, as an alternative to fossil fuels, is continuing to increase, what is a result of population growing, exhaustion of fossil fuels, global warming and oil price fluctuations [1]. Biodiesel is an acceptable alternative fuel for diesel engine, due to its technical, environmental and strategic advantages. Biodiesel, defined as the monoalkyl esters of long chain fatty acids, is produced from several types of conventional and non-conventional vegetable oils and animal fats [2].

In addition to its renewability, other advantages of biodiesel include non-carcinogenic and non-mutagenic properties, biodegradability, miscibility with petroleum diesel, lubricity, high flash point and cetane number and absence of aromatic compounds [1]. Biodiesel can be used pure or mixed with petroleum distillates to attain blends defined with the abbreviation BXX, where XX stands for the biodiesel percentage (v/v) [3]. It can be used for industrial processes and transport engines. In Slovakia at present, the minimum content of bio-compo-

nents in diesel is 6%, with the percentage of biodiesel being increased as amended by the EU regulation [3].

The content of biodiesel in fuel is possible to determine using various methods, whereby to the most preferred belong gas chromatography with flame ionization detector (GC-FID) or mass spectrometric detector (GC-MS). These methods are able to determine the content of the individual fatty acid methyl esters in the samples, what makes it possible to determine the origin of the oil used to prepare fatty acid methyl ester [4]. The disadvantage of these methods is the relatively long analysis time, which in some cases takes almost an hour. A more rapid and inexpensive method for determining bio-components in diesel is the use of infrared spectroscopy, where the presence of the C=O group is monitored. The limitation of infrared spectroscopy method is that for correct bio-compound content determination in diesel is necessary to know the origin or the composition of the individual fatty acid methyl esters. Furthermore, other components containing C=O group present in diesel can provide a positive signal, not necessarily belonging to the bio-components. By default, the biodiesel content in diesel is determined according to STN EN 14078 by infrared spectroscopy.

The aim of this work is to develop a new method, which combines the benefits of the previously proposed methods, as rapid analysis (infrared spectroscopy) and high reliability (as GC-FID; GC-MS methods), where the possibility of interference with other substances present in fuel is minimized.

## 2. Experimental

### 2.1 Chemicals and sample preparation

Samples of plant oils (rapeseed, sunflower, palm oils) were bought on local market and biodiesel was purchased from local gas station. Sodium methoxide, oxalic acid, methanol, hexane were purchased from Sigma-Aldrich (Steinheim, Germany). The methyl esters of fatty acids were prepared using basic transesterification by adding 100 mm<sup>3</sup> of a 0.5 mol dm<sup>-3</sup> solution of sodium methoxide in dry methanol to the samples in 1000 mm<sup>3</sup> hexane. Samples were mixed and reacted at 40 °C for 15 minutes. In the next step 60 mm<sup>3</sup> of oxalic acid (0.5 g in 15 cm<sup>3</sup> of diethyl ether) was added to the solution, it was mixed thoroughly and centrifuged at 2000 r min<sup>-1</sup> for 3 minutes to settle the precipitated sodium oxalate. The samples of biodiesel were prepared at the concentration 100 µg mm<sup>-3</sup> in hexane with diethylphtalate as internal standard with concentration 10 mg mm<sup>-3</sup>.

### 2.2 Instrumentation

GC-MS/MS analyses were performed using a Trace GC Ultra gas chromatograph with a TriPlus autosampler and a TSQ Quantum XLS mass spectrometer (Thermo Fisher, Austin, TX, USA). The injector temperature was set to 350 °C. Samples with

injection volume of 1 mm<sup>3</sup> were injected in a 2 m long fused-silica capillary with 50 µm I.D., with a deactivated surface (restrictor) (Agilent Technologies, PaloAlto, CA, USA). Helium was used as a carrier gas with constant flow of 0.01 cm<sup>3</sup>min<sup>-1</sup> in splitless mode. The temperature of the chromatographic oven and transfer line was 350 °C. The main parameters related to the mass spectrometer setup were: the ion source temperature was 230 °C, the collision gas was argon with pressure of 1.5 Pa in the collision chamber, electron energy 70 eV, emission current 50 µA. The mass spectra in SCAN mode were obtained in the range  $m/z = 33-350$ , MS/MS detection was performed using Selected Reaction Monitoring (SRM) transitions experimentally optimized for the selected analytes. The used SRM transitions were  $m/z$  270→101 and 270→73 for C16:0,  $m/z$  292→121 and 292→33 for C18:3,  $m/z$  294→81 and 294→95 for C18:2,  $m/z$  296→101 and 296→81 for C18:1,  $m/z$  298→101 and 298→73 for C18:0,  $m/z$  326→121 for C20:0 with collision energy set to 15 V, and for diethyl phthalate as internal standard 177→149 with collision energy 15 V, with a scan time of 20 msec each.

Comparative analyzes were performed using GC-FID 6890N (Agilent Technologies, PaloAlto, CA, USA). The injector temperature was set to 300 °C. Volume of 1 mm<sup>3</sup> of samples were injected in split mode (70:1). Helium was used as a carrier gas at constant pressure 255.1 kPa. Chromatographic separation was carried out on a DB-23 60 m × 0.25 mm × 0.25 µm capillary column. The oven temperature was set to 70 °C for 2 min and gradually increased to 150 °C at a rate of 25 °C min<sup>-1</sup>, than the temperature was increased to 240 °C at a rate of 5 °C min<sup>-1</sup> and held 5 min. The detector temperature was 280 °C. Total analysis time was 28.2 min.

### 3. Results and discussion

To study the suitability of the newly developed method for the fatty acid methyl esters determination in diesel, methyl esters of most used oils in the production of biofuels were prepared. Table 1 shows the percentages of individual fatty acids in

**Table 1**

Fatty acid compositional profiles of fats and oils (as fatty acid methyl ester) in percentages.

Fatty acid			Palm oil		Rapeseed oil		Sunflower oil	
Name	Abb.	$t_r$ / min	meas.	publ.	meas.	publ.	meas.	publ.
Myristic acid	14:0	12.0	1.1	1.1	0.1	0	0.1	0.1
Palmitic acid	16:0	14.5	44.3	42.5	4.8	4.2	6.2	6.4
Palmitoleic acid	16:1	14.9	0.5	0.2	0.5	0.1	0.1	0.1
Stearic acid	18:0	17.2	4.4	4.1	1.9	1.6	3.7	3.6
Oleic acid	18:1	17.6	39.9	41.3	63.3	59.5	23.8	21.7
Linoleic acid	18:2	18.3	9.9	9.5	19.2	21.5	64.5	66.3
Linolenic acid	18:3	19.2	0.0	0.3	7.7	8.4	0.3	1.5
Arachidic acid	20:0	20.0	0.0	0.3	0.6	0.4	0.4	0.3
Gondoic acid	20:1	20.3	0.0	0.1	1.5	2.1	0.2	0.2
Behenic acid	22:0	22.6	0.0	0.1	0.3	0.3	0.7	0.6
Erucic acid	22:1	23.0	0.0	0	0.3	0.5	0.0	0.1

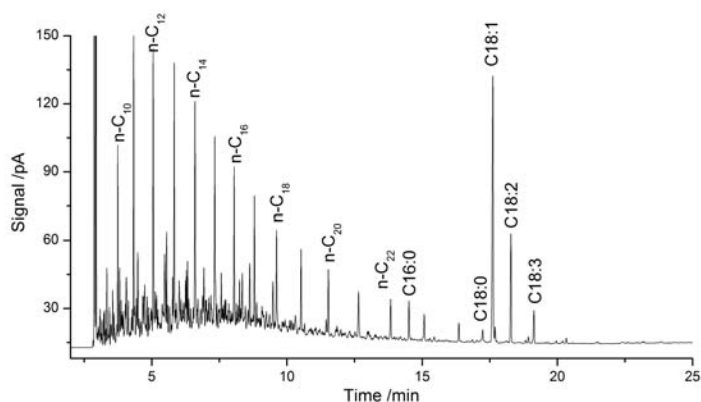


**Fig. 1** GC-FID chromatogram of diesel purchased on local gas station.

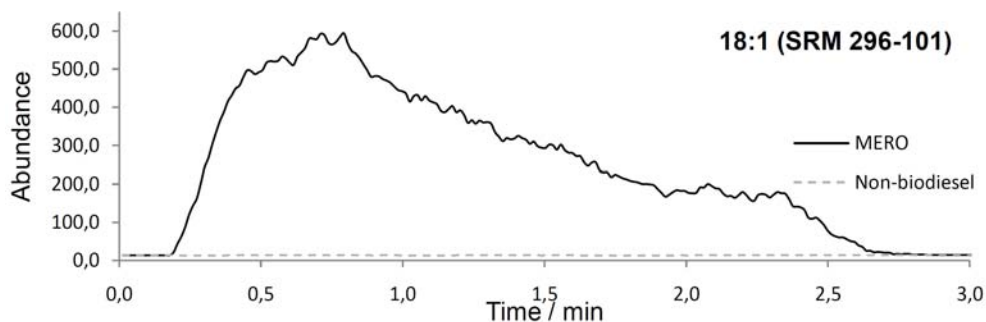


**Fig. 2** GC-MS/MS chromatographic record of oleic acid in biodiesel and diesel without bio-components. The methyl esters of rapeseed oil are marked with abbreviation MERO.

oils obtained by GC-FID analysis after basic transesterification. The individual fatty acid contents (percentages) vary significantly depending on the oil used. In Central Europe, rapeseed oil is most often used for biodiesel production. For this reason, we observed a mixture of methyl esters obtained mainly from rapeseed oil. Fig. 1 shows the GC-FID chromatographic record of diesel purchased on a local gas station.

Using a given separation system, bio-components (biodiesel components originating from plant oils) can be reliably distinguished from those derived from crude oil (Fig. 1). Total GC-FID analysis time is 25 minutes plus several minutes to cool and equilibrate the chromatographic system.

Fig. 2 shows a GC-MS/MS chromatographic record of oleic acid in diesel containing bio-component and without bio-component. From Fig. 2 is apparent, that it is possible to clearly distinguish diesel with fatty acid methyl ester addition (biodiesel) from diesel without fatty acid methyl ester addition. The individual

**Table 2**

Characteristics of the calibration curves for rapeseed fatty acid methyl ester.

Fatty acid methyl ester	SRM	<i>a</i> (slope)	<i>b</i> (intercept)	<i>R</i> <sup>2</sup>
C16:0	270-101	925	18900	0.996
	270-73	9600	7970	0.992
C18:3	292-121	9320	8030	0.993
	292-93	1510	4730	0.995
C18:2	294-81	42900	21300	0.994
	294-95	22900	10350	0.994
C18:1	296-101	2460	20480	0.995
	296-81	9730	17800	0.996
C18:0	298-101	2220	10700	0.995
	298-73	460	4780	0.993
C20:0	326-101	-1500	3740	0.995

SRM transitions, characteristics of the calibration curves for the individual fatty acid methyl ester originating from rapeseed oil are shown in Table 2.

The newly developed method based on MS/MS detection without chromatographic separation allows to monitor the content of individual fatty acid methyl ester in diesel at a concentration range of 0.5–40.0% (v/v) with a high linearity of the method (*R*<sup>2</sup> in the range 0.992–0.996). From the calibration curves listed in Table 2 we calculated the content of bio-components in diesel purchased at the local gas station. The determined biodiesel contents were 5.9% (v/v) using GC-FID method and 6.1% (v/v) using the GC-MS/MS method. The average RSD of the individual fatty acid methyl ester in biodiesel is 3.1%.

#### 4. Conclusion

The newly developed analytical method makes it possible to determine the fatty acid methyl esters content in the range of 0.5–40.0% (v/v) in diesel. The advantage of this method compared to the official method based on infrared spectroscopy is the possibility to determine the content of individual fatty acid methyl ester in diesel, what means that the type of plant oil used as bio-component can be determined. Also, the high selectivity of the method makes it possible to filter out various impurities that give positive response using infrared spectroscopy. Compared to the classic GC-FID or GC-MS method, our method provides comparable data about the composition of fatty acid methyl ester, however is 10 times faster.

#### Acknowledgments

This work was supported by the Slovak Research and Development Agency under the contract number APVV-15-0466.

## References

- [1] Hoekman S.K., Broch A., Robbins C., Cenicerros E., Natarajan M.: Review of biodiesel composition, properties, and specifications. *Renew. Sust. Energ. Rev.* **16** (2012), 143–169.
- [2] Knothe G.: Analyzing biodiesel: Standards and other methods. *J. Am. Oil. Chem. Soc.* **83** (2006), 823–833.
- [3] Mogollon N.G.S., Ribeiro A.L.F., Lopez M.M., Hantao L.W., Poppi R.J., Augusto F.: Quantitative analysis of biodiesel in blends of biodiesel and conventional diesel by comprehensive two-dimensional gas chromatography and multivariate curve resolution. *Anal. Chim. Acta.* **796** (2013), 130–136.
- [4] Ragonese C., Tranchida P.Q., Sciarrone D., Mondello L.: Conventional and fast gas chromatography analysis of biodiesel blends using an ionic liquid stationary phase. *J. Chromatogr. A* **1216** (2009), 8992–8997.

# New biosensor matrices based on carbon nanomaterials for tyrosinase immobilization

KAROLINA STARZEC\*, JOLANTA KOCHANA

Department of Analytical Chemistry, Faculty of Chemistry, Jagiellonian University in Kraków, Gronostajowa 2, 30-387 Kraków, Poland ✉ karolina.wapiennik@doctoral.uj.edu.pl

## Keywords

biosensors  
titania gel  
tyrosinase  
voltammetry

## Abstract

Biosensor matrices based on titania gel modified with carbon nanomaterials: multi-walled carbon nanotubes (MWCNTs) and mesoporous carbon CMK-3 were examined. Matrix composites were additionally enriched by poly(diallyldimethylammonium), gold nanoparticles, Nafion® and glutaraldehyde. Tyrosinase was used as model active biological component. To choose the optimum matrix composite, cyclic voltammetry measurements were carried out in a catechol solution. Sensitivity of each biosensor toward catechol and corresponding value of Michaelis-Menten constants, an indicator of biological affinity of biosensor to substrate, were estimated. The morphology of matrix nanocomposites was characterized by SEM images.

## 1. Introduction

A biosensor is a small measuring device which allows the biological response to be transformed into analytically useful signal, most commonly electrical [1]. The scheme of biosensor is shown in Fig. 1. Biosensors based on tyrosinase are the most sensitive sensors used for the determination of phenolic compounds. Tyrosinase is a copper containing enzyme belonging to the class of oxidoreductases (EC 1.14.18.1). Tyrosinase catalyzes the oxidation of monophenols by molecular oxygen to form *o*-diphenols, which are then transformed by dehydrogenation to *o*-quinones. The resulting *o*-quinones can be reduced at the electrode surface by generating a signal (current) enabling the electrochemical determination of phenolic compounds [2].

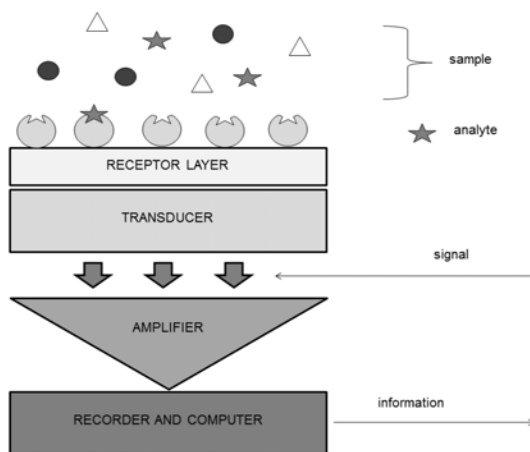


Fig. 1 Scheme of electrochemical biosensor.

Crucial step in the development of new biosensors is the immobilization of bioelement in the receptor layer in the way to retain its catalytic activity [3, 4]. Additionally, the matrices should provide easy access of analyte to bioreceptor, resulting from developed surface area, be characterized by high mechanical strength and, for electrochemical biosensors, the excellent electron transfer [5]. There are several methods of immobilizing biocatalytic elements on the transducer surface like physical adsorption, covalent binding, matrix entrapment, intermolecular cross-linking and encapsulation [6].

In the scientific reports various kinds of biosensors using tyrosinase-enzyme as a biocatalytic element have been reported, like screen-printed carbon electrodes modified by gold nanoparticles [7], graphene modified carbon working electrodes by cross-linking with glutaraldehyde [8], or graphene-gold nanoparticles [9].

Currently, carbon materials including multiwalled carbon nanotubes (MWCNTs) and mesoporous carbon CMK-3 are very promising materials in biosensing research [10, 11]. Both mentioned carbon materials are very attractive because of its applications and properties. Carbon materials are characterized by high specific pore volume (CMK-3), large surface area, hydrophobicity, thermal stability and chemical inertness [6, 12]. Moreover, the use of carbon nano and mesoporous materials have become important due to their excellent conductivity resulting in the improvement of electron transfer between the enzymes and the electrode surfaces [10, 13].

The goal of the presented research was to develop, study and compare various matrices of tyrosinase biosensors based on titanium dioxide gel modified with two type of nanostructured carbon materials: multiwalled carbon nanotubes and mesoporous carbon CMK-3. Matrix composites were additionally enriched with gold nanoparticles (AuNPs), Nafion®, glutaraldehyde (GA) or polycationit, poly(diallyldimethylammonium) chloride (PDDA). For verification purposes, multi-component matrices deposited on the graphite electrode surface were examined with respect to the mechanical durability. Sensitivity of each biosensor toward catechol, the model substrate of enzyme, and corresponding value of Michaelis-Menten constants, an indicator of biological affinity of biosensor to substrate, were estimated.

## 2. Experimental

### 2.1. Reagents and chemicals

Catechol ( $\geq 99\%$ ), tyrosinase from mushroom (EC1.14.18.1; 1881 U mg<sup>-1</sup> and 3130 U mg<sup>-1</sup>), poly(diallyldimethylammonium chloride) PDDA (average  $M_w < 100,000$ , 35 wt% in water), glutaraldehyde (70%), Nafion (5%, w/v, solution in mixture of low aliphatic alcohol and water) and multi-walled carbon nanotubes were purchased from Sigma-Aldrich (USA); mesoporous carbon CMK-3 was

synthesized in Department of Chemical Technology at the Jagiellonian University in Krakow, ethanol (96%),  $\text{HNO}_3$  (65%), 2-propanol, L-(+)-ascorbic acid,  $\text{KH}_2\text{PO}_4$  and  $\text{Na}_2\text{HPO}_4 \cdot 2\text{H}_2\text{O}$  were obtained from Avantor Performance Materials Poland S.A. (Poland);  $\text{HCl}$  (35%),  $\text{NH}_3$  (25% aqueous solution), and acetone were purchased from Lach-Ner (Czech Republic); 0.3 mm alumina powder was from Buehler MicroPolish (USA); acetic acid (100%) was from Merck (Germany). Phosphate buffer solutions of  $\text{pH} = 6.0$  in a concentration of 0.1 M were prepared by mixing appropriate volumes of  $\text{KH}_2\text{PO}_4$  and  $\text{Na}_2\text{HPO}_4$  solutions. Tyrosinase (0.048 mg/10  $\mu\text{L}$ ) solution was prepared in 0.1 M phosphate buffer solution  $\text{pH} = 7.0$ . Ultrapure water was used throughout. All chemicals were analytical-grade reagents.

## 2.2 Instrumentation

Measurements by means of cyclic voltammetry were realized with using of M161 electrochemical analyzer (mtm-anko, Poland) in thermostatic cabinet (Pol-Eko-Aparatura, Poland). All experiments were carried out with using a conventional three-electrode electrochemical cell equipped with the saturated silver/silver chloride reference electrode, a platinum wire as a counter electrode and a graphite working electrode coated with enzymatic matrix composite. As a supporting electrolyte phosphate buffer solution of  $\text{pH} = 6$  (0.1 M) was used. The studies were performed in potential range from  $-0.3$  to  $0.5$  V (vs. saturated  $\text{Ag}/\text{AgCl}$ ) at a scan range of  $62.5 \text{ mV s}^{-1}$  and at temperature of  $25^\circ\text{C}$ .

## 2.3 Biosensor preparation

To prepare all tyrosinase-based biosensors, titania sol was synthesized by acid hydrolysis and then polycondensation of titanium(IV) isopropoxide [14]. In order to prepare the  $\text{Tyr}/\text{TiO}_2/\text{CNTs}/\text{Nafion}$  composite MWCNTs were dispersed in  $\text{TiO}_2$  solution. Then, the mixture of tyrosinase was added to the remaining suspension and shaken. In the last step, Nafion was added to the composite and then all mixture was shaken. To receive homogenous composite, the mixture was sonicated. For the others of prepared matrix composites the method of preparation was similar. However, also the modification of the order of addition the titania sol and tyrosinase have been examined. The amounts of each components of the studied matrix composites are presented in Table 1.

To prepare biosensor two  $10 \mu\text{L}$  portions of nanocomposite were deposited on the surface of the graphite electrode, drying after each portion in air for 10 min. Afterwards, the electrodes were left to dry over saturated disodium phosphate solution for 20 h at  $4^\circ\text{C}$ . Biosensors were stored at  $4^\circ\text{C}$  in 0.1 M phosphate buffer solution ( $\text{pH} = 6.0$ ).

**Table 1**  
The composition of the studied biosensor matrices with the corresponding quantities of each component for one electrode (CMK – mesoporous carbon CMK-3, MWNTs – multiwalled carbon nanotubes, AuNPs – gold nanoparticles, PDDA – poly(diallyldimethylammonium), GA – glutaraldehyde.

Matrices	Components								
	Tyrosinase/ $\mu\text{L}$	TiO <sub>2</sub> / $\mu\text{L}$	CMK-3/mg	MWNTs/mg	Nafion/ $\mu\text{L}$	AuNPs/ $\mu\text{L}$	PDDA/ $\mu\text{L}$	GA/ $\mu\text{L}$	
Tyr/TiO <sub>2</sub> /CNTs/Nafion	7.15	7.15	-	0.04	5.7	-	-	-	
	7.15	7.15 <sup>a</sup>	-	0.04	5.7	-	-	-	
Tyr/TiO <sub>2</sub> /CNTs/Nafion/PDDA	7.15	6.12	-	0.04	5.7	-	1.0	-	
	7.15	6.12 <sup>a</sup>	-	0.04	5.7	-	1.0	-	
Tyr/TiO <sub>2</sub> /CNTs/AuNPs/Nafion	7.15	5.70	-	0.04	5.7	-	1.4	-	
	7.15	8.16	-	0.04	5.7	2.0	-	-	
Tyr/TiO <sub>2</sub> /CNTs/Nafion/GA	7.15	7.15	-	0.04	5.7	-	-	5.0	
Tyr/TiO <sub>2</sub> /CMK-3/Nafion	7.15	7.15	0.04	-	5.7	-	-	-	
Tyr/TiO <sub>2</sub> /CMK-3/PDDA	9.5	9.5	0.06	-	-	-	0.95	-	
Tyr/TiO <sub>2</sub> /CMK-3/Nafion/GA	7.15	7.15	0.04	-	5.7	-	-	1.0	
Tyr/TiO <sub>2</sub> /CMK-3/Nafion/PDDA	7.15	6.5	0.04	-	5.7	-	0.6	-	
	7.15	6.12	0.04	-	5.7	-	1.0	-	
	7.15	6.12 <sup>a</sup>	0.04	-	5.7	-	1.0	-	
	7.15	6.12	0.04	-	5.7	-	1.4	-	

<sup>a</sup> Modification of the order of addition the titania sol and tyrosinase (MWNTs or CMK-3 were dispersed in TiO<sub>2</sub> or tyrosinase solution).

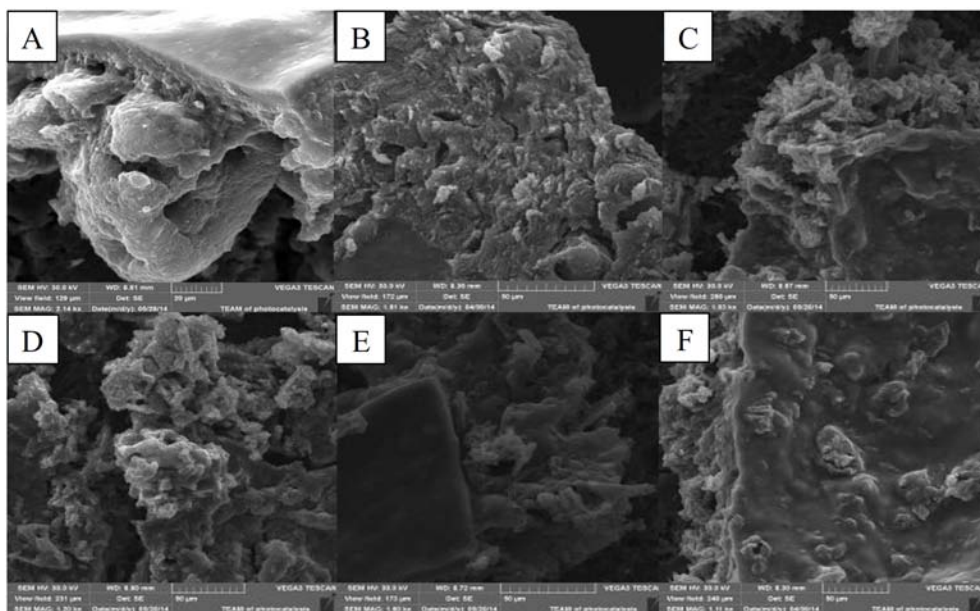


**Fig. 2** SEM images of (A) TYR/TiO<sub>2</sub>/CNTs/Nafion, (B) TYR/TiO<sub>2</sub>/CNTs/Nafion/PDDA, (C) TYR/TiO<sub>2</sub>/CMK-3/Nafion, (D) TYR/TiO<sub>2</sub>/CMK-3/PDDA, (E) TYR/TiO<sub>2</sub>/CMK-3/Nafion/GA, and (F) TYR/TiO<sub>2</sub>/CMK-3/Nafion/GA composites supported on the graphite electrode surface.

### 3. Results and discussion

#### 3.1 SEM images of matrices composites

To characterize the morphology of developed matrix composites scanning electron microscopy have been employed. The obtained images are presented in the Fig. 2. Each modification of the matrix composite noticeably change the morphology of biosensor surface. Three-dimensional porous structure for each biosensor layer with visible convexities inside the cracks can be observed.

#### 3.2 Analytical characteristics of biosensors

The analytical characterization of the prepared biosensors included calculation the Michaelis-Menten constant and sensitivity to the catechol used as the reference substance. The aim of the above-mentioned tests was to examine and compare both parameters for biosensors based on different multi-component composites immobilizing the enzyme and selecting a matrix characterized by the highest sensitivity and the lowest value of the Michaelis-Menten constant.

All the constructed biological sensors based on MWCNTs were characterized by good mechanical strength. Whereas, the mechanical strength of the one biosensor based on mesoporous carbon CMK-3 was poor (TYR/TiO<sub>2</sub>/CMK-3/PDDA).

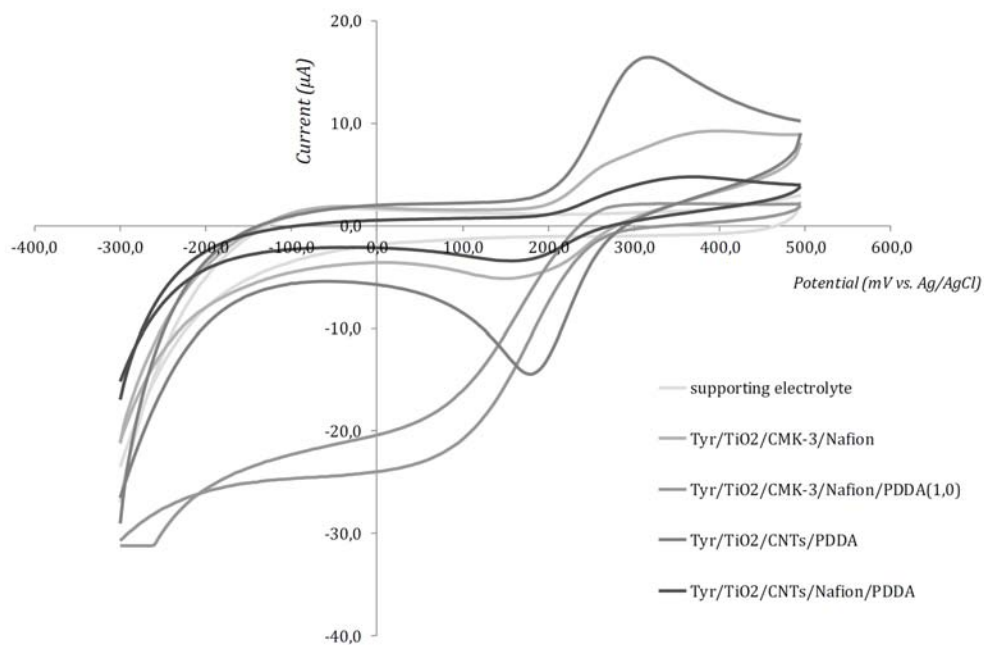


**Fig. 3** Comparison of voltammograms recorded for biosensors with different composition of matrix composites at the catechol solution of  $78 \mu\text{M}$ .

To estimated sensitivity of prepared biosensors the cyclic voltammetry measurements were carried out, first in a supporting electrolyte, and then in a catechol solution of different concentrations in the range of 8 to  $80 \mu\text{M}$ . Based on the obtained results the calibrations graphs were drafted and the sensitivity of each biosensor as a slope of the linear calibration curve were read out.

For the biosensors containing in the matrix composite multiwalled carbon nanotubes the best result of the sensitivity was obtained for the biosensor based on Tyr/TiO<sub>2</sub>/CNTs/Nafion/PDDA ( $1.4 \mu\text{L}$  for one electrode) in a value of  $817.0 \mu\text{A mM}^{-1}\text{cm}^{-2}$ . Analysing the results of sensitivity of the biosensors based on mesoporous carbon CMK-3, definitely higher values of sensitivity, in comparison to the same matrices based on MWCNTs, were observed. Biosensor based on Tyr/TiO<sub>2</sub>/CMK-3/Nafion/PDDA solution in volume of  $1.0 \mu\text{L}$  (for one electrode) was characterized by the highest value of sensitivity  $1247.0 \mu\text{A mM}^{-1}\text{cm}^{-2}$  toward catechol. At the Fig. 3 a comparison of five voltammograms is shown. Each of the voltammogram registered in the catechol solution corresponds to different biosensor. It can be noticed that the composition of the matrix layer had not only a significant impact on the analytical parameters of the tested biosensors, but also on the shape of voltammetric curves.

The dependence of the enzymatic electrode response as a function of the analyte concentration (catechol), by the Michaelis-Menten equation was also described, whereas the enzyme activity is characterized by the Michaelis-Menten

constant ( $K_M$ ). Michaelis-Menten constant value determines the substrate concentration at which half of the active site of molecules in the enzyme structure is occupied. Low value of the Michaelis-Menten constant means the strong affinity of the enzyme to the substrate, while a high value indicates a reverse tendency. For all constructed biosensors the Michaelis-Menten constant was calculated using the Lineweaver-Burk equation, which converts the Michaelis-Menten equation to linear form [15]

$$\frac{1}{I_{\text{cat}} - I_{\text{buf}}} = \left( \frac{K_M}{I_{\text{max}}} \right) \left( \frac{1}{c_{\text{cat}}} \right) + \frac{1}{I_{\text{max}}} \quad (1)$$

where the  $c_{\text{cat}}$  is the concentration of catechol,  $I_{\text{cat}} - I_{\text{buf}}$  is a current corrected by the value registered in the supporting electrolyte,  $I_{\text{max}}$  is the maximum current measured at the moment of complete saturation of the enzyme substrate. The first step of the  $K_M$  value estimation was based on the relationship of the inverse current  $1/(I_{\text{cat}} - I_{\text{buf}})$  as a function of the inverse catechol concentration  $1/c_{\text{cat}}$ . To the designated measurement points trend lines were adjusted in the form of the equation

$$\frac{1}{I_{\text{cat}} - I_{\text{buf}}} = a \cdot \left( \frac{1}{c_{\text{cat}}} \right) + b \quad (2)$$

Then, knowing that  $b = 1/I_{\text{max}}$ , and  $a = K_M/I_{\text{max}}$ , Michaelis-Menten constants were calculated. In case of CNTs-based biosensors the best results of  $K_M$  constant were obtained for biosensor based on TYR/TiO<sub>2</sub>/CNTs/Nafion/PDDA (1.0 μL), that was not correlated to the best sensitivity. For the biosensors based on CMK-3, the lower value of Michaelis-Menten constant was received for biosensor based on TYR/TiO<sub>2</sub>/CNTs/Nafion/GA did not agreeing with the highest sensitivity. Considering all obtained results that the best biosensor was based on composite of Tyr/TiO<sub>2</sub>/CMK-3/Nafion/PDDA (1.0 μL for one electrode). The biosensor was characterized by the highest value of sensitivity 1247.0 μA mM<sup>-1</sup>cm<sup>-2</sup> toward catechol and relatively low Michaelis-Menten constant, 105.2 μM, as well as exhibited good mechanical strength.

#### 4. Conclusions

The biosensor matrices for tyrosinase immobilizing based on titanium dioxide gel modified with nanostructured carbon materials, additionally enriched with gold nanoparticles, Nafion®, glutaraldehyde or polycationit PDDA (poly(diallyldimethylammonium)chloride) were examined. The performed experiments proved that the carbon materials were an essential components of the matrix composites

influencing the electrochemical biosensor response. Some of the constructed biosensors were characterized by good mechanical strength, high sensitivities and relatively low Michaelis-Menten constant values indicating the high affinity of catechol to the tyrosinase immobilized in these matrix composites. Sensitivities of biosensors and Michaelise-Menten constant values could suggest entrapped of a larger amount of tyrosinase in its catalytically active form suggesting larger surface area of mesoporous carbon CMK-3 in comparison to MWCNTs.

## References

- [1] <http://www1.lsbu.ac.uk/water/enztech/biosensors.html> (accessed 22nd June, 2018)
- [2] Tang L., Yang G.D., Zeng G.M., Cai Y., Li S.S., Zhou Y.Y., Pang Y., Liu Y.Y. Zhang Y., Luna B.: Synergistic effect of iron doped ordered mesoporous carbon on adsorption-coupled reduction of hexavalent chromium and the relative mechanism study. *Chem. Eng. J.* **239** (2014), 114–122.
- [3] Zhao H., Cui Q., Shah V., Xu J., Wang T.: Enhancement of glucose isomerase activity by immobilizing on silica/chitosan hybrid microspheres. *J. Mol. Catal. B* **126** (2016), 18–23.
- [4] Yu J., Du W., Zhao F., Zeng B.: High sensitive simultaneous determination of catechol and hydroquinone at mesoporous carbon CMK-3 electrode in comparison with multi-walled carbon nanotubes and Vulcan XC-72 carbon electrodes. *Electrochim. Acta* **54** (2009), 984–988.
- [5] Bhardwaj T.: A review on immobilization techniques of biosensors. *Int. J. Adv. Res. Technol.* **3** (2014), 294–298.
- [6] Monošíka R., Stredanskýb M., Šturdíka E.: Biosensors - classification, characterization and new trends. *Acta Chim. Slov.* **5** (2012), 109–120.
- [7] Del Torno-De Román L., Asunción Alonso-Lomillo M., Domínguez-Renedo O., Julia Arcos-Martínez M.: Tyrosinase based biosensor for the electrochemical determination of sulfamethoxazole. *Sensor Actuat. B* **227** (2016), 48–53.
- [8] Apetrei I.M., Popa C.V., Apetrei C., Tutunaru D.: Biosensors based on graphene modified screen-printed electrodes for the detection of catecholamines. *Rom. Biotech. Lett.* **19** (2014), 9801–9809.
- [9] Pan D., Gu Y., Lan H., Sun Y., Gao H.: Functional graphene-gold nano-composite fabricated electrochemical biosensor for direct and rapid detection of bisphenol A. *Anal. Chim. Acta* **853** (2015), 297–302.
- [10] Pérez López B., Merkoçi A.: Improvement of the electrochemical detection of catechol by the use of a carbon nanotube based biosensor. *Analyst* **134** (2009), 60–64.
- [11] Park J.A., Kim B.K., Choi H.N., Lee W.Y.: Electrochemical determination of dopamine based on carbon nanotube-sol-gel titania-nafion composite film modified electrode. *Bull. Korean Chem. Soc.* **31** (2010), 3123–3127.
- [12] Kumar S., Zheng D., Al-Rubeaan K., Luong J.H.T., Sheu F.S.: Advances in carbon nanotube based electrochemical sensors for bioanalytical applications. *Biotechnol. Adv.* **29** (2011), 169–188.
- [13] Park E.J., Jin J.H., Kim J.H., Min N.K.: Surface activation of plasma-patterned carbon nanotube based DNA sensing electrodes. *Microchim. Acta* **174** (2011), 231–238.
- [14] Kochana J., Nowak P., Jarosz-Wilkolażka A., Bieroń M.: Tyrosinase/laccase bienzyme biosensor for amperometric determination of phenolic compounds. *Microchem. J.* **89** (2008), 171–174.
- [15] Apetrei C., Rodríguez-Méndez M.L., De Saja J.A.: Amperometric tyrosinase based biosensor using an electropolymerized phosphate-doped polypyrrole film as an immobilization support. Application for detection of phenolic compounds. *Electrochim. Acta* **56** (2011) 8919–8925.

# Carbon containing electrodes modified with the iodate salts of aryldiazonium for electroanalysis

ANNA GUSAR\*, ANNA GASHEVSKYA, ELENA DOROZHKO, KSENIA DERINA

*Division for Chemical Engineering, School of Earth Sciences & Engineering,  
Tomsk Polytechnic University, Lenin av.,30, 634050 Tomsk, Russia* ✉ [anngsa@mail.ru](mailto:anngsa@mail.ru)

## Keywords

aryldiazonium salts  
glassy carbon electrode  
voltammetry

## Abstract

This paper deals with the modification of a glassy carbon electrode with aryldiazonium iodate salts (with different functional groups) by the spontaneous formation of organic layers for different electro-analytical purposes. The results were obtained by cyclic voltammetry, scanning (raster) electron microscopy and IR spectroscopy. The optimal conditions of modification were established. Obtained surfaces could be used for the further development of biosensors.

---

## 1. Introduction

Chemically modified electrodes are effective for electrochemical analysis due to its utility in a wide range of investigations, such as, electrostatic phenomena at electrode surfaces, the relationship of heterogeneous electron transfer and chemical reactivity to electrode surface chemistry, and electron and ionic transport phenomena in polymers. Moreover, chemically modified electrodes are beneficial for the design of electrochemical sensing systems, electro-organic syntheses, energy storage, molecular electronics, corrosion protection. Compared with other electrode concepts in electrochemistry, the distinguishing feature of a chemically modified electrode is that a generally quite thin film (from a molecular monolayer to perhaps a few micrometers-thick multilayer) of a selected chemical is bonded to or coated on the electrode surface to endow the electrode with the chemical, electrochemical, optical, electrical, transport, and other desirable properties of the film in a rational, chemically designed manner [1]. Therefore, the search of novel electrode modifiers is extremely necessary for electroanalysis.

The iodate aryldiazonium salts are prospective as electrode surface modifiers. The salts allows the covalent bonding of aryl functional groups [2] with the electrode surface under electrolysis. The first application of diazonium aromatic salts for surface modification was carried out by Delamar et al. [3]. Traditionally

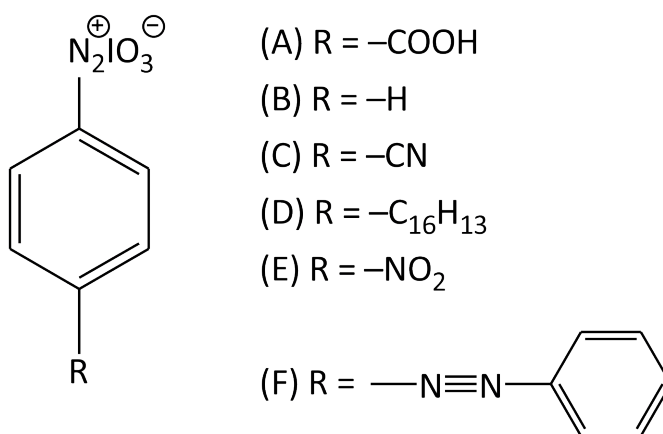


**Fig. 1** Structural formulas of aryldiazonium salts: (A) 4-carboxybenzodiazonium iodate, (B) iodate aryldiazonium; (C) 4-cyanobenzodiazonium iodate, (D) 4-hexadecylbenzodiazonium iodate, (E) 4-nitrobenzodiazonium iodate, (F) 4-(phenyldiazenyl) benzodiazonium iodate.

aryldiazonium salts are used for the modification of solid electrodes. Nevertheless, the control of modifier layer on electrode surface is difficult while electrochemical modification. Therefore, the modifier layer could essentially grow and block the conductive electrode surface [4]. The novelty of present work is obtaining of optimal conditions for nonelectrochemical modification.

## 2. Experimental

### 2.1 Reagents and chemicals

The following iodate salts of aryldiazonium were chosen as modifiers of the electrode surfaces of the glassy carbon electrodes:  $[\text{HOOC}_6\text{H}_4\text{N}_2]\text{IO}_3$ ,  $[\text{NCC}_6\text{H}_4\text{N}_2]\text{IO}_3$ ,  $[\text{O}_2\text{NC}_6\text{H}_4\text{N}_2]\text{IO}_3$ ,  $[\text{C}_6\text{H}_5\text{N}_2]\text{IO}_3$ ,  $[\text{H}_{33}\text{C}_{16}\text{C}_6\text{H}_4\text{N}_2]\text{IO}_3$ . Their structures are depicted in Fig. 1. All reagents were of analytical grade. The water was obtained by water purification system Milli-Q Direct; water resistivity was  $18.2 \text{ M}\Omega \text{ cm}$ . Silver chloride electrodes were used as auxiliary electrode and reference electrode. To select the optimal conditions for spontaneous modification of glassy carbon electrode with iodate salts of aryldiazonium, the concentration of the modifier ( $\text{mg l}^{-1}$ ) and the time of aging of the glassy carbon electrode in the solutions of the corresponding modifiers (sec) were varied. The working concentrations of diazonium salt solutions for modification were  $10, 30, 60 \text{ mg l}^{-1}$ . The time for the maintenance of glassy carbon electrode in the solutions of the modifiers was 2, 5, 10, 30, 60, 120 seconds. To evaluate the reversibility of electrode processes on the glassy carbon electrode, cyclic voltammograms of hexacyanoferrate salts  $[\text{Fe}(\text{CN})_6]^{3-/4-}$  of concentration  $0.25 \text{ M}$  (background  $0.5 \text{ M KCl}$ ) were recorded before and after chemical modification.

## 2.2 Instrumentation

A universal electrochemical workstation TA-2 (Tomanalyt, Tomsk, Russian Federation) with a three electrode cell was used. Silver chloride electrodes and glassy carbon electrodes for modification were purchased from LLC Tomanalyt (Tomsk, Russian Federation). Investigations of the cutoffs of the electrode were carried out using a scanning (raster) electron microscope JEOL JSM-7500FA. To further confirm the presence of organic functional groups on the glassy carbon electrode surface, IR reflection spectra were obtained. The investigations were carried out using the Cary 660 IR spectrometer (manufactured by Agilent).

## 3. Results and discussion

To assess the effectiveness of modifying the glassy carbon electrode with different modifiers under the conditions of changing the concentration of the modifier and the time of aging of the glassy carbon electrode, the value of  $\Delta I$  (%) was calculated

$$\Delta I = \frac{(I_1 - I_0)}{I_0} \cdot 100 \quad (1)$$

where  $I_0$  is current of  $[\text{Fe}(\text{CN})_6]^{3-/4-}$  without modifier,  $I_1$  is current of  $[\text{Fe}(\text{CN})_6]^{3-/4-}$  after aging in the solution of the modifier.

In the course of the study (Fig. 2), it was established that the oxidation and reduction currents of  $[\text{Fe}(\text{CN})_6]^{3-/4-}$  are maximal for 4-carboxybenzodiazonium iodate of the glassy carbon electrode modifier at the time of holding the electrode in its solution for 5 seconds and the modifier concentration  $10 \text{ mg l}^{-1}$  ( $\Delta I = 230\%$  cathode scan and  $\Delta I = 185\%$  anode scan).

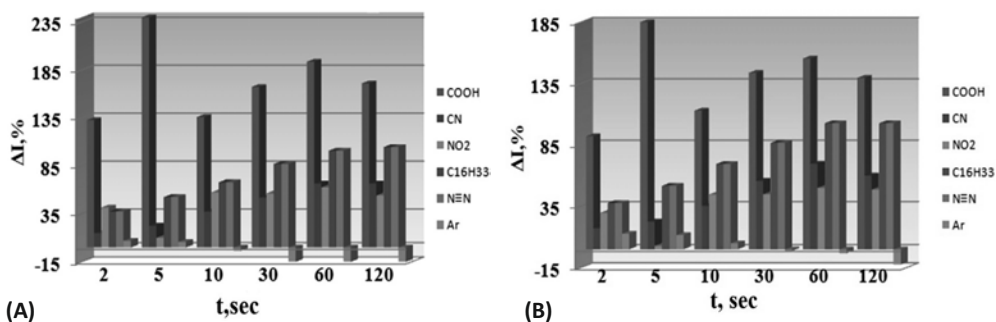


**Fig. 2** Dependence of the change in the currents of  $[\text{Fe}(\text{CN})_6]^{3-/4-}$  ( $\Delta I$ , %) on the time of aging of SEM in the solution of the 4-carboxybenzodiazonium iodate modifier at different concentrations: 1–10  $\text{mg l}^{-1}$ ; 2–30  $\text{mg l}^{-1}$ ; 3–60  $\text{mg l}^{-1}$ : (A) cathode potential sweep, (B) anode potential sweep. The background electrolyte is KCl 0.5 M,  $\nu = 80 \text{ mV s}^{-1}$ .

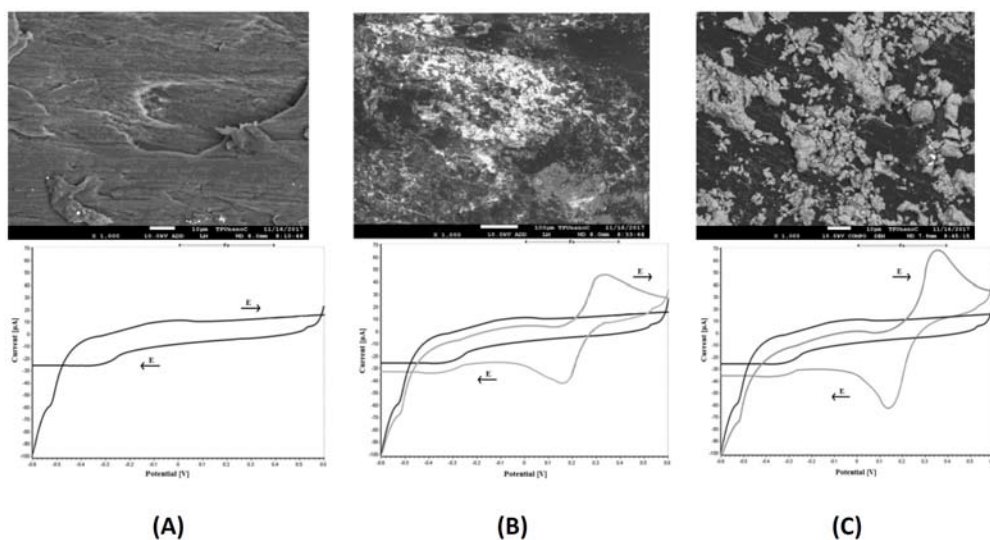


**Fig. 3** Scanning electron microscopy of glassy carbon electrode surfaces and corresponding cyclic voltammograms: (A) glassy carbon electrode without a modifier; (B) glassy carbon electrode after the addition of the reversible  $[\text{Fe}(\text{CN})_6]^{3-/4-}$  pair to the cell; (C) glassy carbon electrode after modification of the solution of the 4-carboxybenzodiazonium iodate modifier ( $10 \text{ mg l}^{-1}$ ) for 5 sec.

For a more accurate description of the mechanism of the processes occurring at the electrode, a study of the morphology of the electrode surface was required (Fig. 3). The first sample is the surface of pure glassy carbon electrode, before the reversible  $[\text{Fe}(\text{CN})_6]^{3-/4-}$  pair is added to the cell. On the sample surface, selective microporosity is observed (Fig. 3A). The pore size does not exceed  $10 \mu\text{m}$ . On the surface there is a slight contamination with an extraneous phase, which has the form of globular particles. Presumably, this phase is a particle of salt, which is part of the background electrolyte. The second sample is the surface of the glassy carbon electrode after introducing a reversible  $[\text{Fe}(\text{CN})_6]^{3-/4-}$  pair into the cell. On a microscopic photograph,  $[\text{Fe}(\text{CN})_6]^{3-/4-}$  aggregates are observed on the surface of the electrode, covering the micropores of glassy carbon. Areas with inclusions of a spherical shape are observed (Fig. 3 B). Presumably, this phase corresponds to iron-containing hexacyanoferrat. The third sample is the surface of the glassy carbon electrode after modification of 4-carboxybenzodiazonium iodate ( $10 \text{ mg l}^{-1}$ ) for 5 seconds. On a microscopic image (Fig. 3C), laminated aggregates of irregular shape are observed confirming the flow of adsorption on the surface of the electrode substrate, which proves the fact of the chemical reaction on the glassy carbon electrode surface between the carbon and the diazonium modifier. It is obvious that a covalent modification of the glassy carbon electrode is possible without imposing a potential in a very short period of time. In addition, after the modification, the current-conducting properties of the SEM are increased due to an increase in the currents of the reversible  $[\text{Fe}(\text{CN})_6]^{3-/4-}$  pair at the potentials of  $0.15 \text{ V}$  and  $0.35 \text{ V}$  under the optimum modification conditions.

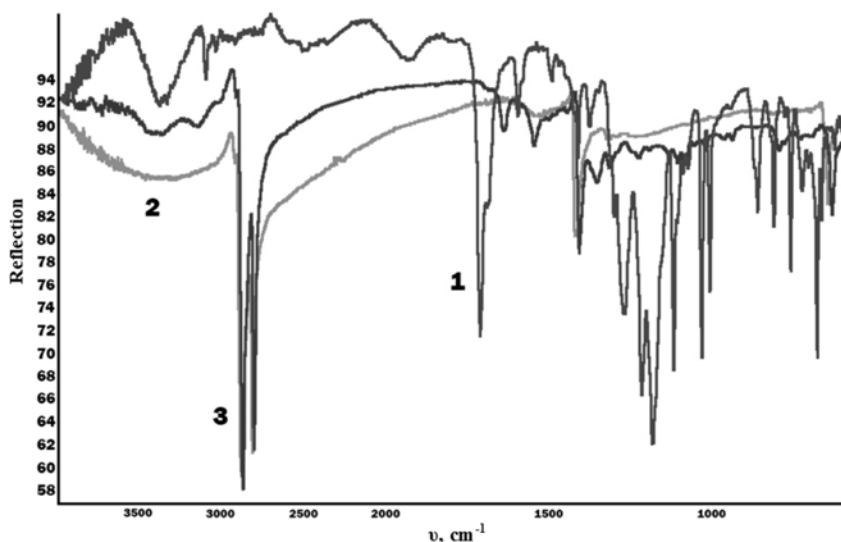


**Fig. 4** The transmission spectrum of the IR surface of the glassy carbon electrode: (1) modifier 4-carboxybenzodiazonium iodate ( $c = 10 \text{ mg l}^{-1}$ ); (2) the initial surface of the glassy carbon electrode; (3) surface of the glassy carbon electrode after modification.

To further confirm the presence of organic functional groups on the glassy carbon electrode surface, IR reflection spectra (Fig. 4) were obtained: 1) 4-carboxybenzodiazonium iodate modifier with a concentration of  $10 \text{ mg l}^{-1}$ ; 2) the initial surface of the glassy carbon electrode; 3) the surface of the glassy carbon electrode after modification. The absorption bands at  $3659, 1685, 1590, 786 \text{ cm}^{-1}$ , corresponding to the carboxyl group and the phenyl nucleus are observed in the spectrum.

#### 4. Conclusions

Thus, it has been established that the most suitable material of the working electrode is the glassy carbon electrode, and the maximum values of the currents are achieved using the 4-carboxybenzodiazonium iodate modifier. The optimum modification conditions were: concentration of 4-carboxybenzodiazonium iodate  $10 \text{ mg l}^{-1}$ , electrode holding time 5 sec.

#### Acknowledgments

The work is supported by grant of Ministry of Education and Science RF for program "Science".

#### References

- [1] Durst R.A., Baumner A.J., Murray R.W., Buck R.P., Andrieux C.P.: Chemically modified electrodes: Recommended terminology and definitions. *Pure Appl. Chem.* **69** (1997), 1317–1323.
- [2] Berger F., Delhalle J., Mekhalif Z.: Hybrid coating on steel: ZnNi electrodeposition and surface modification with organothiols and diazonium salts. *Electrochim. Acta* **53** (2008), 2852–2861.

- [3] Delamar M., Hitmi R., Pinson J., Saveant J.M.: Covalent modification of carbon surface by grafting of functionalized aryl radicals produced from electrochemical reduction of diazonium salts. *J. Am. Chem. Soc.* **114** (1992), 5883–5884.
- [4] Bélanger D., Pinson J.: Electrografting: a powerful method for surface modification. *Chem. Soc. Rev.* **40** (2011), 3995–4048.

# Boron-doped diamond electrode fabricated by microwave plasma enhanced chemical vapour deposition process with linear antenna delivery for neurotransmitters sensing

SIMONA BALUCHOVÁ<sup>a, b, \*</sup>, ANDREW TAYLOR<sup>c</sup>, VINCENT MORTET<sup>b, c</sup>,  
KAROLINA SCHWARZOVÁ-PECKOVÁ<sup>a, b</sup>

<sup>a</sup> UNESCO Laboratory of Environmental Electrochemistry, Department of Analytical Chemistry, Faculty of Science, Charles University, Hlavova 8, 128 43 Prague 2, Czech Republic

✉ [simona.baluchova@natur.cuni.cz](mailto:simona.baluchova@natur.cuni.cz)

<sup>b</sup> Faculty of Biomedical Engineering, Czech Technical University in Prague, Sítňá Sq. 3105, 272 01 Kladno, Czech Republic

<sup>c</sup> Institute of Physics of the Czech Academy of Sciences, Na Slovance 2, 182 21 Prague, Czech Republic

## Keywords

boron-doped diamond  
cyclic voltammetry  
dopamine  
linear antenna  
Raman spectroscopy

## Abstract

Morphological, spectral and electrochemical characterization of boron-doped diamond (BDD) electrode deposited by microwave plasma enhanced chemical vapour deposition process with linear antenna delivery apparatus was performed by scanning electron microscopy, Raman spectroscopy and cyclic voltammetry. Fast electron transfer kinetics was confirmed for studied redox markers at as-deposited hydrogen-terminated BDD surface (H-BDD) and also after applying anodic activation resulting in oxidized surface. Moreover, the voltammetric behaviour of dopamine, an essential biologically active compound of which abnormal levels in physiological fluids are associated with neurological disorders, was examined. Due to the substantial fouling of the H-BDD film during dopamine oxidation process, anodically activated BDD film was chosen to perform further experiments with this neurotransmitter. Concentration dependency for dopamine in phosphate buffer pH=7.4 was constructed and detection limit of  $1.22 \mu\text{mol L}^{-1}$  was achieved.

---

## 1. Introduction

Boron-doped diamond (BDD) has become a well-established electrode material for neurotransmitters detection, especially biogenic amines, due to its exceptional characteristics including biocompatibility, resistance to fouling, and sufficiently

wide potential window in the region of positive potentials for sensitive electrochemical sensing of dopamine, (nor)adrenaline, and serotonin [1].

Boron-doped diamond thin films can be grown by using one of several energy-assisted chemical vapour deposition methods, the most popular being hot-filament and microwave plasma enhanced (MW-PECVD) [2]. However, typical cavity based MW-PECVD are restricted to an area of diameter of 15 cm and high growth temperatures above 600 °C. Conversely, MW-PECVD system with linear antenna delivery (MW-LA-PECVD) enables growth with good homogeneity over large areas at low temperatures (< 600 °C) [3], therefore making it more attractive for many applications, including coverage of glass platforms for microelectrode arrays (MEA) used favourably for neurotransmitters sensing. Nevertheless, in such linear antenna systems the addition of oxygen species, typically in the form of CO<sub>2</sub>, is necessary which leads to, on one hand, enhanced growth rates and diamond quality, but on the other hand, reduced active boron incorporation manifested by decreased electrical conductivity [4].

Hence, within this study, nanocrystalline BDD samples deposited by MW-LA-PECVD system were characterized by scanning electron microscopy (SEM), Raman spectroscopy and electrochemically by cyclic voltammetry (CV) using different redox probes. The possibility of dopamine determination was also verified.

## 2. Experimental

### 2.1 Reagents and chemicals

Analytical grade reagents were used as-received without any further purification: dopamine hydrochloride, hexaammineruthenium chloride (both Sigma-Aldrich, Darmstadt, Germany), potassium chloride, potassium hexacyanoferrate trihydrate, sodium dihydrogen phosphate dihydrate (all Lach-Ner, Neratovice, Czech Republic), sodium hydroxide and sulfuric acid (both Penta, Chrudim, Czech Republic). All aqueous solutions were prepared with deionized water (Millipore Mili plus Q system, Billerica, USA) with resistance of not less than 18.2 MΩ.

### 2.2 Instrumentation

A MW-LA-PECVD system was used for the preparation of BDD samples, further details are reported in [3]. The surface morphology of deposited layers was observed by SEM using a Tescan FERA 3 tool. Raman spectroscopy was carried out at room temperature using a Renishaw InVia Raman Microscope at a wavelength of 488 nm and a laser power of 6 mW at the sample to assess the quality and diamond layer composition.

Cyclic voltammetry measurements with a scan rate of 100 mV s<sup>-1</sup> were carried out by a computer-driven Eco-Tribo Polarograph with PolarPro 5.1 software (Eco-Trend Plus, Prague, Czech Republic). A three-electrode set-up was used in which

linear antenna BDD sample was placed in a laboratory-made Teflon electrode body [5] to form a working electrode. A silver chloride electrode ( $\text{Ag} | \text{AgCl} | 3 \text{ mol L}^{-1} \text{ KCl}$ ) and a platinum wire (both Elektrochemické detektory, Turnov, Czech Republic) served as a reference and counter electrodes, respectively. pH measurements were performed using a digital pH meter 3510 with a combined glass electrode (Jenway, Essen, UK). All electroanalytical experiments were carried out at laboratory temperature ( $23 \pm 1^\circ\text{C}$ ).

The concentration dependency was constructed from the average of four replicate measurements for each dopamine standard solution and evaluated by the least squares linear regression method. Limit of detection (*LOD*) was calculated as a threefold and limit of quantification (*LOQ*) as a tenfold of the standard deviation of the peak currents (ten runs) of the lowest measurable concentration, divided by the slope of the concentration curve *k*.

### 3. Results and discussion

SEM images of investigated layers were found to be closed and free of pinholes. Layers exhibited a distinct crystalline structure with grains consisting of a mixture of orientations. Raman spectra showed peaks related to  $\text{sp}^3$  carbon at  $1332 \text{ cm}^{-1}$  as well as broad features relating to transpolyacetylene lying in grain boundaries at  $1150 \text{ cm}^{-1}$  and  $1490 \text{ cm}^{-1}$ . Furthermore, additional peaks were observed at  $1360 \text{ cm}^{-1}$  and  $1585 \text{ cm}^{-1}$  belonging to  $\text{sp}^2$  carbon, and two peaks at  $500 \text{ cm}^{-1}$  and  $1230 \text{ cm}^{-1}$  related to boron incorporation.

Electrochemical characterization of the linear antenna BDD electrode was performed by recording CVs of the inner-sphere  $[\text{Fe}(\text{CN})_6]^{3-/4-}$  and the outer-sphere  $[\text{Ru}(\text{NH}_3)_6]^{3+/2+}$  redox markers (both of  $1 \text{ mmol L}^{-1}$  in  $1 \text{ mol L}^{-1} \text{ KCl}$ ). BDD film was tested as-received with hydrogen-terminated surface (H-BDD) directly after the deposition procedure, and also after its anodic activation (performed in acidic medium of  $0.5 \text{ mol L}^{-1} \text{ H}_2\text{SO}_4$  by applying highly positive potential  $E_{\text{ACT}} + 2.4 \text{ V}$  for 20 min; in the region of water decomposition leading to the hydroxyl radical evolution and subsequently the oxygen formation) resulting to the introduction of various oxygen-functionalities at the BDD surface (O-BDD) [6]. Evaluated  $\Delta E_p$  values were 81 mV and 66 mV at H-BDD, and 87 mV and 64 mV at O-BDD for  $[\text{Fe}(\text{CN})_6]^{3-/4-}$  and  $[\text{Ru}(\text{NH}_3)_6]^{3+/2+}$ , respectively, indicating that conversion to oxidized surface did not significantly altered the redox behaviour of studied probes. Hence, fast electron transfer kinetics was confirmed at H-BDD as well as at O-BDD surface.

The electrochemical behaviour of  $1 \text{ mmol L}^{-1}$  dopamine in  $0.1 \text{ mol L}^{-1}$  phosphate buffer pH = 7.4 was investigated by cyclic voltammetry. Dopamine oxidation on H-BDD occurred at +0.35 V and the peak heights continuously decreased by 57% within the set of five consecutive scans, confirming electrode fouling. Noticeably higher positive oxidation potential of +0.44 V was observed at O-BDD surface, and repeatable signals were obtained because anodic activation was applied between the individual scans ( $E_{\text{ACT}} + 2.4 \text{ V}$  for 30 s) ensuring resistance

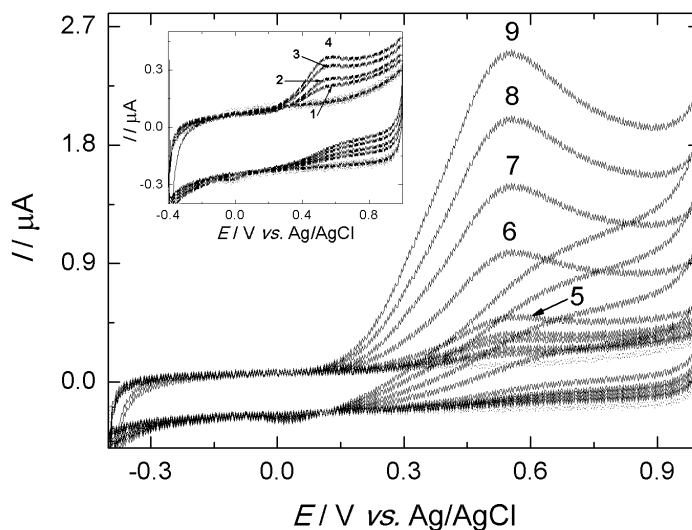


**Fig. 1** Cyclic voltammograms of dopamine in 0.1 mol L<sup>-1</sup> phosphate buffer pH = 7.4 recorded at anodically activated BDD film. Following dopamine concentration levels were measured: (1) 4 μmol L<sup>-1</sup>, (2) 6 μmol L<sup>-1</sup>, (3) 8 μmol L<sup>-1</sup>, (4) 10 μmol L<sup>-1</sup>, (5) 20 μmol L<sup>-1</sup>, (6) 40 μmol L<sup>-1</sup>, (7) 60 μmol L<sup>-1</sup>, (8) 80 μmol L<sup>-1</sup>, and (9) 100 μmol L<sup>-1</sup>. Dotted line represents supporting electrolyte.

towards electrode surface passivation. The reversibility of dopamine oxidation process was suppressed at O-BDD which was manifested by indistinctive cathodic peak in the reverse scan of the recorded CVs. Clearly, the oxidation of dopamine is strongly influenced by surface termination of the BDD sample. Consecutively, on anodically activated BDD sample the concentration dependence of dopamine in 0.1 mol L<sup>-1</sup> phosphate buffer pH = 7.4 was recorded by cyclic voltammetry (Fig. 1) within the linear range from 4 to 100 μmol L<sup>-1</sup> and it can be described by the following equation

$$I_p \text{ (nA)} = 29.9 \pm 22.5 \text{ (nA)} + 23.6 \pm 0.5 \text{ (nA } \mu\text{mol}^{-1} \text{L)} \times c \text{ (}\mu\text{mol L}^{-1}\text{)} \quad (1)$$

$$R = 0.9985$$

The calculated *LOD* and *LOQ* values are 1.22 μmol L<sup>-1</sup> and 4.06 μmol L<sup>-1</sup>, respectively.

#### 4. Conclusions

Within this study, BDD electrode produced by MW-LA-PECVD process was characterized by using a range of techniques and preliminary results with neurotransmitter dopamine were obtained, which suggest that linear antenna BDD is a perspective material for dopamine sensing and it may be used advantageously

for many applications such as fabrication of BDD based MEA device. The comparison of linear antenna BDD samples with other types of BDD, including conventional planar and nanostructured samples prepared by MW-PECVD apparatus will be performed.

### Acknowledgments

The research was carried out within the framework of Specific University Research (SVV 260440). It was financially supported by the Czech Science Foundation (project 17-15319S) and the J. E. Purkyně fellowship awarded to V. Mortet by the Czech Academy of Sciences.

### References

- [1] Garrett D.J., Tong W., Simpson D.A., Meffin H.: Diamond for neural interfacing: A review. *Carbon* **102** (2016), 437–454.
- [2] Xu J.S., Granger M.C., Chen Q.Y., Strojek J.W., Lister T.E., Swain G.M.: Boron-doped diamond thin-film electrodes. *Anal. Chem.* **69** (1997), 591–597.
- [3] Taylor A., Fekete L., Hubik P., Jager A., Janicek P., Mortet V., Mistrik J., Vacik J.: Large area deposition of boron doped nano-crystalline diamond films at low temperatures using microwave plasma enhanced chemical vapour deposition with linear antenna delivery. *Diam. Relat. Mat.* **47** (2014), 27–34.
- [4] Taylor A., Ashcheulov P., Cada M., Fekete L., Hubik P., Klimsa L., Olejnicek J., Remes Z., Jirka I., Janicek P., Bedel-Pereira E., Kopecek J., Mistrik J., Mortet V.: Effect of plasma composition on nanocrystalline diamond layers deposited by a microwave linear antenna plasma-enhanced chemical vapour deposition system. *Phys. Status Solidi A-Appl. Mat.* **212** (2015), 2418–2423.
- [5] Cizek K., Barek J., Fischer J., Peckova K., Zima J.: Voltammetric determination of 3-nitrofluoranthene and 3-aminofluoranthene at boron doped diamond thin-film electrode. *Electroanalysis* **19** (2007), 1295–1299.
- [6] Hutton L.A., Iacobini J.G., Bitziou E., Channon R.B., Newton M.E., Macpherson J.V.: Examination of the Factors Affecting the Electrochemical Performance of Oxygen-Terminated Polycrystalline Boron-Doped Diamond Electrodes. *Anal. Chem.* **85** (2013), 7230–7240.

# Fluorometric method of creatinine determination employing 3,5-dinitrobenzoic acid

IZABELA LEWIŃSKA<sup>a,\*</sup>, MICHAŁ MICHAŁEC<sup>a,b</sup>, ŁUKASZ TYMECKI<sup>a</sup>

<sup>a</sup> Faculty of Chemistry, University of Warsaw, Pasteura 1, 02-093 Warsaw, Poland

✉ i.lewinska@student.uw.edu.pl

<sup>b</sup> College of Inter-Faculty Individual Studies in Mathematics and Natural Sciences, University of Warsaw, Banacha 2C, 02-097 Warsaw, Poland

## Keywords

3,5-dinitrobenzoic acid  
creatinine  
fluorimetry

## Abstract

A fluorometric method of creatinine determination was investigated. As a reagent 3,5-dinitrobenzoic acid is employed. The fluorometric 3,5-dinitrobenzoic acid-creatinine complex is formed in alkaline conditions with excitation and emission maxima at 410 nm and 480 nm, respectively. The conditions of the assays like solvent for 3,5-dinitrobenzoic acid, base concentration and reaction time were optimized. A linear calibration curve in the range from 10 to 500  $\mu\text{mol L}^{-1}$  of creatinine was obtained. However, the substrate (3,5-dinitrobenzoic acid in organic solvent) is unstable, which limits application of proposed method.

## 1. Introduction

Creatinine is one of most common analytes in the clinical analysis [1]. It is formed in muscles in one of two possible processes: either in nonenzymatic dehydration and dephosphorylation of creatine phosphate or in enzymatic creatine dehydration. Creatinine serves no biological functions in the organism and is filtrated by kidneys and removed with urine. However, due to the fact that creatinine is synthesized in muscles, its level is related to the muscle mass as well as it is regarded to be a renal function marker [2]. The physiological range of creatinine is 0.6–1.3 mg dL<sup>-1</sup> in serum and 800–2000 mg in 24-hour urine.

A commonly used method for creatinine determination in biological samples is Jaffé method, proposed by Max Jaffé in 1886 [3] and adapted for clinical analysis purposes by Otto Folin [4]. It bases on an orange complex formation when creatinine reacts with picric acid in alkaline solution. Although Jaffé method dominates in clinical laboratories, it is highly nonspecific. Compounds such as glucose, pyruvate, bilirubin, albumin, cephalosporins and many others are causing a bias in determined creatinine level [5]. To overcome these obstacles, a kinetic variant

of Jaffé method is widely employed, which bases on a two-point absorbance measurement. The difference between obtained values is treated as an analytical signal. This approach allows to eliminate the influence on the measurement of compounds reacting with picric acid with a different rate than creatinine.

As another solution to the problem of many interferences, in 1936 three groups – Bollinger [6], Langley and Evans [7], and Benedict and Bahre [8] independently proposed an alternative method for the determination of creatinine. Instead of picric acid, 3,5-dinitrobenzoic acid was employed as a chromophoric residue. Since then only a few papers have been published on this matter [9–13]. The 3,5-dinitrobenzoic acid-based method is reported to exhibit fewer interferences than Jaffé assay. However, a systematic and comprehensive research in this area is still missing from the literature. It will be a subject of further investigation in our group and will be published elsewhere.

Furthermore, the reaction between creatinine and 3,5-dinitrobenzoic acid is suitable not only for colorimetric but also for fluorometric determination of creatinine [14]. Inorganic base in a concentration above  $0.25 \text{ mol L}^{-1}$  promotes the formation of fluorescent product with the excitation and emission maxima 410 nm and 475 nm, respectively. 3,5-dinitrobenzoic acid ( $0.05 \text{ mol L}^{-1}$ ) was dissolved in an organic solvent. According to [14], solvents like 1,4-butanediol, isopropanol, dimethylsulfoxide (DMSO), dimethylformamide (DMF) and ethanol can be employed to prepare 3,5-dinitrobenzoic acid solution and facilitate fluorescence. The greatest sensitivity was achieved in 1,4-butanediol solution. However, the greatest fluorescence intensity was observed in DMSO solution. The linear range of the assay is up to  $800 \mu\text{mol L}^{-1}$  of creatinine and the limit of detection is below  $1 \mu\text{mol L}^{-1}$ . This method of creatinine determination was patented [15]. In this contribution, we verify results obtained by Blass and optimize the conditions to potentially apply fluorometric creatinine assay to a single-point creatinine determination.

## 2. Experimental

### 2.1 Reagents and chemicals

The creatinine and 3,5-dinitrobenzoic acid were pure grade and obtained from Sigma Aldrich (USA). Other reagents like 1,4-butanediol, sodium hydroxide, ethanol, methanol, DMSO of analytical grade were obtained from Avantor Performance (Poland). Water used in all experiments was the first level of purity.

### 2.2 Instrumentation

For fluorometric measurements, a Scinco FS-2 (South Korea) fluorimeter was employed. In all experiments disposable, polystyrene fluorometric cuvettes obtained from Sarstedt (Germany) were used.

### 3. Results and discussion

A solution of  $0.05 \text{ mol L}^{-1}$  3,5-dinitrobenzoic acid was prepared in various solvents: 1,4-butanediol, DMSO, ethanol, methanol, and  $0.45 \text{ mol L}^{-1}$  NaOH. The kinetics were recorded for 410 nm and 480 nm excitation and emission wavelengths, respectively. The measurements were conducted in a volume ratio of 3,5-dinitrobenzoic acid solution:NaOH:sample equal to 1:1:2. As shown in Fig. 1 out of all five solvents, a fluorescent signal after addition of creatinine was developed only in 1,4-butanediol, contrary to Blass' findings. In case of 3,5-dinitrobenzoic acid dissolved in DMSO, a purple colour was developed and a rise in the solution temperature was noticed after creatinine addition. However, the product was not fluorescent. For further experiments, 1,4-butanediol was selected as a solvent for 3,5-dinitrobenzoic acid.

Next, the effect of NaOH concentration on 3,5-dinitrobenzoic acid-creatinine complex fluorescence was investigated. According to original publication [13], the increase of base concentration resulted in faster development of signal. Kinetics shown in Fig. 2 confirm these observations. A higher signal is obtained with the increase of NaOH concentration. However, a faster decay in fluorescence intensity is also observed. For  $3 \text{ mol L}^{-1}$  NaOH a steady-state is reached instantly. For further measurements,  $1 \text{ mol L}^{-1}$  was chosen due to the highest fluorescence intensity of formed product. The highest emission of the product is reached after 9 minutes after reaction initiation by mixing 3,5-dinitrobenzoic acid in 1,4-butanediol with NaOH and creatinine standard.

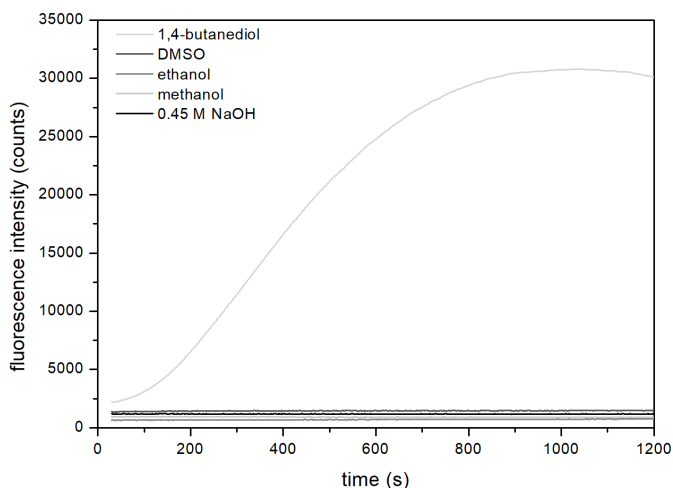


**Fig. 1** Kinetics of fluorescent product formation after reaction of  $0.05 \text{ mol L}^{-1}$  3,5-dinitrobenzoic acid dissolved in 1,4-butanediol, ethanol, methanol, DMSO or  $0.45 \text{ mol L}^{-1}$  NaOH with  $500 \mu\text{mol L}^{-1}$  of creatinine standard and  $1 \text{ mol L}^{-1}$  NaOH recorded at 410 nm excitation wavelength and 480 nm emission wavelength.

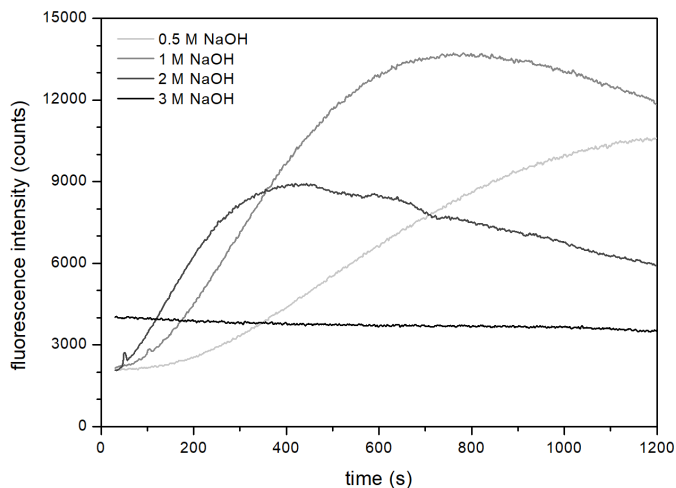


**Fig. 2** Kinetics of fluorescent product formation after reaction of  $0.05 \text{ mol L}^{-1}$  3,5-dinitrobenzoic acid dissolved in 1,4-butanediol with  $500 \mu\text{mol L}^{-1}$  of creatinine standard in different concentrations of NaOH: 0.5, 1.0, 2.0 and  $3.0 \text{ mol L}^{-1}$  recorded at 410 nm excitation wavelength and 480 nm emission wavelength.

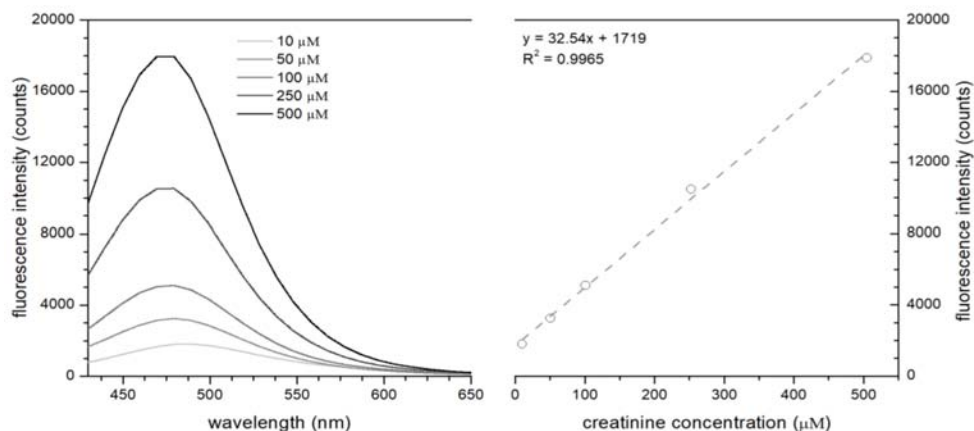


**Fig. 3** Emission spectra (left) of consecutive creatinine standards ( $10, 50, 100, 250$  and  $500 \mu\text{mol L}^{-1}$ ) and a corresponding calibration curve (right).

A calibration curve for creatinine was prepared in the concentration range from  $10$  to  $500 \mu\text{mol L}^{-1}$  and is shown in Fig. 3 with the emission spectra of consecutive creatinine standards.

However, a significant decay in obtained signal was noticed after storing 3,5-dinitrobenzoic acid in 1,4-butanediol for several hours in a closed volumetric flask. A 50% decrease in signal was achieved after 48 hours of storing the reagent and an 80% decrease after 72 hours of storage in a closed volumetric flask, as

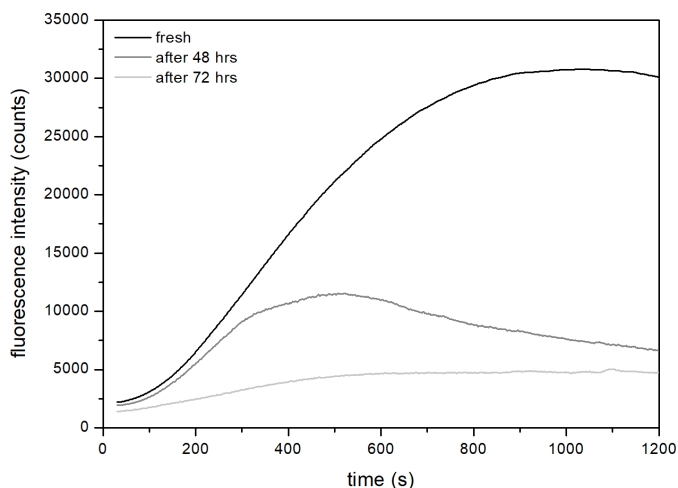


**Fig. 4** Kinetics of fluorescent product formation after reaction of  $0.05 \text{ mol L}^{-1}$  3,5-dinitrobenzoic acid dissolved in 1,4-butanediol with  $500 \mu\text{mol L}^{-1}$  of creatinine standard and  $1 \text{ mol L}^{-1}$  NaOH recorded at 410 nm excitation wavelength and 480 nm emission wavelength. The reagent was freshly prepared, stored for 48 hours or stored for 72 hours.

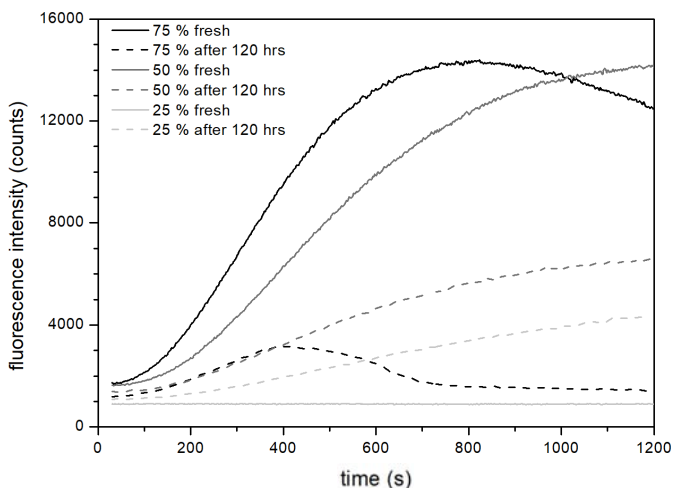


**Fig. 5** Kinetics of fluorescent product formation after reaction of  $0.05 \text{ mol L}^{-1}$  3,5-dinitrobenzoic acid dissolved in 75%, 50% or 25% 1,4-butanediol solution in water with  $500 \mu\text{mol L}^{-1}$  of creatinine standard and  $1 \text{ mol L}^{-1}$  NaOH recorded at 410 nm excitation wavelength and 480 nm emission wavelength. The reagents were freshly prepared or stored for 120 hours.

shown in Fig. 4. This is a major obstacle to implementing this method in real samples analysis. An attempt to stabilize the substrate by addition of water was undertaken. The results are presented in Fig. 5. Even then, not only a smaller signal was developed than in pure 1,4-butanediol, but also similar decay in signal was

observed in case of 75% and 50% 1,4-butanediol solution in water used as a solvent for 3,5-dinitrobenzoic acid. An opposite trend is noticed in case of 25% 1,4-butanediol solution in water. A possible explanation of this is that 3,5-dinitrobenzoic acid was not completely soluble in 25% butanediol and its storage for 120 hours resulted in the increase of the amount of 3,5-dinitrobenzoic acid dissolved.

#### 4. Conclusions

Despite the fact, that the conditions were successfully optimized and a linear calibration curve was obtained, this fluorometric creatinine assay is not suitable for real samples analysis and found as highly unpractical. A new batch of 3,5-dinitrobenzoic acid in 1,4-butanediol is required for every set of measurements because the substrate is not stable in such a solution. What is more, a reaction that lasts 9 minutes is not an attractive alternative for creatinine determination according to Jaffé protocol, which lasts up to 1 minute.

#### Acknowledgments

These investigations were supported by the Polish National Science Centre, projects: Preludium NCN no. 2017/25/N/NZ5/01556 and Opus NCN no. 2014/13/B/ST4/04528. Helpful comments to this paper from Prof. Robert Koncki (University of Warsaw) are kindly acknowledged.

#### References

- [1] Delanghe J.R., Speeckaert M.M.: Creatinine determination according to Jaffe - What does it stand for? *NDT Plus* **4** (2011), 83–86.
- [2] Narayanan S., Appleton H.D.: Creatinine: A review. *Clin. Chem.* **26** (1980) 1119–1126.
- [3] Jaffe M.: Ueber den Niederschlag, welchen Pikrinsäure in normalem Harn erzeugt und über eine neue Reaction des Kreatinins. *Z. Physiol. Chem.* **10** (1886), 391–400.
- [4] Otto F., Wu H.: A system of blood analysis. *J. Biol. Chem.* **38** (1919), 81–110.
- [5] Peake M., Whiting M.: Measurement of serum creatinine – current status and future goals. *Clin. Biochem. Rev.* **27** (2006), 173–184.
- [6] Bollinger A.: The colorimetric determination of creatinine in urine and blood with 3,5-dinitrobenzoic acid. *Med. J. Aust.* **2** (1936), 818–821.
- [7] Langley W., Evans M.: The determination of creatinine with sodium 3,5-dinitrobenzoate. *J. Biol. Chem.* **4** (1936), 333–341.
- [8] Behre J.A., Benedict S.: Studies in creatine and creatinine metabolism. IV. On the question on the occurrence of creatinine and creatine in blood creatinine and creatine in blood. *J. Biol. Chem.* **52** (1922), 11–33.
- [9] Carr J.: Reactions of aromatic nitro compounds with active methyl, methylene, methine groups in presence of base. *Anal. Chem.* **25** (1953), 1859–1863.
- [10] Sabbagh M., Rick W., Schneider S.: Eine kinetische Methode zur direkten Bestimmung des Kreatinins im Serum mit 3,5-Dinitrobenzoesäure ohne Enteiweißung. *J. Clin. Chem. Clin. Biochem.* **26** (1988), 15–24.
- [11] Parekh A.C., Cook S., Sims C., Jung D.: A new method for the determination of serum creatinine based on reaction with 3,5-dinitrobenzoyl chloride in an organic medium. *Clin. Chim. Acta* **80** (1976), 221–231.
- [12] Sims C., Parekh A.C.: Determination of serum creatinine by reaction with methyl-3,5-dinitrobenzoate in methyl sulfoxide. *Ann. Clin. Biochem.* **14** (1977), 227–232.

- [13] Cocco C., Schinella M., Lippi U., Clin C., Maggiore O.C.: New kinetic method for creatinine measurement now automated in the cobas fara centrifugal analyzer. *Clin. Chem.* **34** (1988), 2577.
- [14] Blass K.G.: Reactivity of creatinine with alkaline 3,5 -dinitrobenzoate: A new fluorescent kidney function test. *Clin. Biochem.* **28** (1955), 107–111.
- [15] Blass K.G.: Sensitive and highly specific quantitative fluorometric assay for creatinine in biological fluids. US Pat. 5,507,708 (1996).

# Screening of pesticide in apple ciders by liquid chromatography-high resolution mass spectrometry

VERONIKA ZUŠŤÁKOVÁ<sup>a, b, \*</sup>, MARTIN DUŠEK<sup>a</sup>, JANA OLŠOVSKÁ<sup>a</sup>

<sup>a</sup> *Research Institute of Brewing and Malting, Inc., Lípová 15, 120 44 Prague 2, Czech Republic*

<sup>b</sup> *Department of Analytical Chemistry, Faculty of Science, Charles University, Hlavova 8, 128 43 Prague 2, Czech Republic* ✉ [zustakov@natur.cuni.cz](mailto:zustakov@natur.cuni.cz)

## Keywords

apple cider  
HPLC-HR/MS  
pesticides residues  
QuEChERS

## Abstract

The present study is focused on separation and detection of pesticides residues in apple ciders. The main target of this experiment was not only to determine the concentrations of these residues carrying over from apple peels into the beverages but also to evaluate their potential risk to consumer's health. For the extraction the QuEChERS method was used in combination with additional column SPE sample clean-up to achieve the lowest detection limit possible due to low concentrations of pesticide residues. The samples were analysed using a high-resolution accurate-mass (HPLC-HR/AM) instrument and this applied method assured the quantification of pesticide residues in the ciders possible at 0.2 ppb level for most of fifty target pesticides. Additionally, non-target screening mode enabled to verify presence of over 300 pesticides using comprehensive library including retention times, empirical formulas, and verified fragments.

---

## 1. Introduction

The pesticides have very important the role in the agriculture [1–2]. They help to increase efficiency profitability and quality products. On the other hand, their application to farmland increasing rapidly over the world, and the contamination occurs of agricultural produce, water, air, and soil. The apples belong to commodities treated wide scale of various agrochemicals. The most used pesticides for treatment of apples are insecticides, such as acetamiprid, chlorpyrifos-methyl, methoxyfenozide, pirimicarb and fungicides, such as boscalid, carbendazim, cyprodinil, dithiocarbamate, fluopyram, and mandipropamid [3–4].

Based on the trend of increasing consumption of apple ciders in the Czech Republic, especially ciders produced in domestic craft cider houses, we designed an experiment which provides information about levels of pesticides residues in these kinds of beverages. The samples were obtained mainly from local ciders and several foreign ciders were involved into the study. Several organic ciders were

also analysed in order to confirm the pesticide free declaration. In this study, the QuEChERS based extraction method in combination with column SPE addition sample clean-up to achieve the lowest detection limit of pesticide residues in the samples [5]. The Q-Exactive instrument and this applied method made quantification of pesticide residues in ciders possible at 0.2 ppb level for most of fifty target pesticides.

## 2. Experimental

### 2.1 Reagents and chemicals

Acetonitrile, methanol, formic acid and ammonium formate (all LC-MS grade), sodium citrate tribasic dihydrate and sodium hydrogencitrate sesquihydrate were and purchased from Sigma-Aldrich (Steinheim, Germany). Sodium chloride (anal. grade) was obtained from Lach-Ner (Neratovice, Czech Republic). Magnesium sulfate (anal. grade, >98%) was obtained from Penta (Prague, Czech Republic). Pure water was obtained from a Milli-Q purification system (Merck-Millipore).

Pesticide standards abamectin, acephate, acetamiprid, ametoctradin, azoxystrobin, bifenthrin, boscalid, bupirimate, carbendazim, chlorantraniliprole, chlorpyrifos, clothianidin, cyazofamid, cymoxanil, diflubenzuron, dimethomorph, etoxazole, fenpropimorph, fenpyroximate, flonicamid, fludioxonil, fluopicolide, fluopyram, hexythiazox, imazalil, imidacloprid, indoxacarb, malaoxon, malathion, mandipropamid, mepanipyrim, metalaxyl, methoxyfenozide, metrafenone, myclobutanil, oxadiazon, penconazol, pendimethalin, pirimicarb, propamocarb, propargite, propiconazol, pyraclostrobin, pyridaben, quinoxyfen, spirodiclofen, spirotetramat, spiroxamine, tebuconazole, tebufenozide, tebufenpyrad, thiabendazole, thiacloprid, thiamethoxam, triadimefon, triadimenol, trifloxystrobin, triflumizole, and internal standards azoxystrobin-d4, thiamethoxam-d3, triphenyl phosphate were purchased from Sigma Aldrich (St. Louis, USA).

Standard and internal standard stocks solutions ( $1.0 \text{ mg mL}^{-1}$  for all except  $0.2 \text{ mg mL}^{-1}$  for ametoctradin, carbendazim and chlorantraniliprole) were prepared in acetonitrile or, in case of solubility problem, in methanol or acetone and stored at  $-20^\circ\text{C}$ . A standard mixture solution, with all 58 pesticides, was prepared in acetonitrile at  $1 \text{ } \mu\text{g mL}^{-1}$  of each pesticide.

### 2.2 Instrumentation

HPLC-MS was carried out using a Dionex UltiMate 3000 UHPLC system (Thermo Scientific, Germering, Germany) consisted of a binary pump (HPG-3400RS), an autosampler (WPS-3000TRS), a degasser (SRD-3400) and a column oven (TCC-3000RS). Detection was carried out by a Q Exactive hybrid quadrupole-orbitrap mass spectrometer (Thermo Scientific, Waltham, MA, USA). Analytes were separated on a reversed-phase C18 Atlantis T3 column ( $2.1 \times 100 \text{ mm}$ ,  $3 \text{ } \mu\text{m}$ ) from Waters (Milford, MA, USA) with a corresponding guard C18 column (Security-

Guard ULTRA) from Phenomenex (Aschaffenburg, Germany). The LC-MS system was equipped with a heated electrospray ionization source (HESI-II) and Trace-Finder software version 4.1. Chromatographic separation was realized using gradient elution with 2 mM ammonium formate containing 0.1% formic acid in water as solvent A and methanol as solvent B; LC gradient: 0 min: 85% of solvent A + 15% of solvent B, 0.5 min: 85% A + 15% B, 9 min: 5% A + 95% B, 15 min: 95% A + 5% B with a flow rate of 340  $\mu\text{L}$  per minute was used. The column oven was heated to 40°C and injection volume was 2  $\mu\text{L}$ .

In the positive electrospray ionization (ESI) mode, the ion spray voltage was set at 2.8 kV, the sheath gas flow was at 32 arbitrary units, the auxiliary gas flow rate was kept at 7 arbitrary units, the capillary temperature was set at 295 °C and the auxiliary gas heater temperature was set at 295 °C. In the negative ESI mode, the ion spray voltage was set at -2.5 kV. Nitrogen was used as both sheath and auxiliary gas.

The mass spectrometer was generally operated in parallel reaction monitoring (PRM). The precursor ions in the inclusion list were, within the retention time window  $\pm 0.3$  min, filtered in the quadrupole at isolation window (target  $m/z \pm 0.7$  amu), fragmented in HCD collision cell, product ions were collected in the C-trap at 17,500 resolution (FWHM, full width at half maximum, at  $m/z$  200), AGC target value of  $2e5$ , and maximum ion injection time of 40 ms and finally two specific pairs of precursor-product ion transitions were monitored for each compound of interest. A mass tolerance of 5 ppm was employed. The normalized collision energy (NCE) was optimized for each compound. The instrument was externally calibrated prior to each measurement using the mixture of mass calibrants.

### 2.3 Standard preparation

Stock solutions ( $1 \text{ mg mL}^{-1}$ ) of each compound of interest were prepared by adding 10 mg (corrected for purity) of the analytical grade compound to separate 10 mL volumetric flasks and bringing up to volume with acetonitrile (except carbendazim, which was diluted with methanol). The stock solutions were stored generally at -20 °C. A high level fortification solution was prepared by taking 0.1 mL aliquots of each stock solution and diluting up to volume in a 100 mL volumetric flask with acetonitrile, resulting in a  $1 \mu\text{g mL}^{-1}$  mixed solution.

### 2.4 Cider sample preparation

Fifteen samples of the apple ciders originally from Czech Republic (CZ) were: Cider Hop Hop; Cider Magnetic Apple – chmelený; Tátův sad – chmelený; BB cidre; Cider Bohemia; Cider Magnetic Apple – original; 12PragCider; Cider DRY; Tátův sad cider; První Prajzské jablko; Českorájský cider; Redbrook cider; Rychnovský cider; Johannes cyder; Cidre 99 dry, and five foreign ciders: Val de Rance (FR); Dunkertons (GB); Aspoll Suffolk (GB); Sidra Bere (ESP); Opre'Cidery (SK) were

involved in the experiment. The samples were prepared using a modified QuEChERS method: (1) 10 mL of degassed sample was added into a 50 mL PFTE centrifugation tube, 50  $\mu$ L of internal standard solution (triphenyl phosphate,  $c = 10 \text{ mg L}^{-1}$ ) was added and the tubes were mixed thoroughly; (2) 10 mL of acetonitrile was added (the tubes were tightly closed) and 1 minute mixed on the Vortex shaker; (3) then was added the mix of salts (4 g  $\text{MgSO}_4$ , 1 g NaCl, 1 g sodium citrate tribasic dihydrate, 0.5 g sodium hydrogencitrate sesquihydrate) and (4) the samples were manually shaken for 1 minute; (5) The samples were centrifuge 7 minutes at 4500 rpm; (6) 6 mL of organic phase from sample was took into the centrifugation tubes (15 mL) with 0.9  $\text{MgSO}_4$  and the tubes were again centrifugation for 7 minutes at 4500 rpm. In the second step, the samples were cleaned-up using SPE technique. A SPE columns with PSA sorbent (200 mg, 3 mL tube; Supelco) was conditioned with 2 mL acetonitrile priors clean-up. Then was added 2 mL sample (from 15 mL centrifugation tube). The eluent was collect into the heart shaped flask and subsequently the SPE columns were washed with 10 mL of acetonitrile. Then the samples were evaporated to dryness on the evaporator (40 min/35  $^{\circ}\text{C}$ ). At the last, the samples were dissolved with 1 mL 0.1% formic acid in mixture of 50% methanol in water.

### 3. Results and discussion

In this study, 12 pesticides residues were found in twenty samples of apple ciders that were reliably quantified. At least two pesticides residues were detected in each sample. The most occurring pesticide was pirimicarb, an insecticide for aphid control in a wide range of crops. It was detected in seventeen samples, in four samples was quantified, and the highest concentration was 3.6 ppb in "Johannes Cyder" (CZ). The second most occurred pesticide was boscalid, a fungicide active against a wide range of fungal pathogens. It was detected in fourteen samples, in eight samples was quantification, and the highest concentration was 14.1 ppb in "Bohemia cider" (CZ). The frequently found pesticide residue was also methoxyfenozide, an insecticide used to control various insect moths, butterflies. It was detected in eleven samples, in seven was quantification, and the highest concentration 1.2 ppb was in apple cider with hops addition "Cider Magnetic Apple – chmelený" (CZ). Acetamiprid (an insecticide used for the control aphid) was pesticide residue found quite often in ciders and it was quantification in five samples at the highest concentration was 4.5 ppb in dry cider "Cider Magnetic Apple – original" (CZ), and in other five samples were only detected. Fluopyram, a broad-spectrum fungicide for use as a foliar application and as a seed treatment to control various diseases, was detected in eight samples with the highest concentration 1 ppb in "Cider Bohemia" (CZ) and mandipropamid were detected in four samples, in two samples at the highest concentration 2.1 ppb. The remaining pesticide residues (for example abamectin B1A, carbendazim, imazalil, myclobutanil, pyraclostrobin, thiacloprid) were only detected due to their low concentration.

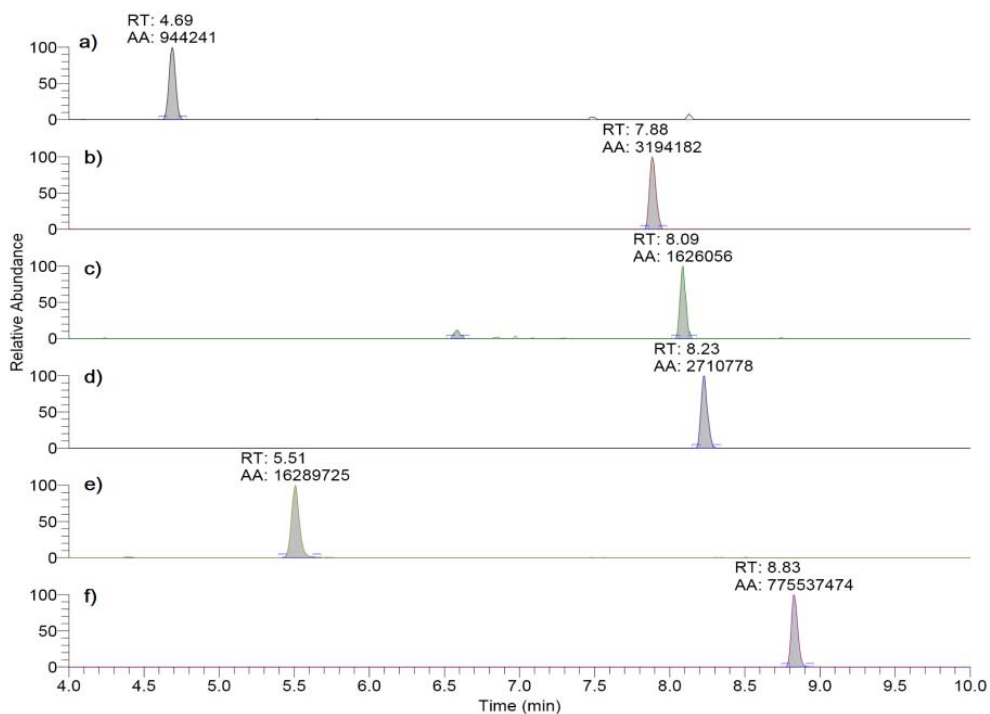


**Fig. 1** Selected ion chromatograms of pesticides residues in sample apple cider “Tátův sad – chmelný”: (a) acetamiprid ( $m/z = 223.0745$ ,  $t_r = 4.69$  min), (b) boscalid ( $m/z = 343.0399$ ,  $t_r = 7.88$  min), (c) methoxyfenozide ( $m/z = 369.173$ ,  $t_r = 8.09$  min), (d) fluorpyram ( $m/z = 397.0537$ ,  $t_r = 8.23$  min), (e) pirimicarb ( $m/z = 239.1503$ ,  $t_r = 5.51$  min), (f) triphenyl phosphate, i.e., internal standard ( $m/z = 327.0780$ ,  $t_r = 8.83$  min).

We had in our experiment also three organic ciders (“Cider hop hop” (CZ); “Apple cider dry” (CZ); “Dunkertons” (GB)). In “Cider hop hop” were detection boscalid (0.5 ppb) and mandipropamid (<0.5 ppb), in the “Apple cider dry” were boscalid (1 ppb) and myclobutanil (<0.5 ppb), and in “Dunkertons” were identified abamectin B1A (0.6 ppb) and pirimicarb (<0.5 ppb).

Five samples of apples ciders were made with hops addition for bitter taste and aroma. Unfortunately, hops belong between commodities treated by wide scale of the agrochemicals. Thus, hops as a raw material could be a potential donor of pesticides residues carried over into ciders. The cider “Opre’ dry hopped cider” originate from Slovakia contained a quite high concentration of imidacloprid (5.3 ppb) and imazalil (2.6 ppb). Presence of imazalil suggests that the apples could be determined for post harvest storage originally. The sample “Cider Magnetic Apple – chmelný” (CZ), which contained acetamiprid at 1.2 ppb, boscalid at 2.6 ppb, methoxyfenozide at 1.2 ppb, fluopyram at <0.5 ppb, mandipropamid at 2.1 ppb, and pirimicarb at <0.5 ppb. In samples “Tátův sad – chmelný” were acetamiprid at <0.5 ppb, boscalid at 1.1 ppb, methoxyfenozide at 0.9 ppb, fluopyram at <0.5 ppb, pirimicarb at 1.1 ppb, and mandipropamid at

<0.5 ppb. The selected ion chromatograms of pesticides residues in sample for this sample is in Fig.1. In the sample “Cider Hop Hop” were detected only boscalid (0.5 ppb) and mandipropamid (<0.5 ppb), and in the sample “BB cidre” were detected boscalid (<0.5 ppb) too and pirimicarb (<0.5). The occurrence of mandipropamid was observed only in case of ciders with hop, thus this pesticide residue coming from the hop most probably. The apples quality is not the only influencing factor for the occurrence of pesticides residues.

#### 4. Conclusions

The found concentrations of pesticide residues in cider as a processed food were evaluated base on acceptable daily intake (ADI,  $\text{mg kg}^{-1}\text{bw day}^{-1}$ ) for each pesticides. The result showed that the even highest determined concentration of boscalid at 14.1 ppb represent only small part of ADI for 80 kg weigh man. The levels of found pesticide residues thus could not be risk for consumers health. Nevertheless, the monitoring of pesticide residues in this type of beverages products is important because they contain various pesticide residues, which long-term consumption could be potentially hazardous for consumer’s health.

#### Acknowledgments

The study was supported by the project of Ministry of Education Youth and Sports of the Czech Republic No. LO 1312.

#### References

- [1] Simon S., Brun L., Guinaudeau J., Sauphanor B.: Pesticide use in current and innovative apple orchard Systems Agronomy. *Agron. Sustain. Dev.* **31** (2011), 541–555.
- [2] [www.food.gov.uk](http://www.food.gov.uk) (accessed 15th May 2018)
- [3] [www.sitem.herts.ac.uk](http://www.sitem.herts.ac.uk) (accessed 10th June 2018)
- [4] Lozowicka B.: Health rick for children and adults consuming apples with residue. *Sci. Total Environ.* **502** (2015), 184–198.
- [5] Lehatay J.S, Anastassiades M., Majers E.R.: The QuEChERS revolution. *LC-GC Europe* **23** (2010), 418–429.

# Chromato-desorption microsystems for determination of biomarkers in the exhaled breath

IGOR ARTEMYEVITCH PLATONOV<sup>a</sup>, IRINA NIKOLAEVNA KOLESNICHENKO<sup>a</sup>,  
ASTKHIK EDIKOVNA IGITKHANIAN<sup>b,\*</sup>, DIANA DAVIDOVNA KARAPETIAN<sup>b</sup>

<sup>a</sup> *Department of Chemistry, Samara University,  
34, Moskovskoye shosse, 443086 Samara, Russia* ✉ [pia@ssau.ru](mailto:pia@ssau.ru)

<sup>b</sup> *Institute of Space Rocket Engineering, Samara University,  
34, Moskovskoye shosse, 443086 Samara, Russia* ✉ [asyaigithanyan@mail.ru](mailto:asyaigithanyan@mail.ru)

## Keywords

biomarkers  
breath acetone  
chromato-desorption  
microsystems  
diabetes  
non-invasive diagnostics

## Abstract

Chromato-desorption microsystems have been developed in this research work. They can be used to increase the accuracy of quantitative determination of biomarkers in the exhaled air. The evaluation of the accuracy determination of acetone in model gas mixtures shows an advantage in comparison with standard methods.

---

## 1. Introduction

Analysis of exhaled air is an attractive area of non-invasive medical diagnostics, because this method excludes invasive interventions and can be implemented repeatedly. It provides an opportunity to study thoroughly the dynamics of physiological processes. Also, the analysis of exhaled air allows to reveal a pathology at those stages of development, when other methods of diagnostics are insensitive, nonspecific and uninformative.

The exhaled air contains about three thousand volatile organic compounds [1], which are the products of physiological and biochemical processes in the organism. Many of them are biomarkers of functional disorders of human body, about 20 of them are used as predictors of some diseases. The acetone is one of the selective biomarkers. It is formed as a result of the oxidation of fats. Increased concentration of acetone in the exhaled air signals about excess level of glucose in the blood [2, 3].

The development of non-invasive diagnostics is hampered by the lack of an optimized method for the quantitative determination of micro quantities of biomarkers in the exhaled air. The limiting factors which determine the accuracy and the rate of measurements are appropriate sampling and sample preparation that eliminate the possibility of additional sample contamination.

The purpose of the research is the development of methodological techniques and the quantitative determination of acetone in the exhaled air.

## 2. Experimental

### 2.1 Reagents and chemicals

We have chosen four types of sorbents for micro systems: Chromaton N-AW-MCS+25% CaCl<sub>2</sub>, Chromaton N-AW-MCS+25% CoCl<sub>2</sub>, Al<sub>2</sub>O<sub>3</sub>, fiberglass+50% polyethylene glycol and filled with them developed chromato-desorption microsystems. We have used acetone as a target component to conduct experiment.

### 2.2 Instrumentation

Developed chromato-desorption microsystems and methods allow to concentrate trace contaminants of aliphatic volatile organic compounds from exhaled air samples by solid phase microextraction technique. Chromato-desorption microsystems have been made from medical needles (inner diameter 0.5 mm) and filled with sorbents. Fig. 1 shows stages of chromato-desorption microsystem preparation. We have used scanning electron microscope Tescan VEGA for analysis of sorbent surface microstructures (Fig. 2).

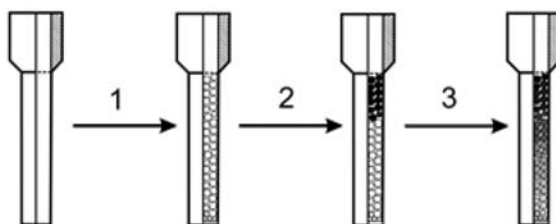


**Fig. 1** Stages of chromato-desorption microsystem preparation: (1) filling with a sorbent, (2) saturation chromato-desorption system with a target component, (3) preparation procedure.

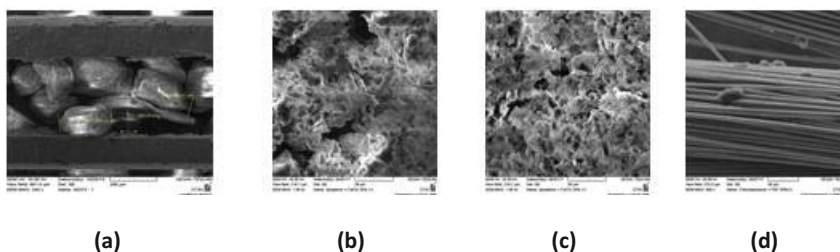


**Fig. 2** Microphotograph of sorbent surfaces: (a) Al<sub>2</sub>O<sub>3</sub>, (b) Chromaton N-AW-MCS+25% CaCl<sub>2</sub>, (c) Chromaton N-AW-MCS+25% CoCl<sub>2</sub>, (d) fiberglass+50% polyethylene glycol.

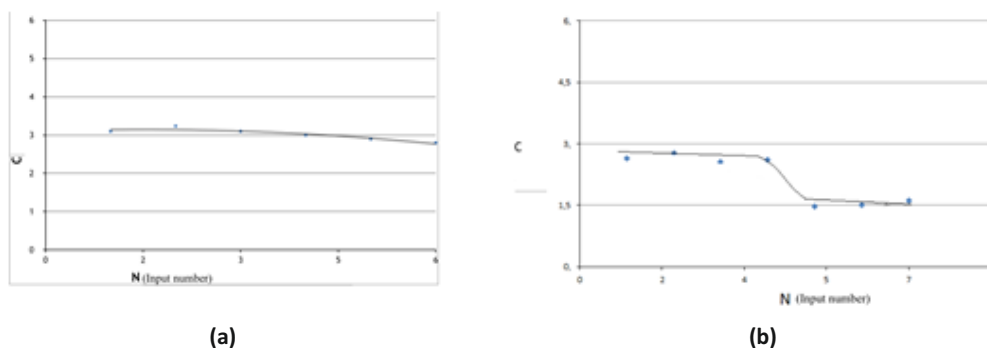


**Fig. 3** Acetone concentration in dependence on use chromatodesorption microsystem filled with (a) Cromaton N-AW-DMCS + 25% CaCl<sub>2</sub>, (b) fiberglass+50% polyethylene glycol.

### 3. Results and discussion

It is known that surface-layer sorbents, modified with sorption-active inorganic salts, have a large adsorption capacity, chemical inactivity and thermal stability, allow the process of concentrating a sample with direct thermal desorption of impurities to transfer them to a gas chromatograph, thereby shortening the time, increasing the sensitivity analysis. In this connection, it is expedient to study the potential use of sorbents of this type for the manufacture of chromatographic desorption microsystems designed to produce gas mixtures containing microquantities of acetone. Chromaton N-AW-DMCS with modification of 25% CaCl<sub>2</sub> and Chromaton N-AW-DMCS with modification of 25% CoCl<sub>2</sub> acquire a strongly developed surface structure, which greatly increases its surface area, moreover sorbent particles are small and have irregular geometric form, whereby the packing density of chromatodesorption microsystem increases. The cumulative effect of these factors makes it possible to predict an increase in sorption capacity of the system. A similar effect of increasing the sorptive capacity of the system due to the large surface area and is shown to Al<sub>2</sub>O<sub>3</sub>, the capacity reduction is not observed.

The system with fiberglass+50% polyethylene glycol showed high throughput. The salt is planted partially on the fiberglass. This sorbent has a special configuration, so the dead volume is almost absent. It was established experimentally that chromatodesorption microsystem life of dispensing discrete gas mixture of at least six cycles with a standard deviation  $\delta = 15\%$  (Fig. 3).

### 4. Conclusions

Analytical micro concentrating systems and methods for concentrating trace aliphatic hydrocarbons from exhaled air samples have been developed. Characteristics of chromatodesorption microsystems filled with Chromaton N-AW-DMCS+25% CaCl<sub>2</sub>, Chromaton N-AW-DMCS+25% CoCl<sub>2</sub>, Al<sub>2</sub>O<sub>3</sub>, fiberglass+50% polyethylene glycol have been determined. It is reasonable to use

chromato-desorption microsystem filled with Chromaton modified with sorption-active inorganic salts and with fiberglass+50% polyethylene glycol to concentrate volatile organic compounds from breath air samples. Chromato-desorption microsystem method meets green chemistry principles as it reduces dramatically chemical agent consumption.

### Acknowledgments

The study was supported by the Ministry of Education and Science of the Russian Federation under project number 4.6875.2017/8.9.

### References

- [1] Копылов Ф.Ю., Сыркин А.Л., Чохамидзе П.Ш., Быкова А.А., Шалтаева Ю.Р., Беляков В.В., Першенков В.С., Самотаев Н.Н., Головин А.В., Васильев В.К., Малкин Е.К., Громов Е.А., Иванов И.А., Липатов Д.Ю., Яковлев Д.Ю.: Перспективы диагностики различных заболеваний по составу выдыхаемого воздуха. *Клиническая медицина* **10** (2013), 16–21.
- [2] Zhou M.G., Liu Y., Li W.W., Yuan X., Zhan X.F., Li J., Duan Y.X., Liu Y., Gao Z.H., Cheng Y., Cheng S.Q., Li H., Liang Y.: Investigation and identification of breath acetone as a potential biomarker for type 2 diabetes diagnosis. *Chin. Sci. Bull.* **59** (2014), 1992–1998.
- [3] Galassetti P.R., Novak B., Nemet D., Rose-Gottron C., Cooper D.M., Meinardi S., Newcomb R., Zaldivar F., Blake D.R.: Breath ethanol and acetone as indicators of serum glucose levels: an initial report. *Diabetes Technol. Ther.* **7** (2005), 115–123.

# A novel way of establishing the quantitative composition of gravimetrically prepared standard solutions of volatile compounds in water-ethanol matrix

ANTON KORBAN<sup>a, b</sup>

<sup>a</sup> *Department of Analytical Chemistry, Chemistry Faculty, Belarusian State University, Leningradskaya Str. 14, 220030 Minsk, Belarus* ✉ [karbonat7@gmail.com](mailto:karbonat7@gmail.com)

<sup>b</sup> *Institute for Nuclear Problems of Belarusian State University, Bobruyskaya Str. 11, POB 220030, Minsk, Belarus*

## Keywords

ethanol  
gravimetric preparation  
standard solution  
successive iterations,  
volatile impurities

## Abstract

The iteration method of volatile compounds concentrations and calibration coefficients calculation in water-ethanol standard solutions was proposed. It lies in the gravimetric preparation of a mixture which contains impurities at much higher concentrations than those in initial ethyl alcohol applied as a blending agent. The "Ethanol as Internal Standard" method is then used for the calculation of Relative Response Factors of zero-order approximation for each analysed volatile. Ethyl alcohol used for preparation is then measured by gas chromatography and the adulterants concentrations in it are determined. Further the volatiles concentrations in standard solution and Relative Response Factors are specified. Finally the process of taking into consideration the adulteration of initial ethanol allows correct determination of low volatiles concentrations in prepared standards solutions. The efficiency of the method was demonstrated experimentally.

---

## 1. Introduction

Each and every quantification analysis undoubtedly cannot proceed correctly without preliminary calibration process. Speaking about water-ethanol mixtures excellent exponents of their application sphere are alcoholic beverages and the materials of their origin, such as distillates. Among lots of control tests of this output volatile compounds quantification is the topmost quality parameter, as chemical content of alcoholic beverage influence both organoleptic parameters (flavour and taste) and safety. Consequently analytical chemists challenge is to establish the concentrations of volatile compounds in the testing sample as accurately as possible.

**Table 1**  
Limits of volatile concentrations in ethyl alcohol.

Component(s)	Concentration limit of absolute alcohol / mg L <sup>-1</sup>		
	EP monograph	EC 110/2008	Open commercial sources
acetaldehyde (+ acetal)	8	50	8–40
methanol	165	300	80–300
higher alcohols/other volatiles	240	50	80–240

Separation and detection of components in ethanol-containing products is mainly performed with gas chromatography (GC) method as the most robust, rapid and modern. Thus, lots of international legislative documents establish the GC way of quantitative determination of volatile compounds in alcoholic products [1–5]. But the standard solutions preparation algorithm differs from document to document. European regulation [1] concerns the GC method of volatile compounds quantification in spirit drinks and describes the whole procedure of standard solutions gravimetric preparation from water and ethyl alcohol free from volatile impurities. Oppositely, the European Pharmacopeia (EP) monographs concerning ethanol (96%) and anhydrous ethanol analysis establish the preparation of reference solutions on the basis of testing substance [5]. In addition, the authors of a major part of research articles concerning the determination of contaminants in alcoholic products prepare standard solutions in their own way, applying methods different from those described in the legislative documents. In this case both External and Internal standard methods are applied although the latter is predominant.

Eventually let us describe the problem which unavoidably exists during standard solutions preparation. The fact is that ethyl alcohol cannot be 100% pure as it always contains volatile impurities. And the challenge is to take the ethanol adulterants concentrations into consideration during final calculation of standard solutions composition. Table 1 includes the information about limits of volatiles concentrations in ethyl alcohol found in both legislative documents and open official commercial sources, such as Sigma-Aldrich. Finally in some cases the concentrations of volatiles in standard solutions are comparable with those in the initial ethyl alcohol. This phenomenon causes a problem of incorrect establishment of certified values. The problem can be solved by the proposed iteration method.

Firstly, a standard solutions which contains analysed volatile compounds at the concentrations near to 500 mg l<sup>-1</sup> absolute alcohol (AA) is to be prepared gravimetrically according to ASTM recommendations [6]. Zero-order approximated concentration (mg l<sup>-1</sup> AA) of *i*-th volatile in the prepared standard solution  $c_i^{\text{st}}(0)$  is determined according to the formula

$$c_i^{\text{st}}(0) = \rho_{\text{eth}} \frac{c_i^i m_i^{\text{st}}}{c_{\text{eth}}^{\text{st}} m_{\text{st}}} \quad (1)$$

where  $\rho_{\text{eth}} = 789300 \text{ mg l}^{-1}$  is the ethanol density;  $c_i^i$  and  $m_i^{\text{st}}$  are the purity of  $i$ -th compound in the  $i$ -th substance ( $\text{mg mg}^{-1}$ ) and recorded mass of added  $i$ -th substance;  $c_{\text{eth}}^{\text{st}}$  is the mass concentration ( $\text{mg mg}^{-1}$ ) of ethanol in prepared standard solution and  $m^{\text{st}}$  is the mass (mg) of standard solution. Further the zero-order approximated Relative Response Factors ( $RRF$ ) are determined according to the "Ethanol as Internal Standard" method [7–8] by the following equation

$$RRF_i^{\text{eth}}(0) = \frac{c_i^{\text{st}}(0)}{A_i^{\text{st}}} \frac{A_{\text{eth}}^{\text{st}}}{\rho_{\text{eth}}} \quad (2)$$

where  $A_i^{\text{st}}$  and  $A_{\text{eth}}^{\text{st}}$  are the values of GC response to  $i$ -th volatile and ethanol, for instance, peak area. Hereafter it is necessary to establish volatiles concentrations in the initial ethyl alcohol, that is why it should be measured by GC. The concentrations of impurities are then calculated according to the following formula

$$c_i^{\text{eth}}(0) = RRF_i^{\text{eth}}(0) \frac{A_i}{A_{\text{eth}}} \rho_{\text{eth}} \quad (3)$$

The obtained  $\text{mg l}^{-1}$  AA concentration units fully comply with the international regulatory documents [1–5]. Most common volatiles presented in pure ethyl alcohol are acetaldehyde, ethyl acetate, methanol and higher alcohols (fusel oils). Then the volatiles concentrations in standard solutions must be clarified by taking into consideration the amount of impurities established according to the Eq. (3). It is done according to the following formula

$$c_i^{\text{st}} = \rho_{\text{eth}} \frac{c_i^i m_i^{\text{st}} + \frac{c_i^{\text{eth}}(0) c_{\text{eth}}^{\text{st}} m_{\text{st}}}{\rho_{\text{eth}}}}{c_{\text{eth}}^{\text{st}} m_{\text{st}}} \quad (4)$$

This is how the iteration circle is closed. Further it is necessary to make one or two additional iterations by subsequent usage of Eqs. (2)–(4). After this the quantitative analysis of a test sample proceeds according to the Eq. (3) but with clarified  $RRF_i^{\text{eth}}$  values.

In order to show the influence of ethanol spoilage on the establishment of certified concentrations values the relative bias is applied

$$\text{Bias} = \frac{|c_i^{\text{st}}(0) - c_i^{\text{st}}|}{c_i^{\text{st}}} \cdot 100 [\%] \quad (5)$$

## 2. Experimental

### 2.1 Reagents and chemicals

Initial high-purity ethanol was purchased from JSC “Dyatlovo Wine and Distillery Plant Algon” (Belarus).

### 2.2 Instrumentation

The samples were analysed with a Chromatec-Kristall 5000 gas chromatograph equipped with FID and an autosampler. Instrument control and data analysis were performed with UniChrom software (New Analytical Systems, Minsk, Belarus). The gas chromatograph was fitted with capillary column Rt-Wax, 60 m × 0.53 mm with 1 μm phase thickness. The oven temperature was the following: the initial isotherm at 75 °C for 9 min was raised to 130 °C at a rate of 5 °C min<sup>-1</sup> then raised to 180 °C at a rate of 10 °C min<sup>-1</sup> with final isotherm of 155 °C for 5 min. The carrier gas was nitrogen (≥99.99 % purity); the gas flow was 6.9 ml min<sup>-1</sup>; the injector temperature was 160 °C; the detector temperature was 200 °C; the injector volume was 1 μL; the split ratio was 1:7. Analytic balance OHAUS PA-214C with a precision of 0.2 mg was used for gravimetric preparations.

### 2.3 Standard solutions preparation and analysis

Six standard water-ethanol solutions with 40% ethanol by volume were prepared gravimetrically according to [6] recommendations by subsequent addition of individual chemical substances or solutions into initial water-ethanol mixture. The added individual chemical substances were: acetaldehyde, methyl acetate, ethyl acetate, methanol, 2-propanol, 1-propanol, isobutyl alcohol, 1-butanol, and isoamyl alcohol.

## 3. Results and discussion

The concentrations of volatiles in the prepared standard solutions were nearly the following: 3, 10, 50, 200, 250 and 500 mg l<sup>-1</sup> AA. Each sample was measured triply in repeatability conditions. The standard solutions “WES-B”, which contained nearly 500 mg l<sup>-1</sup> AA of each component was used as a calibration solution. Then the  $RRF(0)$  values were calculated according to the Eq. (2) and initial ethyl alcohol was also triply measured by GC. It was found that initial ethanol contained only three impurities, which were acetaldehyde, methanol and 2-propanol (Fig. 1). Then the abovementioned iterations were done in accordance with Eqs. (2)–(4). The detailed results of iterations are given in Table 2. Then the biases were calculated according to the Eq. (5) and transferred into graphical form (Fig. 2). As there were only three impurities in the initial ethyl alcohol, there are three lines on

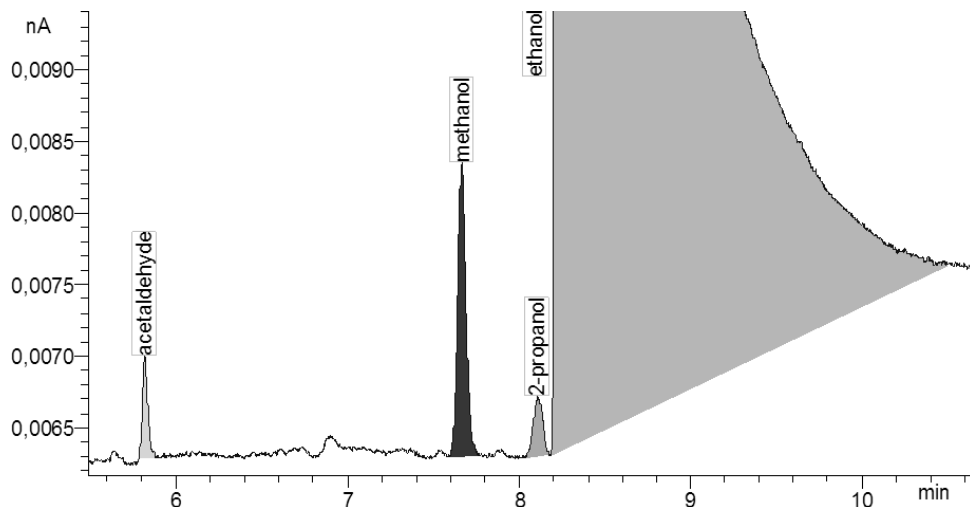


Fig. 1 The chromatogram of ethyl alcohol used for standard solutions preparation.

Table 2

The establishment of volatiles concentrations in standard solutions and the specification of Relative Response Factors (RRF).

Component	Concentration of absolute alcohol / mg L <sup>-1</sup>			Average detector response /nA min	RRF(0)	RRF(I)	RRF(II)
	Zero-order approximation in standard solutions WES-B	In the initial ethyl alcohol	Specified in SS WES-B				
acetaldehyde	435.9	1.85	437.8	4.80	1.290	1.295	1.295
methyl acetate	487.2	–	487.2	4.54	1.524	1.524	1.524
ethyl acetate	476.1	–	476.1	5.04	1.342	1.342	1.342
methanol	526.2	18.16	544.3	6.32	1.182	1.222	1.223
2-propanol	512.2	1.15	513.3	8.26	0.881	0.883	0.883
ethanol	789300	789300	789300	11210	1.000	1.000	1.000
1-propanol	532.4	–	532.4	11.32	0.668	0.668	0.668
isobutyl alcohol	553.0	–	553.0	12.34	0.636	0.636	0.636
1-butanol	531.8	–	531.8	11.96	0.631	0.631	0.631
isoamyl alcohol	555.7	–	555.7	12.64	0.624	0.624	0.624

the corresponding diagram. It can be seen, that in case of standard solutions with volatiles at very low concentrations, e.g. solutions with 3 and 10 mg l<sup>-1</sup> AA volatiles contamination, biases reach extremely high values. As methanol concentration in ethyl alcohol is the biggest among other volatiles, its corresponding graph is the most rapid of all. It is clear that the relative bias constantly decreases when speaking about more saturated solutions but still takes rather great values for methanol.

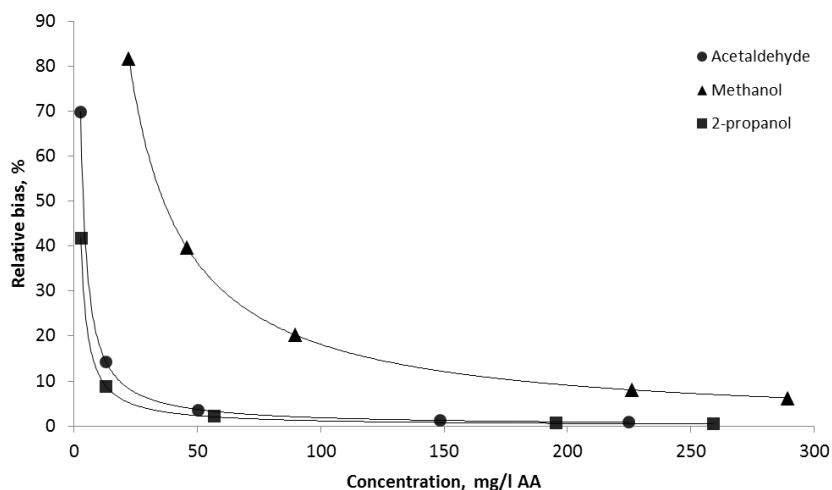


Fig. 2 The diagram of relative biases caused by disregarding of ethanol spoilage.

#### 4. Conclusions

The current study revealed the problem of the correct establishment of standard solutions certified values as ethyl alcohol initially contains analysed volatiles. The successive iterations method of volatile compounds concentrations and calibration coefficients calculation in water-ethanol standard solutions was proposed and experimentally tested. The analysis of obtained results shows that the method allows the accuracy of volatile compounds certified values increase greatly. The most intelligent application of the method seems to be during preparation of standard solutions with congeners at low concentrations. There is no necessity in any expensive materials, additional instruments or labour-cost operations, that is why the proposed method can be applied as an easy, accurate and cheap problem solution.

#### Acknowledgments

Author thanks his scientific advisers Dr. Siarhei Charapitsa and Dr. Svetlana Sytova from Institute for Nuclear Problems of Belarusian State University.

#### References

- [1] Commission Regulation (EC) No 2870/2000 of 19 December 2000 laying down Community reference methods for the analysis of spirits drinks. *Official Journal of the European Communities* L333/20.
- [2] AOAC Official Methods 972.10 and 972.11. *Alcohol (higher), methanol and ethyl acetate in distilled liquors (2005). Alternative gas chromatographic method.*
- [3] International Organization of Vine and Wine (OIV). Compendium of international methods of analysis of spirituous beverages of viti-vinicultural origin. *Determination of the principal volatile substances of spirit drinks of viti-vinicultural origin.* OIV-MA-BS-14: R2009.
- [4] European Standard EN 15721. *Ethanol as a blending component for petrol – Determination higher alcohols, methanol and volatile impurities – Gas chromatographic method, 2009.*

- [5] *European Pharmacopoeia. 9th Ed.* Strasbourg, Council of Europe 2017, p. 2417–2420.
- [6] ASTM D 4307-99. *Standard Practice for Preparation of Liquid Blends for Use as Analytical Standards.*
- [7] Charapitsa S.V., Kavalenka A.N., Kulevich N.V., Makoed N.M., Mazanik A.L., Sytova S.N., Zayats N.I., Kotov Y.N.: Direct determination of volatile compounds in spirit drinks by gas chromatography. *J. Agric. Food Chem.* **61** (2013), 2950–2956.
- [8] Charapitsa S., Sytova S., Korban A., Boyarin N., Shestakovich I., Čabala R.: The establishment of metrological characteristics of the method “Ethanol as Internal Standard” for the direct determination of volatile compounds in alcoholic products. *Journal of Chemical Metrology* **12** (2018), 59–69.

# Method of cyclic voltammograms in the determination of Sn(II) in strongly acid electrolytes for tin electrodeposition

MARINA SHIKUN<sup>a,\*</sup>, OLGA VRUBLEVSKAYA<sup>b</sup>

<sup>a</sup> *Inorganic Chemistry Department, Chemistry Faculty, Belarusian State University, Leningradskaya Str. 14, 220030 Minsk, Republic of Belarus* ✉ [mariawerner21@gmail.com](mailto:mariawerner21@gmail.com)

<sup>b</sup> *Research Institute for Physical Chemical Problems of the Belarusian State University, Leningradskaya Str. 14, 220030 Minsk, Republic of Belarus*

## Keywords

Sn(II)  
Sn(IV)  
cyclic voltammetry  
current density

## Abstract

The way of Sn(II) quantitative determination in the presence of Sn(IV) in acid electrolytes which are used for the tin electrodeposition is proposed. The method is based on the analysis of current density in the maximum of the first stage of Sn(II) reduction.

---

## 1. Introduction

Tin coatings are widely used as a finishing coating for food industry equipment working surfaces, for storage packs from steel, in electronics, in the production of printed circuit board, in the automotive industry and the production of details used in friction.

Strongly acidic electrolytes for industrial electrochemical deposition of tin are demanded mostly due to the possibility to obtain shiny decorative coatings and due to high stability and deposition rate in comparison with the known weakly acidic and alkaline electrolytes. Strongly acidic electrolytes consist of: Sn(II) sulphate or chloride as a metal sources; citrate-, tartrate-ions as ligands for the increasing of solution stability owing the formation of Sn(II) bidentate complexes. pH of solutions is regulated by using a sulphuric, methanesulphonic or hydrochloric acid [1]. Different surfactants such as 2-naphthol, gelatin, polyethylene glycol, peptone [1, 2] are used in the electrolytes for fine-crystalline closely-packed coatings electroplating. Sn(IV) is formed during the electrolytes storage and exploitation both by reaction of Sn(II) oxidation by dissolved oxygen and anodic oxidation of Sn(II). In order to prevent partly these processes the usage of antioxidants, such as quinones, ascorbic acid, is needed.

Sn(II) ions could exist in high mentioned sulphuric electrolytes in next forms:  $\text{Sn}^{2+}$ ,  $\text{SnSO}_4$ ,  $\text{Sn}(\text{SO}_4)_2^{2-}$ ,  $\text{SnL}_2$ ,  $\text{SnL}^+$ , which are presented simultaneously at the  $\text{pH} = 0.5\text{--}2.0$  (ref. [3]), as well as Sn(IV) compounds. The presence of different

Sn(II) forms in the solution causes the complicate (for example two stage) process of its reduction.

During the electrolyte exploitation Sn(II) concentration reduces with coating deposition and the usage of soluble tin anodes does not compensate the decrease in Sn(II) concentration. The adjustment of Sn(II) concentration and other solution components is needed for the long-term electrolytes exploitation. Correction of the solution composition is required if the residual concentration of Sn(II) close to 30–40% of the initial concentration.

Quantitative determination of Sn(II) compounds in aqueous solutions can be proceeded by chemical methods such as: iodometric titration [4]; precipitation with insoluble Sn(II) sulphide formation; complexometry titration, based on the formation of a sufficiently stable Sn(II) complex with ethylenediaminetetraacetic acid. Physicochemical methods such as atomic absorption spectroscopy and inductively coupled plasma atomic emission spectroscopy [5] are also used for quantitative tin analysis. Chemical methods require a lot of time and may be inaccurate if there are many components in the solution. Physicochemical methods are two or three orders of magnitude more accurate than chemical methods, but require special equipment and specially trained personnel.

The purpose of the work was to analyse the possibility of quantitative analysis of Sn(II) compounds in a multicomponent solution in the presence of Sn(IV) compounds by cyclic voltammetry (CV).

## 2. Experimental

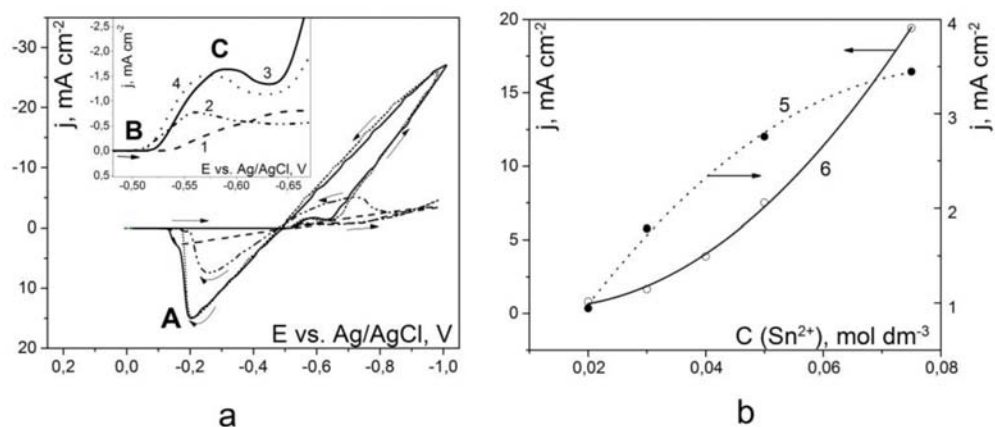
### 2.1 Reagents and chemicals

Model solutions for Sn-coatings electrodeposition are presented in Table 1. All chemicals were purchased from Sigma-Aldrich.

**Table 1**

Compositions of model solutions for tin deposition.

Component	Concentration / mol dm <sup>-3</sup>		
	Sulphate solution	Chloride solution	Chloride solution with Sn(IV)
SnSO <sub>4</sub>	0.020–0.100	–	–
SnCl <sub>2</sub> ·2H <sub>2</sub> O	–	0.020 – 0.100	0.020 – 0.075
SnCl <sub>4</sub> ·5H <sub>2</sub> O	–	–	0.020 – 0.030
Thiourea	0.053	0.053	0.053
Hydroquinone	0.005	0.005	0.005

**Fig. 1**

- (a) CV curves for chloride solutions with Sn(II) concentration 0.050 mol dm<sup>-3</sup> (curve 1) and 0.100 mol dm<sup>-3</sup> (curve) and sulphate solutions with Sn(II) concentration 0.05 mol dm<sup>-3</sup> (curve 2) and 0.10 mol dm<sup>-3</sup> (curve 4)
- (b) The dependences between maximum anodic current density and Sn(II) concentration in chloride (curve 5) and sulphate (curve 6) solutions.

## 2.2 Instrumentation

Voltammetric measurements were carried out in three-electrode cell with carbon working electrode (with working square 0.38 cm<sup>2</sup>). Ag/AgCl/KCl(sat) electrode and a platinum wire were used as reference and counter-electrodes correspondingly. All potentials are referred to the Ag/AgCl/KCl(sat) electrode. Cyclic voltammetry was carried out at scan rate 10 mV s<sup>-1</sup> with the usage of programmer PR-8 and potentiostat PI-50-1.1 (Russia) controlled by software. The surface layer of carbon working electrode was delayed mechanically before each experiment.

## 3. Results and discussion

For the analysis of the possibility of usage cyclic voltammograms for the quantitative determination of Sn(II) concentration CV curves were received for the sulphate and chloride solutions (Fig. 1a). It is possible to allot three areas of CV curves perspective for the data comparison for quantitative analysis of Sn(II). Such areas are the maximum current density of anodic peak of the volt-ampere curves (area A) characterizing the dissolution of tin deposited on the working electrode; the potentials of the Sn(II) reduction beginning (area B); the maximum current density of the peak on the cathodic branch of the volt-ampere curves characterizing Sn(II) reduction on the first stage which is in the range from -0.50 V to -0.52 V for sulphate solutions and in the range from -0.53 V to -0.57 V for chloride solution (area C).

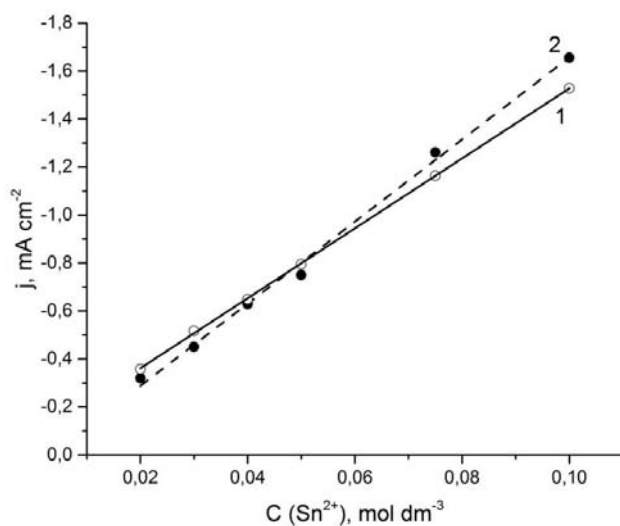


**Fig. 2** The dependence of Sn(II) concentration on the current density in the maximum of Sn(II) reduction (area C) for sulphate (1) and chloride (2) solutions.

The dependence of Sn(II) concentration in sulphate and chloride solutions on current density at the maximum of the anodic branch of volt-ampere curves is shown in Fig.1b. The abovementioned dependences were not linear and could not be used as a calibrator. There was no any dependence of Sn(II) concentration in the electrolyte on the potentials of the Sn(II) reduction beginning (area B). Area C is suitable for the quantitative analysis of Sn(II). Insert in Fig 1a is the cathodic scans of volt-ampere curves in the range of potentials from  $-0.48$  V to  $-0.67$  V for sulphate and chloride containing  $0.050$  and  $0.100$  mol dm<sup>-3</sup> Sn(II). It was found that the dependences between maximum cathodic current and the Sn(II) concentration for sulphate and chloride solutions are linear. Calibration curves are presented in Fig. 2.

Mixed chloride solutions containing SnCl<sub>4</sub>·5H<sub>2</sub>O in concentrations  $0.010$ – $0.030$  mol dm<sup>-3</sup> and Sn(II) in concentration equal to  $0.100$  mol dm<sup>-3</sup> were prepared in order to analyse the possibility of quantitative Sn(II) determination in the solutions with Sn(IV). Cathodic branches of CV curves are presented in Fig. 3. According to the analysis of the cathodic branch of CV curve for chloride solution containing only Sn(IV) (Fig. 3, curve 3) it is obvious that reduction potential of the Sn(IV) is equal to  $-0.63$  V. It is necessary to note that in case of highest concentration of Sn(II) ( $0.100$  mol dm<sup>-3</sup>) in chloride electrolyte the maximum of current density is observed at  $-0.57$  V that is more positive in comparison with Sn(IV) reduction.

In case of mixed chloride solutions the maximum of the current density of Sn(II) reduction is observed at the  $-0.65$  V potential and the process of Sn(IV) reduction is started at  $-0.63$  V. So, in the presence of Sn(IV) it is impossible to observe the

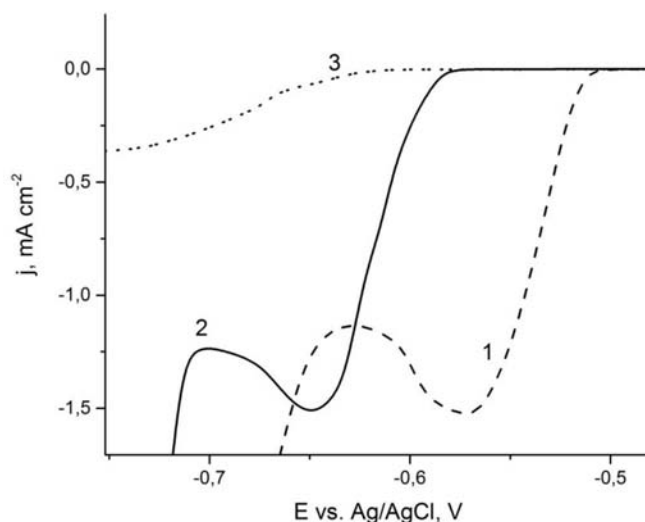


**Fig. 3** Cathodic branches of CV curves for sulphate (curve 1) and chloride (curve 2) electrolytes containing Sn(II) in concentration  $0.100 \text{ mol dm}^{-3}$ ; the solution containing Sn(IV) in concentration  $0.020 \text{ mol dm}^{-3}$  (curve 3).

**Table 2**

The results of quantitative determination of Sn(II) in the presence of Sn(IV) in the chloride model solutions.

$c(\text{Sn(IV)})$ / $\text{mol dm}^{-3}$	$c(\text{Sn(II)})$ / $\text{mol dm}^{-3}$	mole ratio Sn(II):Sn(IV)	$j/\text{mA cm}^{-2}$	$c_{\text{defined}}$ / $\text{mol dm}^{-3}$	Relative error <sup>a</sup> /%
0.02	0.040	2:1	0.696	0.042	4.8
0.02	0.050	2.5:1	0.840	0.051	1.9
0.02	0.075	3.75:1	1.251	0.075	–
0.03	0.040	1.3:1	0.712	0.043	6.9
0.03	0.050	1.7:1	0.872	0.053	5.7
0.03	0.075	2.5:1	1.257	0.075	–

<sup>a</sup> calculated by mean-square error method

current density peak of Sn(II) reduction. The comparison of the current densities corresponding to the maximum of cathode currents densities in solutions without Sn(IV) allows to determine Sn(II) concentrations in mixed chloride electrolyte. The results of quantitative determination of Sn(II) in the presence of Sn(IV) are given in Table 2. It is necessary to note that concentration of Sn(IV) ions in case of electrolyte exploitation for electrochemical tin deposition in manufactory is one order of magnitude less than for Sn(II).

The results of the experimental work show that in case of Sn(II):Sn(IV) mole ratio equal to 3.75:1 the relative error is minimal. With the decreasing of Sn(II) concentration when Sn(II):Sn(IV) = 1.3:1 the relative error reaches 6.9%.

## 4. Conclusions

The express way of Sn(II) concentration determination in sulphate and chloride solutions for electrochemical tin deposition was found. It is based on the analysis of the current density in the maximum of the first stage of Sn(II) reduction. The analysis could be held in the presence of Sn(IV) compounds accumulated in the solution during its exploitation. The relative error reaches the highest value of 6.9% in the case of Sn(II):Sn(IV) mole ratio equal to 1.3:1 and the lowest one of 1.9% at 2.5 : 1 mole ratio. The Sn(II) : Sn(IV) ratio is 10 : 1 in the conditions of electrolytes exploitation in manufactory. That is why it is possible to conclude that proposed method is applicable for the high accuracy tin (II) quantitative determination.

## Acknowledgments

The study was supported by the Belarusian Republican Foundation for Fundamental Research under Project No. X18M-060.

## References

- [1] Walsh F.C., Low C.T.J.: A review of developments in the electrodeposition of tin. *Surf. Coat. Technol.* **288** (2016), 79–94.
- [2] Zaikoska S.P., Mulone A., Hansal W.E.G., Klement U., Mann R., Kautek W.: Alkoxyated  $\beta$ -naphthol as an additive for tin plating from chloride and methane sulfonic acid electrolytes. *Coatings* **8** (2018), 79–96.
- [3] Survila A., Mockus Z., Kanapeckaitė S., Stalnionis G.: Kinetics of Sn(II) reduction in acid sulphate solutions containing gluconic acid. *J. Electroanal. Chem.* **667** (2012), 59–65.
- [4] <http://www.ecitechnology.com/articles/control-tinlead-solutions-electrodeposition-bumps> (accessed 22th June, 2018)
- [5] Rončević S., Benutić A., Nemet I., Gabelica B.: Tin content determination in canned fruits and vegetables by hydride generation inductively coupled plasma optical emission spectrometry. *Int. J. Anal. Chem.* 2012, Article ID 376381.

# Adsorption of Sc(III) on oxidized carbon nanotubes for separation and preconcentration from aqueous solutions – study of mechanism

MATEUSZ PEGIER<sup>a, b, \*</sup>, KRYSZYNA PYRZYNSKA<sup>a</sup>, KRZYSZTOF KILIAN<sup>b</sup>

<sup>a</sup> Faculty of Chemistry, University of Warsaw,  
Pasteur 1 st., 02-093 Warsaw, Poland ✉ pegier@slcj.uw.edu.pl

<sup>b</sup> Heavy Ion Laboratory, University of Warsaw, Pasteur 5a st., 02-093 Warsaw, Poland

## Keywords

adsorption  
carbon nanotubes  
scandium

## Abstract

Oxidized multiwalled carbon nanotubes (CNT-COOH) has been recently proposed for separation and preconcentration of scandium ions from water samples. In the present study adsorption behaviour of scandium cations on CNT-COOH have been investigated. The results show that at pH > 4 removal of Sc(III) from solution can be mainly attributed to precipitation of insoluble scandium hydroxide, while dominating mechanism in the pH range 1–3 is adsorption. Properties of CNT-COOH as excellent sorbent are confirmed by sorption capacity of 40.1 mg g<sup>-1</sup> at pH = 3.0 and 25 °C. As far as the adsorption parameters is concerned, equilibrium data are in good agreement with Freundlich isotherm. Adsorption kinetics is best represented by pseudo-second order model with film diffusion as main controlling factor.

---

## 1. Introduction

Scandium together with yttrium and lanthanides are counted among rare earth elements. Scandium and its compounds, due to its interesting properties is more and more widely applied among others in optical, chemical, laser, superconductor, medical treatment industries [1]. Growing use of scandium in high-tech poses a threat for its release and accumulation in environment. Due to these facts there is a need for simple and accurate analytical methods for determination of scandium in environmental samples, such as water. The main obstacle for application of methods that are used for metal determination in water samples, namely inductively coupled plasma optical emission spectrometry and mass spectrometry (ICP OES and ICP MS, respectively) is low concentration of scandium. For this reason application of preconcentration techniques that allow for separation of analytes from matrix, with solid phase extraction as the most popular, are

essential for obtaining accurate results. Carbon nanotubes (CNTs) have been proven to be effective sorbents for the removal of a wide variety of organic and inorganic pollutants dissolved in aqueous media [2]. Oxidized CNTs, obtained after introduction of oxygen containing functional groups (such as  $-OH$ ,  $-C=O$  and  $-COOH$ ) on their surface with several show exceptionally high sorption capacity and efficiency for removal of heavy metal ions [3]. They have been applied for preconcentration of scandium from water samples [4, 5].

## 2. Experimental

### 2.1 Reagents and chemicals

Solutions of scandium were prepared from  $1000 \text{ mg L}^{-1}$  stock solution from Merck by stepwise dilution. Multiwalled carbon nanotubes carboxylic acid functionalized (purity > 95%, length 1–5  $\mu\text{m}$  and average diameter of 9.5 nm) were purchased from Sigma Aldrich and were used without further purification.

### 2.2 Instrumentation

A Thermo Scientific iCAP 6000 ICP OES spectrometer was used for scandium determination. The pH values were measured using Hanna Instruments HI2210-01 pH-meter supplied with glass-combined electrode. Boehm titrations were made using Metrohm Titrando automatic titrator. Porous structure of CNT-COOH was evaluated using the Micrometrics ASAP 2010 analyzer.

### 2.3 Characterization of CNT-COOH

Content of surface carboxylic groups was evaluated using Boehm titration. The specific surface area was calculated by the Brunauer-Emmer-Teller (BET) method. The pore size distribution was obtained using the Barrett-Joyner-Halenda method. The pore volumes were obtained from the volume of  $N_2$  adsorbed at or near  $P/P_0 = 0.99$ . The porous structure of CNT-COOH was evaluated by nitrogen adsorption isotherms at 77 K.

### 2.4 Kinetic study

The adsorption kinetics experiments were carried out in order to establish the kinetics of the adsorption process for an initial  $\text{Sc(III)}$  concentration of  $2 \text{ mg L}^{-1}$  and a  $\text{pH} = 3.0$  as a function of contact time in the range of 1–50 min.

### 2.5 Adsorption studies

The sorption studies were conducted by equilibrating 50 mg of CNT-COOH with 10 mL of  $5 \text{ mg L}^{-1}$  of  $\text{Sc(III)}$  solution having specified acidity for 4 h at room

temperature. The supernatants were then decanted and the concentrations of Sc(III) was measured. The amount of retained metal ions were calculated as the difference between the initial and final concentration at equilibrium. The results are based on at least three replicate experiments for each pH value. Simultaneously, to check the possibility of scandium removal by precipitation in the studied pH range, similar experiments but in the absence of carbon nanotubes were conducted. The solutions containing  $5 \text{ mg L}^{-1}$  of Sc(III) and appropriate pH were passed through a  $0.2 \text{ }\mu\text{m}$  filter (Whatmann) to trap a possible precipitate. Subsequently, scandium from the filter was eluted by  $\text{HNO}_3$  and determined by ICP OES.

For estimation of the sorption capacity, 50 mg of CNTs was mixed with 10 mL of Sc(III) solution at  $\text{pH} = 3.0$  and concentration range of  $1\text{--}300 \text{ mg L}^{-1}$ . After shaking the solution for 4 h, the metal concentration was determined. The sorption capacity  $q_e$  ( $\text{mg g}^{-1}$ ) were calculated using the following equation

$$q_e = [(c_o - c_e)V]/m \quad (1)$$

where  $c_o$  and  $c_e$  are the initial and equilibrium Sc(III) concentrations ( $\text{mg L}^{-1}$ ), respectively,  $V$  the volume of solution and  $m$  is the weight of an sorbent.

### 3. Results and discussion

#### 3.1 Characterization of CNT-COOH

The  $\text{N}_2$  adsorption-desorption isotherm of CNT-COOH is of type IV, typical for mesoporous materials. The specific surface area was calculated to be  $352 \text{ m}^2 \text{ g}^{-1}$  and total pore volume  $0.72 \text{ cm}^3 \text{ g}^{-1}$ . The content of surface acidic groups evaluated by the Boehm titration method was  $2.41 \text{ mmol g}^{-1}$ .

#### 3.2 Effect of solution pH

As the acidity influences not only the adsorbent surface charge but also the metal species present in solution it is one of the most important parameters in the adsorption of metal ions. The adsorption of Sc(III) ions on CNT-COOH was investigated at pH in the range of 1–7. The experimental results, shown in Fig. 1 (next page), indicate that adsorption quickly increases at pH ranging from 1 to 4 and remains almost constant at higher pH values and removal of Sc(III) is quantitative.

The results obtained for experiments without CNT-COOH were presented also in Fig. 1. For pH values up to 3, there was a little or no precipitation but significant increase of scandium removal was observed in the pH range of 3–7. Precipitation of scandium hydroxide from our solution ( $0.11 \text{ mmol L}^{-1}$ ) is effective at  $\text{pH} = 4.77$  based on its  $K_{\text{sp}}$  value of  $2.22 \times 10^{-31}$ . Until  $\text{pH} = 3$  Sc(III) is the predominant species present in the solution and in the pH range of 4–9 it exists simultaneously as  $\text{Sc}(\text{OH})_2^+$ ,  $\text{Sc}(\text{OH})_3$  and  $\text{Sc}_2(\text{OH})_2^{4+}$ .

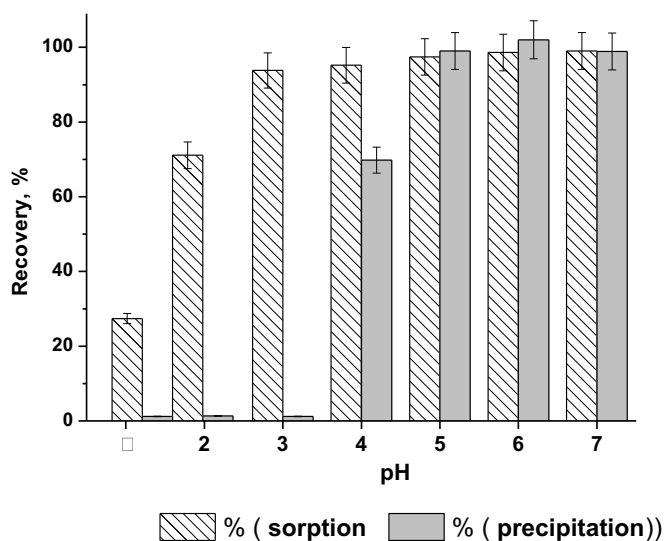


**Fig. 1** Effect of pH on the sorption and precipitation of Sc(III). Metal concentration  $5 \text{ mg L}^{-1}$ ; 50 mg of CNT-COOH.

The results of both series indicated that removal of Sc(III) in the pH range of 1–3 could be mainly attributed to its sorption on carbon nanotubes, while at  $\text{pH} > 4$  the results obtained in the presence of CNT-COOH overlap with the precipitation, indicating insignificance of adsorption. Therefore, further experiments were performed at  $\text{pH} = 3.0$ . It is the advantage in the view of application of CNT-COOH for separation of Sc(III) from heavy metal ions as they exhibit very low affinity for carbon nanotubes under these conditions [6].

### 3.3 Kinetic study

Results for kinetics showed that the adsorption rate rapidly increased during the first 10 min and then, as the number of surface sites for sorption comes down, gradually tended to equilibrium and adsorption of Sc(III) was over 95% during the first 2 min, which indicated that kinetics adsorption equilibrium was very fast.

In order to investigate mechanism of Sc(III) adsorption four different kinetic models were applied to test the experimental data. Estimated models and kinetic parameters are listed in Table 1 (next page). It can be concluded, that adsorption of Sc(III) follows pseudo-second order kinetic model and the mechanism of that process might be chemisorption. Furthermore, intra-particle diffusion model was used to investigate the contribution of intraparticle and film diffusions into adsorption process. The linear plot of experimental data to Weber-Morris equation shows early adsorption step up to 10 min the process is generally controlled by both factors. The subsequent adsorption step, characterized by lower slope, is mainly controlled by the film diffusion.

**Table 1**  
Parameters of various kinetic models fitted to experimental data.

Kinetic model	Equation	Parameters
Pseudo-first order kinetic	$\ln(q_e - q_t) = \ln q_e - k_1 t$	$k_1 = 0.0643 \text{ min}^{-1}$ $R^2 = 0.8488$
Pseudo-second order kinetic	$t/q_t = 1/k_2 q_e^2 + (1/q_e) t$	$k_2 = 0.032 \text{ g mg}^{-1} \text{ min}^{-1}$ $R^2 = 1.000$
Elovich equation	$q_t = \beta \ln(\alpha\beta) + \beta \ln t$	$\alpha = 4.4 \times 10^{92} \text{ mg g}^{-1} \text{ min}^{-1}$ $\beta = 0.0019 \text{ g mg}^{-1}$ $R^2 = 0.9785$
Intra-particle diffusion	$q_t = \theta + k_i t^{0.5}$	$k_i = 0.393 \text{ min}^{-1}$ $\theta = 0.3930$ $R^2 = 0.8845$

### 3.4 Adsorption studies

In order to describe Sc(III) adsorption behaviour on carbon nanotubes, the experimental data was analyzed by three isotherm models. The Freundlich model describes adsorption on heterogeneous surfaces and is represented by equation

$$q_e = K_F C_e^{-1/n} \quad (2)$$

where  $K_F$  and  $n$  are the Freundlich isotherm constants related to adsorption capacity and intensity, respectively.

The Langmuir model, which assumes monolayer coverage is described by the equation

$$q_e = q_{\max} K_L C_e (1 + K_L C_e)^{-1} \quad (3)$$

where  $q_{\max}$  and  $K_L$  are the maximum monolayers adsorption capacity and the adsorption energy related constant, respectively.

The Tempkin isotherm assumes that sorption energy decreases linearly with surface coverage and has been generally applied in the following form

$$q_e = RT/b \ln(A_T C_e) \quad (4)$$

where  $A_T$  is the Tempkin isotherm equilibrium constant,  $b$  is the Tempkin constant related to heat of sorption and  $T$  is the absolute temperature.

The adsorption data for Sc(III) a little better fit the Freundlich equation ( $R^2 = 0.9974$ ) than for Langmuir isotherm model ( $R^2 = 0.9881$ ) as well as Tempkin model ( $R^2 = 0.7476$ ) reflecting multilayer adsorption. Freundlich isotherm is often used for cases of heavy metal adsorption onto carbon materials [3].

## 4. Conclusions

CNT-COOH has high adsorption ability towards scandium ions for their preconcentration and removal from aqueous solutions. The multilayer adsorption of Sc(III) was observed at pH = 3.0. The adsorption kinetics onto carbon nanotubes was fast and the removal of Sc(III) was over 95% during the first 2 min. The obtained data were fitted using the pseudo-second order kinetic model and the film diffusion is the main controlling factor. As compared with other reported methods regarding the adsorption of Sc(III) on different solid materials, carbon nanotubes offer high adsorption capacity and fast sorption kinetics.

## References

- [1] Pyrzynska K., Kilian K., Pegier M.: Separation and purification of scandium: From industry to medicine. *Sep. Pur. Rev.*, in press, DOI: 10.1080/15422119.2018.1430589.
- [2] Pyrzynska K.: Use of nanomaterials in sample preparation. *Trends Anal. Chem.* **43** (2013), 100–108.
- [3] Abbas I.A., Al-Amer A.M., Laoui T., Al-Marri M.J., Nasser M.S., Khraisheh M., Atieh M.A.; Heavy metal removal from aqueous solution by advanced carbon nanotubes: Critical review of adsorption applications. *Sep. Purif. Technol.* **157** (2016), 141–161.
- [4] Jerez J., Isaguirre A.C., Bazan C., Martinez L.D., Cerutti S.: Determination of scandium in acid mine drainage by ICP OES with flow injection on-line preconcentration using oxidized multi-walled carbon nanotubes. *Talanta* **124** (2014), 89–94.
- [5] Pegier M., Kilian K., Pyrzynska K.: Enrichment of scandium by carbon nanotubes in the presence of calcium matrix. *Microchem. J.* **137** (2018) 371–375.
- [6] Stafiej A., Pyrzynska K.: Solid phase extraction of metal ions using carbon nanotubes. *Microchem. J.* **89** (2008), 29–33.

# Behavior and fate of pesticides during beer brewing

VLADIMÍRA JANDOVSKÁ<sup>a, b, \*</sup>, MARTIN DUŠEK<sup>b</sup>

<sup>a</sup> Department of Analytical Chemistry, Faculty of Science, Charles University, Hlavova 8/2030, 128 43 Prague 2, Czech Republic ✉ vl.jandovska@gmail.com

<sup>b</sup> Research Institute for Brewing and Malting, Prague PLC, Lípová 15, 120 44 Prague 2, Czech Republic

## Keywords

beer  
fate  
hops  
pesticide

## Abstract

The article deals with studying of the fate of 16 pesticides, commonly used to treat hops in Czech Republic during beer, brewing to estimate their risk of their carryover into beer. Organic hops were contaminated using pesticides in the level of 20 ppm and the beer was brewed with thus spiked hops on laboratory scale. The samples were taken after each stage of brewing for determination of pesticide residues and the analysis was carried out using by LC/HR-MS in positive and negative mode. The percentages of residues carryover into hopped wort and the percentages of decay reduction relative to the amount spiked on hops were calculated. The pesticide residues were divided into three groups, that characterized behavior of pesticides, among other things, based on their partition coefficients *n*-octanol-water ( $\log P$  values).

---

## 1. Introduction

Raw materials used for beer brewing are water, malt, hops and yeast. The quality of beer bases on the quality of these raw materials [1]. The hop, *Humulus lupulus*, is a poplin plant belong to the family *Cannabaceae*, whose female gender produces cones, strobiles. This hop cones contain compounds that are used in brewing for their aromatic and flavoring properties, especially as a bittering agent. The cost of hops is related to the yield per plant, because growers must combat bacterial diseases, fungus and mildew, virus diseases, as well as pests and parasitic invasion to produce a commodity that is both high in yield and quality with using pesticides [2].

And the main sources of pesticides in beer are hops and barley as well as. Pesticides are applied at many stages of barley cultivation and during post-harvest storage especially against microbial pathogens and insects, fungi and for weed control [1]. Malting process includes several stages, during some of them may occur to reduce of some pesticide residues, especially in the case of water-soluble residues during the steeping [3]. The hop belongs to agricultural crops with

intensive protection by pesticides. These compounds have prominent or potentially negative health effect [4] and they can persist in the crop for a long time. Based on that the maximum residue levels (MRLs) of pesticide residues were established for dried hops (but not for beer) and the control of these chemical agent and their residues became necessity. The aim of this work is answer the question: what is the fate of some commonly used pesticides during beer brewing?

## 2. Experimental

### 2.1 Chemical and material

Pesticide standards of abamectin, azoxystrobin, boscalid, cymoxanil, fenpyroximate, flonicamid, hexythiazox, imidacloprid, mandipropamid, metalaxyl, pyraclostrobin, quinoxyfen, spirotetramat, tebuconazole, thiamethoxam, trifluzazole and internal standard azoxystrobin-d4, thiamethoxam-d3, triphenyl phosphate (TPP) were purchased from Sigma Aldrich (St. Louis, MO, USA).

Standard and internal standard stocks solutions ( $1.0 \text{ gL}^{-1}$  for all) were prepared in acetonitrile or, in case of solubility problem, in methanol or acetone and stored at  $-20^\circ\text{C}$ . A standard mixture solution, with all 16 pesticides, was prepared in acetonitrile at  $1 \text{ mgL}^{-1}$  of each pesticide.

Acetone (99.9% purity), acetonitrile, methanol, formic acid, ammonium formate (LC-MS grade) were purchased from Sigma Aldrich (USA). Sodium chloride (analytical grade) was obtained from Lachner (Neratovice, Czech Republic) and magnesium sulfate (analytical grade) was obtained from Penta (Prague, Czech Republic). Sodium citrate tribasic dihydrate (99% purity), disodium hydrogen citrate sesquihydrate (99% purity) were purchased from Sigma-Aldrich (Germany). Pure water was obtained using by Milli-Q purification system (Merck-Millipore).

For beer brewing in laboratory scale a malt, organic hops (Saaz variety, Czech Republic, The Hop Research Institute Co.) and yeast (*Saccharomyces pastorianus*, RIMB 95, The Research Institute of Brewing and Malting, Prague PLC) were used.

### 2.2 Preparation hops spiked with pesticides

For spiking the organically grown, pesticide-free, dried hop cones were used. A 10 g portion of these ground hop cones were applied to Petri dish in thin layer and subsequently spiked by pesticide mixture contains 200  $\mu\text{g}$  of the each above pesticide. For spiking was used 100 ml glass bottle with spray head. After application of pesticides the bottle was added 3 ml of acetonitrile to rinse the rest of pesticides. Thus prepared hop sample was dried at room temperature overnight. Next day the hop sample was ground again.

**Table 1**Temperature program for infusion mashing (the rate of heating  $1\text{ }^{\circ}\text{C min}^{-1}$ ).

$t/^{\circ}\text{C}$	Heating time at the temperature/min	Process
50	20	Protein rest
62	30	Lower saccharification rest
71	20	Higher saccharification rest
78	20	Mash-off rest

### 2.3 Brewing beer with experimental prepared hops

Infusion mash was prepared using mashing device. Into each of 5 mashing beakers was mixed 73.5 g of ground malt with 400 mL of brewing water heated on  $44\text{ }^{\circ}\text{C}$ . The mashing device was controlled by a computer software with setup of temperature gradient showed in Table 1. During whole process the mash was mixing. Thus prepared mashes in beakers were cooled down on  $60\text{ }^{\circ}\text{C}$  and filtered by using a folder paper filter (type), which was in advance rinsed by hot water. The wort from the beakers were combined, the total volume of wort was approximately 1700 mL and the original gravity was established to  $12.25\text{ }^{\circ}\text{P}$ . After addition of 380 mL of brewing water, the original gravity of sweet wort was adjusted at  $10.04\text{ }^{\circ}\text{P}$ . Hopped wort was transferred into boiling flask (4 L) and heated under reflux, when the wort started to boil then 5 g (2.5 g per liter of sweet wort) of the spiked hop was added. Hopping of wort was carried out for 90 min. Subsequently, the hop wort was left at room temperature for 30 min with occasional rounded mixing to precipitating solid particular in cooled down wort. The cold wort was filtered by using folder filtration paper rinsed in advance with hot water. The spent hops were kept for further analysis. Clear hopped wort was cooled rapidly to  $15\text{ }^{\circ}\text{C}$ . Then 10 g of activated yeast in wort was added and the primary fermentation was concluded in a fermentation vessel with air access at  $12\text{ }^{\circ}\text{C}$  for 7 days. The process of maturing carried out in 2L tightly closed bottle at  $3\text{ }^{\circ}\text{C}$  for 6 weeks.

### 2.4 Sample preparation and extraction

Prepared samples for analysis can be divided to two groups: hop samples and liquid samples. Group of hop samples include spiked hops and spent hops, to liquid samples belong to hopped wort, green beer and finish beer. The spent hops were transferred on original filtration paper onto Petri dish and spread in thin layer. The dish was covered by a filtration paper and let dry at room temperature for two days. Dried spent hops were gently minced to crush lumps.

A 1 g portion of hops or spent hops samples was placed into a 50 mL centrifuge tube, 10 mL of water was added and the sample was mixed using vortex for 1 min and let to soak for next 30 min. Then 10 mL of acetonitrile and 50  $\mu\text{L}$  of internal

standard ( $1 \text{ mg L}^{-1}$ ) were added and the content was mixed by vortex for 1 min. Subsequently, the mixture of 4 g of anhydrous magnesium sulfate, 1 g of sodium chloride, 1 g trisodium citrate dehydrate, and 0.5 g disodium hydrogen citrate sesquihydrate were added, the tube was thoroughly capped and shaken vigorously by hand for 1 min. After 7 min of centrifugation at 4500 rpm 6 mL of upper acetonitrile layer was transferred to a 15mL centrifuge tube with 900 mg of magnesium sulfate. The tube was mixed for 30 s using vortex and centrifuged for 7 min at 4500 rpm. Finally, a 2 mL portion of the QuEChERS extracts were diluted with acetonitrile in 20mL volumetric flasks.

A volume of 10 mL of liquid samples were pipetted into 50ml centrifuge tube, 10 mL of acetonitrile were added, and the process of extraction was the same like in case of hops samples. Liquid samples were analyzed undiluted.

### *2.6 Standard addition method*

The method of standard addition was used for quantification of pesticides. Dilution extract (hop samples) of volume of 200  $\mu\text{L}$  was pipetted in four 2 mL vials for each sample. The standard solution ( $1 \text{ mg L}^{-1}$ ) was added to three of these vials at volume corresponding 50, 100 and 150% or original amount. The acetonitrile of the appropriate volume was added to make a final volume of 600  $\mu\text{L}$  in each vial. For analysis of liquid undiluted samples, the volume of 400  $\mu\text{L}$  was pipetted in four 2 mL vials for each sample and the standard solution was added in the same ration as the previous case.

### *2.6 Analysis using LC-MS/MS*

LC/HR-MS consisted of the chromatographic system Dionex UltiMate 3000 UHPLC (Thermo Scientific, Germany) included a binary pump HPG-3400RS, an autosampler WPS-3000TRS, a degasser SRD-3400 and a column over TCC-3000RS, and mass spectrometer Q Exactive hybrid quadrupole-orbitrap (Thermo Fisher Scientific Inc. Waltham, USA) with a heated electrospray ionization source (HESI II). TraceFinder software version 4.1 was used for evaluation of results.

Analytes were separated on a reverse-phase C18 Atlantis T3 column ( $2.1 \times 100 \text{ mm}$ ,  $3 \mu\text{m}$ ) (Waters Milford, USA) with corresponding guard C18 column SecurityGuard ULTRA (Phenomenex, Aschaffenburg, Germany). Separation was realized using by gradient elution: 0 min: 85% of solvent A + 15% of solvent B, 0.5 min: 85% A + 15% B, 9 min: 5% A + 95% B, 15 min: 95% A + 5% B with a flow rate of  $340 \mu\text{L min}^{-1}$ , when the solution 2 mM ammonium formate containing 0.1% formic acid in water was used as solvent A and methanol was used as solvent B. The column temperature was  $40^\circ\text{C}$  and injection volume was 2  $\mu\text{L}$ .

Ions were ionized in positive and negative electrospray ionization mode and the ion spray voltage was set at 2.8 kV and  $-2.5 \text{ kV}$ , respectively. The sheath gas flow was at 32 arbitrary units, the auxiliary gas flow rate was kept at 7 arbitrary units,

the capillary temperature was 295 °C and the auxiliary gas heater temperature was set at 295 °C. Nitrogen was used as sheath and auxiliary gas.

The mass spectrometer was generally operated in parallel reaction monitoring (PRM). The precursor ions from scheduled inclusion list were, within the retention time window  $\pm 0.3$  min, filtered in the quadrupole at isolation window (target  $m/z \pm 0.7$  amu), fragmented in HCD collision cell, product ions were collected in the C-trap at 17.500 resolution (FWHM, full width at half maximum, at  $m/z = 200$ ), AGC target value of  $2e5$ , and maximum ion injection time of 40 ms and finally two specific pairs of precursor-product ion transitions were monitored for each compound of interest. A mass tolerance of 5 ppm was employed. The instrument was externally calibrated prior to each measurement using the mixture of mass calibrants.

### 3. Results and discussion

The QuEChERS method used for extraction of pesticides from hop matrix was modified and validated [5]. The concentration of spiked pesticides was chosen to be  $20 \text{ mg kg}^{-1}$  to allow dilution to overcome matrix effects that are massive for this type of matrix. The amount of hop for hopping was modified to set up the pesticide residue concentration to  $35\text{--}40 \mu\text{g L}^{-1}$  of wort.

Analytes were quantified using by standard addition method.

The transfer rates (in percentages) of each pesticide determined in spent hops and hopped wort to the original residue concentration in the pesticide enriched hops were calculated (Table 2). All analytes were then sorted into three groups based on their behavior during the beer brewing: (group A) the carryover percentages into hopped wort against the amount in contaminated hop were at least 55%; (group B) pesticides remained in spent hop or that were extracted less than from 45%; (group C) pesticides which were not detected at all or were detected at trace level.

The results clearly showed that 90 min boil has a significant influence on amount of a few pesticides sorted into group A and B as well. These carryovers of pesticides could be relating to their partition coefficients between *n*-octanol and water ( $\log P$  values) [1, 6] and solubility in water. The results show that water soluble pesticides ( $\log P < 3$ ) were extracted at  $>70\%$  and pesticides that have low  $\log P$  value, being  $<2$ , were almost fully extracted from hops to hopped wort. Pesticides in group B were not extracted at all or only minimally ( $0.001 \text{ mg L}^{-1}$  for hexythiazox and quinoxifen in hopped wort), corresponding to their  $\log P$  value. Total amount of pesticides such as triflumizole (71%), was reduced more than about 50% due to unspecified thermal decomposition, pyrolysis, hydrolysis or/and adsorption onto insoluble components which represent the dominant and common reason for losses pesticides during hopping wort [7]. Percentages of these losses were calculated and are listed in Table 2 for each pesticide. The ability of pesticides to be carried over into hopped wort was expressed as residual ratio

**Table 2**

Concentration for each pesticide in spiked hops, spent hops, hopped wort, green beer and beer, and wort ( $R_w$ ) and residual ratio of pesticide in beer to the original residue concentration in hopped wort

Group	Compound	Concentration in hops/mg kg <sup>-1</sup>	Concentration in spent hops /mg kg <sup>-1</sup>	Transfer rate to spent hops /%	Concentration in hopped wort/%
A	Azoxystrobin	15.54	2.17	14	0.028
	Boscalid	15.16	4.28	28	0.025
	Flonicamid	12.35	<i>n.d.</i>	–	0.032
	Imidacloprid	15.86	0.51	3	0.037
	Mandipropamid	16.67	4.11	25	0.024
	Metalaxyl	16.31	0.54	3	0.043
	Tebuconazole	14.41	<i>n.d.</i>	–	0.024
	Thiamethoxam	13.70	<i>n.d.</i>	–	0.036
B	Abamectin B1A	12.54	5.81	46	<i>n.d.</i>
	Fenpyroximate	16.18	9.98	62	<i>n.d.</i>
	Hexythiazox	14.21	11.91	84	0.001
	Quinoxifen	14.41	9.47	66	0.001
C	Cymoxanil	13.04	<i>n.d.</i>	–	<i>n.d.</i>
	Pyraclostrobin	15.53	<i>n.d.</i>	–	<i>n.d.</i>
	Spirotetramat	18.76	<i>n.d.</i>	–	<i>n.d.</i>
	Triflumizole	6.65	1.11	17	0.002

( $R_w$ ; Table 2) and calculated on the basis of pesticide amount in hopped wort compared to the sum of amounts of the pesticide in spent hops and hopped wort. From the brewing trial conducted with pesticide spiked hops, the concentrations of pesticide residues were determined in hopped wort prior the addition of yeast, after seven days of fermentation and finally after 4 weeks of fermentation in tighten plastic bottle. All 8 pesticides carried over into hopped wort (group A) were found in green beer and remained in beer at various rates of initial to final concentration ( $R_b$  values; Table 2), which seemed to be also related to log  $P$  values of these pesticides. Results shows that pesticides with a log  $P$  values (<3) tended to remain in the final beer.

#### 4. Conclusions

In the study, a brewing trial simulated the preparation of a beer from pesticide spiked hops as in mass production scale. The results showed that half of the analyzed pesticides (group A) were carried over at an appreciable level. The pesticide residue transfer rates were calculated from hops to final beer for most analytes. The above results confirmed that the transfer rate of pesticide residues mainly depends on its octanol-water partition coefficient (log  $P$ ) and water solubility. If the pesticides log  $P$  values less than 3.75, they tended to be carried over to final beer. Otherwise, the high log  $P$  values (>4) of pesticides indicate that these pesticides such as fenpyroximate (log  $P$  = 5.01), quinoxifen (log  $P$  = 4.66), largely remained in spent hops. The list of 16 LC-amenable pesticides involved in

their log  $P$  and water solubility values. The calculated residual ratio of pesticide after hopping of after fermentation ( $R_b$ ), transfer rates (carryovers) and decomposition rate during wort hopping.

Transfer rate to hopped wort/%	Decomposition rate/%	Concentration in green beer /mg L <sup>-1</sup>	Concentration in beer /mg L <sup>-1</sup>	$R_w$ /%	$R_b$ /%	log $P$	Solubility in water /mg L <sup>-1</sup>
71	15	0.029	0.024	0.84	0.88	2.50	6.7
65	7	0.022	0.018	0.70	0.72	2.96	4.6
103	0	0.028	0.027	1	0.86	-0.24	5200
93	4	0.033	0.033	0.97	0.89	0.57	610
57	18	0.024	0.019	0.70	0.81	3.20	4.2
105	0	0.035	0.036	0.97	0.84	1.65	8400
68	32	0.017	0.018	1	0.75	3.70	36
105	0	0.033	0.032	1	0.89	-0.13	4100
-	54	<i>n.d.</i>	<i>n.d.</i>	-	-	4.40	<i>n.a.</i>
-	38	<i>n.d.</i>	<i>n.d.</i>	-	-	5.01	0.023
3	13	<i>n.d.</i>	<i>n.d.</i>	0.03	-	2.67	0.1
4	31	<i>n.d.</i>	<i>n.d.</i>	0.05	-	4.66	0.047
-	100	<i>n.d.</i>	<i>n.d.</i>	-	-	0.67	780
-	100	<i>n.d.</i>	<i>n.d.</i>	-	-	3.99	1.9
-	100	<i>n.d.</i>	<i>n.d.</i>	-	-	2.51	29.9
13	71	<i>n.d.</i>	<i>n.d.</i>	0.43	-	4.77	10.5

this study cover majority of commonly used pesticides for treatment hop plants in Czech Republic. Based on the data gathered from the measurements shown in Table 2, the carryover of pesticide residues found on commercially treated hops can be easily estimated.

### Acknowledgments

This study was supported by the project of Ministry of Education Youth and Sports of the Czech Republic No. LO 1312.

### References

- [1] Navarro S., Pérez G., Navarro G., Vela N.: Decline of pesticide residues from barley to malt. *Food Addit. Contam.* **28** (2007), 851–859.
- [2] Hengel M.J., Miller M.: Analysis of pesticides in dried hops by liquid chromatography-tandem mass spectrometry. *J. Agric. Food Chem.* **56** (2008), 6851–6856.
- [3] Miyake Y., Hashimoto, K., Matsuki, H., Ono M., Tajima R: Fate of insecticide and fungicide residues on barley during storage and malting. *J. Am. Soc. Brew. Chem.* **60** (2002), 110–115.
- [4] Fantke P., Friedrich R., Jolliet O.: Health impact and damage cost assessment of pesticides in Europe. *Environ. Int.* **49** (2012), 9–17.
- [5] Dušek M., Jandovská V., Olšovská J.: Analysis of multiresidue pesticides in dried hops by LC-MS/MS using QuEChERS extraction together with dSPE clean-up. *J. I. Brewing*, in press, DOI: 10.1002/jib.490.
- [6] Miyake Y., Tajima R.: Fate of pesticide metabolites on malt during brewing. *J. Am. Soc. Brew. Chem.* **61** (2003), 33–36.
- [7] Inoue T., Nagatomi Y., Suga K., Uyama A., Mochizuki N.: Fate of pesticides during beer brewing. *J. Agric. Food Chem.* **59** (2011), 3857–3868.

# Design of Experiment approach for lipid extraction optimisation in lipidomics

INAL BAKHYTKYZY \*, WERONIKA HEWELT-BELKA, AGATA KOT-WASIK

*Department of Analytical Chemistry, Faculty of Chemistry, Gdansk University of Technology, 11/12 Narutowicza St., 80-233 Gdansk, Poland ✉ inbakh@gmail.com*

## Keywords

Design of Experiment  
lipidomics  
lipid extraction

## Abstract

Lipidomics is a lipid targeted metabolomics approach that aims at comprehensive analysis of lipids in given sample. Lipids are structurally and functionally diverse group of small molecules that play multiple important roles in biological systems. The large diversity in structure and function of lipids makes it a huge challenge to develop a comprehensive lipid extraction method. In the study, an optimization of lipid extraction method based on Design of Experiments has been described. A two level full-factorial experimental design was used as a multivariate strategy for the evaluation of the effects of varying several variables at once. The effects of four different variables elution solvent, ratio of stationary phase, extraction and elution vortexing time, on the number of extracted molecular features have been investigated. From these studies, certain variables showed up as significant.

---

## 1. Introduction

Lipidomics is a part of “omics” science that allows to study the biochemical and molecular characterisation of lipids present in a given biological system, fluid, cell or tissue [1], and lipid changes that were induced by some factors [2–3]. Lipids are a large number of structurally and functionally diverse molecular species that cover a broad range of polarity, from non-polar (e.g., triacylglycerides) to polar (e.g., phospholipids) [4–5]. In a biological sample, lipids sometimes are present in significantly ranging levels, from femtomole level up to micromole level [6]. These differences in lipid structures and levels of presence in biological sample introduce considerable challenges to complete efficient lipidome extraction. Careful sample preparation is a critical step in analytical chemistry to generate sample for a chemical measurement accurately. It is critical to develop sample preparation methods for lipidomics that are reproducible, fast, and enables extraction of a wide range of analytes with different polarities and concentration [7].

Conventional methods of optimising a process require varying one parameter per trial [8]. This approach is very time-consuming [9–10]. Taking into account the vast number of parameters that can affect a successful lipid extraction, it is

clear that the implementation of Design of Experiment approach is needed to be economical, by saving time and money on chemicals.

The important features of designing an experiment using statistical tools are to be time effective, enhance capability, and increase process feasibility. The main intent of using Design of Experiment in this work is to simultaneously examine the various factors affecting the lipid extraction efficiency. This approach helps to eliminate the less significant factors and focus on optimising only the most important ones. The full factorial design is a commonly used two-level design. It is described as  $2^k$  design where 2 stands for the number of factor levels and  $k$  is the number of factors, each with a low and high value [12].

The goal of this research is to optimise human breast milk lipid extraction process using Factorial Design. Human breast milk is used as a model biological matrix because it is complex and contains lipid classes with considerable difference in abundance and chemical structure.

## 2. Experimental

### 2.1 Reagents and chemicals

LC-MS grade methanol, HPLC grade hexane were purchased from Merck (Germany), 2-propanol and ammonium formate (99.9% purity) were purchased from Sigma-Aldrich (USA). Deionized water was purified by an HLP5 system (Hydro-lab, Poland).

### 2.2 Experimental design

Four variables affecting the extraction efficiency were selected to define the experimental domain. These variables were:

1. elution solvent,
2. stationary phase ratio (HybridSPE-Phospholipid and C18 both from (Sigma-Aldrich, USA)),
3. extraction time,
4. elution time.

Four variables at 2 levels give  $2^4$  full factorial design. The total number of experiments including replicates and one control sample for each set was 48. The variables considered, the code used, the low and high levels studied, and responses are shown in Table 1 (next page).

### 2.3 Samples and sample treatment

The pooled sample, which was prepared by mixing 150  $\mu\text{L}$  of previously collected ( $n=71$ ) human breast milk samples, was used for lipid extraction method development and optimization using factorial design. Milk samples were stored in polypropylene tube at  $-80\text{ }^\circ\text{C}$  prior to analysis.

**Table 1**

Experimental variables, levels, design matrix, and responses in the 2<sup>4</sup> fractional factorial design for lipid extraction from human breast milk.

Variable	Coded	Level	
		Low (-)	High (+)
elution solvent, methanol:2-propanol:NH <sub>3</sub>	X <sub>1</sub>	81:14:5 (v/v/v)	14:81:5 (v/v/v)
stationary phase ratio	X <sub>2</sub>	9:1 (w/w)	1:9 (w/w)
extraction vortex time	X <sub>3</sub>	1 min	5 min
elution vortex time	X <sub>4</sub>	1 min	5 min

Run	X <sub>1</sub>	X <sub>2</sub>	X <sub>3</sub>	X <sub>4</sub>	Number of molecular features
1	-	-	-	-	415
2	+	-	-	-	531
3	-	+	-	-	439
4	+	+	-	-	732
5	-	-	+	-	388
6	+	-	+	-	604
7	-	+	+	-	431
8	+	+	+	-	777
9	-	-	-	+	415
10	+	-	-	+	579
11	-	+	-	+	413
12	+	+	-	+	749
13	-	-	+	+	368
14	+	-	+	+	578
15	-	+	+	+	422
16	+	+	+	+	782

Sample preparation was based on the extraction of lipids contained in human breast milk with the use of Solid Phase Dispersive Extraction technique. First, 30 mg of an appropriate stationary phase was weighed in 1.7 mL Eppendorf microtubes (VWR International, Poland). Protein precipitation was done as follows: 100 µL of human breast milk sample was transferred to 15 mL polypropylene tube and mixed with 900 µL of 1% formic acid in methanol. After vortexing for 30s, sample was centrifuged for 5 min at 10 000 rpm. 900 µL of supernatant was transferred to the Eppendorf microtubes and vortexed. After the stationary phase was precipitated, the supernatant was carefully discarded using Glass Pasteur Pipette (150 mm, VWR International, Gdansk, Poland). Then, 1000 µL of elution solvent was added to the stationary phase and vortexed. The supernatant was carefully collected using a syringe with needle (1 mL, Terumo, Laguna Technopark, Binan, Laguna, Philippines), filtrated and analysed.

## 2.4 Instrumentation

The HPLC system used was an Agilent 1290 LC system equipped with a binary pump, an online degasser, an autosampler and thermostated column

compartment coupled to a 6540 Q-TOF-MS with a dual electrospray ionization (ESI) source (Agilent Technologies, USA).

The chromatographic separation method was previously developed in our group and described in an article which is still in press. Briefly, the separation was carried out by using an Agilent Poroshell 120 EC-C8, (150×2.1 mm I.D., 1.9 μm particle size) column with 0.2 μm in-line filter. The elution program was generated with a mixture of 5 mM ammonium formate in water and methanol (1:4, v/v) (component A) and a mixture of 5 mM ammonium formate in water, *n*-hexane and 2-propanol (1:20:79, v/v/v) (component B) as follows: 0 to 15 min, B (%) 10 to 50 (lineal increase); 15 to 20 min, B (%) 50 to 100 (lineal increase). Subsequently, column was washed for 0.5 min at 100% B and the gradient returned to starting conditions and system was re-equilibrated for 10 min. The flow rate was 0.5 mL min<sup>-1</sup> and the injection volume was 0.5 μL. The column was kept at constant temperature of 45 °C. Data were acquired in ESI+ (SCAN) mode in the range from 200 to 1700 *m/z* in the high-resolution mode (4 GHz). The ESI source condition applied was optimized earlier and described in detail elsewhere [11].

### 2.5 Data Analysis

The TIC chromatograms were first visually examined to detect any retention time shift. Then, data processing was done using molecular feature extraction option in MassHunter Workstation Software Qualitative Analysis, B.03.01 version (Agilent Technologies, USA). Parameters for the molecular feature extract were as follows: extraction algorithm, small molecule; input data range, restricted retention time 0.90–20.00 min, restricted *m/z* = 200–1700; peak filters; peak with height ≥ 1000, ion species, + H, -H; peak spacing tolerance 0.0025 *m/z* plus 7.0 ppm; isotope model, common organic molecules charge state, 2. molecular feature extract resulted in a list of all molecular entities, which included the full TOF mass spectral data for each sample.

Identification of lipids compounds was performed by comparing the mass accuracy of obtained MF against online database - LipidMAPS. Mass error was set to 5 ppm.

## 3. Results and discussion

We applied screening factorial design to evaluate the factors (variables) influencing lipid extraction efficiency. The factors considered in this study were: elution solvent, stationary phase ratio, extraction time, elution time. The variables were chosen according to their importance in extraction process. Number of molecular feature was used as response.

Obtained results of molecular features for each experimental setup are presented in the last column of Table 1. The highest number of molecular features were observed in experimental runs 4, 8, 12 and 16. In these experimental setups

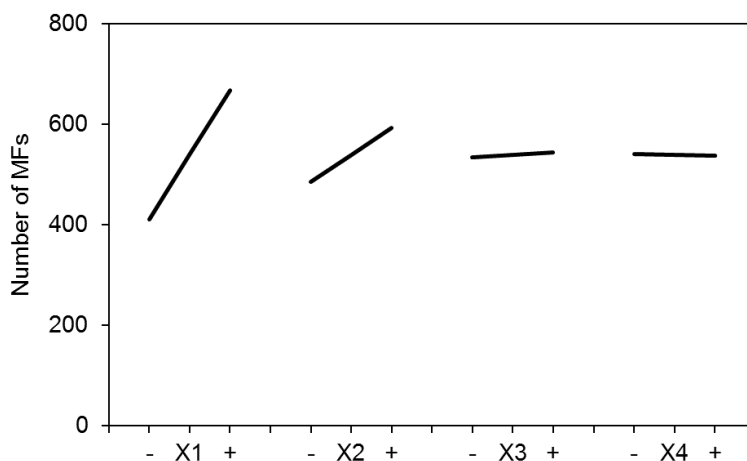


Fig. 1 Main Effects Plot.

$X_1$  and  $X_2$  variables were at the same level, whereas  $X_3$  and  $X_4$  were different. It can be assumed that vortexing time ( $X_3$  and  $X_4$ ) did not influence the number of extracted molecular features. To check the effect of individual factors on the number of extracted molecular features, the main effect ( $ME$ ) of each factor was calculated using equation

$$ME = \frac{\sum_{i=1}^n N_+}{n} - \frac{\sum_{i=1}^n N_-}{n} \quad (1)$$

Fig.1 displays the main effects plot. The slope of the line is proportional to the size of the effect, and it confirms that vortexing time did not influence the number of extracted number of molecular features. Elution solvent and stationary phase ratio positively influenced the number of molecular features. These parameters can be further considered in the optimization design, to obtain optimum conditions.

#### 4. Conclusions

Factorial design is a fast and universal tool for evaluating the significance of a given parameter towards observed response. As could be shown, elution solvent and stationary phase ratio had more impact on the number of extracted molecular features in this extraction method and should be considered during the further optimization designs.

## References

- [1] Navas-Iglesias N., Carrasco-Pancorbo A., Cuadros-Rodríguez L.: From lipids analysis towards lipidomics, a new challenge for the analytical chemistry of the 21st century. Part II: Analytical lipidomics. *TrAC Trends Anal. Chem.* **28** (2009), 393–403.
- [2] Zhao Y.Y., Vaziri N.D., Lin R.C.: Lipidomics: New insight into kidney disease. In: *Advances in Clinical Chemistry*. Makowski G.S. (edit.). Elsevier 2015, p. 153–175.
- [3] Hu C., van der Heijden R., Wang M., van der Greef J., Hankemeier T., Xu G.: Analytical strategies in lipidomics and applications in disease biomarker discovery. *J. Chromatogr. B* **877** (2009), 2836–2846.
- [4] Lam S.M., Shui G.: Lipidomics as a principal tool for advancing biomedical research. *J. Genet. Genomics* **40** (2013), 375–390.
- [5] Sandra K., Sandra P.: Lipidomics from an analytical perspective. *Curr. Opin. Chem. Biol.* **17** (2013), 847–853.
- [6] Quehenberger O., Armando A.M., Brown A.H., Milne S.B., Myers D.S., Merrill A.H., Bandyopadhyay S., Jones K.N., Kelly S., Shaner R.L., Sullards C.M., Wang E., Murphy R.C., Barkley R.M., Leiker T.J., Raetz C.R., Guan Z., Laird G.M., Six D.A., Russell D.W., McDonald J.G., Subramaniam S., Fahy E., Dennis E.A.: Lipidomics reveals a remarkable diversity of lipids in human plasma. *J. Lipid Res.* **51** (2010), 3299–3305.
- [7] Cajka T., Fiehn O.: Comprehensive analysis of lipids in biological systems by liquid chromatography-mass spectrometry. *TrAC Trends Anal. Chem.* **61** (2014), 192–206.
- [8] Dejaegher B., Heyden Y. Vander: Experimental designs and their recent advances in set-up, data interpretation, and analytical applications. *J. Pharm. Biomed. Anal.* **56** (2011), 141–158.
- [9] Kalil S.J., Maugeri F., Rodrigues M.I.: Response surface analysis and simulation as a tool for bioprocess design and optimization. *Process Biochem.* **35** (2000), 539–550.
- [10] Vander Heyden Y., Perrin C., Massart D.L.: Optimization strategies for HPLC and CZE. In: *Handbook of Analytical Separations*. Valko K. (edit.). Elsevier 2000, p. 163–212.
- [11] Garwolińska D., Hewelt-Belka W., Namieśnik J., Kot-Wasik A.: Rapid characterization of the human breast milk lipidome using a solid-phase microextraction and liquid chromatography-mass spectrometry-based approach. *J. Proteome Res.* **16** (2017), 3200–3208.
- [12] Quinn G.P., Keough M.J.: *Experimental Design and Data Analysis for Biologists*. New York, Cambridge University Press 2002.

# Release of active substances from polymeric coatings in medical applications

MAŁGORZATA BOROWSKA<sup>a,\*</sup>, AGATA KOT-WASIK<sup>a</sup>, JUSTYNA KUCIŃSKA-LIPKA<sup>b</sup>

<sup>a</sup> *Department of Analytical Chemistry, Faculty of Chemistry, Gdańsk University of Technology, 11/12 Gabriela Narutowicza Street, 80-233 Gdańsk, Poland ✉ malborow@student.pg.edu.pl*

<sup>b</sup> *Department of Polymer Technology, Faculty of Chemistry, Gdańsk University of Technology, 11/12 Gabriela Narutowicza Street, 80-233 Gdańsk, Poland*

## Keywords

antimicrobial coatings  
catheterization  
urinary catheters  
urinary tract infections

## Abstract

Catheter-associated urinary tract infections are the result of catheterization of the bladder. The risk of infection increases with lengthening time required for catheterization. Bacterial cells can to adhere and create the biofilm on the surface of catheter materials. Microbes that are the integral part of the biofilm show greater resistance to agents used for their degradation. The treatment of urinary tract infections are associated with require the oral administration of large amounts of antimicrobial drugs. An alternative may be the use of antimicrobial release coatings on the surface of catheters. These coatings can to allow target drug delivery and contribute to reducing the dose and improving a drug availability. HPLC-MS system is a very good solution to analysis of release the drug from antimicrobial coatings and it is used in this studies.

---

## 1. Introduction

Urinary catheters are used when the natural urinary output is hindered. One of the indication for catheterization of the urinary bladder is an accurate assessment of the amount of urine output. Catheterization is given to patients undergoing some surgical procedures. Another indication for catheterization is the state of urinary retention occurring involve in bladder inflammation. Catheters are used after urological procedures to heal the urinary tract, when it is necessary. The most frequently complication reported after catheterization are urinary tract infections [1]. Urinary tract infections are the most common infections associated with healthcare and constitute about 40% of all infections in hospitalized patients. Catheter-associated urinary tract infections) are 80% of urinary tract infections and are result from the presence of catheters in the urinary tract [2].

Catheterization may contribute to the disruption of the natural defense system of the urinary tract and can allowing the colonization of bacteria, leading to the creation of biofilms and the development of infections. Microbes have the ability to adhere and create a biofilm on the surface of the catheters materials. It is

importance when the catheters are placed in body for a long time [3]. The risk of developing urinary tract infections is directly proportional to the length of stay of the catheter in the urinary tract. Short-term catheterization (less than 7 days) is the cause of infections in almost 50% of patients. For patients undergoing long-term catheterization (up to 28 days), the risk of infection increases to 100% [2].

Bacteria's biofilm provides protection for the bacteria against antimicrobial agents, antibodies and defences of the human body. It is a serious problem because bacterial cells that are an integral part of biofilm are up to 1000-fold more resistant to antimicrobial agents compared to planktonic form of bacteria [4]. In addition catheter colonized by microbes must be replaced resulting in increased morbidity for the patient and increased cost to the healthcare system [3].

From a prevention urinary tract infections standpoint, the most important aspect are develop catheters with materials that prevent microorganism attachment and biofilm formation [3]. The most effective choice seems to coating of catheter surface with antimicrobial agents or polymer coating loaded with antimicrobial agents [4]. The polymer coating should be degradable, so that during the implementation gradually release the drug substances.

The aim of this study was to prepare antimicrobial coatings from polyvinylpyrrolidone (PVP) with clindamycin which were choose like polymer to prepare the coatings and antimicrobial agent, respectively. Antimicrobial activity of PVP-clindamycin coatings were tested against *Staphylococcus aureus* (Gram-positive bacteria) which is the microorganism most frequently involved in catheter-related infections [3].

## 2. Experimental

### 2.1 Chemicals and reagents

Polyvinylpyrrolidone was purchased from Sigma-Aldrich (USA). Clindamycin was purchased from Pfizer (USA) in form of tablets labeled to contain 300 mg clindamycin per tablet. Saline solution (0.9%) was purchased from Polpharma (Poland). Acetonitrile (HPLC grade) and formic acid (>98%) were purchased from Merck (Germany). Acetonitrile (LC-MS grade) was purchased from VWR Chemicals (USA). Ultrapure water was prepared using HPL5 system from Hydrolab (Poland).

### 2.2 Sample preparation

PVP coatings were prepared by dissolving the appropriate amount of polymer in deionized water. These solutions consisted 1, 3, 5 and 7% of PVP, respectively. After the dissolution of the entire PVP (using mixing and heating), the solutions were poured into Petri dishes for drying. The coating with the best properties was then selected and shells were prepared with the addition of clindamycin, respectively, 1, 3, 5% for the selected concentration of PVP.

### 2.3 Characterization of PVP coatings

Coatings with different PVP concentrations were observed using Optical Microscopy from company Bresser to assess their homogeneity. The degradation of coatings after the impact of 0.9% NaCl was also tested.

### 2.4 Chromatography and mass spectrometry

An Agilent G1379B LC system consisted with binary pump, an on-line degasser, an autosampler and a thermostated column compartment coupled with 1100 Series LC/MSD. Purospher® STAR RP-C18e (125×3 mm, 5 μm; Merck, Germany) column was used during analysis. The flow rate was 1 mL min<sup>-1</sup>, injection volume was 5 μL, column temperature was 30°C. The mobile phase gradient was 0–2 min: 15.0% B, 2–4 min: increase of eluent B to 30.0%, 4–6.5 min: 30.0% B and between 6.5 and 6.6 min change to start conditions (15.0% B), where A was water and B was acetonitrile, both of solvents included of 0.1% formic acid addition. The ESI source was operated with positive ion mode. The fragmentator voltage was set at 80 eV. Nebulizer gas was set at 35 psi and drying gas temperature was set at 300 °C.

### 2.5 Clindamycin release studies

Drug release studies were conducted for the clindamycin modified coatings (5% addition of clindamycin in coatings). The prepared coatings were cut into squares (5×5 mm) and were weighted. In the next stage, the prepared samples were placed in 0.9% NaCl solution for 15, 30 and 60 minutes, respectively. After a predetermined time, a sample solution was taken and tested by HPLC-MS (procedure 2.4).

### 2.6 Microbiology

Antibacterial activities of clindamycin-PVP based coatings (3% PVP coatings with 1, 3 and 5% addition of clindamycin) were evaluated against *Staphylococcus aureus*, Gram-positive bacteria, using disk agar diffusion method. The bacterial cells were refreshed by growing in Luria-Bertani broth medium (10 g NaCl, 10 g peptone, and 5 g yeast extract per liter of distilled water), and incubated at 37 °C for 24 h. Then, the bacterial cultures were diluted 10-fold using Luria-Bertani medium, and 0.1 mL of the bacterial suspensions were spread over the Luria-Bertani agar plates and incubated at 37 °C for 24 h. The polymeric coatings were cut, sterilized with 70% ethanol and followed by drying under UV lamp (30 min). The coatings were gently placed on the agar plates using forceps, and the plates were incubated at 37 °C for 24 h. After incubation, zones of inhibition of bacterial growth were observed.

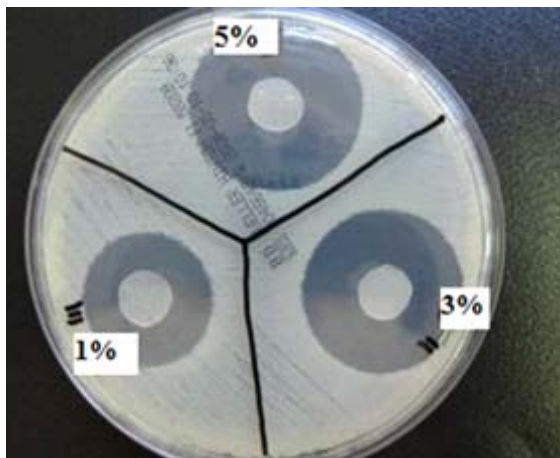


**Fig. 1** The growth inhibition zones of *Staphylococcus aureus* subjected to interaction with antimicrobial coating containing 1, 3 and 5% of clindamycin.

### 3. Results and discussion

#### 3.1 Characterization of PVP coatings

Polymeric coatings containing 1, 3, 5 and 7% of PVP were prepared. In the case of 1 and 3% of PVP coatings, a homogeneous structure was observed while for 5 and 7% amount of PVP in coatings, homogeneity was not obtained. The coating containing 1% PVP turned out to be brittle and unstable in contact with 0.9% NaCl (too fast solubility), which means that it cannot be used in next studies. The remaining coatings (3, 5, 7%) showed good flexibility and sufficient durability. Degradation of these three coatings were slower. In this step coating which include 3% of PVP was choose to prepare coatings with addition of clindamycin.

#### 3.2 Microbiology test

Polymeric coatings containing 3% of PVP and different amount of clindamycin (1, 3, 5%) subjected to interaction with the *Staphylococcus aureus* bacterial strain. The growth inhibition zones of this bacteria are shown in Fig. 1.

Based on the drawing, it is easy to notice that the higher the concentration of antibiotic in the coating, that the growth inhibition of *Staphylococcus aureus* increases. But for 5% of drug amount the inhibition zone is not very much bigger than to 3% containing of clindamycin.

#### 3.3 Clindamycin release from antimicrobial coatings

The analysis of the clindamycin release rate from coatings containing 3% of PVP was carried out at various time intervals (15, 30, 60 min). This is the time from placing the antimicrobial coating fragment in saline solution to take a sample of the solution for analysis by HPLC-MS. The release profile of clindamycin from coatings was defined as the dissolution of PVP with the simultaneous release of

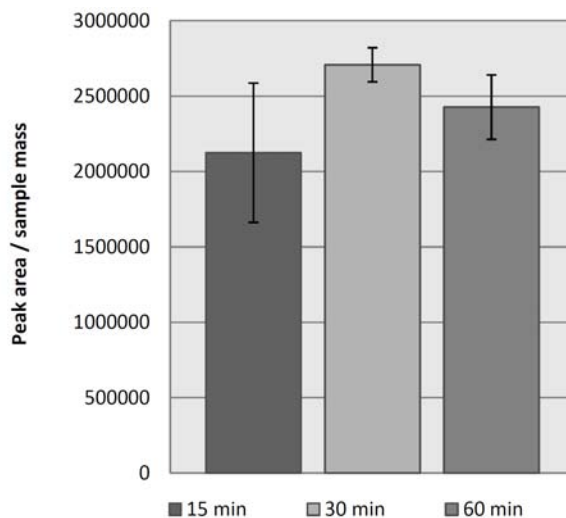


**Fig. 2** Release of clindamycin from polyvinylpyrrolidone-based coatings.

clindamycin at three different time intervals (15, 30, 60 min). The results are shown in Fig. 2 and are presented as the ratio of the peak area to the mass coating immersed in the solution as a function of time.

Release of clindamycin from PVP coatings was occurred immediately. After the first time interval (15 min) was eluted approximately 80% of clindamycin. After 30 minutes was observed maximally concentration of drug in saline solution. After the third point of time (60 min) approximately 90% of clindamycin was released from coating.

At the beginning, release of clindamycin from PVP-based coatings happens quickly and reaches maximum concentration after just 30 minutes. Then there is a slow decrease in the concentration of drug in saline solution. That mechanism releasing of clindamycin can provide a quick counteracting the growth of bacteria. It may help to reduced the risk of infection. In addition, the use of antimicrobial coatings should contribute to the immediate release of antimicrobial agents through targeted delivery and maintenance of high concentrations for a long time.

#### 4. Conclusions

The conducted study proved that the PVP can be used as drug eluting coating. This polymer facilitates quick release of the antimicrobial agent, like clindamycin. Coatings made based on the 3% content of PVP containing antimicrobial drug can be used in medical applications. PVP-clindamycin based coatings prepared in this studies show growth inhibition for *Staphylococcus aureus*. The possibility of using PVP as a catheter's coating will be tested in the next studies.

## References

- [1] Warren J.W.: Catheter-associated urinary tract infections. *Int. J. Antimicrob. Agents* **17** (2001), 299–303.
- [2] Dohnt K., Sauer M., Müller M., Atallah K., Weidemann M., Gronemeyer P., Rasch D., Tielen P., Krull R.: An in vitro urinary tract catheter system to investigate biofilm development in catheter-associated urinary tract infections. *J. Microbial. Methods* **87** (2011), 302–308.
- [3] Kowalczuk D., Ginalska G., Golus J.: Characterization of the developed antimicrobial urological catheters. *Int. J. Pharm.* **402** (2010), 175–183.
- [4] Dayyoub E., Frant M., Pinnapireddy S. R., Liefeyth K., Bakowsky U.: Antibacterial and anti-encrustation biodegradable polymer coating for urinary catheter. *Int. J. Pharm.* **531** (2017), 205–214.

# Multi-criteria decision analysis for selection of the best procedure for PAHs determination in smoked food

MARTA BYSTRZANOWSKA\*, MAREK TOBISZEWSKI

*Department of Analytical Chemistry, Chemical Faculty, Gdańsk University of Technology,  
G. Narutowicza St., 80-233 Gdańsk, Poland ✉ marbystr@student.pg.edu.pl*

## Keywords

green analytical  
chemistry  
Multi-Criteria Decision  
Analysis  
PROMETHEE  
smoked meat

## Abstract

Making a proper decision in multifacitated situation is very challenging task. Especially, if there are many alternatives and criteria, even contradictory ones. The support tools may be application of Multi-Criteria Decision Analysis methods. In this study the application of PROMETHEE (Preference Ranking Organization Method for Enrichment Evaluations) as one of Multi-Criteria Decision Analysis method in selection of the most preferable analytical procedure for polycyclic aromatic hydrocarbons determination in smoked products is presented.

---

## 1. Introduction

The most common analysts' considerations involve the selection of appropriate methods of sample preparation, reagents, analytical techniques, and conditions for analytical determination. Unfortunately, there is a huge number of alternatives, thus making a proper decision is not an easy task. It is necessary to know the decision problem, the need and purpose of the analysis, as well as the criteria of the decision and the available alternatives. It is a difficult task to judge clearly, which of the analytical procedures is the best in a given case. In this situation the application of Multi-Criteria Decision Analysis methods may be a useful and desirable solution. These tools allow describing a given problem using numerical values, and enable to obtain final results also as numerical values. The scores are presented in a form of a full ranking of available options, which allows selecting objectively the best alternative. Moreover, the decision is made in a systematic way. Detailed information about Multi-Criteria Decision Analysis usage in area of chemical sciences, especially analytical chemistry may be found in [1].

One of the most popular tools is PROMETHEE (Preference Ranking Organization Method for Enrichment Evaluations). In this work selection of the most preferable analytical procedure for polycyclic aromatic hydrocarbons (PAHs) determination in smoked products using PROMETHEE is presented and discussed.

## 2. Experimental

### 2.1 Polycyclic aromatic hydrocarbons in smoked products

Polycyclic aromatic hydrocarbons are a large class of organic compounds that are composed of two or more fused aromatic rings [2]. Mainly they are formed through incomplete combustion or pyrolysis of organic matter and during various industrial processes. Additionally PAHs are also formed during food preparation methods such as grilling, roasting and smoking. In Europe about 15% of fish products for consumption are prepared using smoking process [3]. In food industry mostly benzo[*a*]pyrene is controlled as a marker of the carcinogenic PAHs in food with maximum limits in certain foods in the EU [4]. Analytical procedures may involve variety of sample preparation techniques, for instance Soxhlet extraction, solid-phase extraction, and liquid–liquid extraction, pressurized liquid extraction and QuEChERS, etc. [5]. Therefore, which of the analytical procedures is the best for this given purpose?

### 2.2 Components of Multi-Criteria Decision Analysis

#### 2.2.1 Main goal of analysis

Main aim of the analysis is finding the greenest analytical procedure for PAHs determination in smoked products such as meat and fish. Analysis includes assessment only for benzo[*a*]pyrene, as a marker of carcinogenic PAHs in food. In case of analytical procedure consideration, also metrological factors have to be satisfactory but mainly environmental factors are considered.

#### 2.2.2 Criteria of assessment

In Multi-Criteria Decision Analysis methods criteria are factors that are allow to make an evaluation of a given problem, and describe alternatives. Technical evaluation of analytical procedure involve limit of detection (*LOD*) and precision, expressed as relative standard deviation (*RSD*). Criteria as amount of sample, total time needed to perform analysis and number of procedural steps are involved. The information on reagents are designate in a reference to Analytical Eco-Scale approach [6]. On the other hand, solvents evaluation is based on calculations proposed by Tobiszewski and Namieśnik [7]. Criteria with preferences functions are *LOD*, *RSD*, Amount of sample, Time of analysis, Score for solvents, Score for other reagents, Number of procedural steps, all with preference function “the lower the better”. It is possible to differentiate the importance of criteria by assessing appropriate weight values to all criteria. In this particular case study we assumed that all criteria influence similarly on the main goal.

**Table 1**Analytical procedures of benzo[*a*]pyrene determination in smoked meat and fish.

Number	Matrix	Abbreviation	Ref.
1	Smoked fish	ASE-GC-MS	[8]
2	Cold-smoked fish (mackerel)	LLE-GC-MS	[9]
3	Cold-smoked fish (salmon)	LLE-HPLC-FLD	[10]
4	Smoked meat	SPE-GC-FID	[11]
5	Smoked meat	MAE-RP-HPLC-FLD	[12]
6	Smoked fish	MAE-DLLME-GC-MS	[13]
7	Smoke-cured fish products	Sox.-GC-MS	[14]

### 2.2.3 Alternatives

Alternatives are the subject of considerations. They represent possible analytical procedures that may reach the stated goal. Proposed analytical procedures for PAHs determination in smoked products are summarized in Table 1.

### 2.3 PROMETHEE analysis

All the data values are taken directly or indirectly from indicated above scientific papers (Table 1.). Indirectly means, that some of them are calculated into numerical values. The set of data prepared for PROMETHEE analysis consists of alternatives described by criteria. In this work PROMETHEE algorithm is used as commercial computer software - VisualPROMETHEE software.

## 3. Results and discussion

For PAHs determination in smoked fish and meat, all introduced criteria are define as being equally important. With such assumptions, it is possible to obtain result as a complete ranking of alternatives, what is presented in Table 2. Phi presented in Table 2 is a balance between the positive and negative preference flows and it includes both of them and presents as a single score. As it is presented, the best

**Table 2**

Final results of PROMETHEE analysis.

Rank	Alternatives	Number (cf. Table 1)	Phi
1	MAE-RP-HPLC-FLD	5	0.6190
2	ASE-GC-MS	1	0.1905
3	MAE-DLLME-GC-MS	6	0.0714
4	LLE-HPLC-FLD	3	0.0000
5	LLE-GC-MS	2	-0.0714
6	SPE-GC-FID	4	-0.3571
7	Soxhlet-GC-MS	7	-0.4524

analytical procedure for PAHs determination in smoked meat and fish is technique based on high performance liquid chromatography with spectrofluorometric detection, preceded by microwave-assisted extraction. MAE-RP-HPLC-FLD procedure is characterized by the most desired criteria's values in response to other alternatives. On the other hand, the worst analytical procedures are Soxhlet-GC-MS and SPE-GC-FID. Their low positions in the ranking are due to high score for solvents. Thus, highly toxic and hazardous solvents are used, involving their huge amounts. In procedure with Soxhlet extraction as a pre-treatment over 300 mL of dichloromethane is used. Moreover, Soxhlet-GC-MS is characterized by the highest value for limit of detection, what is not desired.

#### 4. Conclusions

Many chemical decision problems are complex and are characterized by interdisciplinary nature. Thus there is a need of comprehensive assessment that includes environmental, economic and metrological point of view. Multi-Criteria Decision Analysis methods combine multioutput information into single value, that is easy to be compared other possibilities. They allow solving complex problems (with many criteria and alternatives) in a technically valid and practically useful way. It was found that the best procedure for PAHs determination in smoked meat and fish is MAE-RP-HPLC-FLD.

#### References

- [1] Bystrzanowska M., Tobiszewski M.: How can analysts use multicriteria decision analysis? *Trends Anal. Chem.* **105** (2018), 98–105.
- [2] European Food Safety Authority (EFSA): Polycyclic aromatic hydrocarbons in food-scientific opinion of the panel on contaminants in the food chain. *EFSA J.* **724** (2008), 1–114.
- [3] Stołyhwo A., Sikorski Z. E.: Polycyclic aromatic hydrocarbons in smoked fish—a critical review. *Food Chem.* **91** (2005), 303–311.
- [4] European Commission: Commission Regulation (EC) No. 1881/2006 of 19 December 2006 setting maximum levels for certain contaminants in foodstuffs. *O. J. EUL* 364/5 (2006).
- [5] Pissinatti R., de Souza S. V.: HC-0A-02: Analysis of polycyclic aromatic hydrocarbons from food. In: *Biodegradation and Bioconversion of Hydrocarbons – Analysis of Polycyclic Aromatic Hydrocarbons from Food*. K. Heimann, O.P. Karthikeyan, S.S. Muthu (Eds.). Springer 2017, p. 67–104.
- [6] Gałuszka A., Migaszewski Z.M., Konieczka P., Namieśnik J.: Analytical Eco-Scale for assessing the greenness of analytical procedures. *Trends Anal. Chem.* **37** (2012), 61–72.
- [7] Tobiszewski M., Namieśnik J.: Scoring of solvents used in analytical laboratories by their toxicological and exposure hazards. *Ecotox. Environ. Safe.* **120** (2015), 169–173.
- [8] Duedahl-Olesen L., Christensen J. H., Højgård A., Granby K., Timm-Heinrich M.: Influence of smoking parameters on the concentration of polycyclic aromatic hydrocarbons (PAHs) in Danish smoked fish. *Food Addit. Contam.* **27** (2010), 1294–1305.
- [9] Yurchenko S., Mölder U.: The determination of polycyclic aromatic hydrocarbons in smoked fish by gas chromatography mass spectrometry with positive-ion chemical ionization. *J. Food Compos. Anal.* **18** (2005), 857–869.
- [10] Visciano P., Perugini M., Amorena M., Ianieri A.: Polycyclic aromatic hydrocarbons in fresh and cold-smoked Atlantic salmon fillets. *J. Food Protect.* **69** (2006), 1134–1138.

- [11] Olatunji O.S., Fatoki O.S., Opeolu B.O., Ximba B.J.: Determination of polycyclic aromatic hydrocarbons [PAHs] in processed meat products using gas chromatography–flame ionization detector. *Food Chem.* **156** (2014), 296–300.
- [12] Purcaro G., Moret S., Conte L. S.: Optimisation of microwave assisted extraction (MAE) for polycyclic aromatic hydrocarbon (PAH) determination in smoked meat. *Meat Sci.* **81** (2009), 275–280.
- [13] Ghasemzadeh-Mohammadi V., Mohammadi A., Hashemi M., Khaksar R., Haratian P.: Microwave-assisted extraction and dispersive liquid–liquid microextraction followed by gas chromatography–mass spectrometry for isolation and determination of polycyclic aromatic hydrocarbons in smoked fish. *J. Chromatogr. A* **1237** (2012), 30–36.
- [14] Essumang D.K., Dodoo D.K., Adjei J.K.: Polycyclic aromatic hydrocarbon (PAH) contamination in smoke-cured fish products. *J. Food Compos. Anal.* **27** (2012), 128–138.

# Metal content in wines of Polish origin

MAGDALENA FABJANOWICZ\*, JUSTYNA PŁOTKA-WASYLKA

*Department of Analytical Chemistry, Faculty of Chemistry, Gdańsk University of Technology,  
11/12 Narutowicza Street, 80-233 Gdańsk, Poland ✉ plotkajustyna@gmail.com*

## Keywords

ICP-MS  
ICP-OS  
metal  
wine

## Abstract

Metals are important in the human diet. However, the excessive intake may be toxic to human body. That is why monitoring of metals in food products and beverages, including wines is of high importance. The aim of given study is to characterize wines coming from different region in Poland, in terms of metal content. Due to desired features like: sensitivity, low limit of detection as well as speed of analysis, the inductively coupled plasma-mass spectrometry (ICP-MS) and the inductively coupled plasma-optical emission spectrometry (ICP-OES) techniques were used to determine the metal concentration in wine samples. Results were satisfied showing allowable concentrations of examined metals according to the toxic levels for metals reported in the literature. Additionally, chemometric analysis was performed in order to find possible correlation between the wine samples or between chemical variables. The chemometric analysis found specific correlation.

---

## 1. Introduction

Metals are important in human diet however, the excessive intake of metals may be toxic and very harmful for human health [1]. Thus, monitoring of metals is crucial in the control of the quality of food products and beverages. Due to the increasing consumption of wines from year to year the monitoring of metal content in given alcoholic beverages is of high importance. The law already established the acceptable levels of particular metal concentrations and in most oenological laboratories it is routinely performed. The accepted limits of metals content in wine is presented in Table 1, on next page, [2]. Metals are strongly impacting the quality of wines due to taste and organoleptic properties changing, what also encourage their controlling [3]. Moreover, the content of some metals might be used to identify the origin of wine (vineyard and regional levels) due to its correlation with the soil type [4]. There was a lot of research performed in this field. However, there is still a lot to study. For the practical issues of legal fingerprinting of wines the multi-element dataset is needed, multivariate statistical techniques are required for data analysis. What is more, inductively coupled plasma – mass spectrometry (ICP-MS) is promising analytical methods for trace and ultra-trace element fingerprinting of wines, which is inexpensive, fast, routine

**Table 1**

The accepted limits of the metals content in wine in different countries and given by International Organization of Vine and Wine (OIV).

Country	Concentration of metals (mg L <sup>-1</sup> )							
	Al	As	Cd	Cu	Na	Pb	Ti	Zn
Australia	-	0.10	0.05	5.00	-	0.20	-	5.00
Germany	8.00	0.10	0.01	5.00	-	0.30	1.00	5.00
Italy	-	-	-	10.00	-	0.30	-	5.00
Poland	-	0.20	0.03	-	-	0.30	-	-
OIV	-	0.20	0.01	1.00	60	0.15	-	5.00

and accurate. Following work is focused on the determination of selected metals in wines from different Polish vineyards. Two analytical techniques were applied: ICP-MS and ICP-OES. Moreover, chemometric analysis were performed using cluster analysis (CA, hierarchical and non-hierarchical with K-means algorithm) and principal components analysis (PCA) to search for the specific relationships between the wine samples or between the chemical variables.

## 2. Experimental

### 2.1 Reagents and chemicals

Metals were analyzed with the use of Certified Reference Material ERM CA713 (sample 125) trace elements in waste water (IRMM – Institute for Reference Materials and Measurements). Calibration involved the ICP IV multi element standard usage (Merc, USA) and single standards: As, Sb, Se, Mo and V (Sigma-Aldrich, USA), Hg (Merc, USA) and internal standards: Sc, Rh, Tb and Ge standards in supra pure 1% HNO<sub>3</sub> (Merc, USA) and deionized water from the Milli-Q Direct 8 Water Purification System (Merc Millipore) for the sample (pre)treatment and sample dilution. To prepare the calibration standard the Sigma Aldrich (USA) stock solution containing Ca, Mg and K (1000 mg L<sup>-1</sup> for each element) were used.

### 2.2 Instrumentation

44 bottles of wine from 9 different vineyards from Poland were analyzed using ICP-OES (Shimadzu ICPE-9820, Japan) by which Ca, K, Mg concentration were investigated. However, ICP-MS analytical technique (ICP-MS 2030 Shimadzu, Japan) was used to determine concentration of: Ag, Al, As, B, Ba, Bi, Cd, Co, Cr, Cu, Fe, Hg, Li, Mn, Mo, Na, Ni, Pb, Sb, Se, Sn, Sr, Ti, Tl, V, Zn, Zr. Moreover, the chemometric tools of multivariate data interpretation, cluster analysis (CA, hierarchical and non-hierarchical clustering) were used [5].

### 3. Results and discussion

In order to characterise Polish wines, coming from different region, in terms of metal content, 30 elements were selected to be analyzed. Almost all chosen metals were determined in Polish wine samples, excluding Ag, Co, Cu, Sn and V, not detected in some samples. The amount of particular element was dependent on the type of specific wine sample. The highest concentrations were observed for: K (97 to 3250 mgL<sup>-1</sup>), Mg (42.7 to 161 mgL<sup>-1</sup>), Ca (32 to 137 mgL<sup>-1</sup>), B (0.333 to 12.1 mgL<sup>-1</sup>) and Mn (0.329 to 9.219 mgL<sup>-1</sup>). Moreover: Mn (18.61 µgL<sup>-1</sup> to 9.219 mgL<sup>-1</sup>), Fe (0.1558 to 2.775 mgL<sup>-1</sup>), Na (5.33 µgL<sup>-1</sup> to 3.823 mgL<sup>-1</sup>), Al (64.12 µgL<sup>-1</sup> to 2.729 mgL<sup>-1</sup>) and Zn (74.71 µgL<sup>-1</sup> to 2.339 mgL<sup>-1</sup>) were at high concentration levels. The lowest concentrations were noted for such metals as: Hg (0.31 to 0.51 µgL<sup>-1</sup>), Ag (<0.001 to 4.92 µgL<sup>-1</sup>), Co (<0.002 to 6.98 µgL<sup>-1</sup>), Cd (0.023 to 2.54 µgL<sup>-1</sup>), and Ti (0.54 to 2.37 µgL<sup>-1</sup>).

There is observed a correlation between the color of wine sample and the concentration level of marked metals. This is well visible on the example of silver, which the concentration is higher in the white wine than in the red wine samples. The same relationship is observed in case of: As, Bi, Co, Sb, Se, Sn, V and Zn. And opposite for: B, Ba, Fe, K and Mn, which were present at higher concentration in samples of red wines. Chemometry analysis was applied to find more complex correlations. It was used to examine specific correlations between 44 wine (red and white) samples (object of the study), coming from different regions of Poland like West Pomerania, Kyuavian Pomerania, Subcarpathia, Lesser Poland and Masovia) and between 30 metal concentrations, variables in order to classify the wines according to their metal content in a way being discriminating chemical indicators for each cluster group of wine type.

The hierarchical cluster analysis (HCA) was used to group chemical variables, Fig. 1 (next page). The unsupervised clustering lead to the formation of 4 clusters:

- K1: Zn, Pb, Cu, Co
- K2: Cd, Mg, Ca, K, Mn, Ba
- K3: Ni, Fe, Li, Cr, Sr, B, V, Na, Zr, Al
- K4: Tl, Ti, Se, Sb, Mo, Sn, Bi, As, Hg, Ag.

Later, the principal components was used to explain over 80% of the total variance of the system:

- PC1(27%) – indicates high correlation between Ag, As, Bi, Hg, Mo, Sb, Se, Sn, Tl and Ti – one can noticed it is entire K4 from HCA;
- PC2 (>10%) showing high factor loading for Al, V and Zr.
- PC3 (~10%) pointing out significant loading factor of Ba, K, Mg, Ti.
- PC4 (~7%) showing the relationship between B, Na and Sr.
- PC5 (9%) indicating correlation between Ca, Co, Cu and Zn.
- PC6 (7%) showing high loading factor of elements like: Cr, Fe, Li, Ni.
- PC7 and PC8 (explaining together >10% of total variance) pointing out the simple impact of Cd and Pb.

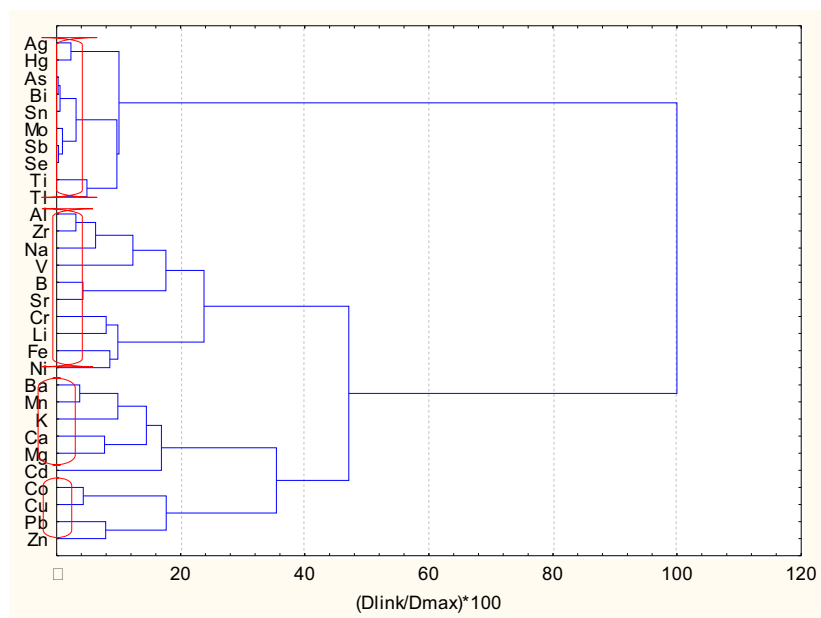


Fig. 1 Hierarchical dendrogram for 30 chemical variables analyzed in wine samples.

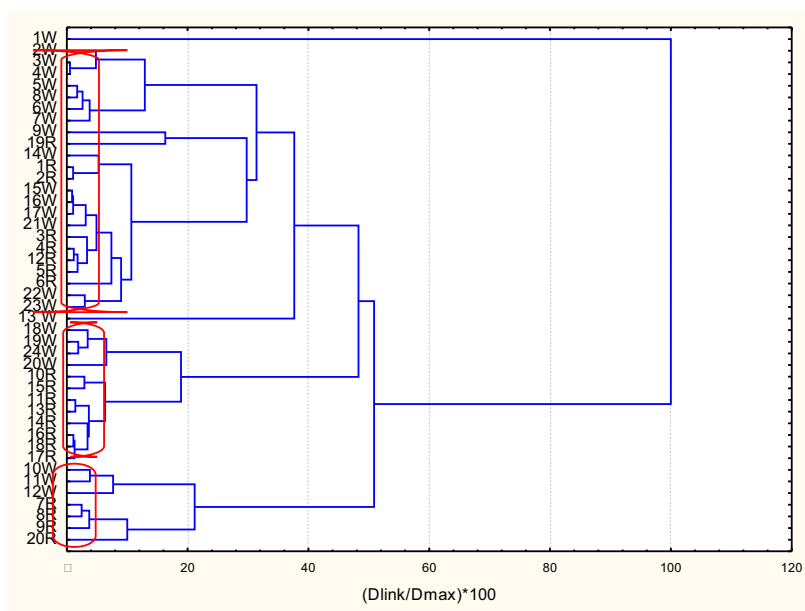


Fig. 2 Hierarchical dendrogram for 44 wine samples, coming from different region in Poland.

PCA broaden the information about the relationship of analyzed variables, showing similar trend as in HCA demonstrated before, at the same time.

Next step included the more important task which was to detect the similarity groups of wine samples. The results are present on Fig. 2, where 3 significant clusters were created:

- K1: **10w, 11w, 12w, 7r, 8r, 9r, 20r**
- K2: **18w, 19w, 20w, 24w, 10r, 11r, 13r, 14r, 15r, 16r, 17r, 18r**
- K3: **2w, 3w, 4w, 5w, 6w, 7w, 8w, 9w, 13w, 14w, 15w, 16w, 17w, 21w, 22w, 23w, 1r, 2r, 3r, 4r, 5r, 6r, 12r, 19r**

**1w** is an outlier.

It shows, that K1 the smallest cluster consists of equal number of white and red wines, including the Subcarpathia wines. K2 is dominated by red wines in the relation of 2:1 to the white wines, from Masovia. K3, the biggest cluster, consists mostly of white wines in relation of 2:1 to the red wines, from West Pomerania, Pomerania and Kyuavian Pomerania.

Furthermore, the supervised classification by the use of K-means non-hierarchical cluster method was used to determine the discriminant chemical variables. The analysis entirely confirmed the results from the HCA. One outlier was obtained and three clusters having the same number of wine samples.

Outlier (**1w**) is a wine sample of a specific characteristic: highest level of Ag, As, Bi, Hg, Mo, Sb, Se, Sn, Ti, Tl (those are metals having high factor scores in PC1 which could be conditionally named "toxicated" by soil conditions) and lowest levels of Al, V, Zr (elements from PC2), B, Ba, K, Mg, Mn (PC3), i.e. earth constituents or "specific" soil conditions). It is much different wine sample from West Pomerania than others from the same region.

Cluster 1 is of the same characteristic as K3 in HCA and includes all different Pomeranian wines. No discriminating species were detected. It characterized by "background" levels of all metals. It can be concluded, that the soil conditions are very appropriate for the grapes ensuring high wine quality.

Cluster 2 is the same as K2 in HCA and includes Masovian wines and is characterized by similar quality as Pomeranian wines. The soil conditions may be considered as good (no "toxic" or "specific" soil conditions impacting the wine quality).

Cluster 4 is the same as K1 in HCA and consists of Subcarpathian wines. Their characterization is closer to the outlier wine sample than Masovian or Pomeranian wine samples. There were enhanced levels of Al, B, Co, Fe, Li, Na, Ni, Sr, Zr observed, thus becoming subject to soil specificity (of natural, nor anthropogenic origin) in the region.

#### 4. Conclusions

Almost all 30 selected metals were determined in Polish wine samples, excluding Ag, Co, Cu, Sn and V. However, the type of analyte and quantity depends on the

specific wine sample. K, Mg, Ca, B and Mn were present at highest amount, whereas Hg, Ag, Co, Cd and Ti were present at lowest concentrations. The content of metals in all analysed wine samples was within the acceptable limits according to the toxic levels of metals stated in the literature. Polish wines may be considered as safe in terms of metal content. The level of selected metals strongly depends on the colour of wine, specific elements content in a particular wine sample. There were higher concentrations of metals like: Ag, As, Bi, Co, Sb, Se, Sn, V and Zn in white wine samples than red ones. However, B, Ba, Fe, K and Mn were present at higher concentrations in red wine samples than white. In order to see more complex correlations the chemometric analysis were performed which helped to find, that wine quality strongly depends on soil natural composition as well as soil toxic metals content. Wine would be successfully separated on geographic objectives and to discriminate metal variables for each region. Further research would be helpful to find possible sources of the metal content both natural and anthropogenic.

### Acknowledgments

Justyna Płotka-Wasyłka would like to thank Faculty of Chemistry, Gdańsk University of Technology for financial support within the minigrant program (Decision no. 4914/E-359/M/2017). The authors would like to thank Zodiak Vineyard, PrzyTalerzyku Vineyard, Kozielec Vineyard, Pod Orzechem Vineyard, Stok Vineyard, Spokaniówka Vineyard, and Dwór Kombornia Vineyard for the samples of wine.

### References

- [1] Płotka-Wasyłka J., Rutkowska M., Cieślik B., Tyburcy A., Namieśnik J.: Determination of selected metals in fruit wines by spectroscopic techniques. *J. Anal. Meth. Chem.* (2017), Article ID 5283917.
- [3] Pyrzyńska K.: Chemical speciation and fractionation of metals in wine. *Chem. Speciation Bioavailability* **19** (2007), 1–8.
- [4] Greenough J.D., Mallory-Greenough L.M., Fryer B.J.: Geology and wine: regional trace element fingerprinting of Canadian wines. *Geosci. Can.* **32** (2005), 229–137.
- [5] Massart D.L., Kaufman L.: *The Interpretation of Analytical Chemical Data By the Use of Cluster Analysis*. Amsterdam, Elsevier 1983.

# New sample preparation strategies for comprehensive lipidomics of human breast milk

DOROTA GARWOLIŃSKA\*, WERONIKA HEWELT-BELKA, JACEK NAMIEŚNIK,  
AGATA KOT-WASIK

*Department of Analytical Chemistry, Faculty of Chemistry, Gdansk University of Technology,  
11/12 Narutowicza St., 80-233 Gdansk, Poland ✉ [dorota.garwolinska@pg.edu.pl](mailto:dorota.garwolinska@pg.edu.pl)*

## Keywords

human breast milk  
untargeted lipidomics

## Abstract

Global profiling analysis of human breast milk lipids is hindered by complex composition of human breast milk. This problem is huge from analytical point of view, since due to that detection of all human breast milk lipids during one analytical run is limited. Thus, sample preparation step constitutes a crucial step in untargeted lipidomic analysis of human breast milk, especially when semi-quantitative analysis is assumed. Herein, we present a comparison of published and proposed by us sample preparation procedures used in lipidomic study of human breast milk, including indication of advantages, drawbacks and possible application.

---

## 1. Introduction

Human breast milk is considered as the gold standard in nutrition of the newborn [1]. Despite a huge contribution of human breast milk lipids to the total amount of human breast milk nutrients and their impact on the proper child development, they remain the least understood part of milk. Due to the inefficiency and time-consuming of prior available traditional analytical methods for lipid analysis, the extension of knowledge about human breast milk lipids was limited. The application of untargeted lipidomics that offers investigation of lipids in a fast and precise way allows for detailed characterization of an enormous number of human breast milk lipids species, even those unidentified previously, in one analytical run.

One of the main concerns in untargeted lipidomic study is to achieve high lipidome coverage using simple, reproducible sample preparation strategy and limited number of analytical techniques. In human breast milk, the significant variety in concentration level of lipid species occurs. Some lipid classes are dominant with concentration ( $\mu\text{M}$  to  $\text{mM}$  range) in contrast to other one, which are much less abundant ( $\text{pM}$ – $\text{nM}$  range). This applies primarily for low abundant

glycerophospholipids and sphingophospholipids [2], and compared with glycerophospholipids and sphingophospholipids high abundant glycerolipids [3]. This problem is important from analytical point of view, since due to that detection of all human breast milk lipids during one analytical run is limited. Low abundant lipids require enriching step to break the limit of detection, whereas lipids at high concentration levels frequently require dilution step to avoid saturation of MS signal. Therefore, the proper sample preparation is the crucial step in lipidomics analysis of human breast milk.

## 2. Experimental

### 2.1 Reagents and chemicals

LC-MS-grade methanol and HPLC-grade chloroform and hexane were purchased from Merck (Germany), and HPLC-grade 2-propanol, ammonium formate (99.9% purity) formic acid and ammonia p.a were purchased from Sigma-Aldrich (USA). Deionized water was purified on an HLP5 system (Hydrolab, Wiślina, Poland).

### 2.2 Sample preparation procedure

For the global lipidomics of human breast milk we developed two sample preparation protocols. First one has been based on solid-phase microextraction (SPME) technique [4] and the second one involves combination of solid-phase extraction (SPE) and liquid-liquid extraction (LLE) techniques [5]. The flowcharts of sample preparation strategies for global lipidomic of human breast milk are presented on Fig. 1 and 2 respectively.

The first sample preparation protocol was described in details in previous research [4]. In short, prior to adsorption, the SPME tip that consisted of a fiber coated with a silica-based sorbent modified with C18 groups (Supelco, Sigma-Aldrich, USA) was preconditioned in a mixture of solvents (MeOH/H<sub>2</sub>O). Then, it

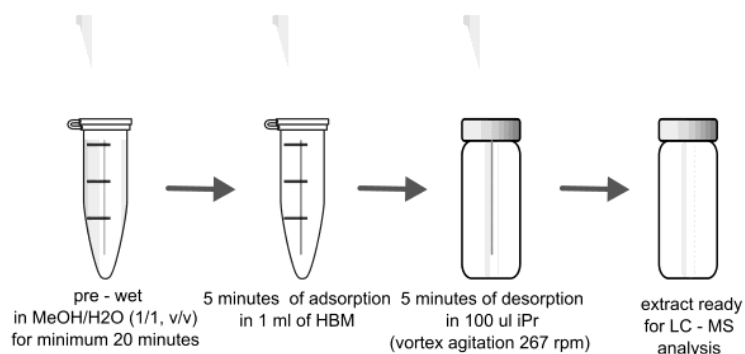
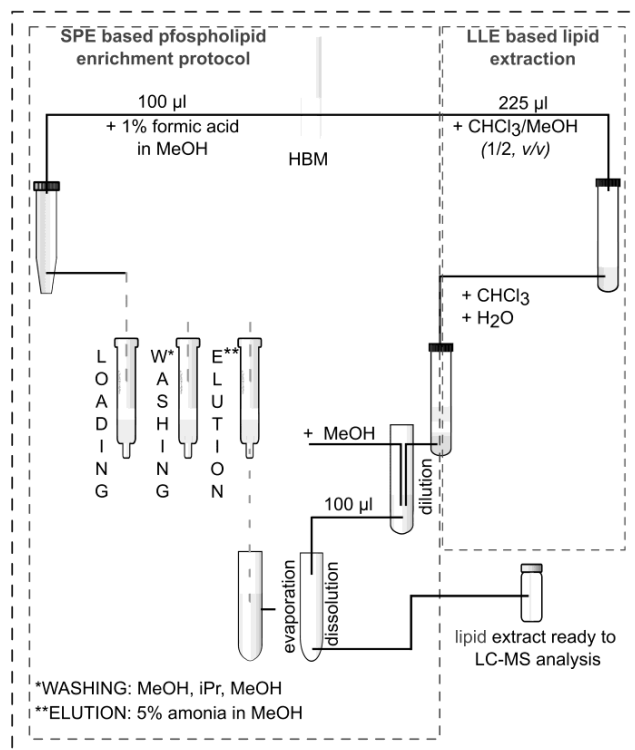


Fig. 1 Optimized protocol for human breast milk lipid extraction using SPME technique [4].



**Fig. 2** Lipid extraction by SPE and LLE based approach [5].

was immersed in 1 mL of human breast milk. After lipid adsorption, the SPME tip was transferred to a LC vial containing a glass insert filled with 2-propanol for lipid desorption. After desorption with shaking, the SPME tip was removed. The obtained lipid extract was subsequently analyzed using LC-Q-TOF-MS.

The second developed sample preparation strategy for comprehensive characterization of human breast milk lipids with used LLE and SPE technique [5] included two basis steps:

1. SPE based phospholipids enrichment: 100  $\mu\text{L}$  of human breast milk sample has to be mixed with the solution of 1% formic acid in methanol and subsequently vigorous vortexing and centrifuged in order to precipitate proteins. Next supernatant has to be loading to the HybridSPE-Phospholipid cartridge (Supelco, Sigma Aldrich, USA). After stationary phase washing, phospholipids can be eluted with 5% ammonia in methanol. The obtained extract has to be evaporated to dryness and dissolved with the use of lipid extract obtained in the second step of sample preparation procedure.
2. LLE based lipid extraction, where just 225  $\mu\text{L}$  of human breast milk sample has to be mixed with the chloroform/methanol mixture and vortexed. Next, appropriate volume of chloroform and water has to be added and after vigorous vortexing sample has to be centrifuged to separate aqueous and organic

phase. The lower organic phase containing lipids has to be diluted and next, 100  $\mu\text{L}$  of diluted extract has to be used as a dissolving solution for enriched phospholipid fraction (obtained in the first step).

Finally, the prepared human breast milk lipid extract can be transferred to the chromatographic vial and analysed by LC-Q-TOF-MS

### 2.3 Instrumentation

The RP-LC-Q-TOF-MS analysis of obtained extract was performed using Agilent 1290 LC system equipped with a binary pump, an online degasser, an autosampler and thermostated column compartment coupled with a 6540 Q-TOF-MS with a Dual electrospray ionization (ESI) source (Agilent Technologies, USA).

Lipid extracts obtained by SPME based strategy were chromatographically separated on an Agilent ZORBAX SB-C18 column (50 $\times$ 2.1 mm, 1.8  $\mu\text{m}$  particle size) in the condition described in details in previous research [4].

To reduce time of analysis lipid extracts obtained by SPE and LLE based strategy were chromatographically separated on a reversed-phase column (Poroshell 120 EC-C8, 150 $\times$ 2.1 mm, 1.9  $\mu\text{m}$  particle size, Agilent) with a 0.2  $\mu\text{m}$  in-line filter. The column and autosampler temperature throughout the analysis were maintained at 45  $^{\circ}\text{C}$  and 4  $^{\circ}\text{C}$ , respectively.

In both cases the injection volume was 0.5  $\mu\text{L}$  and mobile phase consisted of mixture of 5 mM ammonium formate in water and methanol (1:4,  $v/v$ ) as component A and a mixture of 5 mM ammonium formate in water, hexane and 2-propanol (1:20:79,  $v/v/v$ ) as component B). The mobile phase was pumped at 0.5  $\text{mL min}^{-1}$  within a total run time of 30.5 min. The gradient elution program was initiated with 10% eluent B during the first 10 minutes and was then ramped from 10% to 50% B from 10 to 15 minutes and 50% to 100% B from 15 to 20 minutes. Then, after 0.5 minute, the gradient was switched to 10% eluent B for 10 min for equilibration prior to the next run.

The ESI source condition and data analysis parameters were described in details elsewhere [8].

### 3. Results and discussion

Human breast milk lipid analysis is hindered by huge diversity of this compounds and their wide range of concentration. Due to that the sample preparation step is crucial. According to available literature data, previously reported methods for human breast milk lipid analysis by HPLC-MS approach including LLE [6] and single phase extraction [6], [7] as sample preparation step. We developed two another methods for lipid extraction, one based on SPME technique, and second one based on SPE and LLE techniques.

Sample preparation method, based on SPME technique allows for rapid and simple comprehensive characterization of lipids in human breast milk samples.

Our sample preparation method offers significant improvements over other published methods for human breast milk lipid extraction. It does not require protein precipitation (extraction is performed directly from human breast milk samples), what minimizes sample preparation step time and significantly reduces the organic solvents use. Moreover, the development of a SPME method in combination with LC-Q-TOF-MS enables detection of broad range of human breast milk lipids. Comparison of the individual lipid classes extracted from human breast milk using different extraction procedures revealed that all extraction procedures provide similar lipidome coverage [4]. However, due to the low precision it can be only use for qualitative purpose. The relative standard deviation of the 69% of molecular feature volumes (detected in three extraction replicates of the same human breast milk sample) was higher than 20%, which does not meet the criteria for semi-quantitative analysis. We assumed that main reason of low precision of develop extraction method, may be high level of glycerolipids concentration, which can cause nonlinear isotherm. Sample dilution may improve precision of extraction procedure, but low level of concentration of some other lipids, limits it. Moreover, due to the wide concentration range of different lipid classes in the human breast milk samples, the MS signal obtained for some of lipids was saturated and required dilution for quantification, and the MS signals for other lipid classes were very low and limit dilution. Thus, the simultaneous quantification of all detected lipid classes in one analytical run was limited also for this reason. However, in our study we focused on developed method for rapid qualitative analysis and for this purpose, developed sample preparation method, even with low repeatability, is sufficient.

To overcome drawbacks of previously evaluated method, we have developed sample preparation method, based on SPE and LLE techniques. The combination of these two extraction techniques enables the enrichment of low abundant human breast milk lipids containing the phosphate moiety (glycerophospholipids and sphingomyelins), and dilution of human breast milk lipids that are at the high concentration level in human milk (glycerolipids). To confirm usefulness of developed lipid extraction protocol the human breast milk lipid chromatograms obtained with the previous and developed method are presented on Fig. 3.

The lipidome coverage obtained by implementation of this enrich-dilute strategy was higher than those described in previously reports [8, 10, 11], particularly in the term of phospholipids content (approximately fourfold more human breast milk lipids containing phosphate moiety were identified. This extraction procedure enables both highly effective separation of phospholipids and glycerolipids. Thus, the developed sample preparation strategy represents valuable tool for comprehensive analysis of human breast milk lipids.

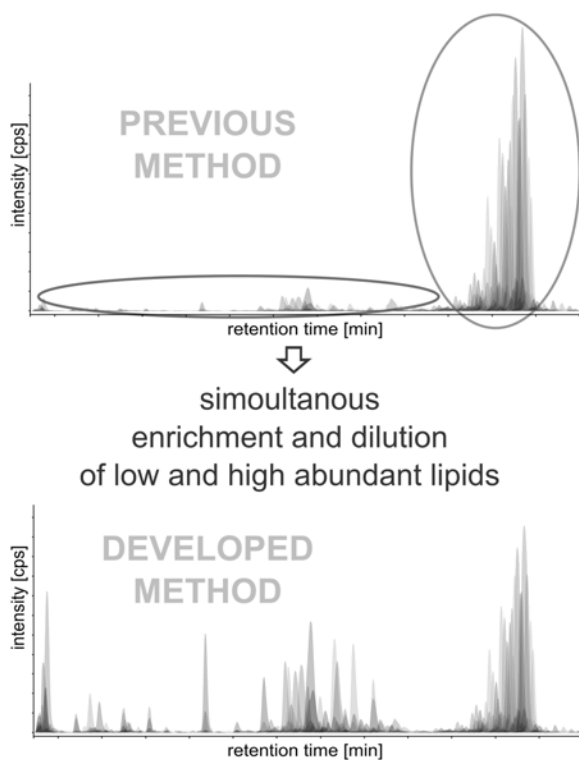


**Fig. 3** Lipid chromatograms obtained with the previous and developed method based on SPE and LLE and LC-MS techniques.

#### 4. Conclusions

Preparation of human breast milk sample to lipid analysis performed in untargeted manner is a challenge. Many of available lipid extractions are not suitable for isolation of human breast milk lipids, due to the huge diversity of these compounds and their wide range of concentration. We have developed two sample preparation procedures and compared them with other sample preparation strategies used in analysis of human breast milk lipids. One of them ensures similar lipid coverage to those described in previous reports, but is not suitable for quantitative analysis. However, the second one provides higher lipid coverage than those described in previous reports and is suitable for both qualitative and semi-quantitative lipid analysis performed in untargeted manner.

#### References

- [1] World Health Organization: *Global strategy for infant and young child feeding*. UNICEF 2003.
- [2] Tavazzi I, Fontannaz P, Lee L.Y., Giuffrida F: Quantification of glycerophospholipids and sphingomyelin in human milk and infant formula by high performance liquid chromatography coupled with mass spectrometer detector. *J. Chromatogr. B* **1072** (2018), 235–243.
- [3] Sokol E, Ulven T, Færgeman N.J., Ejsing C.S.: Comprehensive and quantitative profiling of lipid species in human milk, cow milk and a phospholipid-enriched milk formula by GC and MS/MS(ALL). *Eur. J. Lipid Sci. Technol.* **117** (2015), 751–759.

- [4] Garwolińska D., Hewelt-Belka W., Namieśnik J., Kot-Wasik A.: Rapid Characterization of the human breast milk lipidome using a solid-phase microextraction and liquid chromatography-mass spectrometry-based approach. *J. Proteome Res.* **16** (2017), 3200–3208.
- [5] Hewelt-Belka W., Garwolińska D., Belka M., Bączek T., Namieśnik J., Kot-Wasik A.: *unpublished data*.
- [6] Andreas N.J. Hyde M.J., Gomez-Romero M., Lopez-Gonzalvez M.A., Villaseñor A., Wijeysekera A., Barbas C., Modi N., Holmes E., Garcia-Perez I.: Multiplatform characterization of dynamic changes in breast milk during lactation. *Electrophoresis* **36** (2015), 2269–2285.
- [7] Villasenor A., Garcia-Perez I., Garcia A., Posma J.M., Fernández-López M., Nicholas A.J., Modi N., Holmes E., Barbas C.: Breast milk metabolome characterization in a single-phase extraction, multiplatform analytical approach. *Anal. Chem.* **86** (2014), 8245–8252.

# Determination of amikacin and ciprofloxacin by liquid chromatography with pre-column derivatization to evaluate sustained delivery of antibiotics from Drug-Eluting Biopsy Needle

MARTA GLINKA<sup>a,\*</sup>, JUSTYNA KUCIŃSKA-LIPKA<sup>b</sup>, ANDRZEJ WASIK<sup>a</sup>

<sup>a</sup> Department of Analytical Chemistry, Faculty of Chemistry, Gdańsk University of Technology, 11/12 Gabriela Narutowicza Street, 80-233 Gdańsk, Poland ✉ marglink@student.pg.edu.pl

<sup>b</sup> Department of Polymer Technology, Faculty of Chemistry, Gdańsk University of Technology, 11/12 Gabriela Narutowicza Street, 80-233 Gdańsk, Poland

## Keywords

antibacterial antibiotics  
derivatization  
drug delivery systems  
high performance liquid  
chromatography

## Abstract

Determination of chosen antibacterial antibiotics: amikacin and ciprofloxacin was carried out by hplc-uv after derivatization with 9-fluorenylmethyl chloroformate and in their native form by HPLC-MS/MS. Developed methods have been applied to control the kinetics of antibiotic release from polymer-based controlled drug delivery system.

---

## 1. Introduction

Amikacin and ciprofloxacin are the most commonly used antibiotics used to fight bacterial infections mainly caused by *Escherichia coli* [1]. Thanks to their efficiency these antibiotics are used to prevent possible infections in the case of a transrectal prostate biopsy. Nowadays, for this purpose, medicine willingly uses the “controlled drug delivery systems”, i.e., polymer-based drug-eluting biopsy needles. This approach allows administration of antibiotics during the biopsy directly into the tissue, elimination of onerous antibiotic therapy and decrease possibility of infection complications.

Amikacin is an aminoglycoside antibiotic especially effective against Gram-Negative bacteria. Chemically amikacin consist of aminosugars (D-glucosamine, D-kanosamine) which are connected to aminocyclitol by glycosidic bonds.

Ciprofloxacin is a second generation quinolone derivative. In comparison to amikacin, ciprofloxacin is characterized by completely different chemical properties such as lower polarity and water solubility (Table 1).

**Table 1**

Selected properties of amikacin and ciprofloxacin (dissociation exponents predicted from Chem-Axon).

Name	Molecular formula	$M/g\ mol^{-1}$	Log $P$	Water solubility	$pK_a$	$pK_b$
amikacin	$C_{22}H_{43}N_5O_{13}$	585.6	-7.40	185 g L <sup>-1</sup> (25 °C)	12.1	9.79
ciprofloxacin	$C_{17}H_{18}FN_3O_3$	331.3	0.28	30 g L <sup>-1</sup> (20 °C)	5.76	8.68

As a result of the aforementioned differences, the chromatographic determination of amikacin and ciprofloxacin may cause problems due to their completely different retention behaviour during separation. In addition, due the lack of chromophores and high polarity, direct analysis of amikacin in its native form, especially under reversed phase conditions is difficult and the derivatization step is required [2]. Derivatization of antibiotics with amino-groups is realized mainly with: 9-fluorenylmethyl chloroformate, 6-aminoquinolyl-*N*-hydroxysuccinimidyl carbamate, ortho-phthalaldehyde with 3-mercaptopropionic acid, etc. However, derivatization often results in the decrease of precision and increase of costs and time of analysis [2–4]. The procedure for precolumn derivatization of amikacin and ciprofloxacin with 9-fluorenylmethyl chloroformate was proposed. Additionally obtained results were compared with direct analysis of the antibiotics in their native forms using high performance liquid chromatography coupled with tandem mass spectrometry (HPLC-MS/MS). Proposed procedure was applied to control the kinetic of antibiotics release from polymer-based controlled drug delivery system, namely the trans-rectal biopsy needle.

## 2. Experimental

### 2.1 Reagents and chemicals

Amikacin and Ciprofloxacin were purchased from Interquim (Cuautitlán Izcalli, Mexico) and Aarti Drugs Limited (Maharashtra, India) respectively. 9-fluorenylmethyl chloroformate ( $\geq 99\%$ ), acetonitrile (LC-MS grade) and glycine were purchased from Sigma Aldrich. Ultrapure water was prepared using HLP5 system from Hydrolab (Wiślna, Poland). Formic acid was purchased from Merck. Boric acid, phosphoric acid, sodium hydroxide and potassium chloride were purchased from POCH (Gliwice, Poland). Borate buffer was prepared by titrating the water solution of boric acid (0.2 M) and potassium chloride (0.2 M) with sodium hydroxide to pH = 7.3. Polymer-coated biopsy needles with different concentrations of hydrophilic polymers and antibiotics were prepared in cooperation with Department of Polymer Technology (Gdańsk University of Technology, Poland).

**Table 2**

Multiple reaction monitoring mode parameters.

Analyte	Multiple reaction monitoring	Declustering potential/V	Collision energy/V
amikacin	586.4–163.1	81	47
	586.4–425.3	81	27
ciprofloxacin	332.3–288.1	91	27
	322.3–231.0	91	49

## 2.2 Instrumentation

HPLC-UV determination of antibiotic was performed using an Agilent 1200 LC system consisting of degasser, binary pump, ALS autosampler, thermostated column compartment and diode array detector (DAD) detector. The separation of antibiotics was carried out using Kinetex C18, 1.7  $\mu\text{m}$  (50 $\times$ 2.1 mm) chromatographic column working at 40 $^{\circ}\text{C}$ . As a mobile phase water (component A) and acetonitrile (component B) both with 0.5% (v/v) of diluted phosphoric acid (in a mass ratio 1:1 with deionized water) were used in following gradient elution: 0 min – 20% B, 15 min – 95% B, 20 min – 95% B, 20.1 min – 20% B, 24.5 min – 20% B. Flow rate of 0.3 mL min $^{-1}$  was used and the injection volume was 2  $\mu\text{L}$ .

HPLC-MS/MS determination of antibiotics in multiple reaction monitoring mode (Table 2) was performed using an Agilent 1200 Series Rapid Resolution LC system (USA) consisting of an online degasser, a binary pump, a high-performance SL autosampler and a thermostated column compartment. The system was coupled to the Q-Trap 4000 triple quadrupole mass spectrometer (AB SCIEX, USA) with electrospray ionization (ESI) source working in positive ion mode. Other parameters of ESI source were as follows: curtain gas pressure: 20 psi, source temperature: 550  $^{\circ}\text{C}$ , nebulizer gas pressure: 30 psi, heater gas pressure: 30 psi and capillary voltage: 4000 V. For separation ZORBAX Eclipse XDB-C18 1.8  $\mu\text{m}$  (50 $\times$ 4.6 mm) chromatographic column was used. Temperature of column was maintained at 35  $^{\circ}\text{C}$ . Separation was carried out in isocratic conditions with mixture of acetonitrile and water (85:15, v/v) with 0.1% of formic acid as a mobile phase. Flow rate of 0.8 mL min $^{-1}$  was used and the injection volume was 2  $\mu\text{L}$ . The time of analysis was 3 minutes.

## 2.3 Sample preparation

Two sets of biopsy needles were prepared with two different compositions and thickness of coatings (8 needles for each set) and injection simulation test was performed. For this purpose, pork prostates obtained from a local slaughterhouse were used. Prostates were frozen and heated to approx. 37  $^{\circ}\text{C}$  on the test day. Additionally, in order to simulate the real biopsy procedure, the special biopsy gun was used. For each of 8 needles from a given series (with the same coatings),

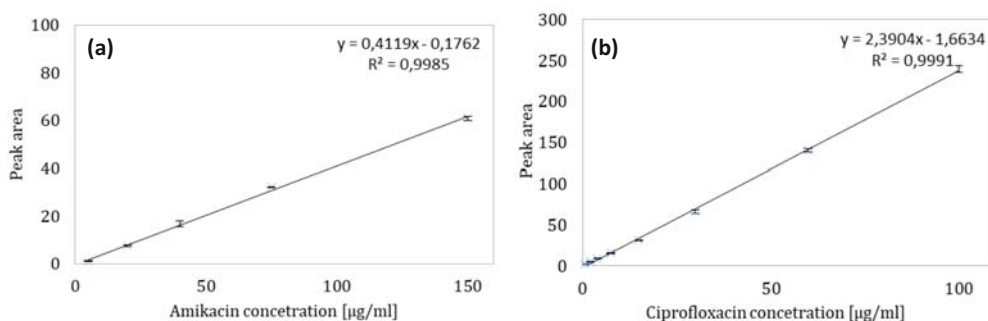


**Fig. 1** Calibration curve of (a) amikacin ( $5\text{--}150\ \mu\text{g ml}^{-1}$ ), and (b) ciprofloxacin ( $0.5\text{--}100\ \mu\text{g ml}^{-1}$ ).

a different number of tissue injections were performed: 0 (without injection – reference sample), 1, 3, 5, 7, 9, 11 and 12 injections. Subsequently, each needle was immersed in 5.5 mL of deionized water in dedicated test-tube for 40 min. After that, the solution was transferred into Eppendorf vials and vortex for 5 minutes. The clarified solution was transferred to the vials and analysed by HPLC-MS/MS.

In the case of HPLC-UV analysis, the modified Chang's [4] procedure was applied. The clarified solution was mixed with acetonitrile in volume ratio 1:1. The 200  $\mu\text{L}$  of this mixture was introduced in to the vial with 200  $\mu\text{L}$  borate buffer (0.2 M, pH = 7.3). For derivatization, 200  $\mu\text{L}$  of 9-fluorenylmethyl chloroformate acetonitrile solution (2.5 mM) was added and mixed. After 20 minutes, the 50  $\mu\text{L}$  of glycine (0.1 M) was added and mixed for stopping the derivatization reaction. After all, samples were analysed by HPLC-UV.

#### 2.4 Calibration curves

Stock solution of amikacin ( $10\ \text{mg mL}^{-1}$ ) and ciprofloxacin ( $1\ \text{mg mL}^{-1}$ ) were prepared in deionized water. Working standard solutions were prepared freshly by mixing volumes of stock solutions with water in graduated flasks. Amikacin and ciprofloxacin LC-MS/MS calibration standard solutions of 0.5, 1, 5, 15, 25, 50, 100  $\mu\text{g mL}^{-1}$  were prepared. In the case of LC-UV method, calibration standards of 5, 20, 40, 75, 150  $\mu\text{g mL}^{-1}$  for amikacin and 0.5, 2, 4, 7.5, 15, 30, 60, 100  $\mu\text{g mL}^{-1}$  for ciprofloxacin after derivatization with 9-fluorenylmethyl chloroformate were used.

### 3. Results and discussion

In the case of derivatization procedure, the buffer pH (7.3 and 8.5), concentration of 9-fluorenylmethyl chloroformate (1, 2.5, 3.5, 5 and 25 mM) and time of reaction (1, 3, 5, 15, 20 and 45 minutes) were optimized (data not shown). The optimal conditions were summarized in section 2.3.

Validation of pre-column derivatization HPLC-UV method was performed. It consisted of estimation of linearity, limits of detection (LOD) and limits of

**Table 3**

Comparison of amikacin and ciprofloxacin content in polymer-based coatings after injection simulation test obtained by pre-column derivatization HPLC-UV and derivatization-less HPLC-MS/MS methods ( $n = 3$ ).

Coating number	Injection number	$c(\text{amikacin}) \pm \text{SD} / \mu\text{g mL}^{-1}$		$c(\text{ciprofloxacin}) \pm \text{SD} / \mu\text{g mL}^{-1}$	
		HPLC-UV	HPLC-MS/MS	HPLC-UV	HPLC-MS/MS
1	0	68.4±6.2	60.9±1.8	48.63±0.51	45.1±1.6
	1	44.2±7.1	39.2±1.3	37.60±0.46	35.0±1.7
	3	28.7±4.8	26.23±0.67	23.85±0.47	24.0±1.6
	5	17.1±1.3	13.27±0.55	15.61±0.57	16.8±1.4
	7	20.9±2.1	17.50±0.92	25.2±2.2	23.5±1.9
	9	6.86±0.88	3.96±0.52	4.53±0.33	4.82±0.65
	11	<i>n.a.</i>	1.60±0.63	0.55±0.13	<i>n.a.</i>
	12	5.0±1.1	2.84±0.58	1.56±0.22	1.46±0.35
2	0	59.9±4.1	44.92±0.32	39.42±0.72	42.1±1.3
	1	44.5±8.3	38.9±1.5	40.83±0.84	40.0±1.9
	3	35.6±1.1	25.50±0.54	36.3±2.2	33.7±2.1
	5	42.0±4.1	34.75±0.97	35.52±0.73	37.3±2.4
	7	16.24±0.37	14.08±0.31	20.15±0.17	19.0±1.5
	9	<i>n.a.</i>	1.051±0.051	0.96±0.21	0.92±0.11
	11	9.69±0.71	11.19±0.75	13.99±0.51	16.4±1.9
	12	6.86±0.24	7.24±0.61	8.95±0.28	10.79±0.56

quantification (LOQ). Both calibration curves (Fig. 1) were linear within the studied concentration ranges. Determination coefficients were satisfactory.

Also the limits of detection ( $LOD = \text{calibration curve intercept standard deviation multiplied by } 3.3 \text{ and divided by the slope of the calibration curve}$ ) and limits of quantitation ( $LOQ = 3 \times LOD$ ) were established. For amikacin the  $LOD = 3.2 \mu\text{g mL}^{-1}$  and  $LOQ = 9.6 \mu\text{g mL}^{-1}$ , whereas for ciprofloxacin 0.65 and  $1.95 \mu\text{g mL}^{-1}$  respectively.

Results of real-world sample analysis (with and without pre-column derivatization) are summarized in Table 3. Developed HPLC-UV method can be applied for determination of antibiotics in polymer matrix. Both HPLC-UV and HPLC-MS/MS methods produces similar results. For ciprofloxacin, HPLC-UV method involving the derivatization step gives more precise results while the accuracy remains similar. In case of amikacin results obtained with the help of HPLC-UV method are less precise than those provided by direct HPLC-MS/MS method. This is most probably caused by inconsistent derivatization reaction efficiency. On the other hand we can observe that the results obtained with the HPLC-MS/MS method are slightly lower than those produced by HPLC-UV. This phenomenon can be explained by the fact that amikacin was not retained on C18 stationary phase and eluted in a dead time together with other signal suppression causing components.

## 4. Conclusions

The results obtained with the developed HPLC-UV method are similar to those obtained by HPLC-MS/MS analysis of the antibiotics in their native forms. It can be used to study the kinetics of amino-antibiotic drug release from drug's controlled-delivery systems. In relation to amikacin it is slightly less sensitive than HPLC-MS/MS method but seemingly the accuracy is better. With regard to ciprofloxacin the developed method seems to be superior over the HPLC-MS/MS since the precision of the results is higher while accuracy stays the same. Also the instrumentation is simpler, cheaper and widely available.

## References

- [1] Sieczkowski M., Gibas A., Wasik A., Kot-Wasik A., Piechowicz L., Namieśnik J., Matuszewski M.: Drug-Eluting biopsy needle as a novel strategy for antimicrobial prophylaxis in transrectal prostate biopsy. *Technol. Cancer Res. Treat.* **16** (2017), 1038–1043.
- [2] Farouk F., Azzay H.M.E., Niessen W.M.A.: Challenges in the determination of aminoglycoside determination, a review. *Anal. Chimica Acta* **890** (2015), 21–43.
- [3] Baranowska I., Markowski P., Baranowski J.: Simultaneous determination of 11 drugs belonging to four different groups in human urine samples by reversed-phase high-performance liquid chromatography method. *Anal. Chimica Acta* **570** (2006), 46–58.
- [4] Chang X.-J., Peng J.-D., Liu S.-P.: A simple and rapid high performance liquid chromatographic method with fluorescence detection for estimation of amikacin in plasma – application to preclinical pharmacokinetics. *J. Chin. Chem. Soc.* **57** (2010), 34–39.

# Poultry meat freshness assessment based on the biogenic amines index

KAJA KALINOWSKA\*, WOJCIECH WOJNOWSKI, JUSTYNA PŁOTKA-WASYLKA,  
JACEK NAMIEŚNIK

*Department of Analytical Chemistry, Faculty of Chemistry, Gdansk University of Technology,  
11/12 Narutowicza St., 80-233 Gdańsk, Poland ✉ kajkalin@student.pg.edu.pl*

## Keywords

biogenic amines  
food analysis  
meat freshness

## Abstract

In order to safeguard the well-being of the consumers, it is important to accurately determine the shelf life of poultry and poultry-based products. In this work, it was evaluated whether the measurement of the concentration of cadaverine, putrescine, histamine and tyramine can be used to assess the shelf-life of poultry meat stored in the different types of the containers. Based on the results it can be concluded that the collective measurement of the biogenic amines can be successfully used in the poultry meat freshness assessment and could potentially supplement more traditional methods of quality and shelf-life evaluation.

---

## 1. Introduction

Poultry meat is an important part of most diets due to its being a source of a wholesome protein essential for proper functioning of the human body. In terms of the nutritional value, poultry meat surpasses pork and beef, as it contains more proteins and less fat. It is an easily digestible source of minerals, such as potassium, calcium, phosphorus and iron [1]. As a result, poultry is one of the most popular types of meat and its consumption is steadily increasing. It is established that it constitutes 40% of the overall meat consumed in European Union [2]. Moreover, poultry meat is becoming an important component of the diet of Poles. Since the year 2000, its annual consumption increased by as much as 63.3% and at the present moment reaches 29 kg per capita [3, 4].

The growing demand for safe meat products has caused an increased interest in new methods of poultry's spoilage assessment, both at the industrial and retail levels. The quality evaluation is necessary to ensure the consumers' satisfaction, as well as their safety since the consumption of spoiled meat, can be a cause of serious health hazards [5].

It was reported that the deterioration of meat's quality due to chemical changes accompanying bacterial growth can be quantified by the measurement of total volatile basic nitrogen. This method is used mostly for the evaluation of fish

freshness since the volatile nitrogenous bases that are primarily formed in the process of the enzymatic decarboxylation of certain amino acids are often associated with the aroma of spoiled fish [6, 7]. However, it was determined that the value of total volatile basic nitrogen increases with the poultry meat's spoilage and thus may be used as one of the meat freshness indicators [8–10].

The alternative approach to meat quality evaluation is the measurement of concentration values of biogenic amines. As volatile nitrogenous bases, they are predominantly formed by the decarboxylation of amino acids due to the activity of various microorganisms. Even though there are several polyamines occurring in fresh meat, biogenic amines such as cadaverine and histamine are mainly formed during processing and storage of meat and thus may serve as quality indicators of poultry and poultry-based produce [11–14]. Moreover, there is a growing interest in their determination not only because of their potential use in meat spoilage assessment but also due to the toxicological effect that can be related to the ingestion of biogenic amines. It was reported that the consumption of products with high levels of certain amines (e.g., tyramine and histamine) may cause food poisoning and migraines [15–16].

Since the concentration of individual biogenic amines may differ depending on the numerous factors, meat quality assessment may yield a better result with the application of methods based on the measurement of the levels of several amines. Veciana-Nogués et al. [17] proposed the use of biological amines index in which the values of histamine, cadaverine, putrescine and tyramine are added up. This method is employed primarily in fish freshness evaluation; however, it has found an application in the spoilage assessment of poultry and poultry-based products [18].

## 2. Experimental

### 2.1 Samples

Fresh chicken breast muscle, pork loin and beef loin were sourced from a local distribution centre in Gdańsk, Poland. Animals were slaughtered on the evening prior to the first day of the analysis and then transported to the distribution centres, in which the carcasses were processed. On the first day of the experiment, meat was transported in a portable cooler to the laboratory, where it was refrigerated at 4°C. Samples of each meat were stored in three different containers: polypropylene co-polymer vacuum food box, aerobically in a standard polypropylene co-polymer food box and aerobically in a standard high-density polyethylene refrigerator bag. On the 1st, 3rd, and 5th day of the experiment, the concentration of the four biogenic amines was determined using a previously described method [14].

## 2.2 Reagents

Standards of cadaverine, histamine, putrescine, tyramine, as well as the internal standard (hexylamine) were supplied by Sigma Aldrich. For derivatization, isobutyl chloroformate (Sigma Aldrich) was used. As extractive solvent, chloroform of high purity HPLC analysis grade, also supplied by Sigma Aldrich, was used. Both hydrochloric acid and high-purity grade dispersive solvent methanol were obtained from Fluka. In order to prepare the solution of alkaline methanol, potassium hydroxide was dissolved in methanol until saturation.

## 2.3 Biogenic amines determination

In situ derivatization with isobutyl chloroformate coupled to dispersive liquid-liquid microextraction was used as sample preparation methodology prior to the final determination with gas chromatography-mass spectrometry.

## 2.4 Multivariate data analysis method

Data analysis was performed using a dedicated Python toolbox Orange v. 3.13 [19]. The concentration values of the four biogenic amines were normalised and used as inputs for both principal component analysis and for supervised machine learning algorithms. The performance of the latter was assessed using a stratified 10-fold cross-validation. Hierarchical cluster analysis was performed based on Euclidean distances between the data points with Ward linkage.

## 3. Results and discussion

The aim of the experiment was to determine whether it is possible to assess the freshness of poultry meat stored in different containers based on the concentration of cadaverine, tyramine, putrescine and histamine. During the course of the experiment, the overall concentration of biogenic amines in all samples (listed in Table 1) has increased significantly. The differences between the results obtained for the samples stored in different containers were noticeable, but not prominent.

The averaged concentration of biogenic amines has been used as input values for chemometric analysis. First of all, principal component analysis (PCA) has been performed. First two principal components covered 99% of variance. A scatter plot obtained with the use of PCA is presented in Fig. 1. As it can be seen, data points corresponding to samples analysed on different days of storage form distinctly separated groups. Moreover, the within-group variance increased after the first day of storage, as the differences between the concentrations of biogenic amines in the samples stored in various containers become more pronounced over time.

**Table 1**

Information on concentration of biogenic amines in samples on different days of storage: (I) food box, (II) vacuum food box, (III) high-density polyethylene refrigerator bag. Averaged concentration 100 mg g<sup>-1</sup>.

Biogenic amine	Storage	Concentration/mg g <sup>-1</sup>		
		Day 1	Day 3	Day 5
cadaverine	I	<i>n.d.</i>	870.6±4.4	1041.4±4.8
	II	<i>n.d.</i>	781.8±1.2	980.6±4.7
	III	<i>n.d.</i>	915.0±1.9	1104.2±3.2
tyramine	I	<i>n.d.</i>	311.6±1.3	410.0±2.1
	II	<i>n.d.</i>	241.8±1.5	305.0±3.8
	III	<i>n.d.</i>	413.0±1.1	531.4±3.6
putrescine	I	98.84±0.19	111.60±0.17	179.58±0.58
	II	98.86±0.17	103.3±1.7	153.78±0.52
	III	99.140±0.040	115.0±0.2	197.7±1.4
histamine	I	148.14±0.46	433.2±3.2	380.6±4.7
	II	148.00±0.47	411.4±3.0	365.4±3.7
	III	148.46±0.05	507.8±4.8	338.0±1.9

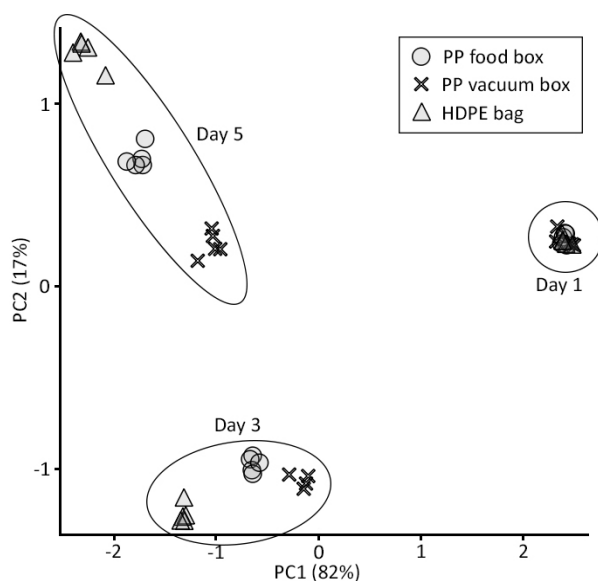


**Fig. 1** Results of PCA analysis refrigerated over the period of 5 days.

In Fig. 2, the dendrogram of hierarchical clustering is shown. Data points are grouped primarily based on the time of storage. However, samples stored in different types of containers form separate clusters within the groups. It is also worth noting that the result for the meat stored in a food box and in a bag form a group separated from the results of poultry meat kept in a vacuum food box (a distinct group at the 0.33 cluster analysis cut-off). This is likely due to the fact that limited oxygen access in vacuum food box affects the microbial development.

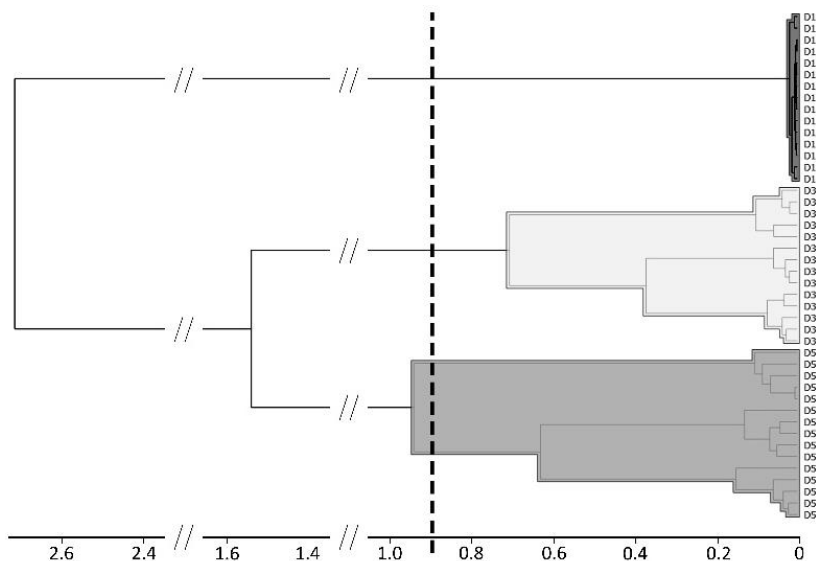


**Fig. 2** The dendrogram of hierarchical clustering with a cut-off line at 33% of the range.

**Table 2**  
Classification parameters.

Method	AUC	CA	Precision
<i>k</i> -nearest neighbours	1.000	1.000	1.000
classification Tree	0.981	0.977	0.398
support vector machines	1.000	1.000	1.000
random forest	1.000	1.000	1.000
Naive Bayes	1.000	0.955	0.960

Furthermore, the classification accuracy of five different algorithms, namely *k*-nearest neighbours, classification tree, support vector machines, random forest and Naive-Bayes, was assessed. As it can be seen in Table 2, it was possible to classify the samples based on the storage time with satisfactory results. It is worth noting that the perfect classification (AUC 1.000, CA 1.000, precision 1.000) was achieved with the use of three out of five algorithms.

#### 4. Conclusions

Based on the results of the experiment, it is possible to conclude that the collective measurement of the concentration of cadaverine, putrescine, histamine and tyramine can be used to assess the shelf-life of meat. The biological amines index proposed by Veciana-Nogués et al. [17] enables the classification of meat based on the duration of storage even when the samples are stored in different types of containers. This suggests that this technique could be used as a supplementary method in production or distribution centres using more traditional methods of quality assessment, such as Total Viable Count.

## References

- [1] Rachwał A.: Cechy chemiczne mięsa drobiowego. *Hod. Drobiu* **2** (2006), 28–33. (In Polish)
- [2] *OECD-FAO Agricultural Outlook 2015*. Paris, OECD Publishing 2016.
- [3] [www.stat.gov.pl/obszary-tematyczne/roczniki-statystyczne/roczniki-statystyczne/rocznik-statystyczny-rzeczypospolitej-polskiej-2016,2,16.html](http://www.stat.gov.pl/obszary-tematyczne/roczniki-statystyczne/roczniki-statystyczne/rocznik-statystyczny-rzeczypospolitej-polskiej-2016,2,16.html). [accessed 21st May, 2018]. (In Polish)
- [4] Nowak M., Trziszka T.: Zachowania konsumentów na rynku mięsa drobiowego. *Żywność. Nauk. Technol. Jakość* **1** (2010), 114–120. (In Polish.)
- [5] Saucier L., Microbial spoilage, quality and safety within the context of meat sustainability. *Meat Sci.* **120** (2016), 78–84.
- [6] Balamatsia C.C., Patsias A., Kontominas M.G., Savvaidis I.N.: Possible role of volatile amines as quality-indicating metabolites in modified atmosphere-packaged chicken fillets: Correlation with microbiological and sensory attributes. *Food Chem.* **104** (2007), 1622–1628.
- [7] Wojnowski W., Majchrzak T., Dymerski T., Gębicki J., Namieśnik J.: Electronic noses: Powerful tools in meat quality assessment. *Meat Sci.* **131** (2017), 119–131.
- [8] Wang Y., Li Y., Yang J., Ruan J., Sun C., Microbial volatile organic compounds and their application in microorganism identification in foodstuff. *Trends Anal. Chem.* **78** (2016), 1–16.
- [9] Khulal U., Zhao J., Hu W., Chen Q.: Intelligent evaluation of total volatile basic nitrogen (TVB-N) content in chicken meat by an improved multiple level data fusion model. *Sens. Actuators B* **238** (2017), 337–345.
- [10] Huang L., Zhao J., Chen Q., Zhang Y.: Nondestructive measurement of total volatile basic nitrogen (TVB-N) in pork meat by integrating near infrared spectroscopy, computer vision and electronic nose techniques. *Food Chem.* **145** (2014), 228–236.
- [11] Franke C., Beauchamp J.: Real-time detection of volatiles released during meat spoilage: a case study of modified atmosphere-packaged chicken breast fillets inoculated with *Br. thermosphacta*. *Food Anal. Methods* **10** (2017), 310–319.
- [12] Balamatsia C.C., Paleologos E.K., Kontominas M.G., Savvaidis I.N.: Correlation between microbial flora, sensory changes and biogenic amines formation in fresh chicken meat stored aerobically or under modified atmosphere packaging at 4 °C: possible role of biogenic amines as spoilage indicators. *Antonie Van Leeuwenhoek* **89** (2006), 9–17.
- [13] Wojnowski W., Majchrzak T., Szweida P., Dymerski T., Gębicki J., Namieśnik J.: Rapid evaluation of poultry meat shelf life using PTR-MS. *Food Anal. Methods* **11** (2018), 2085–2092.
- [14] Wojnowski W., Płotka-Wasyłka J., Kalinowska K., Majchrzak T., Dymerski T., Szweida P., Namieśnik J.: Direct determination of cadaverine in the volatile fraction of aerobically stored chicken breast samples. *Monatsh. Chem.*, in press, doi: 10.1007/s00706-01802218-7.
- [15] Lehane L., Olley J.: Histamine fish poisoning revisited. *Int. J. Food Microbiol.* **58** (2000), 1–37.
- [16] Crook M.: Migraine: A biochemical headache. *Biochem. Soc. Trans.* **9** (1981), 351–357.
- [17] Veciana-Nogués M.T., Mariné-Font A., Vidal-Carou M.C.: Biogenic amines as hygienic quality indicators of tuna. Relationships with microbial counts, ATP-related compounds, volatile amines, and organoleptic changes. *J. Agric. Food Chem.* **45** (1997), 2036–2041.
- [18] Silva C.M., Glória M.B.A.: Bioactive amines in chicken breast and thigh after slaughter and during storage at 4±1 °C and in chicken-based meat products. *Food Chem.* **78** (2002), 241–248.
- [19] Demšar J., Curk T., Erjavec A., Hočevar T., Milutinovič M., Možina M., Polajnar M., Toplak M., Starič A., Stajdohar M., Umek L., Zagar L., Zbontar J., Zitnik M., Zupan B.: Orange: Data mining toolbox in Python. *J. Mach. Learn. Res.* **14** (2013), 2349–2353.

# High resolution liquid chromatography and time of flight mass spectrometry in perfume analysis

DAGMARA KEMPIŃSKA\*, AGATA KOT-WASIK

*Department of Analytical Chemistry, Faculty of Chemistry, Gdańsk University of Technology,  
11/12 Gabriela Narutowicza Street, 80-233 Gdańsk, Poland ✉ dagkempi@student.pg.edu.pl*

## Keywords

HILIC-Q-TOF-MS  
perfumes  
RP-HPLC- Q-TOF-MS

## Abstract

Perfumes consist of a wide range of natural and synthetic compounds that belongs to different chemical classes. Most of these compounds are generally determined by GC. However, in this study RP-HPLC-Q-TOF-MS and HILIC-Q-TOF-MS technique was applied for the determination of ingredients of original perfumes and their imitations. Antioxidants and compounds specific to fragrances of animal origin were found in original perfume samples, whereas carrier oils components were generally determined in their imitations. Furthermore, some components of essential oils were also detected. This research confirmed the theory that results obtained in the analysis of perfume using HPLC can be complementary to those one obtained during GC analysis.

---

## 1. Introduction

Perfumes have been used for thousands of years and nowadays they are considered as an essential part of human life [1, 2]. On average, every 43 hours a new female fragrance appears, while the male one appears once every 96 hours. As a result, it is assessed that the perfume business is a billion-dollar industry [3].

Perfumes have complex matrices that consist of a wide range of natural and synthetic compounds belonging to different chemical classes. Hence, the risk of contact allergy induced by their ingredients is still being the object of scientific debate [1]. Furthermore, due to the adverse effects of some of perfumes components on human health and their potential bioaccumulation, they present a clearly growing threat to health and environment. Besides, the high prices of essential oils cause that fragrance dealers more and more often decide to falsify their products by adding cheaper materials, but still asking for the same price for the mixture. According to these reasons, the use of analytical techniques to assess allergenic properties of perfume components, environmental contamination or adulteration of perfumes is inevitable [4]. Due to the fact that the most perfume ingredients have apolar and (semi-) volatile character, gas chromatography (GC)

is the most popular technique used for perfume application. However, reversed-phase high performance liquid chromatography (RP-HPLC) is technique than can be applied for the determination of non-volatile perfumes ingredients that have low thermostability. Between the variety of detectors, mass spectrometer (MS) is superior for either GC or HPLC, because of its high sensitivity and outstanding identification possibilities. Electronic nose is another popular device used for determining the perfume ingredients [3, 4].

The aim of this study was to show the potential of HPLC-MS technique in direct analysis of original perfumes and their imitations. Two different types of liquid chromatography were presented and compared. Furthermore, the identification of several perfumes ingredients has been done.

## 2. Experimental

### 2.1 Reagents and chemicals

Acetonitrile (HPLC grade) and formic acid (>98%) were obtained from Merck (Germany). Acetonitrile (LC-MS grade) was purchased from VWR Chemicals (USA) and ultrapure water was prepared using HPL5 system from Hydrolab (Wiślina, Poland).

### 2.2 Instrumentation

Both HILIC-Q-TOF-MS and RP-HPLC-Q-TOF-MS analyses were performed using the Agilent 1290 LC system equipped with a binary pump, an online degasser, an autosampler and a thermostated column compartment coupled with the 6540 Q-TOF-MS with a Dual ESI ion source (Agilent Technologies, Santa Clara, USA). The ESI source was operated with positive and negative ion ionization mode. The fragmentor voltage was set at 100 V and the mass range was set at 100–1500  $m/z$  in MS. Furthermore, nebulizer gas was set at 35 psig, capillary voltage was set at 3500 V, and drying gas flow rate and temperature were set at 10 L  $\text{min}^{-1}$  and 300 °C, respectively. The TOF-MS system was calibrated on a daily basis.

In case of RP-HPLC, LiChrospher 100 RP-18e (125×4 mm, 5  $\mu\text{m}$ ; Merck, Germany) column was used in order to separate analytes. Two different solvent mixtures were examined and applied as a mobile phase: one mixture was based on acetonitrile and water mixture with formic acid (0.05%,  $v/v$ ) and the second one was based on acetonitrile acidified with formic acid (0.05%,  $v/v$ ). In both case, the isocratic elution was performed (100% B). The flow rate of mobile phase was 0.8  $\text{mL min}^{-1}$  and the injection volume was 20  $\mu\text{L}$ . The column temperature throughout the separation process was kept at 25 °C.

In case of hydrophilic interaction liquid chromatography (HILIC), Kinetex HILIC 100A (150×4.6 mm, 2.6  $\mu\text{m}$ ; Phenomenex, USA) column was used in order to separate analytes. The mixture of acetonitrile and water mixture with formic acid

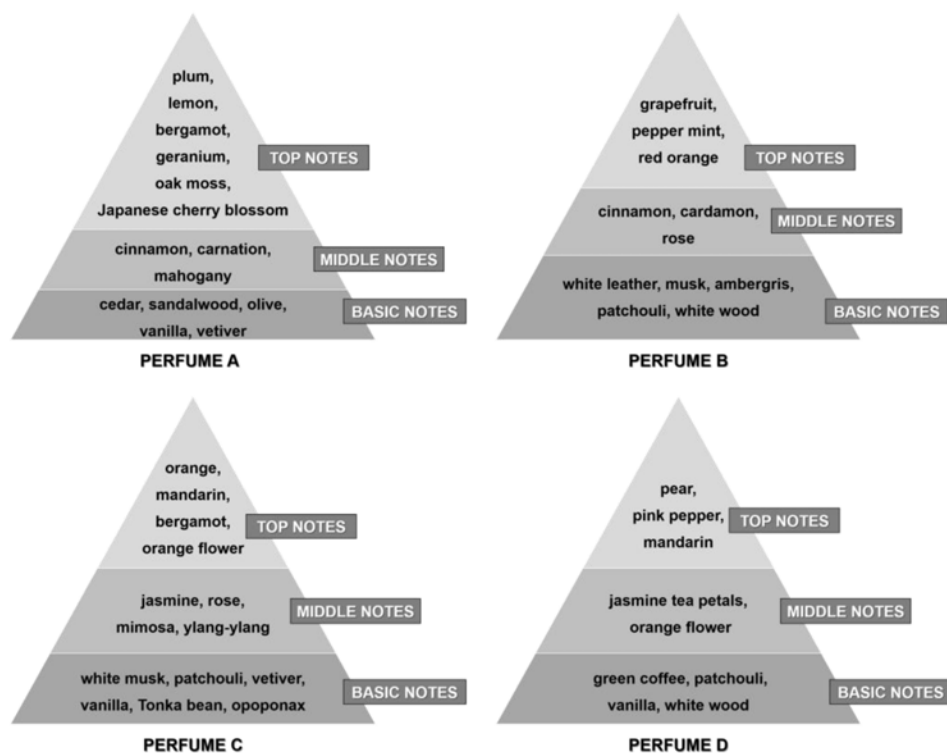


Fig. 1 Fragrance pyramids of original perfumes analyzed by HPLC-MS technique.

(0.05%, v/v) was used as a mobile phase. The other parameters have been set as above.

### 2.3 Sample and sample preparation

In case of this research, two samples of perfumes for men (A, B), two samples of perfumes for women (C, D) and four samples of perfume imitations were analyzed. The original ones were bought in popular perfumery in Gdańsk, whereas their cheaper versions were bought in Chinese shop. The scent compositions of original perfumes are shown at Fig. 1.

Both original and cheaper perfume samples (250  $\mu$ L) were diluted in 250  $\mu$ L of acetonitrile containing 3% of water. Such prepared samples were injected (20  $\mu$ L) directly into the HPLC-Q-TOF-MS system.

## 3. Results and discussion

In this presented study, different chromatographic system has been used in order to determine perfumes components. The samples of original perfumes and their imitations were analyzed by SCAN mode. Each obtained chromatogram LC-HRMS

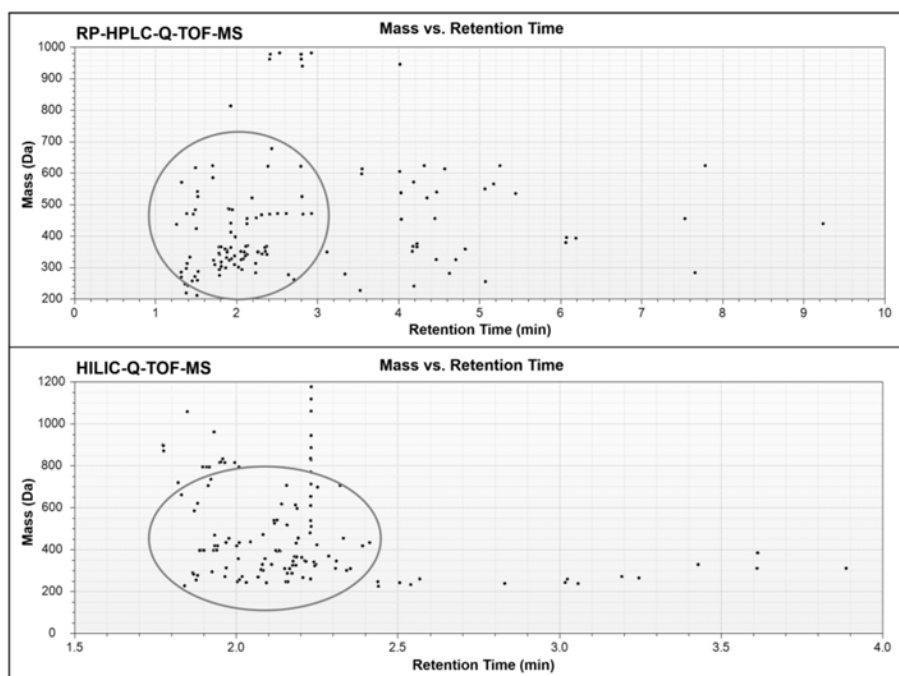


**Fig. 2** The relationship between the mass of chemical species detected in perfumes samples and the retention time.

were processed with Molecular Feature Extraction (MFE) mode. The results achieved for sample A (both ESI modes) are shown in Fig. 2. In case of RP-HPLC-Q-TOF-MS, low molecular compounds (200–500 Da) and medium molecular weight compounds (500 Da < ) were generally detected. In case of HILIC-Q-TOF-MS, the same situation was observed. However, the use of HILIC enabled to determine more compounds with mass higher than 700 Da.

The next step was to identify the perfumes ingredients. Perfumes contain various chemicals that can be classified in six categories: solvents, essential oils, dyes, modifiers, blenders, and fixatives [5]. It was decided that the identification would be based on information about perfumes composition, which is partially available, and the list of compounds used in perfumery published by International Fragrance Association (IFRA). Some compounds detected in the perfume samples were presented in Table 1. The results for two types of perfumes are shown in Table 2.

Compounds belong to fatty acids were detected in all samples. They are the components of carrier oils that are used to dilute essential oils and absolutes. Compounds specific to fragrances of animal origin (musk, ambergris) were found in both original perfume samples. These substances are not only used as base notes in perfumery, but also as fixatives. Due to the limited amount of natural musk and ambergris available on the market, they are very expensive. Furthermore, antioxidants (avobenzone, diethylamino hydroxybenzoyl hexyl benzoate)

**Table 1**

Basic information about compounds detected in perfumes samples.

Compound	Molecular formula	Monoisotopic mass/ Da	Ionization mode	Theoretical $m/z$
ambroxide	C <sub>16</sub> H <sub>28</sub> O <sub>2</sub>	236.2140	Positive	237.2213
atranol	C <sub>8</sub> H <sub>8</sub> O <sub>3</sub>	152.0473	Negative	151.0401
avobenzone	C <sub>20</sub> H <sub>22</sub> O <sub>3</sub>	310.1569	Positive	311.1642
dimethyl benzyl carbinyl butyrate	C <sub>14</sub> H <sub>20</sub> O <sub>2</sub>	220.1463	Positive	221.1536
diethylamino hydroxy- benzoyl hexyl benzoate	C <sub>24</sub> H <sub>31</sub> NO <sub>4</sub>	397.2253	Positive	398.2326
mintlactone	C <sub>10</sub> H <sub>14</sub> O <sub>2</sub>	166.0994	Positive	167.1066
muscone	C <sub>16</sub> H <sub>30</sub> O	238.2296	Positive	239.2369
oleic acid	C <sub>18</sub> H <sub>34</sub> O <sub>2</sub>	282.2559	negative	281.2486
palmitic acid	C <sub>16</sub> H <sub>32</sub> O <sub>2</sub>	256.2402	Negative	255.2329
pentadecanoic acid	C <sub>15</sub> H <sub>30</sub> O <sub>2</sub>	242.2246	Negative	241.2173
stearic acid	C <sub>18</sub> H <sub>36</sub> O <sub>2</sub>	284.2715	Negative	283.2642
vanillin	C <sub>8</sub> H <sub>8</sub> O <sub>3</sub>	152.0473	Positive	153.0546

that are added to perfumes to protect their color and scent composition were detected in original perfumes. In case of perfume A, atranol, dimethyl benzyl carbinyl butyrate and vanillin were detected. These compounds are characteristic for some essential oils. The first one can be determined in oak moss essential oils, the second one in plum essential oils, whereas the third one is specific to vanilla essential oils. In case of its imitation, atranol was only detected. This compound has been identified as the allergen, so its concentration in perfumes should be regulated. Mintlactone was identified in both samples C and C'. It is a fragrance compound that can be found in Tonka bean oils. Coumarin is the second compound that can be detected in this essential oil.

#### 4. Conclusions

The price of perfumes is affected by the cost of their production. Because of the usage of small availability components, some of the perfumes are expensive and still very desirable. For this reason, many perfume imitations are reaching the markets. Most of compounds that vary perfumes and their imitations are commonly detected during GC analyses. However, the determination of essential oil components, musk and other fixatives confirmed that the LC-MS can be used as a complementary technique to GC or GC-MS. Two different chromatographic systems were applied for perfume analysis. In both cases low molecular weight compounds (from 200 Da to 500 Da) were generally detected. Nonetheless, most identified perfumes ingredients were only determined in samples analyzed with RP-HPLC-Q-TOF-MS system.

**Table 2**

Compounds detected in original perfume samples (A, C) and their imitations (A', C') using two different chromatographic system (+ = detected under used conditions, - = not detected under used conditions).

Sample	Compound	Experimental <i>m/z</i>	Mass accuracy /ppm	RP-HPLC	HILIC
A	ambroxide	237.2217	1.81	+	-
	atranol	151.0410	-5.96	+	+
	dimethyl benzyl carbinyl butyrate	221.1537	0.45	+	+
	diethylamino hydroxy- benzoyl hexyl benzoate	398.2331	1.26	+	+
	oleic acid	281.2480	-2.13	+	-
	palmitic acid	255.2332	1.76	+	+
	pentadecanoic acid	241.2178	-2.07	+	+
	stearic acid	283.2639	-1.06	+	+
	vanilin	153.0539	-4.57	+	-
	A'	atranol	151.0406	3.31	+
palmitic acid		255.2339	3.92	+	-
C	ambroxide	237.2214	-0.42	+	-
	avobenzene	311.1644	0.64	+	-
	mintlactone	167.1067	0.56	+	-
	muscone	239.2372	-1.25	+	-
	oleic acid	281.2494	2.84	+	-
	palmitic acid	255.2336	2.74	+	+
	stearic acid	283.2647	1.77	+	+
C'	coumarin	147.0441	0.00	+	-
	mintlactone	167.1064	-1.20	+	-
	oleic acid	281.2491	1.78	+	-
	palmitic acid	255.2338	3.53	+	+
	pentadecanoic acid	241.2180	2.90	+	+
	stearic acid	283.2648	2.12	+	+

## References

- [1] Mondello L., Casilli A., Tranchida P.Q.: Comprehensive two-dimensional gas chromatography in combination with rapid scanning quadrupole mass spectrometry in perfume analysis. *J. Chromatogr. A* 1067 (2005), 235–243.
- [2] Ghergel S., Morgan R.M., Blackman C.S., Karu K., Parkin I.P.: Analysis of transferred fragrance and its forensic implications. *Sci. Justice* 56 (2016), 413–420.
- [3] van Asten A.: The importance of GC and GC-MS in perfume analysis. *Trends Anal. Chem.* 21 (2002), 698–708.
- [4] Abedi G., Telebpour Z., Jamechenarboo F.: The survey of analytical methods for sample preparation and analysis of fragrances in cosmetics and personal care products. *Trends Anal. Chem.* 102 (2018), 41–59.
- [5] Palmer I.: Perfume making-An overview. In: *Perfume, Soap and Candle Making. The Beginner's Guide*. Omaha, Wow Enterprises 2013, p. 11–28.

# Study of the effect of the hybridisation process on the content of terpenes in oroblanco fruit (*Citrus paradisi* × *Citrus grandis*)

MARTYNA LUBINSKA-SZCZYGEŁ\*, ANNA RÓŻAŃSKA, TOMASZ DYMERSKI, JACEK NAMIEŚNIK

Department of Analytical Chemistry, Chemical Faculty, Gdańsk University of Technology, Narutowicza Street 11/12, 80 952, Gdańsk Poland ✉ [martyna.lubinska@pg.edu.pl](mailto:martyna.lubinska@pg.edu.pl)

## Keywords

aroma properties  
fruit hybridization  
sweetie  
terpenes

## Abstract

Fruit hybridization is a process that has been used for many years and results in formation of fruits with new organoleptic and health-promoting properties. The purpose of hybridization is also to improve the fruit's functional properties. The paper presents the comparison of the content of terpenes of hybrid fruit namely oroblanco and its parent fruits, grapefruit and pummelo. By the use of two-dimensional gas chromatography coupled with mass spectrometry it was possible to determine the most abundant terpenes in the volatile fraction of sweetie, grapefruit, and pummelo. A-terpineol and limonene were selected as main terpenes compounds determined in the headspace of sweetie and grapefruit. In the case of pummelo, it was possible to determine only one chemical compound, namely limonene.

---

## 1. Introduction

In recent years, there has been an increasing interest in health food, which is why new varieties of plants with a high content of pro-health substances such as vitamins, minerals and bioactive substances are being sought for. From the point of view of fruit producers, the new varieties should have specific functional properties, such as those associated with greater resistance to climatic factors, higher yields or lack of seeds [1]. One of the popular solutions in recent years is the creation of hybrid plants. Fruit hybridization, or cross-breeding, is the process of botanical mating of two different plant species in order to create hybrids that have all the best qualities of mother plants and none of its disadvantages [2].

One of the commonly available hybrid fruit in recent years is oroblanco called sweetie (*Citrus paradisi* × *Citrus grandis*), hybrid between grapefruit (*Citrus paradisi*) and the giant orange, called pummelo (*Citrus grandis*). It is seedless fruits, less acidic and less bitter than the grapefruit [3], which is related to the different

content of terpenes, aldehydes, esters, ketones and carboxylic acids. According to the literature, terpenes are the most abundant compound in most of citrus fruits [4]. These are compounds belonging to the group of bioactive compounds, showing antioxidant, antibacterial activity, etc. Their presence also determines the taste and aroma of newly-created fruits, which affects their consumption by consumers.

Due to the complex composition of the matrix for the determination of volatile compounds, an analytical technique to give rise to improved resolution and peak capacity is required. In line with the principles of green analytical chemistry, the aim is also to use solvent-free extraction techniques, therefore HS-SPME-GC×GC-TOFMS is pure foreign performed [5]. The aim of the conducted research was to compare the content of terpenes in samples of oroblanco and its parents fruits using two-dimensional gas chromatography.

## 2. Experimental

### 2.1 Reagents and chemicals

Standards of terpenes:  $\alpha$ -pinene, limonene, ocimene, myrcene,  $\gamma$ -terpinene,  $\alpha$ -terpineol (Sigma-Aldrich, USA) were diluted in methanol (Avantor Performance Materials Poland). The fruits for testing were purchased at local distribution points in the Pomeranian Voivodship. Due to the complex composition of the matrix, which are fruits and varied structure and properties of the compounds identified to eliminate the matrix effect, the standard addition method was used.

### 2.2 Instrumentation

An Agilent 6890A gas chromatograph (Agilent Technologies, USA) equipped with a split/splitless injector and a liquid nitrogen-based dual stage cryogenic modulator, coupled with Pegasus IV time-of-flight mass spectrometer. In case of isolation and enrichment of analytes solid phase microextraction was used.

## 3. Results and discussion

The identified compounds were divided into eight chemical classes. As it can be seen at Fig. 1. the dominant class in the fruit samples tested are terpenes. The high content of terpenes can determine the bitter taste of citrus [6]. A significant chemical class, regarding to the amount of identified substances, was the group of alcohols, esters, aldehydes and ketones. These are chemicals with a specific, often intense odour. Their presence and synergistic interactions cause intense aroma of fruits.

Table 1 presents all terpenes identified and quantified in sweetie, pummelo and grapefruit samples. Based on the results it can be stated that pummelo is the

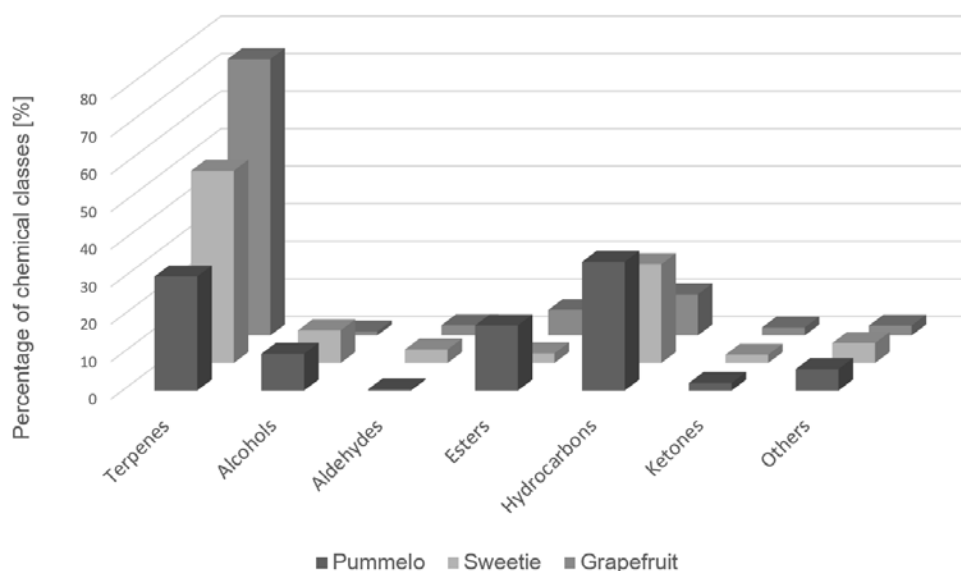


Fig. 1 Content of selected classes of chemicals in samples of sweetie, pummelo and grapefruit.

Table 1

Quantitation of selected terpenes present in the volatile fraction of sweetie, pummelo, and grapefruit.

Compound	$R^2$	Concentration/ $\mu\text{g g}^{-1}$			$LOQ/\mu\text{g g}^{-1}$	$LOD/\mu\text{g g}^{-1}$
		sweetie	pummelo	grapefruit		
$\alpha$ -Pinene	0.999	$0.8241 \pm 0.0096$	<LOQ	$2.851 \pm 0.015$	0.664	0.219
Limonene	0.996	$5.298 \pm 0.058$	$2.057 \pm 0.092$	$15.79 \pm 0.30$	1.431	0.472
Ocimene	0.995	$1.600 \pm 0.097$	<LOQ	$2.057 \pm 0.078$	1.519	0.501
$\beta$ -Myrcene	0.991	$4.1 \pm 0.14$	<LOQ	$3.224 \pm 0.0293$	2.098	0.692
$\gamma$ -Terpinene	0.997	$7.27 \pm 0.34$	<LOQ	$2.566 \pm 0.026$	1.163	0.384
$\alpha$ -Terpineol	0.992	$20.96 \pm 0.70$	<LOQ	$87.9 \pm 2.0$	1.947	0.643

least aromatic one. Despite the use of GC $\times$ GC technique, it was possible to quantify only one substance, namely limonene, in the fruit pulp. In contrast, in the grapefruit and sweetie samples, six chemical compounds, belonging to the terpenes group, were identified and determined. In both cases, the highest content of  $\alpha$ -terpineol was indicated. The four fold more amount of this substance was noted in grapefruit than in sweetie samples. The earthy odor description of  $\alpha$ -terpineol is one of the reasons for the bitter taste of the fruit. The highest content of limonene was noted in the grapefruit, namely  $15.79 \pm 0.30 \mu\text{g g}^{-1}$ . Moreover, sweetie contains more myrcene and  $\gamma$ -terpinene with pleasant citrus aroma which may explain its sweet and less bitter taste compared to grapefruit. Considering the content of individual terpenes in the samples of the sweetie pulp

and its parent fruit, it can be concluded that the hybrid fruit correlates to grapefruit. Due to the high content of chemical compounds in this chemical class, sweetie is a rich source of health-promoting ingredients.

#### 4. Conclusions

Using the analytical procedure during the presented studies, it was possible to determine the content of selected terpenes in the sweetie and its parent fruits samples and to find the reasons for the less bitter and acidic sweetie taste compared to the grapefruit. It was also shown that the high content of terpenes with bioactive activity is a feature that sweetie inherited from the grapefruit during the hybridization process.

#### References

- [1] Sansavini S., Donati F., Costa F., Tartarini S.: Advances in apple breeding for enhanced fruit quality and resistance to biotic stresses: new varieties for the european market. *J. Fruit Ornament. Plant Res.* **12** (2004), 13–52.
- [2] Burke J.M., Arnold B.J.: Genetics and the fitness of hybrids. *Annu. Rev. Genet.* **35** (2001), 31–52.
- [3] Gazit Y., Kaspi R.: An additional phytosanitary cold treatment against *Ceratitis capitata* (diptera: tephritidae) in 'oroblanco' citrus fruit. *J. Econ. Entomol.* **110** (2017) 790–792.
- [4] Dharmawan J., Kasapis S., Curran P., Johnson J.R.: Characterization of volatile compounds in selected citrus fruits from Asia. Part I: freshly-squeezed juice. *Flavour Fragr. J.* **22** (2007), 228–232.
- [5] Lubinska-Szczygeł M., Różańska A., Dymerski T., Namieśnik J., Katrich E., Gorinstein S.: A novel analytical approach in the assessment of unprocessed Kaffir lime peel and pulp as potential raw materials for cosmetic applications. *Ind. Crops Prod.* **120** (2018), 313–321.
- [6] Ren J.N., Tai Y.N., Dong M., Shao J.H., Yang S.Z., Pan S.Y., Fan G.: Characterisation of free and bound volatile compounds from six different varieties of citrus fruits. *Food Chem.* **185** (2015), 25–32.

# Correlation between chemical composition and the presence of selected groups of bacteria in freshwater samples collected from Isfjorden and Billefjorde

FILIP PAWLAK<sup>a,\*</sup>, KATRZYNA JANKOWSKA<sup>b</sup>, ŻANETA POLKOWSKA<sup>a</sup>

<sup>a</sup> *Department of Analytical Chemistry, Faculty of Chemistry, Gdansk University of Technology, 11/12 Narutowicza St., 80-233 Gdańsk, Poland ✉ filpawla@student.pg.edu.pl*

<sup>b</sup> *Department of Water and Waste-Water Technology, Faculty of Civil and Environmental Engineering, Gdansk University of Technology, 11/12 Narutowicza St., 80-233 Gdańsk, Poland*

## Keywords

Arctic  
Bacteria  
pollutants  
Spitsbergen

## Abstract

The average concentrations of pollutants in the arctic water, snow and the atmosphere are much lower than those observed in the temperate climate. Specific conditions occurring in the polar regions have a potential to accumulate the pollutants transported from other parts of the world. In this study, attempts were made to find a correlation between selected chemical components and the bacterial population. The analysis involved 11 samples of water collected from rivers and streams flowing into Isfjorden and Billefjorde in summer 2017 (Spitsbergen, Svalbard). Water samples were analysed in order to determine the concentration of various substances such as PAHs, metals, main cations, and anions. Additionally, parameters such as pH, SEC, TOC, number, average size and biomass of bacterioplankton were also measured. On the basis of the obtained results, it was impossible to determine the relationship between the measured substances and the bacterial community.

---

## 1. Introduction

The interest in the subject of pollution in the Arctic has increased when compounds, whose nearest potential source of emission was several thousand kilometers away, were detected there. Since then, the main focus has been on the impact of pollutants on the higher-order organisms found in this region, and little attention has been paid to microorganisms.[1] It is assumed that the contamination in the polar regions are derived mainly from the emission sources located in regions with temperate climates. It is believed that the transport of the chemicals over large distances is caused by the grasshopper effect. This phenomenon is concerning mainly the light organic compounds characterized by low vapor

pressure. The mechanism of this effect is as follows: volatile compounds evaporate intensely into the atmosphere and then they are transported with warm masses of air to Arctic. In polar regions, the temperature decreases significantly, which leads to the condensation and deposition of pollutants. Solid particles, on which nonvolatile substances can be absorbed, are also carried with warm masses of air. Moreover, pollutants can be transported by sea and river, as well as ice forming on the coast of Siberia [2]. In addition, in some parts of the Arctic local sources of pollution such as human settlements, hard coal mines, power plants, and means of transport may be located [3]. However, concentration of the pollutants is not the only factor that affects the bacterial community. In order to assess its condition, concentration of naturally occurring compounds and elements should also be measured [4]. Moreover, specific climatic conditions such as low average annual temperature, the occurrence of polar night and day, low insolation, presence of ice and snow may contribute to the increase of durability of organic compounds. The global warming and, in effect, rapidly changing climatic conditions in the Arctic caused by global warming can cause remissions of the compounds accumulated in this region [5]. It may create a threat to the fauna and flora of the region. In addition, organisms and microorganisms adapted to life in a colder climate can be supplanted by organisms better adjusted to higher temperatures [6].

## **2. Experimental**

### *2.1 Study area*

The samples were collected from rivers and streams flowing into Isfjorden and Billefjorde in summer 2017 (Spitsbergen, Svalbard). Water samples can be divided into two categories based on the different research areas: three water samples were collected from rivers and lakes that go out to the Billefjorden fjord, and remaining eight were collected from the Isfjorden fjord. Both of these fjords are located in the western part of Spitsbergen. The exact geographical locations are presented on the Fig. 1.

### *2.2 Sampling*

In order to obtain samples representative of the whole watercourse, sampling places were chosen carefully, with morphological and hydrological characteristics of the watercourse, as well as the proximity of the local pollution sources taken under consideration. Samples were collected to hermetically clean 1 L containers with the use of manual sampling technique.

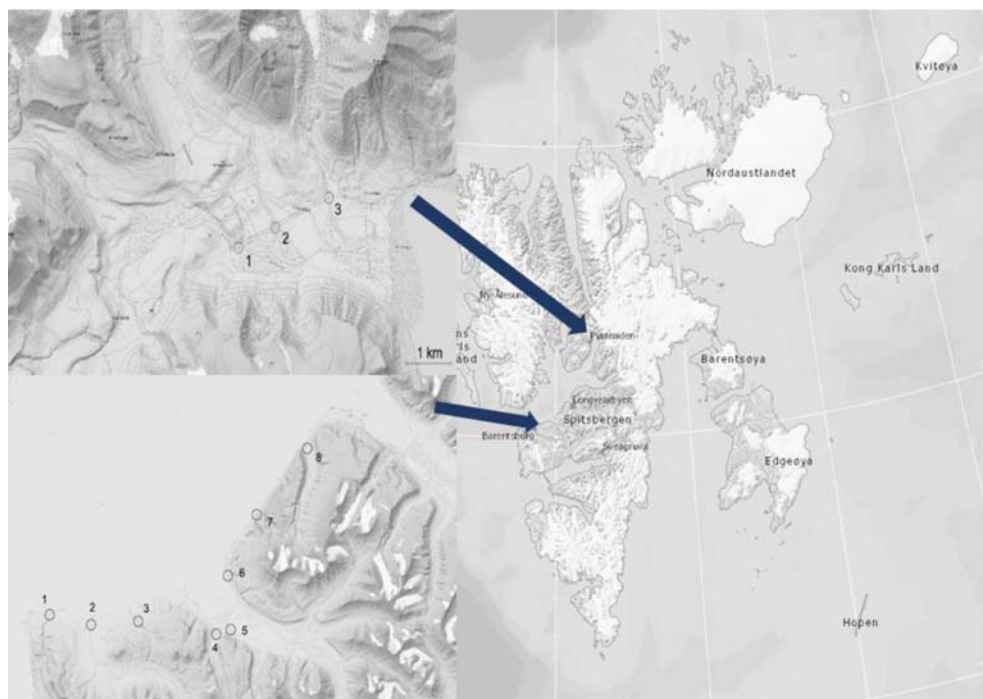
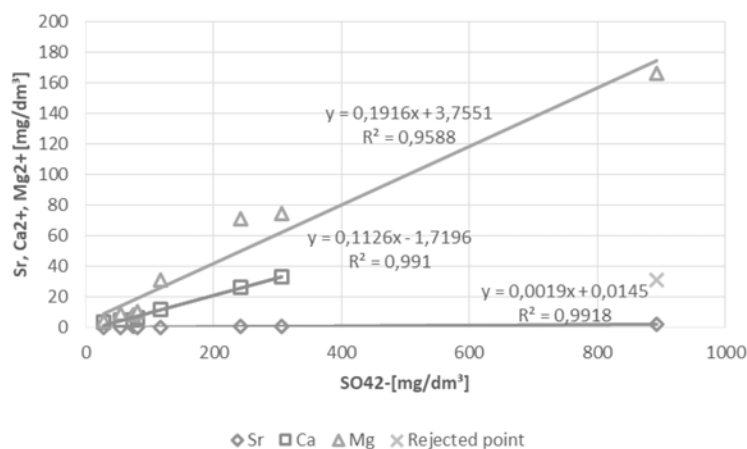


Fig. 1 The map of sampling area with the location of sampling points.

### 2.3 Instrumentation

The following methods were used to determine the analytes: PAHs – gas chromatography (GC Shimadzu 2010 plus) coupled with a mass spectrometry (MS Shimadzu TQ8050), fitted with a detector with the electron ionization Ion chromatography coupled with a conductivity detector (DIONEX ICS-3000) was used in order to analyse the ions, while – while metals were analysed with Inductively Coupled Plasma Mass Spectrometry (Thermo Scientific XSERIES 2 ICP-MS). Sum of phenols and formaldehyde was measured with Spectroquant-Pharo 100 Spectrophotometer, TOC – catalytic oxidation with oxygen at 680 °C with non-dispersive infrared spectroscopy (Total Organic Carbon Analyser TOC-VCSH/CSN). Measurements of pH and electrical conductivity (EC) were performed with the use of microcomputer pH-meter and conductivity meter CPC-411 (Elmetron) equipped with an EC60 conductivity sensor. Microbiological analysis consisted in the estimation of the number, average size and biomass of bacterio-plankton. The direct counting method was used to perform the analysis. The measuring apparatus consisted of a Nikon 80i epifluorescence microscope, a Nikon DS-5Mc-U2 color digital camera. Pre-counting of bacteria was carried out using the NisElements and Multiscan programs. Then the preliminary results were entered into Microsoft Excel and converted into a suitably configured macrodefinition.



**Fig. 2** The relation between the content of magnesium ions, calcium and elemental strontium, and sulphate ions for samples from rivers and streams flowing into Isfiorden.

### 3. Results and discussion

Due to the presence of the suspension obscuring the bacterial cells, the total viable count could not be measured in several samples. The measurement was carried out for 6 out of 11 tested samples. The lack of results prevented a meaningful interpretation of the relationship between the chemical composition of water and bacterial communities.

However, it was possible to find correlations between the concentration of some chemical compounds. In Fig. 2, the interconnection between the content of magnesium ions, calcium, elemental strontium, and sulphate ions in samples from rivers and streams flowing into Isfiorden, can be seen. By setting the trend line for calcium content, the sample taken at point L1 was not taken into account because of the possibility of too much sewage from Barentsburg. The L1 sample was marked on the graph as - Rejected point. The linear relationship between the above-mentioned analytes suggest that they may come from the same origin. It is most likely that they come from the dissolution of local rocks.

The Principal components analysis was performed for selected variables. Variables taken into account are: pH, electrical conductivity, total organic carbon, sum of anion concentrations, sum of cation concentrations, sum of concentrations of polycyclic aromatic hydrocarbons, and sum of selected metals (Ag, As, Bi, Cd, Co, Cr, Cu, Fe, Hg, Mo, Ni, Pb, Sb, Se, V). Some variables have been logarithmized to better show distributions. First two principal components covered 82% of the variance. A scatter plot obtained using PCA is presented in Fig. 3. As it can be seen, samples from two groups: the first of them includes samples L6, L8, Pi1, Pi2, Pi3 taken from rivers and streams occurring near the coal mine, while the second cluster includes samples L2, L3, L5, and L7 collected from rivers and streams around which there are no identified local sources of pollution.

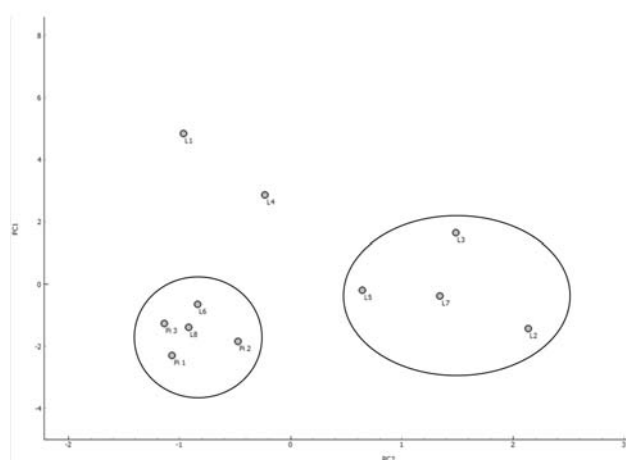


Fig. 3 The result of the PCA analysis.

#### 4. Conclusions

During the course of the experiment, several analysis have been performed: determination of PAHs, ions, formaldehyde, sum of phenol TOC, and selected metals, as well as the measurement of pH, EC, total count and average volume of bacterial cells and biomass. However, no significant correlation between the concentration of the analytes and the condition of bacterial community has been found. Lack of dependence can be caused by the complexity of bacterial metabolism, species diversity of microorganisms, and their environmental adaptation. The lack of full results could make it impossible to observe dependence. However, the analysis of the composition of the tested samples made it possible to find the linear relationship between elements such as calcium, magnesium and strontium, and sulphate ions, which may suggest that they originate from the same source, e.g., local rocks. The analysis of the main components made it possible to visualize the similarity between the samples taken from rivers and streams.

#### References

- [1] Kosek K., Kozak K., Koziół K., Jankowska K., Chmiel S., Polkowska Ż.: The interaction between bacterial abundance and selected pollutants concentration levels in an arctic catchment (southwest Spitsbergen, Svalbard). *Sci. Total. Environ.* **622–623** (2018), 913–923.
- [2] Ma J., Hung H., Macdonald R.: The influence of global climate change on the environmental fate of persistent organic pollutants: A review with emphasis on the Northern Hemisphere and the Arctic as a receptor. *Glob. Planet. Change.* **146** (2016), 89–108.
- [3] Zaborska A., Beszczyńska-Möller A., Włodarska-Kowalczyk M.: History of heavy metal accumulation in the Svalbard area: Distribution, origin and transport pathways. *Environ. Pollut.* **231** (2017), 437–450.
- [4] Grebmeier J., Overland J., Moore S., Farley E., Carmack E. Cooper L., Frey K., Helle J., McLaughlin F., McNutt S.: A major ecosystem shift in the Northern Bering Sea. *Science* **311** (2006), 1461–1464.
- [5] Kozak K., Polkowska Ż., Ruman M., Koziół K., Namieśnik J.: Analytical studies on the environmental state of the Svalbard Archipelago provide a critical source of information about anthropogenic global impact. *Trends Anal. Chem.* **50** (2013), 107–126.

- [6] Kallenborn R, Hung H, Brorström-Lundén E.: Chapter 13 – Atmospheric long-range transport of persistent organic pollutants (POPs) into Polar Regions In.: *Comprehensive Analytical Chemistry*. Vol. 64. E.Y. Zeng (ed.). Elsevier 2015, p. 411–432.

# Influence of terpenes on indoor air quality

KLAUDIA PYTEL\*, RENATA MARCINKOWSKA, BOŻENA ZABIEGAŁA

*Department of Analytical Chemistry, Faculty of Chemistry, Gdańsk University of Technology,  
G. Narutowicza 11/12, 80-233 Gdańsk Poland ✉ klapytel@student.pg.edu.pl*

## Keywords

hairdresser  
indoor air  
d-limonene  
secondary organic  
aerosol  
terpenes

## Abstract

The aim of this study was to investigate air quality in hairdresser salons, focusing on terpenes determination. Terpenes are known reactive volatile organic compounds that contribute to secondary organic aerosol formation. Those compounds are frequently found in cosmetic products as fragrance agents. Hairdresser salons are special kind of environment, where secondary organic aerosol concentration may be elevated. One hairdresser salon in Gdynia was chosen to carry out preliminary research. Indoor air samples from the salon were collected using diffusive samplers and sorbent tubes, which were later desorbed and analyzed by TD-GC-FID and TD-GC-MS. Determined limonene concentration varied between 6–74  $\mu\text{g m}^{-3}$ .

## 1. Introduction

According to United States Environmental Protection Agency 90% of the time people spent in closed spaces, which makes indoor air an important factor that influences human health [1–3]. The problem of indoor air quality arose in late 1960s and 1970s, when the term “sick building syndrome” appeared [4]. This term refers to symptoms like: irritation of upper airway, eyes, mucous membranes and skin [5]. It is believed that sick building syndrome is caused by volatile organic compounds [6] with terpenes as one of the contributors. Terpenes are produced mostly by conifer plants [7–8], however they are also emitted into indoor air from cleaning agents, perfumes, air fresheners and cosmetic products [9–11]. Terpenes most commonly present in indoor air are: d-limonene,  $\alpha$ -pinene and  $\beta$ -pinene [12]. Products formed due to the series of reactions initiated by terpenes oxidation may cause human health deterioration [6; 13–15]. The reason why the presence of terpenes in indoor air may be considered as a threat to human health is because products of their transformations undergo condensation and form secondary organic aerosol [17]. Secondary organic aerosol nanosized particles are able to penetrate deeply human respiratory track and even reach the bloodstream [18].

There were already a lot of studies on terpenes presence in indoor air, but to the best of our knowledge, there was no research concerning terpenes determination in hairdressers salons published yet. In this work we present the preliminary

**Table 1**

Thermal desorption, GC-MS and GC-FID parameters applied during analysis.

	GC-MS	GC-FID
Column	DB5MS 60 m × 0.25 mm × 1 μm (Agilent J&W)	DB1 30 m × 0.32 mm × 5 μm (Agilent Technologies)
Column flow	0.5 ml min <sup>-1</sup>	2.2 ml min <sup>-1</sup>
Temperature program	70 °C held for 1 min, ramped at 15 °C min <sup>-1</sup> to 120 °C and held for 1 min, ramped at 10 °C min <sup>-1</sup> to 280 °C and held for 5 min	40 °C held for 1 min, ramped at 10 °C min <sup>-1</sup> to 125 °C, ramped at 15 °C min <sup>-1</sup> to 240 °C and held for 5 min
Detector temperature	Ion source: 250 °C Quadrupole: 150 °C	250 °C
Thermal desorption prepurge	1 min (split ON)	1 min (split ON)
tube desorption	10 min at 300 °C (split OFF)	10 min at 300 °C (split OFF)
trap desorption	Trap low: 1 °C Trap high: 300 °C (split OFF)	Trap low: 1 °C Trap high: 300 °C (split OFF)

research concerning indoor air quality of this type of public service space. The aim is to determine chemical composition of indoor air, with a special attention paid to terpenes concentration, and its variability in hairdresser salon.

## 2. Experimental

### 2.1 Reagents and chemicals

Methanol (gradient grade for LC, Sigma-Aldrich), (R)-(+)-limonene (Sigma-Aldrich), calibration solutions were of following concentrations: 10; 100; 200 and 500 ng μl<sup>-1</sup>.

### 2.2 Instrumentation

Radiello<sup>®</sup> diffusive passive samplers with Carbograph<sup>®</sup> sorbent and tubes filled with Tenax<sup>®</sup> were applied to sample the indoor air. Passive samplers and sorbent tubes were desorbed using thermal desorption (TD) unit Markes<sup>®</sup>. Gaseous samples were analyzed by gas chromatography coupled to mass spectrometry (GC Agilent Technologies 6890, MS Agilent Technologies 5973) and flame-ionization detector (GC-FID Agilent Technologies 7820A). Parameters of thermal desorption unit and two chromatographic units are presented in Table 1.

### 2.3 Methodology of analytical procedure

All of analytical proceeding stages are presented in Fig.1. Location of Radiello<sup>®</sup> and active sampling with sampling tubes is presented in Fig. 2.

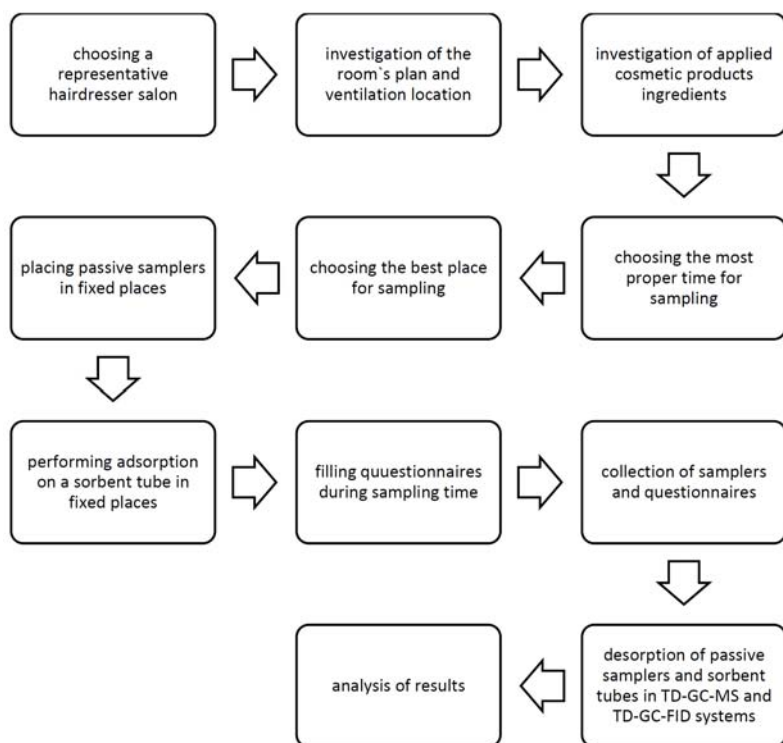


Fig. 1 Analytical proceeding steps applied in this research.

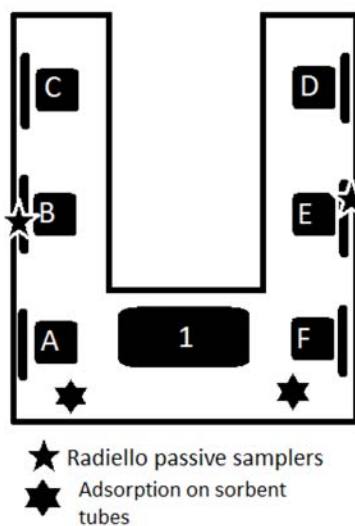


Fig. 2 Location of passive samplers and sorbent tubes sampling points at hairdresser salon.

**Table 2**

Limonene concentration determined in a chosen hairdresser salon.

Day of sampling	Limonene concentration/ $\mu\text{g m}^{-3}$	Total concentration of organic compounds/ $\mu\text{g m}^{-3}$
09.06.2018	6	322
16.06.2018	74	2246
20.06.2018	69	5122

### 3. Results and discussion

Sampling with Radiello<sup>®</sup> samplers last 5 hours (ca. since 10 a.m. to 3 p.m.) each day of sampling, whereas sampling with sampling tubes was performed around 2–3 p.m. each day. Sampling was carried out during the working days and at the weekend. Limonene concentrations calculated on the basis of the mass adsorbed on sampling tubes and determined by TD-GC-FID are presented in Table 2.

According to obtained results, limonene concentrations determined in hairdresser salon were sometimes higher in comparison to an exemplary studies carried out in Germany, which indicated limonene concentration at homes at a level of 15–20  $\mu\text{g m}^{-3}$  [19–22]. All differences in concentration could be caused by activities performed in the salon during the day. For example at 09.06.2018 limonene concentration was the lowest and sampling was carried out very close (1 meter) from the client with a hair dye. The type of hair dyes used in chosen salon does not have terpenes indicated in International Nomenclature of Cosmetic Ingredients and no noticeable scent. The highest concentration determined on the 16.06.2018 may be related to the fact that sampling occurred while hairdresser was using hair spray and other cosmetics in the form of aerosols, with relatively large amount of scented chemicals included. Chromatograms obtained by desorption of Radiello<sup>®</sup> samplers present more precise picture of the complicity of indoor air composition, which can be seen on an exemplary chromatograms obtained by TD-GC-FID and TD-GC-MS (Fig. 3) analysis.

MS detector was applied in order to carry out qualitative analysis and determine components of the indoor air. On the GC-MS chromatogram limonene peak intensity is relatively low in comparison to siloxanes (Fig. 3B). There are also alcohols peaks of high intensity visible at the beginning of chromatogram and their presence is justified due to the fact that they are common cosmetic ingredients. FID detector was applied mainly to get quantitative information about analytes present in the sample. Chromatogram obtained by GC-FID proves that indoor air from hairdresser salon is a complex sample containing a set of different chemicals (a lot of chromatographic peaks on Fig. 3A). Siloxanes are not visible on FID chromatogram, because FID is selective towards compounds that possess C–H bonding in a structure.

Such high concentration of siloxanes in indoor air of hairdresser salon may be explained by the fact that siloxanes are common ingredients of hair cosmetic

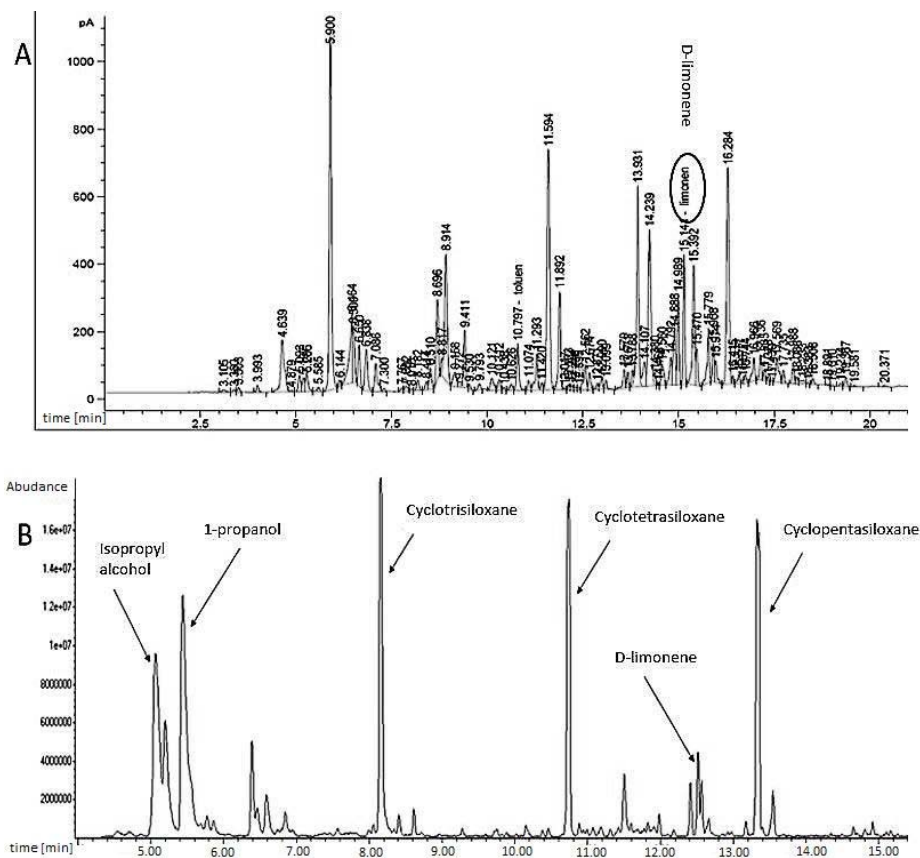


**Fig. 3** Chromatogram obtained by (A) GC-FID, and (B) GC-MS analysis of the sample collected on the fourth day of sampling.

products. Such high concentration of siloxanes may also be considered as a threat for workers and clients health, because according to the literature, siloxanes were determined as components of atmospheric aerosol and may irritate human respiratory system [23].

#### 4. Conclusions

In this paper we proved that indoor air of hairdresser salons contains precursors for secondary organic aerosol formation. It is necessary to continue this research in order to improve analytical approach and obtain more data. It would be very helpful to use in the future particle counters like SMPS (Scanning Mobility Particle Sizers) to determine the exact dependence between the amount of terpenes in indoor air and the amount and spatial distribution of created secondary organic aerosol particles.

## References

- [1] US EPA: *Air Quality Criteria for Particulate Matter. National Center for Environmental Assessment Office of Research and Development. 1. 2001*
- [2] US EPA: *Air Quality Criteria for Particulate Matter. National Center for Environmental Assessment Office of Research and Development. 2. 2004.*
- [3] US EPA: *Air Quality Criteria for Particulate Matter. National Center for Environmental Assessment Office of Research and Development. 3. 1996.*
- [4] Sundell J.: On the history of indoor air quality and health. *Indoor Air* **14** (2004), 51–58.
- [5] Spengler J.D., Samet J.M., McCarthy J.F.: *Indoor Air Quality Handbook*. New York, McGraw-Hill 2001.
- [6] Missia D.A., Demetriou E., Michael N., Tolis E.I., Bartzis J.G.: Indoor exposure from building materials: A field study. *Atmospheric Environ.* **44** (2010), 4388–4395.
- [7] Curci G., Beekman M., Vautard R., Smiatek G., Steinbrecher R., Theloke J., Friedrich R.: Modeling study of the impact of isoprene and terpene biogenic emission on European ozone levels. *Atmospheric Environ.* **43** (2009), 1444–1455.
- [8] Schripp T., Langer S., Salthammer T.: Interaction of ozone with wooden building products, treated wood samples and exotic wood samples. *Atmospheric Environ.* **54** (2012), 365–372.
- [9] Nazaroff W.W., Weschler J.W.: Cleaning products and air fresheners: exposure to primary and secondary air pollutants. *Atmospheric Environ.* **38** (2004), 2841–2865.
- [10] Wolkoff P., Clausen P., Wilkins C., Nielsen G.: Formation of strong airway irritants in terpene/ozone mixtures. *Indoor Air* **10** (2000), 82–91.
- [11] Tsigonia A., Lagoudi A., Chandrinou S., Linos A., Eylogias N., Alexopoulos EC.: Indoor air in beauty salons and occupational health exposure of cosmetologists to chemical substances. *Int. J. Environ. Res. Public Health* **7** (2010), 314–324.
- [12] Hodgson A., Beal D.: Sources of formaldehyde, other aldehydes and terpenes in a new manufactured house. *Indoor Air* **12** (2001), 235–242.
- [13] Holcomb L.C., Seabrook B.S.: Indoor concentrations of volatile organic compounds: implications for comfort, health and regulation. *Indoor Environment.* **4** (1995), 7–26.
- [14] Kotzias D., Geiss O., Tirendi S., Josefa BM., Reina V., Gotti A., Graziella CR., Casati B., Marafante E., Sargiannis D.: Exposure to Multiple air contaminants in public buildings, schools, kindergartens– the european indoor air monitoring and exposure assessment (AIRMEX) study. *Fresenius Environ. Bull.* **18** (2009), 670–681.
- [15] Eriksson K.A., Levin J.O., Sandström T., Lindström-Espeling K., Lindén G., Stjernberg N.L.: Terpene exposure and respiratory effects among workers in Swedish joinery shops. *Scand. J. Work Environ. Health* **23** (1997), 114–120.
- [16] Wolkoff P., Larsen ST., Hammer M., Kofoed-Sørensen V., Clausen P.A., Nielsen G.D.: Human reference values for acute airway effects of five common ozone-initiated terpene reaction products in indoor air. *Toxicol. Lett.* **216** (2013), 54–64.
- [17] Ito K., Harashima H.: Coupled CFD analysis of size distribution on indoor secondary organic aerosol derived from ozone/limonene reaction. *Build. Environ.* **46** (2011), 711–718.
- [18] Borduas N., Lin V.S.: Research highlights: Laboratory studies of the formation and transformation of atmospheric organic aerosols. *Environ. Sci. Process. Impacts* **18** (2016), 425–428.
- [19] Schlink U., Rehwagn M., Damm M., Richter M., Borte M., Herbarth O.: Seasonal cycle of indoor-VOCs: comparison of apartments and cities. *Atmospheric Environ.* **38** (2004), 1181–1190.
- [20] Schlink U., Roder S., Kohajda T., Wissenbach D.K., Franck U., Lehmann I.: A framework to interpret passively sampled indoor-air VOC concentrations in health studies. *Build. Environ.* **105** (2016), 198–209.
- [21] Matysik S., Ramadan A.B., Schlink U.: Spatial and temporal variation of outdoor and indoor exposure of volatile organic compounds in Greater Cairo. *Atmos. Pollut. Res.* **1** (2010), 94–101.

- [22] Rosch C., Kohajda T., Roder S., Bergen M., Schlink U.: Relationship between sources and patterns of VOCs in indoor Air. *Atmos. Pollut. Res.* **5** (2014), 129–137.
- [23] Chandramouli B., Kamens M.R.: The photochemical formation and gas–particle partitioning of oxidation products of decamethyl cyclopentasiloxane and decamethyl tetrasiloxane in the atmosphere. *Atmospheric Environ.* **35** (2001), 87–95.

# Classification of adulterated raspberry juice using ultra-fast gas chromatography

ANNA RÓŻAŃSKA\*, MARTYNA LUBINSKA-SZCZYGEŁ, TOMASZ DYMERSKI, JACEK NAMIEŚNIK

*Department of Analytical Chemistry, Faculty of Chemistry, Gdańsk University of Technology,  
11/12 Gabriela Narutowicza Street, 80-233 Gdańsk, Poland ✉ [anna.rozanska@pg.edu.pl](mailto:anna.rozanska@pg.edu.pl)*

## Keywords

electronic nose  
fruit juices  
gas chromatography  
hierarchical cluster  
analysis

## Abstract

In order to ensure the proper quality of food products, it is important to detect food contaminations. The aim of this work was to present the possibility of using ultra-fast gas chromatography technique to detect the adulteration of raspberry juice. The subjects were Not From Concentrate raspberry and chokeberry juices, as well as mixtures of these juices. Classification of juice samples was carried out using unsupervised statistical method – Hierarchical Cluster Analysis. Based on the results it can be concluded that the using ultra-fast gas chromatography technique coupled with Hierarchical Cluster Analysis method allowed to distinguish adulterated and unadulterated raspberry juice.

---

## 1. Introduction

Consumer awareness is increasing in recent years. They pay more and more attention to the health-promoting properties of food products. Consumers drink more and more pure and naturally cloudy fruit juices, which belong to the group of Not From Concentrate juices. According to the European Fruit Juice Association, the demand for Not From Concentrate juices has increased of about 14.0% (over the past five years) [1]. The most commonly consumed Not From Concentrate juice is orange juice [2], however, it can be noticed that the popularity of juices produced from berries, such as raspberries, blueberries, blackberries and chokeberry increased. These juices are characterized by a high content of bioactive compounds, such as polyphenols, carotenoids or anthocyanins [3–5]. Therefore, the ingestion of these juices as a part of the diet can have a positive effect on health and the human body. Luo et. al. [6] exhibit that consuming raspberry juice may result in improved metabolism. Hatcher [7], on the other hand, has proven that raspberry juice has a positive effect on bone health and protects it against osteoporosis. In Poland, there was a problem with the utilization of chokeberry fruit. Therefore, according to experts' opinions, these fruits can be used as an addition to juices produced from other berries.

In order to provide consumers with safe and high-quality food products, it is extremely important that food does not contain additives. In the case of fruit juices, impurities may be water, dyes or the addition of other cheaper juices [8, 9]. A very important element of this type of products is their aroma, which directly affects the flavour. For this reason, the gas chromatography technique is used to evaluate the aroma profile of raspberry juices [10]. On the other hand, liquid chromatographic techniques are the most commonly used to detect adulteration of these juices [11, 12]. The use of these methods is often labour- and time-consuming. On this account, new rapid procedures to detect adulteration of fruit juice samples are sought.

## 2. Experimental

### 2.1 Samples

Raspberry and chokeberry Not From Concentrate juices were obtained at local distribution centres in Gdansk. The juice mixtures (5 / 10 / 30 / 50% v/v addition of chokeberry) were prepared immediately after their purchase. Samples of  $5.0 \pm 0.1$  grams were poured into 20 cm<sup>3</sup> glass vials and sealed with a cap with a silicone-PTFE membrane. Samples were refrigerated at 4 °C for 24 hours. For each type of samples, the analyses were performed in ten replicates.

### 2.2 Instrumentation

Headspace analysis of fruit juice samples was performed using an ultra-fast gas chromatograph Heracles II (Alpha MOS, Toulouse, France) equipped with the HS 100 autosampler (Gerstel, Mülheim, Germany). The analytes are transferred in a carrier gas stream (hydrogen) to a sorption trap filled with 10 mg of TenaxTA sorbent. Then, the analytes are desorbed and put into two parallel chromatographic columns whose stationary phases are characterized by different polarity (non-polar MTX-5 and medium-polar MXT-1701). After the elution of analytes from chromatographic columns, they were transferred to the flame ionization detectors measuring cells ( $\mu$ FID). Parameters of the chromatographic system that were used are summarized in Table 1. AlphaSoft 12.4 software was used to process the data.

### 2.3 Multivariate data analysis

Data analysis was performed using Orange Canvas Data Mining v. 3.3.9 software (Bioinformatics Lab, University of Ljubljana, Slovenia). The chromatographic peak area values were normalised and used as input data for Hierarchical Cluster Analysis.

**Table 1**  
Ultra-fast GC parameters used during analysis.

Element	Operation	Parameter
Autosampler HS-100	Incubation	Incubation temperature: 40 °C Incubation time: 120 s
	Agitation	Agitation speed: 500 rpm
Heracles II	Injection	Sample volume: 2.5 cm <sup>3</sup> Injector temperature: 200 °C
	Adsorption/desorption of analytes	Trapping temperature: 40 °C Trapping duration: 30 s
	Analysis	Temperature program: from 40 °C with speed 4 °C min <sup>-1</sup> to 200 °C
	Detection of analytes	Detector temperature: 270 °C

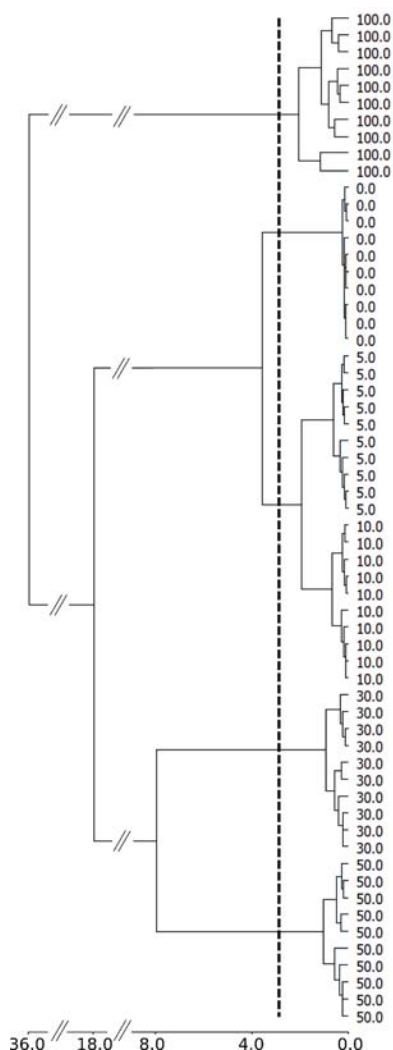


**Fig. 1** The dendrogram of hierarchical clustering (cut-off line at 7.0% of the range).

### 3. Results and discussion

The aim of the research was to determine, whether it is possible to distinguish between adulterated and unadulterated samples of raspberry juice based on its headspace. The changes in the volatile fraction of samples were monitored using an electronic nose device which based on the ultrafast gas chromatography technique. The chromatographic peak areas from the detectors were treated as signals of gas sensors. These results were used as input data for chemometric analysis, namely Hierarchical Cluster Analysis. It is a method of combining groups of the most closely related samples. In the study, the Euclidean distance was used to determine the similarity between the objects. In addition, Ward's linkage method was applied. The result of Hierarchical Cluster Analysis is the dendrogram (Fig. 1), which takes into account the cutoff point (mean distance less than 3.0). In this way, 5 clusters were formed.

The composition of the aroma for 100.0% chokeberry juice samples (marked as 100.0) and 100.0% raspberry juice samples (marked as 0.0) forming two single clusters. Subsequently two separated clusters were obtained for samples of mixtures of raspberry and chokeberry juice containing 50.0% and 30.0% of chokeberry juice (samples 50.0 and 30.0). However, for data for samples containing between 5.0% and 10.0% of chokeberry juice, the distinction is difficult because one cluster has been created for this data. This means that the Hierarchical Cluster Analysis method makes it possible to distinguish samples of unadulterated raspberry juice from samples adulterated with chokeberry juice, however, for some samples this method is insufficient to determine the percentage of chokeberry juice.

### 4. Conclusions

Based on the obtained results, it can be concluded, that it is possible to classify between adulterated and unadulterated raspberry juice samples based on its volatile fraction. This suggests that the use of Hierarchical Cluster Analysis method could be used to determine the authenticity of Not From Concentrate raspberry juice. However, in order to indicate the percentage of the chokeberry juice in raspberry juice with greater precision, supervised statistical methods should be used.

### References

- [1] AIJN European Fruit Juice Association: Fruit Juice Matters 2017 Report. <http://www.aijn.org/-files/default/aijn-fjm-report-final-digital.pdf>
- [2] Liu Y., Heying E., Tanumihardjo S.A.: History, Global Distribution, and Nutritional Importance of Citrus Fruits. *Compr. Rev. Food Sci. Food Saf.* **11** (2012), 530–545.
- [3] Borges G., Mullen W., Crozier A.: Comparison of the polyphenolic composition and antioxidant activity of European commercial fruit juices. *Food Funct.* **1** (2010), 73–81.
- [4] Bobinait R., Viškelis P., Venskutonis P.R.: Variation of total phenolics, anthocyanins, ellagic acid and radical scavenging capacity in various raspberry (*Rubus* spp.) cultivars. *Food Chem.* **132** (2012), 1495–1501.

- [5] Carvalho E., Fraser P.D., Martens S.: Carotenoids and tocopherols in yellow and red raspberries. *Food Chem.* **139** (2013), 744–752.
- [6] Luo T., Miranda-García O., Sasaki G., Shay N.F.: Consumption of a single serving of red raspberries per day reduces metabolic syndrome parameters in high-fat fed mice. *Food Funct.* **8** (2017), 4081–4088.
- [7] Hatcher K.: The effect of whole red raspberry juice on bone density and biomarkers of bone in postmenopausal osteopenic women. *Master Thesis at The Graduate School of Texas Woman's University* 2017. <https://twu-ir.tdl.org/twu-ir/handle/11274/9756>
- [8] Fry J., Martin G., Lees M.: Authentication of orange juice. In: *Production and Packaging of Non-Carbonated Fruit Juices and Fruit Beverages*. Ashurst P. (edits.). Boston, Springer 1994, p. 1–52.
- [9] Elkins A., Heuser J., Chin H.: Detection of adulteration in selected fruit juices. In: *Adulteration of Fruit Juice Beverages*. Nagy S., Attaway J., Rhodes M. (edits.). New York, Marcel Dekker 1988, p. 317–341.
- [10] Duarte W.F., Dragone G., Dias D.R., Oliveira J.M., Teixeira J.A., Silva J.B., Schwan R.F.: Fermentative behavior of *Saccharomyces* strains during microvinification of raspberry juice (*Rubus idaeus* L.). *Int. J. Food Microbiol.* **143** (2010), 173–182.
- [11] Obón J.M., Díaz-García M.C., Castellar M.R.: Red fruit juice quality and authenticity control by HPLC. *J. Food Compos. Anal.* **24** (2011), 760–771.
- [12] Versari A., Biesenbruch S., Barbanti D., Farnell P., Galassi S.: Effects of pectolytic enzymes on selected phenolic compounds in strawberry and raspberry juices. *Food Res. Int.* **30** (1997), 811–817.

# The potential of raw sewage sludge in construction industry

LESŁAW ŚWIERCZEK\*, BARTŁOMIEJ CIEŚLIK, PIOTR KONIECZKA

*Department of Analytical Chemistry, Faculty of Chemistry, Gdańsk University of Technology,  
11/12 Gabriela Narutowicza Street, 80-233 Gdańsk, Poland ✉ lesswier@student.pg.edu.pl*

## Keywords

building industry  
heavy metal  
sewage sludge  
sewage sludge ash  
stabilization

## Abstract

Excess sewage sludge produced in any, municipal or industrial wastewater treatment plant becomes a serious problem due to its increasing amount. This increase is related, e.g., to the improvement of treatment technologies. The use of sewage sludge in building materials eliminates some of the expensive and energy-intensive stages of utilization, therefore the final product obtained is often stable and safe. Heavy metals are not leach out from obtained materials while strange properties are considered satisfying. Due to the occurrence of heavy metals in sewage sludge, their stabilization with mineral and hydraulic binders becomes a promising method of development. This paper presents the results of research on the content of metals in sewage sludge from various steps of the technological process provided in sewage treatment plant. This is one of the key parameters responsible for the durability and strength of cemented products.

---

## 1. Introduction

Sewage sludge management is a challenge for municipal wastewater treatment plants in terms of social, ecological and economic aspects. Their production in recent years shows an upward trend. It is estimated that by 2020 in Europe, the amount of generated sewage sludge on a dry matter basis will reach approx. 13 million tones DM of sludge [1]. There are many methods for their management and the quality of stabilized final products depends mainly on the characteristics of the sewage sludge produced in the treatment plant. The most commonly used methods of management include direct soil application, biological-chemical stabilization (methane fermentation, composting) or thermal neutralization (mono- or co-incineration, gasification, pyrolysis) [2]. In the case of using compost obtained through biological stabilization, concerning legal requirements, the limiting aspect is the content of heavy metals. Therefore, other methods of utilization are sought. One of Best Available Technologies is thermal stabilization, which allows the sludge to be hygienized while reducing their volume. The end product is ash, which due to heavy metal concentration may be considered as

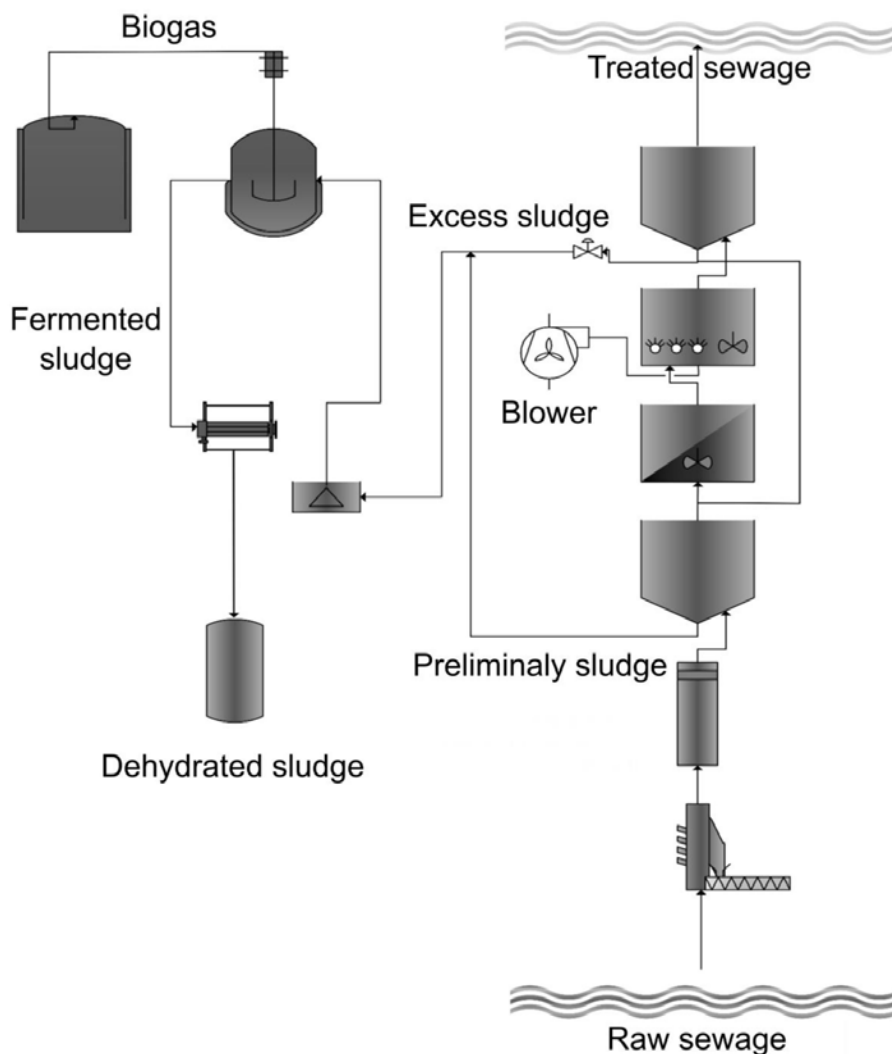


**Fig. 1** Example of sewage sludge treatment technological line.

a hazardous waste. In addition, the process can be energy-consuming due to the drying of sludge before being incinerated [3].

In developed countries, the construction industry plays a significant role. The use of raw sludge as an additive for mortars, concretes or ceramic products is a pro-environmental approach. On the one hand, the environmentally harmful waste is disposed of, on the other hand, a good quality building material is produced, saving raw material at the same time. In addition, such an approach promotes a circular economy [4, 5].

The addition of excess sludge to raw cement and mortar products may be an alternative to the existing methods of its management. In the literature, one can

find approaches using of unhydrated sewage sludge (1–2% DM) to mortar or concrete as a substitute for water. On the other hand, dehydrated sludge can be used as a substitute for fine aggregates [6]. However, significant presence of heavy metals in sewage sludge may negatively affect the bonding reactions of cement products. It is possible to use raw sewage sludge from various steps of the technological process. An example of a sewage treatment plant with emerging sludge is presented in Fig. 1. The purpose of this work was to determine heavy metals (Cd, Cu, Ni, Pb, Zn, Cr, Mg, Mn, Fe) in the primary sludge, dehydrated sludge, digested sludge and excess sludge to check and compare heavy metal content. The obtained data can be used to optimize the production process of cement products that contain raw sewage sludge, and confirm the environmental safety of proposed approaches.

## 2. Experimental

### 2.1 Reagents and chemicals

Sewage sludge was collected from one of the municipal sewage treatment plant in Gdańsk. In order to determine the content of heavy metals in various obtained sludge, dry masses were initially determined. For this purpose, about 2 g of each sludge was weighed, placed in a porcelain crucible and dried at 105 °C to constant weight. Each analysis was done with 3 repetitions. Determination of pseudo total metal concentration consisted in weighing about 1g of each type of sediment into a special vessel (Teflon bomb) and subjecting them to wet pressure mineralization using microwave energy. The Digestion mixture was concentrated with HNO<sub>3</sub> and HCl in a 1: 2 by volume ratio. The mineralization was carried out for 1.5 hours at a maximum temperature of 150 °C. The obtained solutions were quantitatively transferred into 25 cm<sup>3</sup> graduated flasks and made up to volume with deionized water.

Analysis of heavy metals in obtained solutions was carried out using Atomic Absorption Spectrometry with flame atomization. Calibration solutions were prepared from stock solution (1000 mg dm<sup>-3</sup>). Depending on the determined element (Cd, Cu, Ni, Pb, Zn, Cr, Mg, Mn, Fe) proper calibration solutions were prepared (from 0.1 to 5.0 mg dm<sup>-3</sup>). If the concentration of the element was above the range of the calibration curves, the sample solutions were appropriately diluted. Each measurement was repeated 3 to 4 times for uncertainty calculation. On the basis of the results of dry matter and the concentration of heavy metals, the content of heavy metals in particular sewage sludge from various steps of technological line was calculated.

### 2.2 Instrumentation

Microwave assisted mineralization was carried out using the Anton Paar Mineralization system, model Multiwave GO.

**Table 1**

Heavy metals concentration in sewage sludge collected at different step of treatment and processing.

Element	Preliminally sludge /mg kg <sup>-1</sup> DM	Dehydrated sludge /mg kg <sup>-1</sup> DM	Fermented sludge /mg kg <sup>-1</sup> DM	Excess sludge sludge /mg kg <sup>-1</sup> DM	Limit of detection /mg kg <sup>-1</sup> DM
Cd	6.189±0.093	10.88±0.15	<LOD	<LOD	1.8
Cu	186.0±9.4	269±12	230±11	257±13	–
Ni	<LOD	<LOD	<LOD	<LOD	5.0
Pb	<LOD	<LOD	<LOD	<LOD	6.8
Zn	129.0±3.5	1216±47	110.4±3.2	188.9±5.9	1.9
Cr	<LOD	<LOD	<LOD	<LOD	24
Mg	660±179	8147±1947	853±190	2395±565	–
Mn	<LOD	208±24	<LOD	14.3±1.2	5.8
Fe	2069±224	27113±2932	2230±244	6649±938	–

The Atomic Absorption Spectrometer from GBC SCIENTIFIC EQUIPMENT model SensAA was used to analyze heavy metals in the samples. Hollow cathode lamps for every element determination was also supplied by GBC SCIENTIFIC EQUIPMENT.

### 3. Results and discussion

In Table 1 the results of determination of selected metals are presented. Concentrations of metals such as Cu, Cr, Pb or Ni do not differ significantly. The concentrations of the remaining elements vary depending on the purification stage. Differences in content may be related with the formation of stable metal-organic compounds, which can be built-in sewage sludge biota tissues. Mentioned compounds are degraded during mineralization. In addition, unit processes and operations preceded in different steps of the treatment plant technological line causes the sludge to differ significantly, which can also affect the differences in metal content. This is most evident in the case of Fe and Mg. Fe and Al salts are often used as coagulants, thanks to which dewatering of sewage sludge is easier. They are also used to remove phosphates from wastewater, as well as other alkaline salts (Ca(OH)<sub>2</sub>), which simultaneously promotes the precipitation of Mg(OH)<sub>2</sub> [6]. Moreover, mentioned reagents may be added during, previously mentioned, different steps of sludge treatment.

The presence of Fe in the end product is undesirable, due to the fact it may adversely affect the pozzolanic activity of mortar or concrete with additives (e.g., coal burn ash) [7]. The biggest problem of sewage sludge in building industry use is the fact, that the Fe based salt are most commonly used precipitating reagent. Alternatively used Al based reagents are used seldom because of economic aspects (Al based reagents prices are significantly higher). Concentrations of more toxic metals (Cd, Ni, Pb, Cr and Mn) are relatively low and at the same time

comparable with literature values. However, since those could cause environmental hazard and pollution, their concentrations have to be monitored [8–10].

#### 4. Conclusions

Sewage sludge can be considered as a potentially attractive addition to building materials mainly due to, their physicochemical properties. The main mineral components of sewage sludge include: calcium, iron and aluminum and phosphorus compounds, which, in the form of oxides, are included in cement mortars and other commercially used building materials. Thanks to this, there is the possibility of pro-ecological use of sewage sludge, which is very beneficial in the context of the circular economy. When designing a new method of management, it is important to determine broad range of heavy metals due to their possible impact on bonding of cement binders and also for ecological reasons. In addition, such products must meet the strength and leaching criteria included in legislative standards. The effect of the addition of raw sewage sludge on the durability and the risk of leaching of heavy metals from the final products are the target of future research.

#### Acknowledgments

The research was supported by Gdańsk University of Technology, Faculty of Chemistry funds. No specific grants and funding were available.

#### References

- [1] Mininni G., Blanch A. R., Lucena F., S. Berselli: EU policy on sewage sludge utilization and perspectives on new approaches of sludge management. *Environ. Sci. Pollut. Res.* **22** (2015), 7361–7374.
- [2] Cieślík B.M., Namieśnik J., Konieczka P.: Review of sewage sludge management: Standards, regulations and analytical methods. *J. Clean. Prod.* **90** (2015), 1–15.
- [3] Li J., Xue Q., Fang L., Poon C. S.: Characteristics and metal leachability of incinerated sewage sludge ash and air pollution control residues from Hong Kong evaluated by different methods. *Waste Manag.* **64** (2017), 161–170.
- [4] Smol M., Kulczycka J., Henclik A., Gorazda K., Wzorek Z.: The possible use of sewage sludge ash (SSA) in the construction industry as a way towards a circular economy. *J. Clean. Prod.* **95** (2015), 45–54
- [5] Supino S., Malandrino O., Testa M., Sica D.: Sustainability in the EU cement industry: The Italian and German experiences. *J. Clean. Prod.* **112** (2016), 430–442.
- [6] Klaczyński E.: Oczyszczalnia ścieków-chemiczne usuwanie fosforu. *Wodociągi-Kanalizacja* (2013), 26–28. (In Polish.)
- [7] Giergiczny Z., Małolepszy J., Szwabowski J., Śliwiński J.: *Cementy z dodatkami mineralnymi w technologii betonów nowej generacji*. Opole, Górażdże Cement 2002. (In Polish.)
- [8] Tella M., Doelsch E., Letourmy P., Chataing S., Cuoq F., Bravin M.N., Saint Macary H.: Investigation of potentially toxic heavy metals in different organic wastes used to fertilize market garden crops. *Waste Manag.* **33** (2013), 184–192.
- [9] Ščančar J., Milačič R., Stražar M., Burica O.: Total metal concentrations and partitioning of Cd, Cr, Cu, Fe, Ni and Zn in sewage sludge. *Sci. Total Environ.* **250** (2000), 9–19.
- [10] Antunes E., Schumann J., Brodie G., Jacob M. V., Schneider P. A., Biochar produced from biosolids using a single-mode microwave: Characterisation and its potential for phosphorus removal. *J. Environ. Manage.* **196** (2017), 119–126.

# Estimation of the odour intensity of air samples undergoing biofiltration process using electronic nose and artificial neural network

BARTOSZ SZULCZYŃSKI\*, PIOTR RYBARCZYK, JACEK GĘBICKI

*Department of Chemical and Process Engineering, Faculty of Chemistry, Gdansk University of Technology, Narutowicza Street 11/12, 80-233 Gdansk, Poland ✉ bartosz.szulczynski@pg.edu.pl*

## Keywords

biofiltration  
biotrickling  
electronic nose  
odour intensity  
toluene

## Abstract

Biofiltration is one of the techniques used to reduce odorants in the air. It is based on the aerobic degradation of pollutants by microorganisms located in the filter bed. The research presents the possibility of using the electronic nose prototype combined with artificial neural network for estimation of the odour intensity of toluene contaminated air samples. The study was conducted using 3-section biotrickling filter settled with selected environmental isolates of *Candida* fungi during 21 days. As a result of the studies, it was found that the electronic nose prototype along with the proposed artificial neural network can be successfully used to estimate of the odour intensity of toluene contaminated air samples undergoing biofiltration process.

---

## 1. Introduction

Municipal services as well as the industrial activities are the main sources of emissions to the atmosphere of odorous compounds. The dominant group of such compounds are volatile organic compounds. Such compounds are both unpleasant and dangerous for people. Therefore, odorous substances should be effectively removed from air.

There are several air cleaning technologies devoted to the removal of odorous compounds, i.e., catalytic combustion or adsorptive and absorptive methods. Biological methods, including biofiltration, are interesting group of odor abatement technologies. Biofiltration consists in the decomposition of pollutants by means of bacteria and other microbes inhabiting the porous packing of a filter. The mechanism of the process takes advantage of the diffusion of pollutants from gaseous phase to a liquid phase of a biofilm covering the elements of a filter packing. The purified stream of air leaves the biofilter whilst the adsorbed pollutants undergo the process of biodegradation. As a result, pollutants

**Table 1**

Odour intensity scale described in German Standard VDI 3940.

Odour strength	Odour Intensity level
Not perceptible	0
Very weak	1
Weak	2
Distinct	3
Strong	4
Very strong	5
Extremely strong	6

previously harmful to human health are transformed mainly into CO<sub>2</sub>, water and biomass, depending on the polluted air composition [1, 2]. Biofiltration is a highly efficient method for the treatment of large volumes of air polluted with low concentrations of odorants. The most frequently used techniques to evaluate effectiveness of biofiltration process are gas chromatography techniques. They enable separation and determination of concentrations of individual components of the mixture. In terms of the evaluation of the odour quality of purification, such information is not directly useful. Therefore, electronic noses – devices enabling holistic analysis of gas samples – are increasingly used to assess the effectiveness of biofiltration in terms of odour intensity reduction [3]. Odour intensity is one of the most common determined feature of the smell. It is defined as the perceived strength of odor sensation that will be triggered by a specific stimulus. Typically, intensity is assessed by sensory analysis using point scales. An example of a scale according to the German standard is shown in Table 1.

The evaluation of the odour intensity is also possible with the use of electronic noses – devices that are supposed to imitate the human sense of smell. The electronic nose system consists of four main components:

- Sampling system which provides stable and reproducible measuring conditions (temperature, humidity, gas flow velocity) and eliminates all undesirable factors that can affect the sensor response;
- Detection system which is built from the set of sensors located in the measuring chamber. The most commonly used type of sensors are commercially available sensors for detection of volatile organic compounds, e.g., Metal Oxide Sensors [4]. They show different selectivity and sensitivity, but as a whole, produce a characteristic chemical image of the gas mixture (“fingerprint”);
- Data processing system;
- Pattern recognition system which assigns the received set of signals to one of the pattern classes.

As pattern recognition system various chemometric algorithms are used, e.g., Principal Component Analysis, Linear Discriminant Analysis, Support Vector Machine or Partial Least Square. But the most valuable method used in the e-nose system is Artificial Neural Network (ANN). Artificial neural networks are now considered the best method of analyzing data from artificial senses, mainly due to the fact that ANNs in their architecture and functioning resemble the nervous system in humans. The simplest, having only one neuron, ANN is called the perceptron. The main and most important element of the perceptron is the

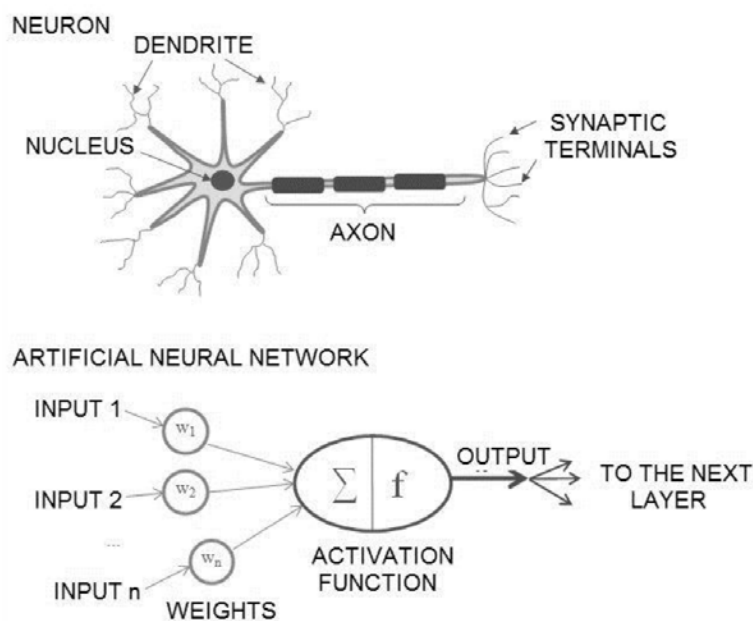


**Fig. 1** Similarity of neuron cell and Artificial Neural Network construction.

McCulloch-Pitts neuron, which is a simplified model of the biological nerve cell. The similarity in the construction of both neurons is presented in Fig. 1.

The use of ANN for data analysis is possible only after prior collection of the training data set – examples of inputs along with defined, corresponding output values. Neural network learning process involves changing its internal parameters (weight coefficients and neuron activation thresholds). This is done using the appropriate algorithm, usually learning under supervision. The most frequently used algorithm for this purpose is the back error propagation algorithm [5]. Its operation consists in the modification of weights and threshold values based on training data in such a way as to minimize the error made by the network while performing its assigned tasks for all data included in the training set.

The article presents estimation of the odour intensity of air samples (contaminated with toluene) undergoing biofiltration process using electronic nose and artificial neural network. The obtained results were compared with the results of sensory analysis.

## 2. Experimental

### 2.1 Biofiltration unit

The studies used a three-section biotrickling filter. The installation diagram is shown in Fig. 2. The biofilter was filled with 10×2.4 mm Rashig ceramic rings (section A) and 6×1.5 mm (sections B and C). The biofilter bed, after sterilization,

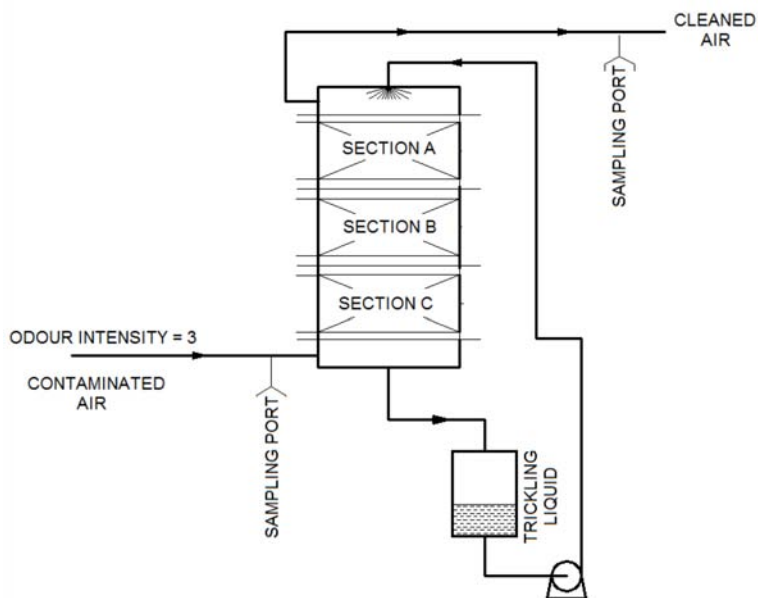


Fig. 2 Biotrickling filter system used during the research.

was settled with selected environmental isolates of *Candida* fungi. The medium with yeast, containing  $K_2HPO_4$ ,  $MgSO_4 \cdot 7H_2O$ ,  $KH_2PO_4$ ,  $NH_4Cl$  and microelements, in a volume of  $1.5 \text{ dm}^3$  was poured into the bioreactor and then circulated for 5 days (at a flow rate of  $50 \text{ cm}^3 \text{ min}^{-1}$ ). After this time, the supply of air contaminated with toluene was started. The toluene concentration in the inlet air stream corresponded to the odour intensity equal to 3. Every third day, approx. 20% of the trickling liquid volume was changed to fresh. Six gas samples were collected at the inlet and outlet of the installation for each day. Samples were collected to the Tedlar bags (with a volume of  $1.5 \text{ dm}^3$ ). Three of them were analyzed by an electronic nose, while the other three were analyzed by sensory analysis.

## 2.2 Sensory analysis

Sensory evaluation of odor intensity was carried out by 4 persons, selected according to the procedure described in [6]. Each member of the panel was responsible for assigning the appropriate odour intensity value to a given sample using a 7-step scale described in German Standard VDI 3940 (Table 1).

## 2.3 Electronic nose analysis

The prepared samples were analyzed using a constructed electronic nose prototype. The device was equipped with eight metal oxide sensors manufactured by Figaro Engineering: TGS2104, TGS2106, TGS2180, TGS2600, TGS2602, TGS2201A, TGS2201B and TGS2611.

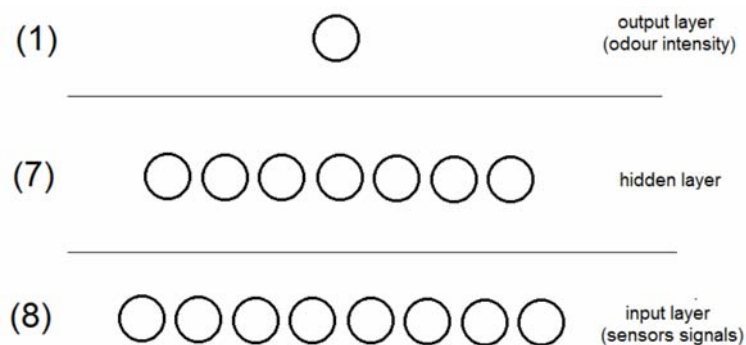


**Fig. 3** Architecture of the Artificial Neural Network.

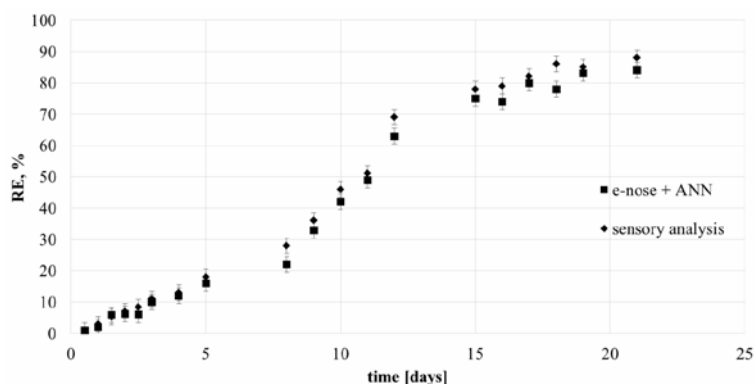


**Fig. 4** Changes in the removal efficiency of toluene as a function of the duration.

The collected samples were sucked by a membrane pump into the e-nose chamber for 15 seconds. The sample was then kept in the chamber for 30 seconds. The purified air was then directed into the chamber for regeneration of the sensors. For data analysis the maximum signal value of each sensor was used.

The odour intensity of the sample was determined using previously designed Artificial Neural Network (topology: 8-7-1). Architecture of the network is presented in the Fig. 3. Three layer neural network was designed. The weights were modified until the error between the measured and predicted values are minimized. RStudio Desktop (v. 1.0.143) software was used as the computational software.

### 3. Results and discussion

The results of sensory analysis compared to the electronic nose with artificial neural network analysis obtained during 21 days of biofilter's work are presented in the Fig. 4. On the basis of the obtained results, the removal efficiency (*RE*) of the tested samples was determined, according to the dependence

$$RE = 1 - \frac{OI_{out}}{OI_{in}} \quad (1)$$

where:  $OI_{in}$  are odour intensities at the inlet, and  $OI_{out}$  are odour intensities at the outlet of the biofiltration system.

The results obtained using the electronic nose combined with Artificial Neural Network are characterized by a large convergence with the results of sensory analysis. In most cases, they are overestimated, so removal efficiency is lower.

#### 4. Conclusions

As a result of the studies, it was found that the electronic nose prototype along with the proposed Artificial Neural Network can be successfully used to estimate of the odour intensity of toluene contaminated air samples undergoing biofiltration process. The research has shown that the use of e-noses instead of sensory analysis is possible which is advantageous due to significantly shorter time and costs of a single analysis. In addition, it is also possible to work this type of devices in on-line mode, which can also be used for continuous monitoring and control of the air biofiltration process, which is now increasingly used deodorization method.

#### Acknowledgments

The investigations were financially supported by the Grant No. UMO-2015/19/B/ST4/02722 from the National Science Centre (Poland).

#### References

- [1] Cheng Y., He H., Yang Ch., Zeng G., Li X., Chen H., Yu G.: Challenges and solutions for biofiltration of hydrophobic volatile compounds. *Biotechnol. Adv.* **34** (2016), 1091–1102.
- [2] Schiavon M., Ragazzi M., Rada E.C., Torretta V.: Air pollution control through biotrickling filters: a review considering operational aspects and expected performance. *Crit. Rev. Biotechnol.* **36** (2016), 1143–1155.
- [3] Szulczyński B., Namieśnik J., Gębicki J.: Monitoring and efficiency of biofilter air deodorization using electronic nose prototype. *Chem. Pap.* **72** (2018), 527–532.
- [4] Szulczyński B., Gębicki J.: Currently commercially available chemical sensors employed for detection of volatile organic compounds in outdoor and indoor air. *Environments* **4** (2017), 21.
- [5] Rumelhart D.E., Hinton G.E., Williams R.J.: Learning representations by back-propagating errors. *Nature* **323** (1986), 533–536.
- [6] Gębicki J., Dymerski T., Rutkowski Sz.: Identification of odor of volatile organic compounds using classical sensory analysis and electronic nose technique. *Environ. Prot. Eng.* **40** (2014), 103–116.

# Supercritical carbon dioxide extraction as a crucial step in the enriching sample in desired group of bioactive compounds

OLGA WRONA<sup>a, b, \*</sup>, KATARZYNA RAFIŃSKA<sup>b, c</sup>, CEZARY MOŻEŃSKI<sup>a</sup>,  
BOGUSŁAW BUSZEWSKI<sup>b, c</sup>

<sup>a</sup> New Chemical Syntheses Institute, Al. Tysiąclecia Państwa Polskiego, 24-110 Puławy, Poland  
✉ [Olga.Wrona@ins.pulawy.pl](mailto:Olga.Wrona@ins.pulawy.pl)

<sup>b</sup> Interdisciplinary Centre of Modern Technologies, Nicolaus Copernicus University, Wilenska 4, 87-100 Toruń, Poland

<sup>c</sup> Department of Environmental Chemistry and Bioanalytics, Faculty of Chemistry, Nicolaus Copernicus University, Gagarina 7, 87-100 Toruń, Poland

## Keywords

carbon dioxide  
fatty acids  
GC-MS  
goldenrod (*Solidago gigantea* L.)  
isolation  
response surface methodology  
supercritical fluids extraction

## Abstract

The main goal of this study was to obtain the optimal conditions of supercritical carbon dioxide extraction of *Solidago gigantea* (goldenrod) at the quarter-technical plant. Criterion for the selection of those conditions was the highest amount of fatty acids methyl esters in obtained extract. Fatty acids, especially unsaturated fatty acids, are valuable compounds due to their health-promoting properties. Fatty acids methyl esters was determined by GC-MS. For optimization purpose, Box-Behnken design was used to analyze the effects of three independent process parameters (pressure, temperature, and flow rate of CO<sub>2</sub>) on selected criterion. Box-Behnken design allows to analyze of obtained results by Response Surface Methodology. A second-order quadratic polynomial model was suitable for the experimental data and obtained results ( $R^2$  for fatty acids methyl esters was 0.90). Therefore, the response surface methodology can be applied to optimize the supercritical carbon dioxide extraction of *Solidago gigantea*. Response Surface Methodology results and ANOVA indicate that the highest amount of desired group is achieved by extracting at 318 K, 35 MPa and the flow of CO<sub>2</sub> 6.3 kg h<sup>-1</sup>.

## 1. Introduction

*Solidago gigantea* (commonly known as goldenrod) is widely spread in Poland and has traditional usage in the diet and as a medicinal plant. Genus of *Solidago* includes over 100 species mainly inhabiting America, Asia and Europe. Two of the most popular species: *S. canadensis* and *S. gigantea* are very invasive and now considered among the most aggressive plant in Europe. Therefore, it is very reasonable to find additional application for those plants. Also literature study

had shown that preparations obtained from goldenrods have a diuretic, spasmolytic, hypotensive, anti-inflammatory, bacteriostatic and analgesic properties [1–4]. All of the properties of the goldenrod preparation are a results of their composition. Goldenrods are rich in secondary metabolites: flavonoids, monoterpenes, diterpenes (clerodane-type), saponins and different nitrogen-containing compound [5, 6].

Supercritical fluid extraction (SFE) is a green technology, providing efficient isolation of valuable components from plant materials. Supercritical fluid extraction offers several advantages over conventional solvent extraction, render higher selectivity and shorter extraction time. The qualitative and quantitative composition of the final extract is determined by the physicochemical properties of the solvent and parameters of the process. Hence the necessity to optimize the process conditions for individual plant materials.

Sample preparation is a crucial first step in the analytical chemistry which may cause an errors in further analysis. At the isolation stage (SFE) it is possible to control the composition of the sample and enrich it with the desired group of compounds. As a result of SFE, free of contamination and enriched product is obtained and sample can be analyzed directly by dissolution of the extract.

## 2. Experimental

### 2.1 Chemicals and reagents

All chemicals and reagents were of analytical grade and were purchased from Sigma Aldrich, Germany.

### 2.2 Plant material

*Solidago gigantea* used in this study were harvested in Choceń, Poland. Goldenrods were dried and ground into 2–3 cm pieces.

### 2.3 Experimental program

In our case, Box-Behnken design was used to analyze the effects of three independent variables on selected criterion. Complete design consisted of 15 experimental steps at the different conditions (Table 1). Three independent variables were: temperature (K) pressure (MPa) and solvent flow rate ( $\text{kg h}^{-1}$ ). To evaluate the effect of those factors, fatty acids methyl esters (FAME) were determined. All the results and statistical analysis were accomplished using Design Expert 9.0. Optimal extraction conditions were determined based on the concentration on selected compounds as a response.

**Table 1**  
Results of Box–Behnken design for the supercritical carbon dioxide extraction of *Solidago gigantea*.

	<i>T</i> /K	<i>P</i> /MPa	<i>S</i> /kg h <sup>-1</sup>	FAME/mg g <sup>-1</sup> DM
NwOE1	333.15	80.00	7.00	22.37
NwOE2	353.15	80.00	5.00	41.31
NwOE3	353.15	20.00	5.00	36.23
NwOE4	313.15	50.00	3.00	114.13
NwOE5	333.15	50.00	5.00	102.43
NwOE6	353.15	50.00	3.00	95.77
NwOE7	333.15	50.00	5.00	48.42
NwOE8	333.15	50.00	5.00	72.11
NwOE9	313.15	80.00	5.00	157.25
NwOE10	333.15	20.00	3.00	101.21
NwOE11	313.15	20.00	5.00	211.94
NwOE12	313.15	50.00	7.00	217.16
NwOE13	333.15	80.00	3.00	134.24
NwOE14	333.15	20.00	7.00	157.22
NwOE15	353.15	50.00	7.00	56.91

#### 2.4 Extraction of the plant material

Extractions were carried out at the quarter-technical plant placed in New Chemical Syntheses Institute in Puławy, according to the Box-Benhken design (the process parameters are included in the Table 1). Briefly, 150 g of plant material were loaded into the 1 L extraction basket (vessel). When equilibrium was reached, CO<sub>2</sub> was fed to the extractor through a high pressure pump. The extract laden CO<sub>2</sub> was sent to a separator. At reduced *T* and *P* conditions, the extract precipitated in the separator, while CO<sub>2</sub> was recycled to the extractor. At the end, after finishing the extraction, the extract contained in the separator was carefully collected in a container and tightly-closed.

#### 2.5 Determination of fatty acids methyl esters

Qualitative and quantitative identification of fatty acids methyl esters (FAME) in obtained extract of *Solidago gigantea* was carried out using a Trace GC Ultra gas chromatograph coupled with Thermo Scientific TSQ Quantum XLS mass spectrometer. 10 mg of extract was weighed, 500 μL of *t*-butylmethylether and 250 μL of TMSH were added, and the mixer was placed in magnetic stirrer for 15 minutes at 40 °C. The prepared sample was left for 30 minutes to establish the equilibrium. After the set time, the sample was analyzed. The analysis was carried out on the TR-FAME polar column (30 m × 0.25 mm × 0.25 μm). Other operating conditions of the gas chromatograph: column temperature control: 90 °C for 1 min, then heated to 140 °C at a rate 4°C min<sup>-1</sup>, hold up at 140 °C for 5 min., then heated to 180 °C at a rate 2°C min<sup>-1</sup>, isothermal at 180 °C for a 5 minutes, and heated to 220 °C at a rate 10°C min<sup>-1</sup> and maintained at 220 °C for 2 min; carrier

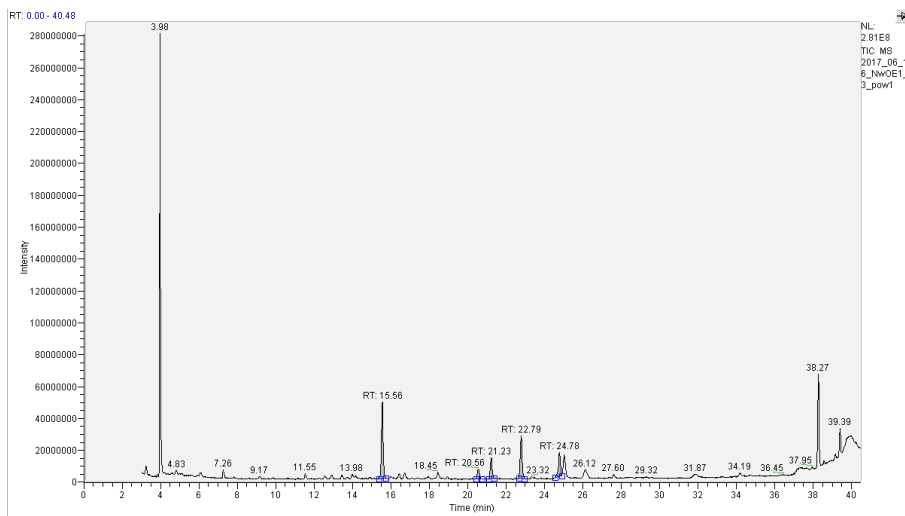


**Fig. 1** MS mass spectrum of *Solidago gigantea* extract: palmitic acid methyl ester ( $t_r = 15.56$  min), stearic acid methyl ester ( $t_r = 20.56$  min), oleic acid methyl ester ( $t_r = 21.23$  min), linoleic acid methyl ester ( $t_r = 22.79$  min), and  $\alpha$ -linolenic acid methyl ester ( $t_r = 24.78$  min).

gas flow  $1.1 \text{ mL min}^{-1}$ ; split 100:1; injection volume  $1 \mu\text{L}$ ; electron energy 70 eV; ion source temperature  $230 \text{ }^\circ\text{C}$ ; temperature of sample inlet  $230 \text{ }^\circ\text{C}$ .

The sample components were identified by comparing obtained results to mass spectra from NIST mass database. The quantitative analysis was made on the basis of the previously prepared curves for the five methyl esters fatty acids standard.

### 3. Results and discussion

GC-MS is very useful technique for separation and identification of compounds extracted from complex matrix. As a result of qualitative analysis, by comparing obtained results to mass spectra from NIST mass database, palmitic, oleic, stearic, linoleic and  $\alpha$ -linolenic acids methyl esters were identified (with the highest accuracy, over 99.9%) (Fig. 1).

The quantitative analysis was made on the basis of the previously prepared curves for those five methyl esters fatty acids standard. The results are listed on the Table 1. The concentration of those compound is high despite the fact that goldenrod is non-oily plant material). This is due to the fact that fatty acids are non-polar compounds, which are very easily extractable by non-polar carbon dioxide.

Box-Behnken design allows analyzing obtained results by Response Surface Methodology (RSM). RSM is a statistical tool that can be used to evaluate the effect (correlation) between responses and independent variables as well as their interactions which allows finding the levels of input variables ( $P$ ,  $T$ ,  $S$ ) that optimize a particular response of a extraction process. The obtained results

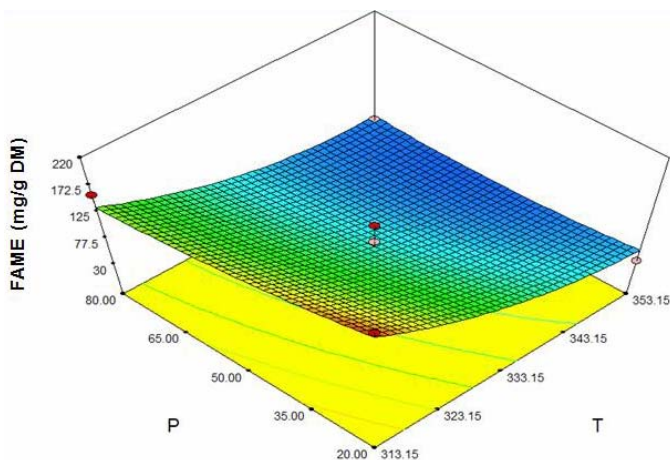


**Fig. 2** Dependence on the concentration of FAME in extract on the pressure and temperature.

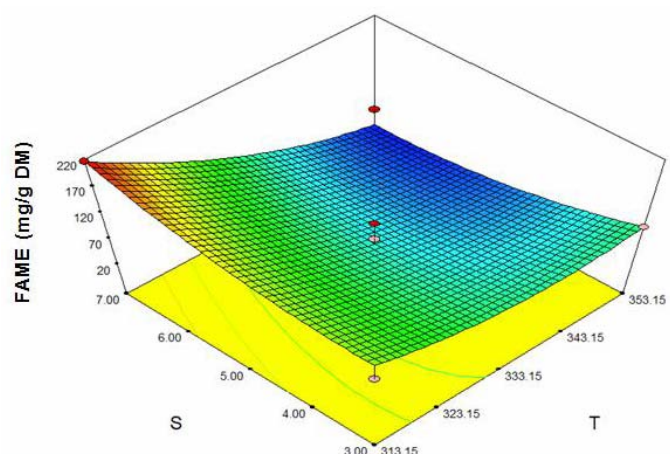


**Fig. 3** Dependence on the concentration of FAME in extract on the flow rate of carbon dioxide and temperature.

showed the influence of the process parameters on concentration of fatty acids methyl esters (Fig. 2–4). All of the process parameters have a great impact on the response; the slopes of the response surface at  $P$ ,  $T$ ,  $S$  are significant.

Regression coefficient of 0.90 indicates that the adopted model explains 96% the dependence of responses on input variables. High values of regression coefficient and the adjusted coefficient prove the accuracy of the adopted model. Non-statistically significant lack of fit and statistically significant  $p$ -value test admit that the model describes well the dependence of input and output variables (Table 2).

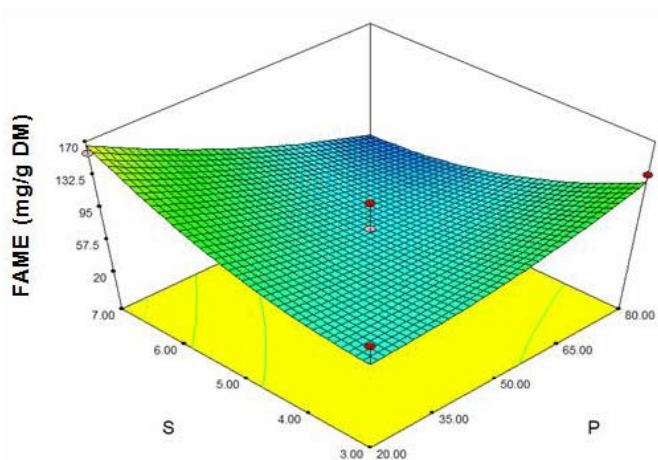


**Fig. 4** Dependence on the concentration of FAME in extract on the flow rate of carbon dioxide and pressure.

**Table 2**

Values of important statistical parameters of the adopted model for obtained results (critical values:  $R^2 > 0.8$ ;  $p < 0.0001$  very highly significant,  $p < 0.01$  very significant,  $p < 0.05$  significant,  $p > 0.1$  not statistically significant;  $LOF > 0.05$ ).

Regression coefficient $R^2$	0.90
Adjusted $R^2$	0.72
Lack of fit ( $LOF$ )	1.70
$p$ -value	0.0443

As a result of process optimization, by using the analysis of variation, for individual input variables the following optimal parameters were obtained: 318 K, 35 MPa and the flow  $6.3 \text{ kg h}^{-1}$ . In order to verify the correctness of the adopted model, extractions in optimal parameters were carried out. As results, we obtained the concentration of  $218 \text{ mg FAME g}^{-1} \text{ DM}$ , which was the highest obtained value and which was within the confidence interval.

#### 4. Conclusion

Supercritical fluid extraction can be considered as an analytical method that provides a very pure and rich sample for further determinations. To produce a high quality extract for further application, supercritical carbon dioxide extraction of *Solidago gigantea* was developed. Our studies showed that the best conditions of the extraction of fatty acids methyl esters were 318 K, 35 MPa and the flow  $6.3 \text{ kg h}^{-1}$  which indicated the highest amount of FAME.

#### Acknowledgments

This study was supported by PLANTARUM project No. BIOSTRATEG 2/298205/9/NCBR/2016 from National Centre for Research and Development, Poland.

## References

- [1] Radusiene J., Marska M., Ivanauskas L., Jakstas V., Karpaviciene B.: Assessment of phenolic compound accumulation in two widespread goldenrods. *Ind. Crops Prod.* **63** (2015), 158–166.
- [2] Paun G., Neagu E., Albu C., Radu G.L.: *Verbascum phlomoides* and *Solidago virgaureae* herbs as natural source for preventing neurodegenerative diseases. *J. Herb. Med.* **6** (2016), 180–186.
- [3] Amtmann M.: The chemical relationship between the scent features of goldenrod (*Solidago canadensis* L.) flower and its unifloral honey. *J. Food Compost. Anal.* **23** (2010), 122–129.
- [4] Kundel D., van Kleunen M., Dawson W.: Invasion by *Solidago* species has limited impacts on soil seedbank communities. *Basic Appl. Ecol.* **15** (2014), 573–580.
- [5] Weber E., Jakobs G.: Biological flora of central Europe: *Solidago gigantea* Aiton. *Flora* **200** (2005), 109–118.
- [6] Henderson M.S., McCrindle R., McMaster D.: Constituents of *Solidago* species. Part V. Non-acidic diterpenoids from *Solidago gigantea* var. *serotina*. *Can. J. Chem.* **51** (1973), 1346–1358.

# Development of a voltammetric method for detection of ethyl nitrite

VALENTINA POPOVA\*, ANNA KRIVOSHEINA, ELENA KOROTKOVA

*Chemical Engineering Department, National Research Tomsk Polytechnic University,  
30 Lenin Avenue, 634050 Tomsk, Russia* ✉ [vap25@tpu.ru](mailto:vap25@tpu.ru)

## Keywords

carbon ink  
ethyl nitrite  
graphite electrode  
voltammetry

## Abstract

A simple and sensitive voltammetric method was developed to determine of ethyl nitrite at graphite electrode in Britton-Robinson buffer solution with a pH=4.02. Surface of graphite electrode was modified with carbon ink. The ethyl nitrite was pre-accumulated on the electrode surface at +0.4 V for 4 s. A well-defined oxidation peak was obtained at 0.9 V. Anodic voltammetry in differential mode was applied for the calibration plot and detection limit ( $3.8 \times 10^{-7} \text{ mol L}^{-1}$ ).

---

## 1. Introduction

Despite the emergence of new drugs and therapeutic approaches in the field of oncology, the performance indicators of antitumor treatment of non-small cell lung cancer remain low. One of the reasons that non-small cell lung cancer is so hard to treat is that in the late stages malignant cells develop novel properties, such as the avoidance of immunological surveillance [1].

Increased production of nitric oxide has been implicated in the development of malignancy [2]. The development of a sensitive and selective methodology for the determination nitric oxide concentrations directly in biological systems requires is required to understand its role in the pathogenesis of malignant tumors. Many papers in this field have been published, yet, there is still no developed test system for determining nitric oxide (II) in biological fluids and the problem is still relevant [3].

## 2. Experimental

### 2.1 Reagents and chemicals

All solutions were prepared with nanopure water. Britton-Robinson buffer solution was prepared by mixing of  $0.2 \text{ mol L}^{-1}$  sodium hydroxide with the mixture of  $0.04 \text{ mol L}^{-1}$  of boric, acetic and phosphoric acid.

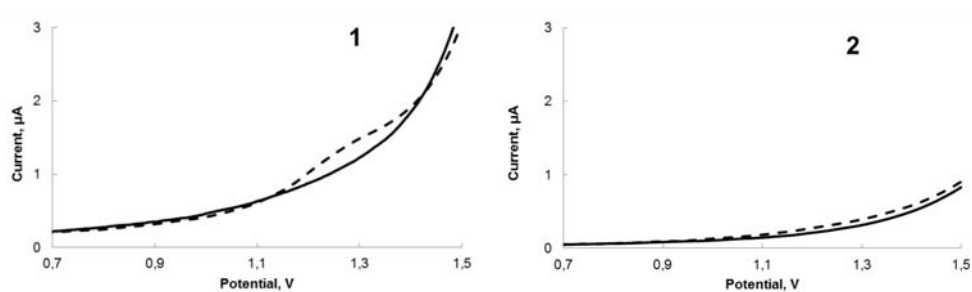


**Fig. 1** Anodic voltammograms of  $C_2H_5ONO$  at (1) graphite electrode, or (2) carbon-containing working electrode in Britton-Robinson buffer solution (pH = 4.02) (----). Background electrolyte (- - -). Conditions:  $c(C_2H_5ONO) = 7 \times 10^{-4} \text{ mol L}^{-1}$ , scan rate  $90 \text{ mV s}^{-1}$ .

For modification of the electrode surface the carbon ink was prepared by mixing 0.01 g of polystyrene, 0.09 g of carbon powder (particle size of 3.5–5.5  $\mu\text{m}$  Aldrich) and 0.5 mL of 1,2-dichloroethane (99.97%, Aldrich).

## 2.2. Instrumentation

All measurements were carried out using analyzer TA-2 (Tomsk, Russia). The three-electrode electrochemical cell was equipped with the: Ag/AgCl 1M KCl reference and auxiliary electrode, graphite electrode and carbon-containing working electrode. The pH was measured with a pH-meter/ionomer ITAN, Tomanalyt, Russia.

## 3. Results and discussion

Firstly, the optimal pH for ethyl nitrite determination was found. The Britton-Robinson buffer solution in the pH range from 2.4 to 9.1 were controlled. The highest and the best developed peak was obtained in the pH = 4.02. Britton-Robinson buffer pH = 4.02 was chosen as the optimal medium.

Moreover, two types of material of working electrodes for ethyl nitrite determination were studied: graphite electrode; carbon-containing working electrode with a renewable surface. Measurements was carried out in the potential range from +0.4 to +1.4 V.

Ethyl nitrite gives well developed peak in potential range between 1.15 V and 1.4 V at graphite electrode ( $E_p = 1.2 \text{ V}$ ). On the carbon-containing working electrode carbon-containing working electrode electrochemical signal was not observed (Fig. 1).

To increase the sensitivity the surface of electrodes were modified by carbon ink. The modifier was prepared according to the procedure described above. The efficiency of the modification was evaluated on a standard oxidation-reduction pair  $[Fe(CN)_6]^{3-}/[Fe(CN)_6]^{4-}$ . The highest and the best developed peak of ethyl

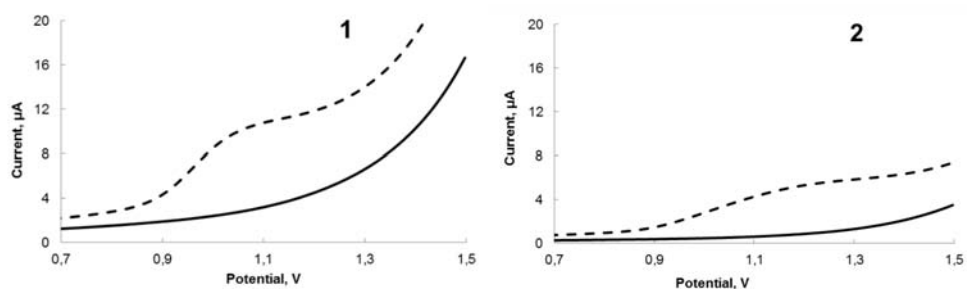


**Fig. 2** Anodic voltammograms of  $C_2H_5ONO$  on (1) graphite electrode, or (2) carbon-containing working electrode in Britton-Robinson buffer solution (pH = 4.02) after modification (----). Background electrolyte (- - -). Conditions:  $c(C_2H_5ONO) = 7 \times 10^{-4} \text{ mol L}^{-1}$ , scan rate  $90 \text{ mV s}^{-1}$ .

nitrite was obtained on electrodes after their modification by carbon ink (Fig. 2). Peak of ethyl nitrite oxidation was obtained at the  $E_p = 1.0 \text{ V}$  on graphite electrode, and at the  $E_p = 1.13 \text{ V}$  on carbon-containing working electrode. For future measurements graphite electrode was chosen as working electrode.

The influence of potential and time pre-accumulation have been tested. Optimal working conditions are: potential pre-accumulation:  $+0.4 \text{ V}$ ; time pre-accumulation:  $4 \text{ s}$ .

The dependence of the peak current on the concentration of ethyl nitrite was linear in the range from  $1$  to  $10 \mu\text{mol L}^{-1}$  with the regression equation

$$I [\mu\text{A}] = 0.0786 c [\text{mg L}^{-1}] - 0.0537 \quad (1)$$

$$R^2 = 0.9959$$

The detection limit calculated by equation  $LOD = 3s/b$ , where  $s$  is the standard deviation in the measurement of the signal of blank sample;  $b$  is the instrumental sensitivity factor of the slope of the straight section of the calibration curve, was  $3.8 \times 10^{-7} \text{ mol L}^{-1}$ .

#### 4. Conclusions

In this research, electrochemical signal from ethyl nitrite at different electrode surfaces was controlled. Optimal working conditions were found. These studies will be used to evaluate NO metabolites in biological objects to determine their activity in human and animal cancer cells.

#### Acknowledgments

The authors thank Tomsk Polytechnic University for financial support of this work (Russian Fund for Basic Research, research project No. 4.5752.2017/BP, Russian State assignment "Science").

**References**

- [1] Janakiram N.B., Rao C.V.: iNOS-selective inhibitors for cancer prevention: promise and progress. *Future Med Chem.* **17** (2012), 2193–2204.
- [2] Gow A.J., Davis C.W., Munson D.: Immunohistochemical detection of S-nitrosylated proteins. *Methods Mol. Biol.* **279** (2004), 167–172.
- [3] Ischiropoulos H., Gow A.: Pathophysiological functions of nitric oxide-mediated protein modifications. *Toxicology* **208** (2005), 299–303.

# Control of electrochemical signal from silver nanoparticles at different modification steps for electrochemical immunosensor development

YEKATERINA KHRISTUNOVA<sup>a, b, c, \*</sup>, JIŘÍ BAREK<sup>a</sup>, BOHUMIL KRATOCHVÍL<sup>b</sup>,  
VLASTIMIL VYSKOČIL<sup>a</sup>, ELENA KOROTKOVA<sup>c</sup>, ELENA DOROZHKO<sup>c</sup>

<sup>a</sup> UNESCO Laboratory of Environmental Electrochemistry, Department of Analytical Chemistry, Faculty of Science, Charles University, Hlavova 8, 128 43 Prague 2, Czech Republic

✉ yekaterinakhristunova@gmail.com

<sup>b</sup> Department of Solid State Chemistry, University of Chemistry and Technology, Prague, Technická 5, 16628 Prague 6, Czech Republic

<sup>c</sup> National Research Tomsk Polytechnic University, Lenin Avenue 30, 634050 Tomsk, Russia

## Keywords

electrochemical  
immunosensor  
silver nanoparticles  
tick-borne encephalitis

## Abstract

Development of electrochemical immunosensors towards antibody detection consists of several steps. Specific attention was paid to exclude the non-specific electrochemical signal from silver nanoparticles at different modification steps. A tick-borne encephalitis virus antigen was attached to glutaraldehyde on a glassy carbon electrode modified with gold nanoparticles and cysteamine. Cyclic voltammetric studies demonstrate the electrochemical situation on the electrode surface by electron transfer of Fe<sup>II/III</sup> as a probe. Detection of the SNPs was performed by anodic stripping voltammetry of Ag<sup>+</sup> at the glassy carbon electrode.

---

## 1. Introduction

In the past decade, electrochemical immunoassays have become an attractive option for high-throughput analysis combined with advantages of easy handling, enhanced sensitivity, high selectivity, and rapidity of data collection [1–3]. The main idea of this research is to develop an electrochemical immunosensor for the quantitative detection of antibodies against tick-borne encephalitis. Tick-borne encephalitis virus is one of the endemic flaviviruses in Russia, which can cause serious infections in humans that may result in encephalitis/meningoencephalitis [4]. In this work, silver nanoparticles (SNPs) were used as direct signaling markers for the antibody detection, and their signal was recorded by voltammetry. Such types of electrochemical immunosensors based on a signal from metal nanoparticles represent an upcoming trend in analytical chemistry [5, 6].

Preparation of the electrochemical immunosensor is performed in several steps: i) immobilization of tick-borne encephalitis virus antigen on the electrode surface; ii) production of silver nanoparticle–antibody (against tick-borne encephalitis virus) conjugates; iii) incubation of the electrode with the antigen in the silver nanoparticle–antibody bioconjugate solution; iv) silver dissolution from the surface of the electrochemical immunosensor; v) recording of voltammograms corresponding to the oxidation of cathodically pre-accumulated silver on the bare glassy carbon electrode (GCE). Immobilization of the antigen on the electrode surface is one of the most significant preparation steps, and it is critically important to control the electrochemical signal from SNPs after each modification step. Results of this research are important for understanding the nature of SNP signals and could help avoiding questions about non-specific interactions of SNPs.

## 2. Experimental

### 2.1 Reagents and chemicals

HAuCl<sub>4</sub>·3H<sub>2</sub>O (99.99%), NaBH<sub>4</sub> (99%), AgNO<sub>3</sub> (99.99%), cysteamine (95%), glutaraldehyde solution (25% in H<sub>2</sub>O), K<sub>4</sub>[Fe(CN)<sub>2</sub>]·3H<sub>2</sub>O (99%), KNO<sub>3</sub>, HNO<sub>3</sub> (65%) were obtained in analytical grade purity from Sigma-Aldrich, Germany. An antigen against tick-borne encephalitis virus was supplied by Vector-Best, Novosibirsk, Russia. All solutions were prepared with nanopure (deionized) water (18 MΩ cm).

### 2.2 Instrumentation

Voltammetric measurements were carried out in a three-electrode system with a GCE as a working electrode (3 mm diameter, Metrohm, Switzerland), an auxiliary platinum wire electrode (Eco-Trend Plus, Czech Republic), and a Ag|AgCl (3M KCl, Elektrochemické detektory, Czech Republic) reference electrode. The GCE was polished prior to measurements with aqueous slurry of alumina powder (1.1 μm) to mirror-like appearance. Linear-sweep ASV was carried out using scan rate of 0.1 V s<sup>-1</sup>, potential scan range from -0.2 to +0.6 V, accumulation potential of -0.8 V, and accumulation time of 60 s. CV measurements were carried out from -0.9 to +1 V at scan rate of 0.05 V s<sup>-1</sup>. ASV and CV were carried out on μAutolab III (Metrohm) controlled by Nova 1.11 software (Metrohm).

## 3. Results and discussion

In the initial research stage, spherically shaped SNPs (5.3±1.2 nm in size) were synthesized by the method of Mulfingher and Solomon [7]. In the UV/Vis absorption spectra (Fig. 1), the maximum absorption of SNPs is in the range of

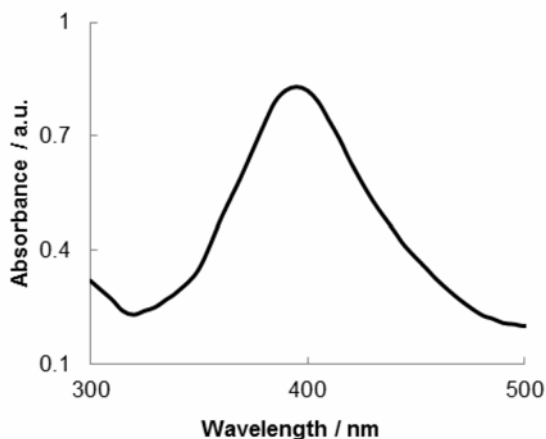


**Fig. 1** UV/Vis absorption spectra of clear yellow colloidal Ag (SNPs), optical path length of 1.0 cm, blank – deionized water.

395–400 nm, which is in accordance with the average SNP size of  $5.3 \pm 1.2$  nm calculated from the transmission electron microscopic (TEM) observations.

Afterwards, an aliquot (2 mL) of silver colloid solution was centrifuged at 8,000 rpm for 10 min. The pellet was collected and resuspended in deionized water.

Preparation of electrochemical immunosensor was as follows. The GCE was chosen as a platform for antigen immobilization. Firstly, gold nanoparticles were deposited electrochemically on the surface of the GCE [8]. During the second stage, the thiolation of Au-GCE surface was performed by dipping it into 2 mL of a cysteamine solution ( $0.05 \text{ mol L}^{-1}$ ) for 2 hours at room temperature. After rinsing the electrode with deionized water, the electrode was placed into a glutaraldehyde solution (2.5%) for 45 minutes at room temperature. Afterwards, the electrode was rinsed with a phosphate buffer (pH=7.4) three times, and the antigen was then immobilized on the electrode surface. The electrode incubation time was 1 hour at room temperature.

Electrochemical signals from SNPs were checked after each modification step. The electrode was immersed into the SNP solution for 30 min. Chemical dissolution of silver from the electrode surface with  $1 \text{ mol L}^{-1} \text{ HNO}_3$  followed by ASV at the GCE was found as a suitable technique for the determination of the SNPs. In further investigations, both the electrode surface and the solution were controlled because of the possibility of the SNP residues remaining on the surface. Electrochemical situation on the surface of variously modified electrodes demonstrated by CV of  $\text{Fe}^{\text{II/III}}$  as a probe is shown in Fig. 2. The obtained results show that the surface of the electrode was successfully modified. This can be observed via increasing the potential difference between the anodic and cathodic peak, which indicates formation of the next layer, leading to the inhibition of the electron transfer.

Detection of the SNPs was performed by ASV of  $\text{Ag}^+$  at the GCE. Our studies have shown that after the modification of the Au-GCE with cysteamine, signals from

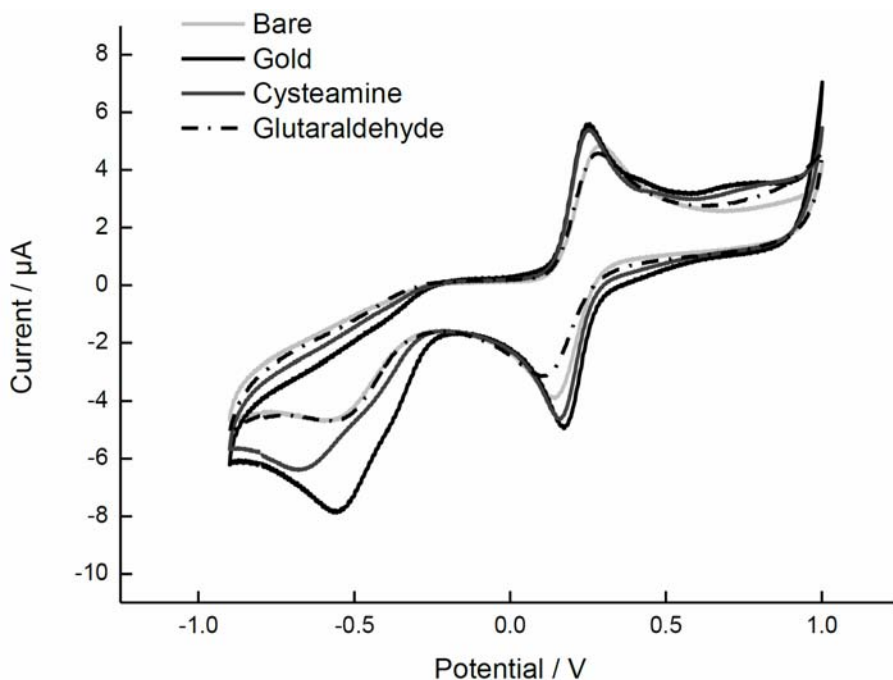


**Fig. 2** Cyclic voltammograms of  $[\text{Fe}(\text{CN})_6]^{4-}$  ( $c = 10 \text{ mmol L}^{-1}$ ) at different electrode surfaces in  $0.1 \text{ mol L}^{-1}$  KCl solution,  $E$  vs. Ag|AgCl, scan rate  $0.05 \text{ V s}^{-1}$ .

SNPs were recorded. The molecule of cysteamine contains an  $-\text{NH}_2$  group which can react with the SNPs. Upon the next modification stage with glutaraldehyde, no signals from SNPs were observed. This excludes the possibility of SNP penetration to the cysteamine layer and avoids questions about non-specific interactions of SNPs. Moreover, in the case of the subsequent modification with the antigen, signals from SNPs were recorded again. This problem could be solved within the construction of the future immunosensor, where antigen firstly binds to unlabeled antibodies and the whole electrode surface should, moreover, be blocked with a protein – thus, there would be no possibility of non-specific binding of free SNPs.

#### 4. Conclusions

In this research, electrochemical signal from SNPs at different modification steps was controlled. The obtained data showed that after all steps of modification, there is no possible binding of free SNPs through the individual modification layers. Result of this research are equally important for understanding the nature of SNP signal and for confirmation that the final signal is received as a result of the antigen–antibody (against tick-borne encephalitis virus) interaction.

## Acknowledgments

This work was financially supported by the Grant Agency of the Czech Republic (Project P206/12/G151). The authors also thank Tomsk Polytechnic University for financial support of this work (Russian Fund for Basic Research; Research Project No. 4.5752.2017/BP). This research was also supported by the project „Research in Pharmaceuticals and Biomaterials“ (grant No. A1\_FCHT\_2017\_004).

## References

- [1] Zhang K., Lv S., Lin Z., Li M., Tang D.: Bio-bar-code-based photoelectrochemical immunoassay for sensitive detection of prostate-specific antigen using rolling circle amplification and enzymatic biocatalytic precipitation. *Biosens. Bioelectron.* **101** (2018), 159–166.
- [2] Wang R., Liu W.D., Wang A.J., Xue Y., Wu L., Feng J.J.: A new label-free electrochemical immunosensor based on dendriticcore-shell AuPd@Au nanocrystals for highly sensitive detection of prostate specific antigen. *Biosens. Bioelectron.* **99** (2018), 458–463.
- [3] Wan Y., Zhou Y.G., Poudineh M., Safaei T.S., Mohamadi R.M., Sargent E.H., Kelley S.O.: Highly specific electrochemical analysis of cancer cells using multi-nanoparticle labelling. *Angew. Chem. Int. Ed.* **53** (2014), 13145–13149.
- [4] Khasnatinov M., Danchinova G., Liapunov A., Manzarova E., Petrova I., Liapunova N., Solovarov I.: Prevalence of tick-borne pathogens in hard ticks that attacked human hosts in Eastern Siberia. *Int. J. Biomed.* **7** (2017), 307–309.
- [5] Haoa N., Li H., Long Y., Zhangb L., Zhaoa X., Xua D., Chena H.Y.: An electrochemical immunosensing method based on silver nanoparticles. *J. Electroanal. Chem.* **656** (2011), 50–54.
- [6] Perez-Lopez B., Merkoci A.: Nanoparticles for the development of improved (bio)sensing systems. *Anal. Bioanal. Chem.* **399** (2011), 1577–1590.
- [7] Mulfinger L., Solomon S.D., Bahadory M.: Synthesis and study of silver nanoparticle. *J. Chem. Educ.* **84** (2007), 322–325.
- [8] Noskova G.N., Zakharova E.A., Chernov V.I.: Fabrication and application gold microelectrode ensemble based on carbon black-polyethylene composite electrode. *Anal. Methods* **3** (2011), 1130–1135.

# Effect of chaotropic salts addition into mobile phases on separation of model analytes on polar stationary phases in hydrophilic interaction chromatography

JANA SMOLEJOVÁ<sup>a,\*</sup>, MICHAL DOUŠA<sup>b</sup>

<sup>a</sup> Department of Analytical Chemistry, Faculty of Science, Charles University, Hlavova 8, 128 43 Prague 2, Czech Republic ✉ jana.smolejova@natur.cuni.cz

<sup>b</sup> Zentiva Group a. s., U Kabelovny 130, 102 37, Prague 10, Czech Republic

## Keywords

chaotropic salts  
formic acid  
hexafluorophosphoric acid  
Hydrophilic interaction chromatography  
TSK-amide column

## Abstract

Effect of addition chaotropic salts into the mobile phases on separation in hydrophilic interaction chromatography was studied. Four columns, twelve modelling analytes and thirteen mobile phases were used. Interesting phenomenon were observed. Ammonium formate buffer with hexafluorophosphoric acid addition has positive effect on retention behaviour of *p*-toluenesulfonic acid, 4-hydroxybenzenesulfonic acid, nicotinic acid and ascorbic acid.

## 1. Introduction

Hydrophilic interaction chromatography belongs to more recent chromatography methods. Currently it is commonly used for separation of very polar compounds which provides a good alternative to NP-HPLC and RP-HPLC. Stationary phases are similar to those used in using in RP-HPLC and mobile phases are similar to those used in NP-HPLC. A mechanism of separation is very complex consisting of hydrophilic partitioning, adsorption, ionic interactions and hydrophobic interaction. [1–6] The process of separation also depends on amount of water content in mobile phase. Lesser the water content in mobile phase, lesser hydrophilic interactions and other phenomenon participates on separation.

Chaotropic salts are substances (Hofmeister serie of salts) which are using for peptide analysis and have “salting in” properties. There are many theories explaining the mechanism behind effect of chaotropic salts in mobile phase of separation in RP-mode. First one is a non-specific “ion association” model [7, 8]. Chaotropic additives are less polar than water and destroy hydrogen bridges while the hydrophobicity increases. Second theory says that mechanism is an analogy of “dynamic ion-exchange” [9]. Large, poorly hydrated anions of chaotropic salts penetrate deeper into the non-polar stationary phase and create charged surface of ion-exchange properties.

## 2. Experimental

### 2.1 Reagents and chemicals

Thiamine hydrochloride (95.7%, Sigma Aldrich, USA), amprolium hydrochloride (99.4%, Sigma Aldrich, USA), adenine ( $\geq 99\%$ , Sigma Aldrich, USA), guanine (98%, Sigma Aldrich, USA), cytosine ( $\geq 99\%$ , Sigma, USA), uracil ( $\geq 99\%$ , Sigma Aldrich, USA), melamine (99%, Sigma, USA), ascorbic acid (99% Sigma Aldrich, USA), nicotinic acid (99%, Sigma Aldrich, USA), *p*-toulenesulfonic acid (*p*-TSA) ( $\geq 99\%$ , Sigma Aldrich, USA) and 4-hydroxybenzenesulfonic acid (4-OH-BSA) (98%, Sigma Aldrich, USA) were used as samples which were prepared as  $1 \text{ mg mL}^{-1}$  solution dissolved in 50% acetonitrile and then diluted by pure acetonitrile (Ultra Gradient HPLC Grade, J. T. Baker, Poland) to  $0.1 \text{ mg mL}^{-1}$  solution.

The following reagents were used for buffers: acetic acid (100% Sigma, USA), formic acid (100%, Merck, Germany), phosphoric acid (85%, Merck, Germany), citric acid (99%, Sigma, USA), malonic acid (99%, Sigma, USA), methansulfonic acid (100%, Sigma, USA), perchloric acid (70%, Aldrich, USA), trifluoroacetic acid ( $\geq 99.5\%$ , Sigma, USA), hexafluorophosphoric acid (55%, Aldrich, USA), ammonium hydroxide (25%, J. T. Baker, Poland), triethylamine ( $\geq 99.5\%$ , Sigma, USA), *tert*-butylamine ( $\geq 99.5\%$ , Sigma, USA), potassium hydroxide (45%, Merck, Germany). There were three types of preparation. First 0.5 L of  $25 \text{ mmol L}^{-1}$  acetic acid, formic acid, phosphoric acid, citric acid or malonic acid were prepared and then titrated by 25% ammonium hydroxide to  $\text{pH} = 3.5$ . Second were buffers with chaotropic salt: 0.25 L of  $25 \text{ mmol L}^{-1}$  methansulfonic acid, perchloric acid, trifluoroacetic acid or hexafluorophosphoric acid were titrated by ammonium hydroxide to  $\text{pH} = 3.5$  or 6.6 then 0.25 L of  $25 \text{ mmol L}^{-1}$  formic acid was added and titrated by 25% ammonium hydroxide to  $\text{pH} = 3.5$  or 6.6. Third were basic buffers: 0.5 L of  $25 \text{ mmol L}^{-1}$  ammonium hydroxide, triethylamine, *tert*-butylamine or potassium hydroxide were prepared and then titrated by 25% formic acid to  $\text{pH} = 3.5$ .

### 2.2 Instrumentation

All experiments were performed on the Waters (USA) Alliance 2695 with PDA 2996 as a detector. The following columns were used: TSKgel® Amide-80  $3 \mu\text{m}$   $4.6 \times 150 \text{ mm}$ , (Sigma Aldrich, USA), Atlantis® HILIC Silica  $5 \mu\text{m}$   $4.6 \times 150 \text{ mm}$  (Waters, USA), Luna®  $3 \mu\text{m}$  HILIC 200 Å  $4.6 \times 150 \text{ mm}$  (Phenomenex, USA) and X-BridgeTH HILIC  $3.5 \mu\text{m}$   $4.6 \times 150 \text{ mm}$  (Waters, USA). Flow rate of mobile phase was  $1 \text{ mL min}^{-1}$ , ration of organic and inorganic part was 80:20(v/v), injection volume was  $5 \mu\text{L}$ , column was thermostated on  $30 \text{ }^\circ\text{C}$  and detection was at 230 nm for melamine, 4-OH-BSA, *p*-TSA and 260 nm for thiamine, amprolium, adenine, cytosine, guanine, uracil, ascorbic acid, nicotinic acid.

### 3. Results and discussion

There are not many works dealing with effect on addition of chaotropic salt into the mobile phase in connection with HILIC columns. Therefore a screening was made. Four columns were used for separation of 12 modelling analytes (from strong acids to strong basis) using 13 different mobile phases. Interesting results were searched. Retention of acids on column was important aspect because of their difficult separation on reverse phases.

Retention of analytes on column TSK-amide with carbamoyl as a stationary phase with  $\text{HCOONH}_4$  and  $\text{HPF}_6$  as mobile phase seemed to be most interesting. Changes in concentration of formic acid and  $\text{HPF}_6$  and in pH were made. Significant drift in retention times were observed only by acids therefore 4-OH-BSA, *p*-TSA, ascorbic acid and nicotinic acid were examined.

Experiments took place by following way: 5, 10, 20 and 30  $\text{mmol L}^{-1}$ .  $\text{HPF}_6$  was added to 10  $\text{mmol L}^{-1}$   $\text{HCOOH}$  and titrated by 25%  $\text{NH}_4\text{OH}$  to pH = 3.5 and 6.6. And then 5, 10, 20 and 30  $\text{mmol L}^{-1}$   $\text{HCOOH}$  was mixed with 25  $\text{mmol L}^{-1}$   $\text{HPF}_6$  and titrated by 25%  $\text{NH}_4\text{OH}$  to pH 3.5 and 6.6.

There are two groups of analytes: strong acids (4-OH-BSA, *p*-TSA) and weak acids (ascorbic acid, nicotinic acid). Group of weak acids are more retained on the column and stronger acid of one group is more retained on the column.

Ascorbic acid is retained more when mobile phase has pH = 6.6 than when pH is 3.5. While opposite trend was observed for all other acids. Analyte with the smallest retention times is *p*-TSA. The biggest retention of *p*-TSA was achieved by using 10  $\text{mmol L}^{-1}$   $\text{HCCONH}_4$  with 25  $\text{mmol L}^{-1}$   $\text{HPF}_6$  and pH = 3.5.

In case of pH = 3.5 (Fig. 1) increasing ionic strength of buffer decreases retention of ascorbic and nicotinic acid but has not an influence on retention time

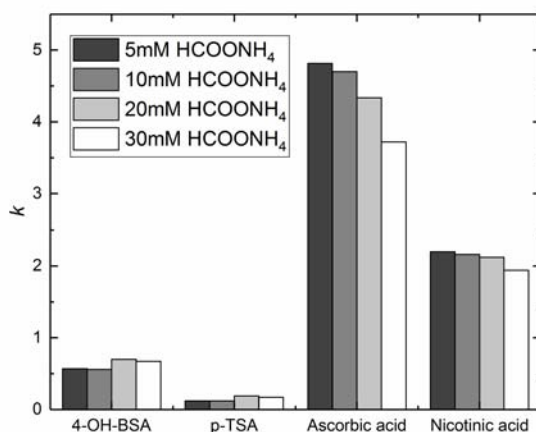


**Fig. 1** Effect of retention factor of 4-OH-BSA, *p*-TSA, ascorbic acid, and nicotinic acid on concentration of  $\text{HCOONH}_4$ . Unchanging conditions: pH = 3.5, 25  $\text{mmol L}^{-1}$   $\text{HPF}_6$ .

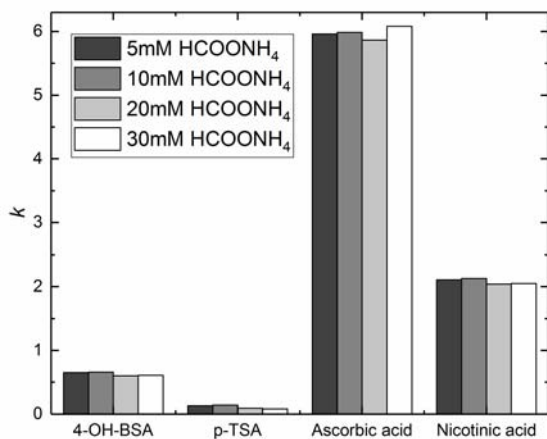


**Fig. 2** Effect of retention factor of 4-OH-BSA, *p*-TSA, ascorbic acid, and nicotinic acid on concentration of HCOONH<sub>4</sub>. Unchanging conditions: pH = 6.6, 25 mmol L<sup>-1</sup> HPF<sub>6</sub>.

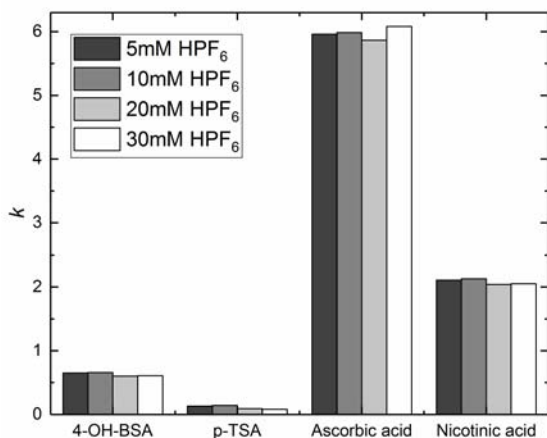


**Fig. 3** Effect of retention factor of 4-OH-BSA, *p*-TSA, ascorbic acid, and nicotinic acid on concentration of HPF<sub>6</sub>. Unchanging conditions: pH = 3.5, 10 mmol L<sup>-1</sup> HCOONH<sub>4</sub>.

of 4-OH-BSA and *p*-TSA. When pH = 6.6 (Fig. 2) retention of acid is not changing because of their p*K*<sub>a</sub>. Interesting effect on retention was observed when concentration of HPF<sub>6</sub> was changed. Increasing concentration of HPF<sub>6</sub> causes increase of retention times for all of 4 acids in case of both pH = 3.5 (Fig. 3) and 6.6 (Fig. 4). Further experiments are necessary and are in progress.

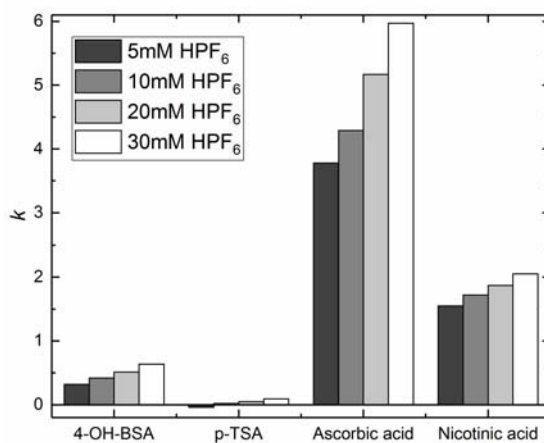


**Fig. 4** Effect of retention factor of 4-OH-BSA, *p*-TSA, ascorbic acid, and nicotinic acid on concentration of HPF<sub>6</sub>. Unchanging conditions: pH = 6.6, 10 mmolL<sup>-1</sup> HCOONH<sub>4</sub>.

#### 4. Conclusions

The effect of presence of chaotropic salts in HILIC mobile phases was investigated. After a screening study combination of TSK-amide column with carbamoyl as a stationary phase and HCOONH<sub>4</sub> with HPF<sub>6</sub> as a mobile phase was selected for detailed study. Increasing ionic strength of buffer with pH = 3.5 decreases retention of ascorbic acid and nicotinic acid and doesn't have an impact on 4-OH-BSA and *p*-TSA. Increasing concentration of HPF<sub>6</sub> increases retention times of all 4 acids.

#### References

- [1] Alpert A.J.: Hydrophilic interaction chromatography for the separation of peptides, nucleic acids and other polar compounds. *J. Chromatogr. A* **499** (1990), 177–196.
- [2] McCalley D.V.: Study of the selectivity, retention mechanism and performance of alternative silica-based stationary phases for separation of ionized solutes in hydrophilic interaction chromatography. *J. Chromatogr. A* **1217** (2010), 3408–3417.
- [3] Jin G., Guo Z., Zhang F., Xue X., Jin Y., Liang X.: Study on the retention equation in hydrophilic interaction chromatography. *Talanta* **76** (2008), 522–527.
- [4] Karazapanis A.E., Fiamegos Y.C., Stalikas C.D.: Study of the behavior of water-soluble vitamins in HILIC on a diol column. *Chromatographia* **71** (2010), 751–759.
- [5] McCalley D.V., Neue U.D.: Estimation of the extent of the water-rich layer associated with silica surface in hydrophilic interaction chromatography. *J. Chromatogr. A* **1192** (2008), 225–229.
- [6] Alpert A.J.: Electrostatic repulsion hydrophilic interaction chromatography for isocratic separation of charged solutes and selective isolation of phosphopeptides. *Anal. Chem.* **80** (2008), 62–75.
- [7] LoBrutto R., Jones A., Kazakevich Y.V.: Effect of counter-anion concentration on retention in high performance chromatography of protonated basic analytes. *J. Chromatogr. A* **913** (2001), 189–196.
- [8] Jones A., LoBrutto R., Kazakevich Y.V.: Effect of counter-anion type and on the liquid chromatography retention of  $\beta$ -blockers. *J. Chromatogr. A* **964** (2002), 179–188.

- [9] Horvath C., Melander W., Molnar I., Molnar P.: Enhancement of retention by ion-pair formation in liquid chromatography with nonpolar stationary phases. *Anal. Chem.* **49** (1977), 2295–2305.

Indexes



## Author Index

- Bakhytkyzy I. 188  
Baluchová S. 140  
Barek J. 51, 82, 280  
Baš B. 37  
Blaško J. 120  
Borowska M. 194  
Braun P. 55  
Bulska E. 19, 25, 44  
Bulycheva E.V. 61  
Buszewski B. 1, 68, 93, 269  
Bystrzanowska M. 200  
Ciesielski W. 77  
Ciešlik B. 258  
Czauderna M. 25  
Dębosz M. 14  
Dejmková H. 82  
Derina K. 134  
Dorozhko E. 134, 280  
Douša M. 285  
Durner B. 7  
Dušek M. 152, 181  
Dymerski T. 236, 253  
Ehmann F. 7  
Fabjanowicz M. 205  
Festinger N. 77  
Fischer J. 51  
Gabrišová L. 120  
Gajdár J. 51  
Galbavá P. 120  
Garwolińska D. 211  
Gashevskya A. 134  
Gawor A. 25  
Gawor A. 44  
Gębicki J.: 263  
Glinka M. 218  
Granica M. 31  
Gusar A. 134  
Halicz L. 19  
Hewelt-Belka W. 188, 211  
Igitkhanian A.E. 114, 158  
Jagielska A. 44  
Jakuczun W. 44  
Jandovská V. 181  
Jankowska K. 240  
Kalinowska K. 224  
Karapetian D.D. 114, 158  
Karasinski J. 19  
Kempińska D. 230  
Khristunova Y. 280  
Kilian K. 175  
Klausová K. 87  
Kochana J. 37, 126  
Kolesnichenko I.N. 114, 158  
Konieczka P. 258  
Konopka A. 25  
Korban A. 162  
Korotkova E. 61, 276, 280  
Kościelniak P. 14  
Kot-Wasik A. 188, 194, 211, 230  
Krata A.A. 19  
Kratochvíl B. 280  
Krejčová A. 87  
Krivosheina A. 276  
Król A. 68, 93  
Kubinec R. 120  
Kucińska-Lipka J. 194, 218  
Lewińska I. 145  
Ligor T. 1  
Linert W. 61  
Lubinska-Szczygeł M. 236, 253  
Madej M. 37  
Macho O. 120  
Makrlíková A. 82  
Malečková M. 105  
Marcinkowska R. 246  
Matysik F.M. 7, 55  
Michalec M. 145  
Mikulec J. 120  
Milanowski M. 1  
Morawska K. 77  
Mortet V. 140  
Možeński C. 269  
Musil S. 100  
Namiešnik J. 211, 224, 236, 253  
Navrátil T. 82  
Nguyen-Marcinczyk C.T. 19  
Nikolaeva A.A. 61  
Nižnanská Ž. 120  
Olšovská J. 105, 152  
Patočka J. 87  
Pawlak F. 240

- Pegier M. 175  
Platonov I.A. 114, 158  
Płotka-Wasyłka J. 205, 224  
Polkowska Ż. 240  
Pomastowski P. 68, 93  
Popova V. 276  
Pyrzynska K. 175  
Pytel K. 246  
Rabl H.P. 55  
Rafińska K. 93, 269  
Railean-Plugaru V. 68, 93  
Rogowska A. 93  
Różańska A. 236, 253  
Rudnicka J. 1  
Ruszczynska A. 25, 44  
Rybarczyk P. 263  
Shikun M. 169  
Schwarzová-Pecková K. 140  
Smarzewska S. 77  
Smolejová J. 285  
Šoukal J. 100  
Starzec K. 126  
Świerczek L. 258  
Szostek M. 44  
Szulczyński B. 263  
Szultka-Młyńska M. 93  
Taylor A. 140  
Tobiszewski M. 200  
Toczyłowska B. 44  
Torres Elguera J.C. 25  
Tymecki Ł. 145  
Vrublevskaya O. 169  
Vrzal T. 105  
Vyskočil V. 82, 280  
Wagner B. 44  
Wasik A. 218  
Wieczorek M. 14  
Wojciechowski M. 19  
Wojnowski W. 224  
Wrona O. 269  
Zabiegała B. 246  
Ziemińska E. 44  
Złoch M. 93  
Zušťáková V. 152

## Keyword Index

- acemetacin 77  
adsorption 175  
analytical calibration 14  
antibacterial antibiotics 218  
antimicrobial coatings 194  
apple cider 152  
Arctic 240  
aroma properties 236  
aryldiazonium salts 134  
atherosclerosis 44  
Bacteria 240  
bacterial aggregation 68  
beer 181  
biodiesel 120  
biofiltration 263  
biogenic amines 224  
biomarkers 158  
biosensors 126  
biotrickling 263  
boron-doped diamond 140  
breath acetone 158  
building industry 258  
calibration mixtures 114  
capillary electrophoresis 68, 93  
carbon dioxide 269  
carbon ink 276  
carbon nanotubes 175  
carbon paste electrode 77  
catheterization 194  
cells clumping 93  
chaotropic salts 285  
chelation 19  
chemiluminescence detector 105  
chromato-desorption microsystems 114, 158  
chromium 19  
citalopram 37  
creatinine 145  
current density 169  
cyclic voltammetry 37, 140, 169  
DeNO<sub>x</sub> systems 55  
derivatization 105, 218  
Design of Experiment 188  
determination 77  
diabetes 158  
diesel 120  
diesel engine 55  
difenzoquat 51  
dinitrobenzoic acid, 3,5- 145  
distance-based detection 31  
d-limonene 246  
dopamine 140  
drug delivery systems 218  
ecological control 114  
electrochemical immunosensor 280  
electrochemistry 37  
electronic nose 253, 263  
ethanol 162  
ethyl nitrite 276  
extraction 105  
fate 181  
fatty acids 269  
fatty acid methyl ester 120  
flow analysis 14  
fluorimetry 61, 145  
food analysis 224  
formic acid 285  
fruit hybridization 236  
fruit juices 253  
gas chromatography 105, 114, 253  
GC-FID 120  
GC-MS 269  
glassy carbon electrode 134  
goldenrod (*Solidago gigantea* L.) 269  
graphite electrode 276  
gravimetric preparation 162  
green analytical chemistry 200  
hairdresser 246  
heavy metal 258  
herbicide 51  
hexafluorophosphoric acid 285  
hierarchical cluster analysis 253  
HILIC-Q-TOF-MS 230  
hops 181  
HPLC 82, 218  
HPLC-HR/MS 152  
HS-SPME-GC/MS 1

- human breast milk 211  
hydrophilic interaction  
  chromatography 285  
ICP-MS 87, 100, 205  
ICP-OS 205  
indoor air 246  
interactive  
  chromatography 7  
interference effects 14  
iodinated contrast  
  agents 87  
iodine 87  
iron 14  
isolation 269  
label-free proteomics 25  
*Lactococcus lactis* 68  
laser ablation 44  
linear and cyclic  
  poly(dimethyl-  
  siloxane) 7  
linear antenna 140  
lipid extraction 188  
lipidomics 188  
MALDI-TOF MS 93  
mass spectrometry 25,  
  44  
meat freshness 224  
mercury meniscus  
  modified silver solid  
  amalgam electrode  
  51  
metal 205  
molybdenum 100  
MS/MS 120  
Multi-Criteria Decision  
  Analysis 200  
NiOOH 55  
nitroso compounds 105  
non-invasive diagnostics  
  158  
odour intensity 263  
 $\mu$ PAD 31  
perfumes 230  
pesticide 181  
pesticides residues 152  
photochemical vapor  
  generation 100  
pollutants 240  
polymer HPLC 7  
precipitation-re-  
  dissolution  
  mechanism 7  
preconcentration 1  
PROMETHEE 200  
Prussian blue 31  
QuEChERS 152  
Raman spectroscopy  
  140  
reduction 19  
response surface  
  methodology 269  
restrictor 120  
RP-HPLC- Q-TOF-MS 230  
RPIP HPLC 19  
saliva 1  
scandium 175  
secondary organic  
  aerosol 246  
selective catalytic  
  reduction 55  
selenoproteins 25  
sewage sludge 258  
sewage sludge ash 258  
silver nanoparticles 280  
simultaneous  
  determination 61  
smoked meat 200  
Sn(II) 169  
Sn(IV) 169  
solid phase extraction  
  82  
sorption 87  
spectrophotometry 14  
Spitsbergen 240  
stabilization 258  
staircase voltammetry  
  37  
standard solution 162  
successive iterations 162  
supercritical fluids  
  extraction 269  
sweetie 236  
synthetic dyes 61  
terpenes 236, 246  
tick-borne encephalitis  
  280  
titania gel 126  
toluene 263  
TSK-amide column 285  
tumor biomarker 82  
tyrosinase 126  
untargeted lipidomics  
  211  
urea decomposition 55  
urinary catheters 194  
urinary tract infections  
  194  
UV 100  
vanillylmandelic acid 82  
volatile impurities 162  
volatile organic  
  compounds 1  
voltammetry 51, 77,  
  126, 134, 276  
wine 205  
yeast 93  
zinc ions 68



---

**Proceedings of the 14th International Students Conference “Modern Analytical Chemistry”**

Edited by Karel Nesměrák.

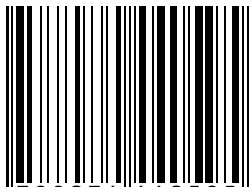
Published by Charles University, Faculty of Science.

Prague 2018.

1st edition – x, 298 pages

ISBN 978-80-7444-059-5

ISBN 978-80-7444-059-5



9 788074 440595